

The University of Leeds
Faculty of Medicine and Health
Leeds Institute of Cardiovascular and Metabolic Medicine

Stimulus-coupled regulation of Weibel-Palade Body trafficking by Rab46

Katarina Tencheva Miteva

Submitted in accordance with the requirements for the degree of
Doctor of Philosophy

June, 2021

Funded by the British Heart Foundation FS/17/43/33003



**British Heart
Foundation**

Intellectual Property and Publication Statements

The candidate confirms that the work submitted is his own and that appropriate credit has been given where reference has been made to the work of others.

This copy has been supplied on the understanding that it is copyright material and that no quotation from the thesis may be published without proper acknowledgement.

The right of Katarina Tencheva Miteva to be identified as Author of this work has been asserted by her in accordance with the Copyright, Designs and Patents Act 1988.

© 2021. The University of Leeds and Katarina Tencheva Miteva

Acknowledgements

This PhD journey has been the biggest challenge in my life, both professional and personal. The past couple of years were filled in with many highs and lows, many tears and above all - tons of laughs, dances, songs and jokes during the countless in the lab. I recently heard the saying that 'Hindsight is 20/20'. In hindsight, now I know that even the bad times were good times. In fact, I am very grateful for the bad times which ultimately made me the scientist, daughter, sister, friend and wife I am today. I had many challenges in submitting this thesis and I would have never made it without the incredible support of the people acknowledged below.

First and foremost, I would like to thank my PhD supervisor Dr Lynn McKeown for being an inspiring mentor and scientist. Your guidance has been instrumental for the completion of this project and thesis. I am immensely grateful for all your patience and support, especially in the last 6 months during my back injury. Your belief in me kept me going during the painfully slow writing of this thesis. I will always miss being a member of your lab and will remember my PhD with a smile on my face.

I gratefully acknowledge Professor David Beech for offering me a PhD in LICAMM and for the guidance throughout my PhD. Your advice and thought provoking lab meetings have helped me keep focused and deliver this project. It is a privilege to know a scientist like yourself.

I would also like to thank Dr Robin Bon for his advice during my project. Although, I still don't understand chemistry very well, I have always found your expertise, research excellence and passion incredibly motivating.

I would like to thank Dr Sally Boxall from Bioimaging facility for all the advice on microscopy, Dr Izzy Jayasinghe for invaluable support on image analysis and Martin Fuller from Astbury Centre for support on electron microscopy.

Massive thank you goes to Professor Mirela Delibegovic and Dr Samantha Le Sommelier from The University of Aberdeen. Mirela, to this day you remain my biggest mentor and my 'academic mum'. You have supported me from applying to this PhD, to surviving it and to finishing it. Sam, without the training you provided me I would've never become half the scientist I am today. I will always be indebted for both of your support and belief in me.

To all past and present members of the McKeown lab: Jane, I will always be grateful for your kindness to me, warm hugs and for your support during the prep and revision of our publication. To Sabina, the busiest bee in the lab,

thank you for helping me out with your masterful molecular biology skills and a joy to be around. To Ash (fierce), as the only boy in the McKeown lab during my time, your calm presence was very much needed! Thank you very much for all the laughs in the lab and for sharing few cold pints with me!

I have been incredibly lucky to work closely with the Beech lab, and I would like to thank all past and present Beech lab members for their support, especially Euli, Melanie, Greg and Vincenza. Hannah has been a huge support from day one, helping me and Lucia figure our way in the lab. I am very grateful for your friendship and support throughout my time in Leeds. Now that you know what a cytokine is, we are all waiting for you to become a CEO and give us jobs! Nikki, thank you for always cheering me up and making me smile during the tough times. I have thoroughly enjoyed sharing few cold wines with you on those crazy nights out.

Marj and Fiona (Fifi), first of all thank you not only for being two of my best friends in the world, but also showing me what is to be an absolutely brilliant scientists. I have always said that if I could be half as brilliant and bright post-doc as you two you are, I would be very successful. Thank you for all laughs in the lab, the French language lessons (les ananases sont mure aussi!), sharing my love for Ca^{2+} signalling, answering my endless silly questions (especially qPCR) and teaching me how to make 2mg/ml BSA solution. Please don't forget that lunch is always at 12.

Thank you to Katie (Mus), you and I have our own way of communicating (sometimes not even using words!). You and I went through some very difficult times and I am so proud of everything you have achieved. I miss dearly those 'share a bottle of wine' sunny afternoons when we never run out of things to say to each other. Upwards and onwards.

To Beth, to this day it still amazes me how our friendship grew along the years and you became my absolute best friend in the entire world when we both needed each other the most. You are my biggest support and partner in pints crime! Your genuine kindness taught me that you could get very far in life by not being afraid to be yourself. As much as I taught you the importance of self-care, you taught me how to truly find joy in life (and some slick dance moves). Thank you also for bringing Briana in my life. I didn't know my heart could open for one more best friend. You two have been instrumental in finishing this thesis, keeping me going through the darkest times when my back pain was at its worst. Looking forward to visiting you in California and living my best life there.

Last but not least, to the person without this project was never going to be possible from start and to finish, Lucia. Thank you for being the absolute best 'Weibel-Palade buddy' and friend throughout this Rab46 journey. I am in awe of your calm, quiet and patient wisdom that have taught me more about integrity, family and friendship, importance of work-life balance, good pasta and the power of a small cup of espresso than anyone else I know. You never complained, never judged me and always responded with a smile when I talked way too much in the lab, patiently listened to my worries, and provided invaluable support when I needed it most. Thank you for all the laughs in and outside the lab, for the help on those late night experiments and for always patiently answering my questions about the scale bars on the DV (I can confirm that I finally know it). Working alongside you and learning from you have been a true privilege and joy. You are a brilliant scientist and I will always cheer you on (and of course, won't stop asking you if you want to move to Scotland!).

I would not recommend injuring a lumbar disc during a world pandemic and having to write a thesis to anyone. That's why, I would like to acknowledge my rehab team without whom the writing of this thesis would've been even slower and more painful. Thank you to Dominique Reed from Unique Physiotherapy for always being patient with my worries and giving me the reassurance that I can indeed get through this back injury. To Dr Dawn Blaser from Blaser Chiropractic, thank you for your expertise and helping me return to leading a normal life. Finally, to Joel Proskewitz from PerformanceRx, your knowledge, expertise and wisdom were key in my recovery. Thank you for helping me find joy in training and life again.

A huge thank you to my parents-in-law, Patty and Frank, you are the kindest people I know. Thank you for your care, love and support throughout this PhD. To Grandma Mary, your 101-year old wisdom and your unrelenting belief in me have been one of the biggest motivators in my life.

I would like to acknowledge my husband, David. You have been the biggest pillar in my life that held strong throughout my PhD and my back injury, ultimately without you none of this would've been possible. Thank you for being the best listener (I am sure you didn't want to always listen about Ca²⁺ and failed Western blots), for reminding me there is a life outside the lab and for always supporting all my aspirations.

To my family whom I am most grateful - Maria, Tencho and Tatyana, I dedicate this thesis to you. Мамо, тате, како, благодаря Ви за безвъзвратната подкрепа през всичките години на тази докторантура. Благодаря Ви, че

никога не ми се сърдихте когато бях уморена, ядосана и в лошо настроение, а вместо това с търпение слушахте когато плачех прекалено пъти по телефона или се оплаквах за лабораторните проблеми. Благодаря Ви, че никога не се отказахте от мен, че вярвате в мен, и че ме подкрепяте в моменти в които аз нямам никаква вяра останала. Без вашата подкрепа и любов, аз нямаше да успея да приключа този проект и да постигна успех. Посвещавам тази докторска степен на вас. Обичам Ви и се надявам че се гордеете с мен, колкото аз се гордея с вас.

Final thank you goes to a truly special charity, the British Heart Foundation, who have kindly funded my PhD studentship. I am truly humbled by this life-changing experience.

Abstract

Endothelial cells (ECs) comprise the innermost lining of the vasculature. ECs maintain and restore vascular homeostasis after vascular injury by regulating a number of functionally distinct processes including haemostasis, thrombosis and inflammation. The endothelium operates these processes by means of exocytosis of cargo from specialised storage organelles named Weibel-Palade bodies (WPBs). WPBs contain cargo that is rapidly released upon demand. This cargo play roles in haemostasis (von Willebrand factor; vWF), inflammation (P-selectin) and angiogenesis (Angiopoietin-2). Several functionally distinct endothelial agonists, such as histamine and thrombin, induce WPB trafficking and exocytosis by raising intracellular Ca^{2+} . It has been previously speculated that ECs can couple stimuli to selective WPB trafficking and exocytosis. However, the underlining mechanisms are not fully understood.

Here, I describe a novel Ca^{2+} sensing Rab GTPase (CRACR2A-L or Rab46) in endothelial cells that is located on WPBs. High resolution imaging reveals that histamine via the H_1R , but not thrombin, evokes retrograde trafficking of Angiopoietin-2-positive WPB subpopulation towards the MTOC that is dependent on GTP-activation of Rab46. Ca^{2+} measurements and immunofluorescent imaging reveal that this retrograde trafficking is independent of cAMP-PKA and intracellular Ca^{2+} signalling. However, further immunofluorescent imaging experiments and mutagenesis of Rab46 Ca^{2+} -sensing EF-hand domain reveal that the dispersal of Rab46-positive WPBs from the MTOC is Ca^{2+} -dependent. Ca^{2+} measurements and immunofluorescent imaging reveals that in ECs the H_1R is coupled to the Ca^{2+} second messenger NAADP that mobilises Ca^{2+} from localised acidic Ca^{2+} stores. Furthermore, Ca^{2+} from these NAADP-sensitive Ca^{2+} stores is responsible for the dispersal of Rab46-positive WPBs from the MTOC. High-resolution imaging shows that in ECs the endogenous localisation of NAADP target Ca^{2+} release channel TPC1 is at the MTOC, demonstrating that there is a potential interaction between the acidic stores and WPBs.

The findings in this thesis indicate that Rab46 is firstly a novel key regulator of differential trafficking of WPB subpopulations and secondly, a sensor of NAADP-sensitive Ca^{2+} stores in ECs, allowing a stimulus appropriate acute immunogenic response whilst avoiding release of excessive pro-thrombotic mediators. Understanding the mechanisms and signalling pathways of Rab46

in the endothelium could be an important avenue for the discovery of novel therapeutic targets for cardiovascular pathologies.

Table of Contents

Acknowledgements	iii
Abstract	vii
Table of Contents	ix
List of Figures	xii
List of Tables	xvi
Abbreviations	xvii
Publications	xix
Communications	xx
Chapter 1 Introduction	1
1.1 Vascular endothelium – homeostasis and pathophysiology.....	2
1.2 Weibel-Palade bodies – the emergency first aid kit of the vasculature	6
1.2.1 WPB biogenesis.....	9
1.2.2 WPB cargo and function	11
1.2.3 WPBs in clinic - When things go wrong	17
1.2.4 Mechanisms underlying WPB exocytosis	19
1.2.5 Exocytotic machinery and signalling pathways of regulated WPB release	22
1.3 Ca ²⁺ toolkit in the endothelium.....	29
1.3.1 Ca ²⁺ entry mechanisms	29
1.3.2 Intracellular Ca ²⁺ stores and signalling.....	34
1.4 Rab GTPases – masters of intracellular transport.....	50
1.4.1 Rab GTPases regulation and function	50
1.4.2 CRACR2A (Rab46) discovery - One gene, two isoforms.....	54
1.5 Summary	61
1.6 Hypothesis, Aim and Objectives.....	62
Chapter 2 Methods	63
2.1 Reagents	63
2.2 Cell culture.....	63
2.2.1 HUVECs.....	63
2.3 Transfection.....	63
2.3.1 Short-interfering RNA (siRNA) transfection.....	63
2.3.2 cDNA transfection	64

2.4	ELISA	65
2.4.1	Angiopoietin-2 ELISA	65
2.4.2	P-selectin surface ELISA	65
2.5	Western blot	66
2.6	Immunoprecipitation	67
2.7	qRT-PCR.....	68
2.7.1	mRNA isolation	68
2.7.2	Reverse transcription	68
2.7.3	qRT-PCR.....	68
2.8	Intracellular Ca ²⁺ measurement.....	70
2.9	Immunocytochemistry.....	71
2.9.1	Microscopy	73
2.9.2	DeltaVision wide-field deconvolution microscopy	73
2.9.3	High-resolution Airyscan microscopy	73
2.9.4	Image analysis	74
2.9.5	Rab46 and WPB distribution	74
2.9.6	P-selectin/Angiopoietin-2 colocalisation.....	77
2.10	Statistical analysis	77
Chapter 3 Stimuli-coupled differential trafficking of Weibel-Palade bodies regulated by Rab46.....		78
3.1	Introduction.....	78
3.2	Histamine evokes perinuclear clustering of Weibel-Palade Bodies	79
3.3	Histamine induces differential trafficking of Weibel-Palade bodies	84
3.3.1	P-selectin and angiopoietin-2 reside in mutually exclusive Weibel-Palade body populations.....	84
3.3.2	Histamine-evoked perinuclear-localized Weibel-Palade Bodies are devoid of P-selectin.....	87
3.3.3	Angiopoietin-2-positive WPBs are mis-localised in Rab46 depleted ECs.....	93
Chapter 4 Rab46 -dependent trafficking of WPBs to the MTOC is independent of cAMP signalling		98
4.1	Introduction.....	98
4.2	Histamine-evoked perinuclear clustering of WPBs is independent of cAMP	99
4.3	Epinephrine-induced perinuclear clustering of WPBs is independent of Rab46	106
Chapter 5 The role of Ca²⁺ in Rab46-dependent WPB trafficking		110
5.1	Introduction.....	110

5.2	Histamine-evoked WPB trafficking is mediated by the H ₁ receptor	111
5.3	Histamine-evoked retrograde trafficking of WPBs is independent of intracellular Ca ²⁺	117
5.3.1	Store-operated Ca ²⁺ entry is not involved in histamine-evoked perinuclear clustering of Rab46-positive WPBs	117
5.3.2	Chelation of intracellular Ca ²⁺ does not prevent histamine-evoked perinuclear clustering of Rab46-positive WPBs.	119
5.4	Intracellular Ca ²⁺ evokes Rab46-dependent dispersal of WPB clusters from the MTOC	123
Chapter 6 NAADP-sensitive Ca²⁺ pool regulates Rab46-dependent Weibel-Palade body trafficking		128
6.1	Introduction	128
6.2	Histamine-evoked intracellular Ca ²⁺ release is coupled to NAADP in endothelial cells	129
6.3	The role of NAADP store in Rab46 trafficking	141
6.3.1	NAADP-sensitive Ca ²⁺ pool is necessary for dispersal of histamine-induced Rab46-positive WPBs clusters.....	141
6.3.2	TPCs are NAADP target channels in ECs	148
6.3.3	Localisation of TPCs	153
6.3.4	Rab46-positive WPBs interaction with the endo-lysosomes.	156
Chapter 7 Discussion		158
7.1	The role of Rab46 in differential trafficking of WPB subpopulations	158
7.2	Histamine-induced WPB retrograde trafficking is independent of cAMP and Ca ²⁺	161
7.3	Rab46 senses Ca ²⁺ release from NAADP-sensitive Ca ²⁺ stores .	166
Chapter 8 Final conclusions and future work		170
8.1	Summary of key findings	170
8.2	Conclusion	170
8.3	Future work.....	171
8.3.1	Rab46 mechanisms	171
8.3.2	Structural studies	174
8.3.3	Transgenic mice.....	174
List of References		176

List of Figures

Figure 1.1 The human cardiovascular system	4
Figure 1.2 Functions of endothelial cells.....	5
Figure 1.3 First micrograph of Weibel-Palade Bodies acquired in 1962	8
Figure 1.4 Biogenesis of Weibel-Palade bodies.....	11
Figure 1.5 Weibel-Palade bodies in action during vascular injury.....	17
Figure 1.6 Current working model of cAMP-dependent Weibel-Palade body exocytosis pathway.	25
Figure 1.7 Differential Ca ²⁺ -dependent Weibel-Palade body exocytosis pathways	28
Figure 1.8 Store-operating Ca ²⁺ entry	31
Figure 1.9 NAADP dose-response curve.	40
Figure 1.10 NAADP-mediated Ca ²⁺ release mode of action and cellular	41
Figure 1.11 Multiple regulators of Two-pore channels affect Ca ²⁺ release from the endo-lysosomes.....	43
Figure 1.12 Two-pore channels function in different tissue types and role in disease.....	44
Figure 1.13 Schematic diagram of EF-hand motif.....	48
Figure 1.14 Endothelial Ca ²⁺ signalling toolkit.....	49
Figure 1.15 Rab GTPase cycling.....	52
Figure 1.16 CRACR2A in endothelial cells.	56
Figure 1.17 Structural similarities between CRACR2A isoforms and other EF-hand proteins.	57
Figure 1.18 Rab46 localises to WPBs.	59
Figure 1.19 Rab46-dependent trafficking of WPBs to the MTOC.	60
Figure 2.1 P-selectin cell surface ELISA.....	66
Figure 2.2 Fluorescence excitation spectra for Fura-2 in solutions containing increasing concentrations of free Ca ²⁺	71
Figure 2.3 AiryScan imaging principle.....	74
Figure 2.4 Quantification of vWF and Rab46 cellular distribution.	76
Figure 3.1 Histamine and thrombin evoke intracellular Ca ²⁺ rise in ECs.....	81
Figure 3.2 Histamine evokes time-dependent perinuclear trafficking of WPBs.	82
Figure 3.3 Thrombin does not evoke perinuclear trafficking of WPBs.	83

Figure 3.4 Angiotensin-2 and P-selectin reside in mutually exclusive WPBs.....	85
Figure 3.5 Angiotensin-2 and P-selectin primary antibodies specificity	86
Figure 3.6 Histamine induces differential trafficking of P-selectin–negative WPBs that contain Angiotensin-2.	89
Figure 3.7 Angiotensin-2 localizes to MTOC in the absence of stimulation with histamine in cells overexpressing Q604L Rab46 mutant.	90
Figure 3.8 Rab46 depletion does not affect P-selectin surface expression.....	91
Figure 3.9 Rab46 depletion prevents histamine- and PMA-evoked Angiotensin-2 secretion.....	92
Figure 3.10 Rab46 depletion decreases total Angiotensin-2 protein levels.....	94
Figure 3.11 Rab46 depletion does not affect mRNA levels of Angiotensin-2	95
Figure 3.12 Rab46 depletion causes a loss of Angiotensin-2 localization to WPBs.....	96
Figure 4.1 H89 inhibits PKA-induced CREB-1 phosphorylation.....	100
Figure 4.2 PKA inhibition does not affect histamine-induced intracellular Ca ²⁺ release.....	101
Figure 4.3 Histamine-evoked perinuclear trafficking of Rab46-positive WPBs is PKA-independent.....	102
Figure 4.4 Rp-cAMP inhibits PKA-induced CREB-1 phosphorylation.....	103
Figure 4.5 cAMP inhibition does not affect histamine-induced intracellular Ca ²⁺ release.....	104
Figure 4.6 Histamine-evoked perinuclear trafficking of Rab46-positive WPBs is cAMP-independent.	105
Figure 4.7 Epinephrine induces perinuclear clustering of Rab46 and WPB solely in the presence of phosphodiesterase inhibitor.	107
Figure 4.8 Epinephrine does not evoke intracellular Ca ²⁺ release from ECs.....	108
Figure 4.9 Rab46 is not necessary for cAMP-dependent trafficking of WPBs.....	109
Figure 5.1 HUVECs express histamine H ₁ receptors.....	112
Figure 5.2 Histamine H ₁ receptor selective agonist, 2-PY, evokes intracellular Ca ²⁺ release and Rab46 and WPB perinuclear clustering.....	113
Figure 5.3 Histamine H ₄ receptor agonist does not trigger perinuclear clustering of Rab46-positive WPBs.....	114

Figure 5.4 H ₁ R selective inverse agonist inhibits 2-PY evoked intracellular Ca ²⁺ release.....	115
Figure 5.5 H ₁ R inverse agonist inhibits histamine-evoked intracellular Ca ²⁺ release.....	116
Figure 5.6 Inhibition of SOCE through Orai channels does not inhibit histamine-induced Ca ²⁺ release from intracellular stores.	118
Figure 5.7 Inhibition of store-operated Ca ²⁺ -entry does not prevent histamine-induced Rab46 and WPB perinuclear clustering.	119
Figure 5.8 BAPTA-AM chelates histamine-evoked intracellular Ca ²⁺ release.....	121
Figure 5.9 Acute histamine-evoked perinuclear trafficking of WPBs is independent of intracellular Ca ²⁺ release.	122
Figure 5.10 Rab46 EF-hand mutant is located at the MTOC in absence of stimulation.	125
Figure 5.11 Intracellular Ca ²⁺ evokes Rab46-dependent WPB dispersal from the MTOC.	126
Figure 5.12 Rab46 EF-hand is necessary for Ca ²⁺ -dependent WPB dispersal from the MTOC	127
Figure 6.1 Histamine-evoked intracellular Ca ²⁺ release is coupled to NAADP-sensitive Ca ²⁺ stores in HUVECs.	133
Figure 6.2 Histamine-evoked Ca ²⁺ release is coupled to NAADP-sensitive Ca ²⁺ stores in HUVECs.	134
Figure 6.3 H ₁ receptor triggers intracellular Ca ²⁺ release from NAADP-sensitive Ca ²⁺ stores.	136
Figure 6.4 H ₁ receptor is coupled to NAADP-sensitive Ca ²⁺ stores.	137
Figure 6.5 NAADP antagonism does not affect intracellular Ca ²⁺ release evoked by thrombin.	138
Figure 6.6 NAADP antagonism does not affect Ca ²⁺ release evoked by thrombin.	139
Figure 6.7 NAADP antagonism does not affect store-operated Ca ²⁺ entry in HUVECs.	140
Figure 6.8 HUVECs have functional endo-lysosomal Ca ²⁺ stores.....	144
Figure 6.9 Ca ²⁺ release from NAADP-sensitive Ca ²⁺ stores governs histamine-induced Rab46 and WPB clusters dispersal from the MTOC.	145
Figure 6.10 High concentrations of histamine does not induce Rab46 and WPB clusters dispersal from the MTOC.....	146
Figure 6.11 Bafilomycin A1 inhibition of V-ATPase activity is not a suitable pharmacological tool to study endo-lysosomal Ca ²⁺ signalling in HUVECs.	147
Figure 6.12 Relative mRNA expression of endo-lysosomal cation channels in HUVECs.....	149

Figure 6.13 TPCs inhibition by tetrandrine decreases histamine-evoked intracellular Ca²⁺ release.	150
Figure 6.14 Tetrandrine does not inhibit intracellular Ca²⁺ release in response to thrombin.	151
Figure 6.15 Ca²⁺ release from TPCs disperses histamine-induced Rab46 and WPB clusters from the MTOC.	152
Figure 6.16 Endogenous TPC1 localises to the MTOC in HUVECs.	154
Figure 6.17 WPBs cluster with TPC1 at the MTOC in response to histamine.	155
Figure 6.18 TPC2 does not colocalise with WPBs.	156
Figure 6.19 Rab46 interacts with TPCs.	157
Figure 8.1 Rab46 depletion decreases Ca²⁺ release and entry in response to histamine.	173

List of Tables

Table 1.1 Known Weibel-Palade bodies cargo and their function.....	12
Table 1.2 Endothelial Rab GTPases.	53
Table 2.1 Western blot buffers.....	67
Table 2.2 qPCR primers.....	69
Table 2.3 Primary antibodies	72
Table 2.4 Secondary antibodies	72

Abbreviations

AC	Adenylyl Cyclase
ACS	Acute Coronary Syndrome
ADAMTS-13	A Disintegrin And Metalloproteinase with Thrombospondin type 1 motif member 13
ADP	Adenosine Diphosphate
AMP	Adenosine Monophosphate
AP-1	Activator Protein-1
AP3	Adaptor Protein 3
APEX	Ascorbate Peroxidase
ATP1 α	Sodium-Potassium ATPase subunit α 1
BA1	Bafilomycin A1
BSA	Bovine Serum Albumin
cADPR	Cyclic ADP-ribose
CaMK	Ca ²⁺ /Calmodulin-dependent Kinase
cAMP α	Cyclic adenosine 3',5'-monophosphate
CC	Coiled-coil
cDNA	Complimentary DNA
CICR	Calcium-induced Calcium Release
CRAC	Calcium Release Activated Channel
CRACR2A	Calcium Release Activated Channel Regulator 2A
CVD	Cardiovascular Disease
DAG	Diacylglycerol
DNA	Deoxyribonucleic Acid
dSTORM	direct Stochastic Optical Reconstruction Microscopy
EBM-2	Endothelial Basal Medium-2
EC	Endothelial Cell
ECE	Endothelin-Converting Enzyme
EF-SAM	EF-Sterile Alpha Motif
EFCAB4B	EF-hand Calcium Binding Domain 4B
ELISA	Enzyme-linked Immunosorbent Assay
EPCR	Endothelial Cell Protein C Receptor
ER	Endoplasmic Reticulum
ERM	Ezrin-radixin-moesin
ET-1	Endothelin-1
FGF	Fibroblast Growth Factor
FVIII	Factor VIII
GAP	GTPase-ctivating Protein
GDI	Rab GDP Dissociation Inhibitors
GDP	Guanine Diphosphate
GDS	Ral Guanine Nucleotide Dissociation Stimulator
GEF	Guanine Nucleotide Exchange Factor
GFP	Green Fluorescent Protein

GMP-140	Granule Membrane Protein 140
GPCR	G Protein-Coupled Receptor
GPI	Glycoprotein Ib
GTP	Guanine Triphosphate
GWAS	Genome-Wide Association Study
HCX	Calcium-proton Exchanger
HMW	High Molecular Weight
HRP	Horse Radish Peroxidase
HUVEC	Human Umbilical Vein Endothelial Cells
IL-8	Interleukin-8
IP ₃	Inositol triphosphate
IP3R	Inositol triphosphate Receptor
IRBIT	Inositol-1,4,5-trisphosphate Receptors Binding Protein
IS	Immunological Synapse
JNK	c-Jun N-terminal kinase
LGCC	Ligand-gated Calcium Channel
LMW	Low Molecular Weight
MCU	Mitochondrial Uniporter Complex
MI	Myocardial Infarction
MTOC	Microtubule Organising Centre
mTOR	Mechanistic Target of rapamycin
MyRIP	Myosin VIIA And Rab Interacting Protein
NAADP	Nicotinic acid adenine dinucleotide phosphate
NAFLD	Non-alcoholic Fatty Liver Disease
NASH	Non-alcoholic steatohepatitis
NCX	Sodium-calcium Exchanger
NFAT	Nuclear Factor of Activated T-cells
NMR	Nuclear Magnetic Resonance
NOS	Nitric Oxide Synthase
NPC	Nuclear Pore Complex
PADGEM	Platelet Activation Dependent Granule-external Membrane Protein
PAR1	Protease-activated Receptor 1
PCR	Polymerase Chain Reaction
PIP ₂	Phosphatidylinositol 4,5-bisphosphate
PKA	Protein Kinase A
PKC	Protein Kinase C
PLC	Protein Lipase C
PLD1	Phospho Lipase D1
PM	Plasma Membrane
PMA	Phorbol 12-myristate 13-acetate
PMCA	Plasma Membrane Calcium ATPase
PRD	Proline-rich Domain
PSGL	P-Selectin Glycoprotein Ligand 1
PTP	Permeability Transition Pore

PVDF	Polyvinylidene Fluoride
qPCR	Quantitative Polymerase Chain Reaction
Rab	Ras-related proteins in brain
Rab11FIP3	Rab11 Family Interacting Protein 3
REP	Rab Escort Protein
RNA	Ribonucleic Acid
ROS	Reactive Oxygen Species
RyR	Ryanodine Receptor
S100A10	S100 Calcium Binding Protein A10
SDS	Sodium Dodecyl Sulphate
SERCA	Sarcoendoplasmic Reticulum Calcium Transport ATPase
SNARE	Soluble N-ethylmaleimide–Sensitive Factor Attachment Protein Receptor
SNP	Single Nucleotide Polymorphism
SOCE	Store-operated Calcium Entry
SPCA1	Calcium-transporting ATPase type 2C member 1
SR	Sarcoplasmic Reticulum
STIM1,	Stromal Interaction Molecule 1
STIM2	Stromal Interaction Molecule 2
Stx1B	Shiga Toxin 1B
TCR	T-cell Receptor
TGN	Trans-Golgi Network
TMB	Tetramethylbenzidine
TKR	Tyrosine Kinase Receptor
TPC1	Two-pore Channel 1
TPC2	Two-pore Channel 2
TPC3	Two-pore Channel 3
TRPA	Transient Receptor Potential Ankyrin
TRPM	Transient Receptor Potential Melastatin
TRPML	Transient Receptor Potential Mucopilin
TRPP	Transient Receptor Potential Polycystin
TRPV	Transient Receptor Potential Vanilloid
ULMW	Ultra-Large Molecular Weight
V2R	V2 Vasopressin Receptor
VEGF	Vascular Endothelial Growth Factor
VGCC	Voltage-gated Calcium Channels
VSMC	Vascular Smooth Muscle Cell
vWD	von Willebrand Disease
vWF	von Willebrand Factor
WPB	Weibel-Palade Body

Publications

Miteva, K., Pedicini, P., Wilson, L., Jayasinghe, I., Slip, R., Marszalek, K., Gaunt, H., Bartoli, F., Deivasigamani, S., Sobradillo, D., Beech, D., McKeown, L. Rab46 integrates Ca²⁺ and histamine signalling to regulate selective cargo release from Weibel-Palade bodies. *The Journal of Cell Biology* 218:2232-2246; (2019).

Pedicini, L., **Miteva, K.**, Hawley, V., Gaunt, H., Appleby, H., Cubbon, R., Marszalek, K., Kearney, M., Beech, D., McKeown, L. Homotypic endothelial nanotubes induced by wheat germ agglutinin and thrombin. *Scientific Reports* volume 8:7569 (2018)

Rubaiy, H.N., Ludlow, M.J., Henrot, M., Gaunt, H.J., **Miteva, K.**, Cheung, S.Y., Tanahashi, Y., Hamzah, N., Musialowski, K.E., Blythe, N.M., Appleby, H.L., Bailey, M.A., McKeown, L., Taylor, R., Foster, R., Waldmann, H., Nussbaumer, P., Christmann, M., Bon, R.S., Muraki, K., Beech, D. Picomolar, selective and subtype specific small-molecule inhibition of TRPC1/4/5 channels. *Journal of Biological Chemistry* 292:8158-8173 (2017)

Communications

Rab46 – a novel regulator of Weibel- Palade trafficking. **K.Miteva**, L.Pedicini LA.Wilson, I.Jayasinghe, DJ. Beech, and L.McKeown. Institute of Integrative Biology, University of Liverpool (2019). **Invited talk.**

Rab46 – a novel regulator of Weibel- Palade trafficking. **K.Miteva**, L.Pedicini LA.Wilson, I.Jayasinghe, DJ. Beech, and L.McKeown. North of England Cell Biology, Manchester (2019). **First prize oral communication.**

Differential trafficking of Weibel Palade bodies. **K.Miteva**, L.Pedicini LA.Wilson, I.Jayasinghe, DJ. Beech, and L.McKeown. Physiology 2019, Aberdeen (2019). **First prize poster communication.**

Ca²⁺ role in differential WPB trafficking. K. Miteva, LA. Wilson, DJ. Beech, and L. McKeown. FASEB Calcium and Cell function, Lake Tahoe, CA, USA (2018)

Statins reduce P-selectin expression and leukocyte adhesion on the endothelial cell surface. **K. Miteva**, L. Pedicini, David J. Beech & Lynn McKeown. IUPS 38th World Congress, Rhythms of Life, Rio de Janeiro (2017)

Chapter 1 Introduction

In 17th century, the Italian biologist and physician Marcello Malpighi described the physical separation between blood and tissue for the first time. Two centuries later, the German pathologist Friedrich Daniel Von Recklinghausen discovered the inner cellular lining of the vascular wall, though it remained only a more detailed description of Malpighi's discovery. This inner lining, nowadays known as the endothelium, was considered to fulfil no other purpose than that of a physical barrier between blood and tissue for many years, until Robert Furchgott and colleagues defined a potent endothelium-dependent vasoreactivity in the 1970s (Furchgott and Zawadzki, 1980; Fishman, 1982).

Henceforth, extensive research on the vasculature has coined the endothelium as the 'corner stone' of the vascular system that is fundamental to human physiology and health. Endothelial cells (ECs) play important roles in physiological processes including, but not limited to, primary haemostasis, inflammation, angiogenesis, regulation of blood flow and blood pressure (Herrmann and Lerman, 2001). ECs have the ability to regulate such a number of physiologically distinct processes through exocytosis of endothelial-specific organelles, named Weibel-Palade Bodies, which contain pre-stored bioactive molecules and factors. On demand, or regulated, exocytosis of WPBs is a pivotal mechanism via which the endothelium can respond to variety of stimuli triggered by, for example, acute vascular injury or inflammation. Endogenous agonists of WPB exocytosis can be grouped into two main categories according to their downstream intracellular signalling pathways: cAMP or Ca²⁺. Ca²⁺ is a ubiquitous signal and its mobilisation from intracellular stores is via ancient and conserved signal transduction mechanisms. Due to the complexity of multi-functional stimuli sharing common downstream pathways, many aspects underlying how ECs achieve such specificity in their response and deliver differential WPB exocytosis, are still poorly understood.

This chapter will offer a short background on the physiological role of ECs, WPBs and the consequences of dysregulated WPB exocytosis. Attention is then turned to the endothelial Ca²⁺ signalling toolkit, part of which drives exocytosis of WPB cargo from ECs. A class of Rab GTPases which possess Ca²⁺-sensing EF-hand domains, will then be described, with a focus on a novel endothelial Rab GTPase, Rab46. Rab46 may have the potential to direct WPB trafficking and also integrate Ca²⁺ signals. Finally, I will describe how understanding how ECs can finely tune their exocytotic response in order to achieve release of bioactive molecules from WPBs according to the physiological context of their environment has the

potential to unveil novel targets for future therapies of haematological and cardiovascular dysfunction.

1.1 Vascular endothelium – homeostasis and pathophysiology

The human cardiovascular network is a closed loop system that enables the transport of oxygenated blood to the body organs and de-oxygenated blood to the respiratory organs. The heart pumps approximately 5 L of blood through the cardiovascular network to vital organs of the body, providing supply of nutrients and oxygen, and removal of waste products and harmful chemicals. This is achieved through an inter-connection of arteries and veins that branch at multiple levels, reaching all parts of the body resulting in an intricate network of vessels (Boulpaep et al., 2009). The walls of larger blood vessels consist of multiple layers (Figure 1.1). The tunica intima, the innermost layer, consists of connective tissues and a thin monolayer of specialised squamous epithelial cells, known as the endothelium. ECs form a flat monolayer, with a thickness ranging between 0.17 and 0.23 μm . The endothelium is estimated to represent the largest organ in the body, comprising around $1\text{--}6 \times 10^{13}$ cells and covering an area of up to 7000 m^2 . In larger vessels, ECs are strategically located between blood flowing through the vessel and the surrounding vascular smooth muscle cells. This forms a semipermeable barrier regulating the transfer of macromolecules between the blood and adjacent tissues, which explains why they have often been described as the ‘tissue-blood barrier’ (Galley and Webster, 2004). ECs are exposed to a frictional force, or ‘shear stress’, as well as a plethora of metabolic and inflammatory signals as blood flows through the vascular system. Therefore, instead of playing merely a passive role as a gatekeeper between the blood and tissues, ECs represent a dynamic organ that regulates its environment and rapidly mediates its response to various stresses (Van Hinsbergh, 2001).

At homeostasis, ECs have a range of functions (Figure 1.2). These mediate vascular contractility, vascular smooth muscle contractility, adhesion of leukocytes, angiogenesis, and endothelial senescence of mature vessels. This myriad of functions stems from the phenotypic heterogeneity across the different and distinct vascular beds described in more detail below. ECs phenotypes differ between organ systems including separate segments of the vasculature within the same organ. At a cell morphology level, orientation of arterial ECs lining, long straight areas of the vessels is dependent on blood flow and its rates. Previous studies have shown that flow-dependent alignment of endothelial cells represents reversible endothelial structural remodeling in response to hemodynamic shear stress (Aird, 2007). Furthermore, spatial and temporal EC heterogeneity depict differences in messenger RNA (mRNA) and protein expression. Interestingly,

there are very few genes that specific only to the endothelium and are expressed constitutively throughout the entire vasculature (i.e. VE-cadherin). The majority of endothelial genes are either constitutively or inducibly expressed in separate endothelial clusters. For example, von Willebrand factor (vWF), a major haemostatic gene is differentially expressed in a constitutive manner across the vascular tree (Mojiri et al., 2019). Moreover, ECs plays a key role in leukocyte adhesion. Leukocytes roll on the endothelial surface, undergo adhesion and extravasation into the target tissue. This process is mediated by the rapid expression of cell adhesion molecules (P-selectin/E-selectin) on the surface of ECs as well as secretion of chemokines (IL-8, MCP-1). Studies have shown that the expression and storage of such molecules is heterogenous across the vascular beds(Aird, 2007). The described examples are particularly important in pathological states of the vasculature where the endothelium is damaged, undergoes remodelling and increases secretion of pro-haemostatic and pro-inflammatory factors, adding another layer of complexity.

As mentioned above, together with heterogeneity, there are many additional factors that affect EC function, including chemical stimuli, such as varying oxygen levels, paracrine signals and inflammatory and metabolic plasma constituents. ECs expertly navigate and operate tight control upon such signals by secreting various factors to maintain vascular tone and blood fluidity to restore homeostasis in the event of intimal injury (Cooke, 2000).

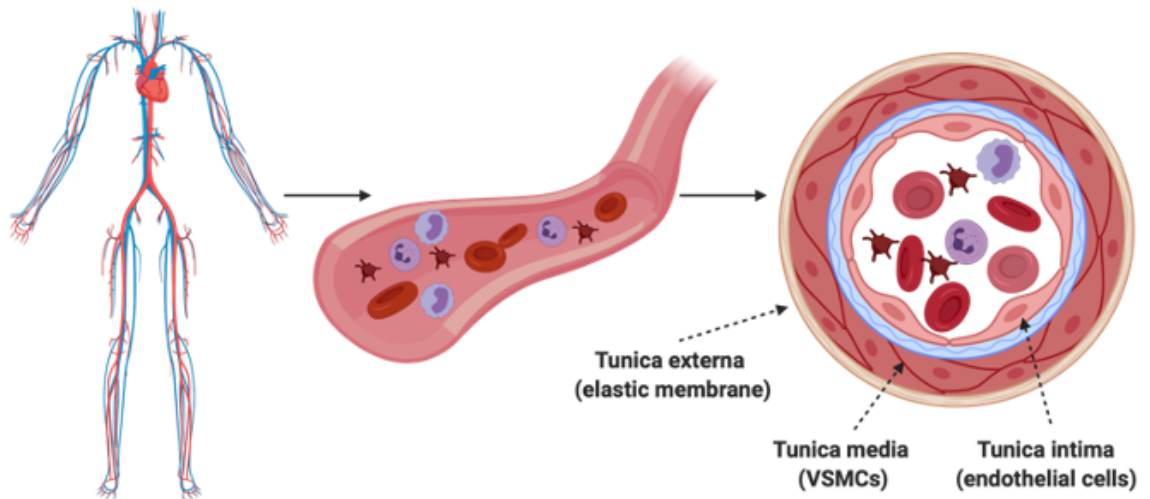


Figure 1.1 The human cardiovascular system

The human cardiovascular system comprises two main components – a heart and a network of blood vessels. The most important function of the cardiovascular system is to carry blood throughout the body, thereby supplying tissues with oxygen and nutrients, and collecting waste products and CO₂ for excretion. Blood vessels transport red blood cells, leukocytes and platelets. By nature, human blood vessels are elastic, tubular structures creating a barrier between the tissues and the blood. Larger vessels are structurally composed of multiple layers, namely the tunica externa (elastic membrane), tunica media (vascular smooth muscle cells: VSMCs) and tunica intima (endothelial cells or endothelium).

To continuously maintain blood in a fluid state, ECs exhibit an anti-coagulatory surface. However, upon acute injury of the vasculature, they secrete multiple protein complexes and factors that congregate on the endothelial surface, at the site of injury, triggering a physiological process called haemostasis. Haemostasis prevents excessive loss of blood while maintaining normal blood flow elsewhere by forming an initial stable blood clot, also known as the primary haemostatic plug, at the endothelial surface. Haemostasis is a tightly regulated process, highly localised to the site of injury and activated within seconds of injury occurrence (Gale, 2011). To initiate primary haemostatic plug formation, ECs release factors promoting platelet recruitment. Platelets are a type of small anuclear blood cells, produced by megakaryocytes in the bone marrow (Schulze and Shivdasani, 2005). For vascular homeostasis and normal blood flow, platelets do not adhere to the endothelial surface, nor aggregate with each other. However, when the endothelium is activated during injury, adhesion and subsequent activation of platelets begins. Platelet-endothelium interactions play an integral role in the formation of the primary haemostatic plug. This is mainly achieved through EC secretion of von Willebrand Factor (vWF) (for more details on endothelial secretion of vWF see Section 1.2.2.1). vWF is a multimeric adhesion glycoprotein

and is released in the form of long strings that 'capture' platelets, promoting further platelet adhesion and aggregation thereafter (Yau et al., 2015). After the injury has occurred and the ECs have prevented excessive bleeding, the healing process begins. The primary haemostatic plug not only seals the subendothelial spaces from further damage, but also acts as the scaffolding during the healing process (Wu et al., 1988). By secreting wound healing factors and cytokines, ECs act as the vector of angiogenesis, the formation of new blood vessels, which is essential for full repair of the wound and vascular homeostasis restoration. Angiogenesis is induced by pro-angiogenic growth factors (e.g. VEGF, angiopoietins, FGF etc.), usually in combination with inflammatory mediators or other factors induced by ischaemia (Kumar et al., 2015).

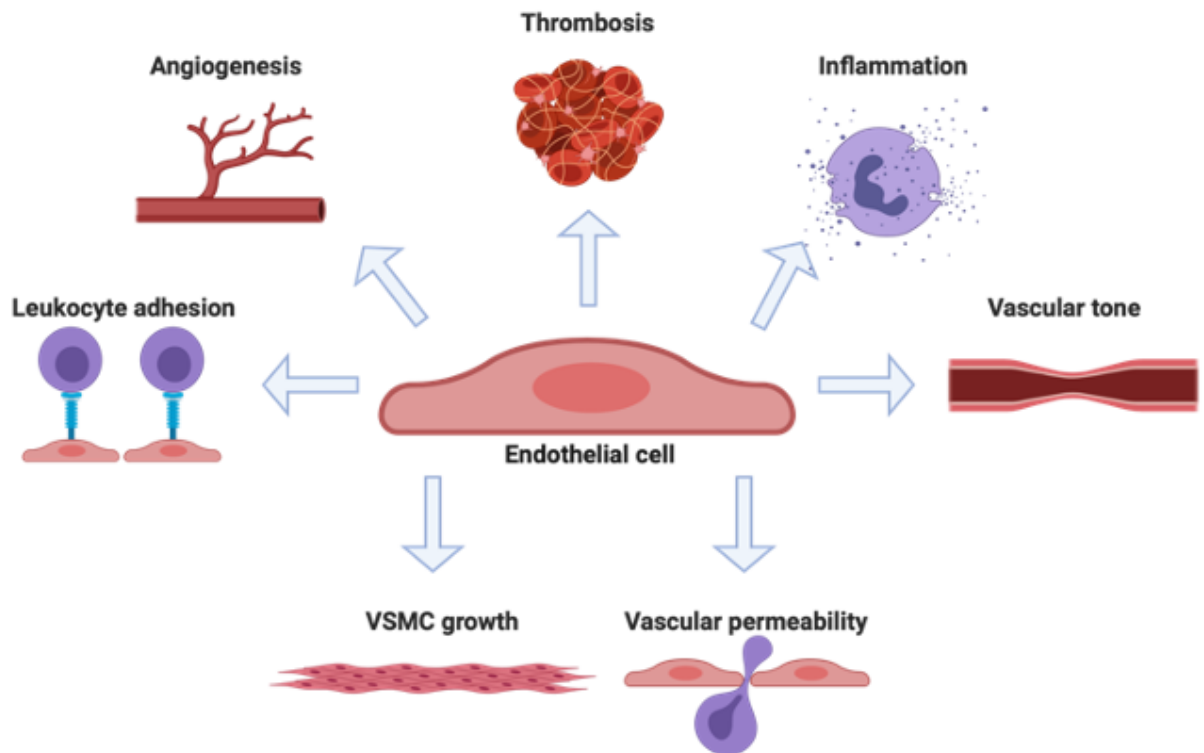


Figure 1.2 Functions of endothelial cells.

Although comprising a mere monolayer of endothelial cells, the endothelium is responsible for the maintenance and post-injury restoration of vascular homeostasis by regulating a myriad of physiological functions.

The importance of ECs in maintaining vascular health is emphasised during thrombosis, a pathophysiological consequence of dysregulation of primary haemostasis and blood clotting. In thrombosis, occlusive clots are formed within a blood vessel, reducing blood flow to tissues and restricting the delivery of oxygen and nutrients, resulting in local necrosis. Large occlusive clots, or thrombi,

can partially break off and embolise to form secondary thrombi in other locations in the body. The process of thrombosis, followed by embolism, is collectively termed 'thromboembolism', and can culminate in a variety of life-threatening disorders. For example, acute thrombosis is initiated by the rupture of atherosclerotic plaques (structures on the surface of endothelium gradually accumulated from fat, cholesterol, oxidative stress, Ca^{2+} etc.), and is the primary cause of myocardial infarctions and strokes. Both conditions lead to death or comorbidities significantly affecting the lifestyle quality of the patients (Lüscher and Noll, 1995; Stoll and Bendszus, 2006).

Overall, the endothelium is a dynamic vascular barrier at the nexus of cardiovascular health that senses multiple cues from the local environment in order to orchestrate a complex network of functionally distinct processes (i.e. haemostasis versus angiogenesis). A clear understanding of how endothelial-derived bioactive molecules and their secretion contribute to homeostasis and injury resolution is therefore vital for the identification of potential therapeutic targets and design of novel therapies for vascular diseases.

1.2 Weibel-Palade bodies – the emergency first aid kit of the vasculature

On 14 February 1962 – St Valentine's day, Ewald Weibel, a member of George Palade's lab group, was scanning a rat pulmonary artery using electron microscopy. In his historical review (Weibel, 2012), he described for the first time, the presence of strange, large bodies in the endothelial cytoplasm. When cut longitudinally, those bodies morphologically appeared long and rod-shaped, primarily residing in the cytoplasm. Studying several other arterial sections, he found many small profiles of round or elliptic shape that could indeed be cross-sections of such a rod-shaped bodies, and that were cut at different angles due to sectioning techniques. Clearly different from mitochondria and lysosomes, they possessed a single membrane, and their content of moderate electron density seemed to contain many tubules (Figure 1.3). Weibel and Palade published the first report of those bodies in 1964, however, they were unable to pinpoint their function (Weibel and Palade, 1964).

In October 1982, 20 years after the first observation by Weibel, Denisa Wagner and co-workers published work demonstrating that these bodies, now named Weibel-Palade bodies (WPBs), contained the large glycoprotein, vWF. It was known that vWF was produced in the endothelium, but its exact location in any of the endothelial compartments was unknown. Later, Wagner's group would identify that P-selectin, a leukocyte adhesion molecule, was also stored in WPBs.

Wagner termed WPBs as 'the perfect first aid kit after an insult to the vasculature' due to its ability to 'allow rapid release of this protein upon appropriate stimulus or physiologic demand' (McEver et al., 1989a).

To date, there has been impressive progress through multiple studies on WPBs, which have underpinned the core knowledge that we have about these enigmatic organelles. Furthermore, studies have now shown that WPBs can be considered acidic organelles and originally evolve from lysosomes (Karampini et al., 2020). They have critically adapted to a highly specialised physiological role allowing storage, clustering and regulated on demand release of not only vWF and P-selectin, but an armour of bioactive components described below.

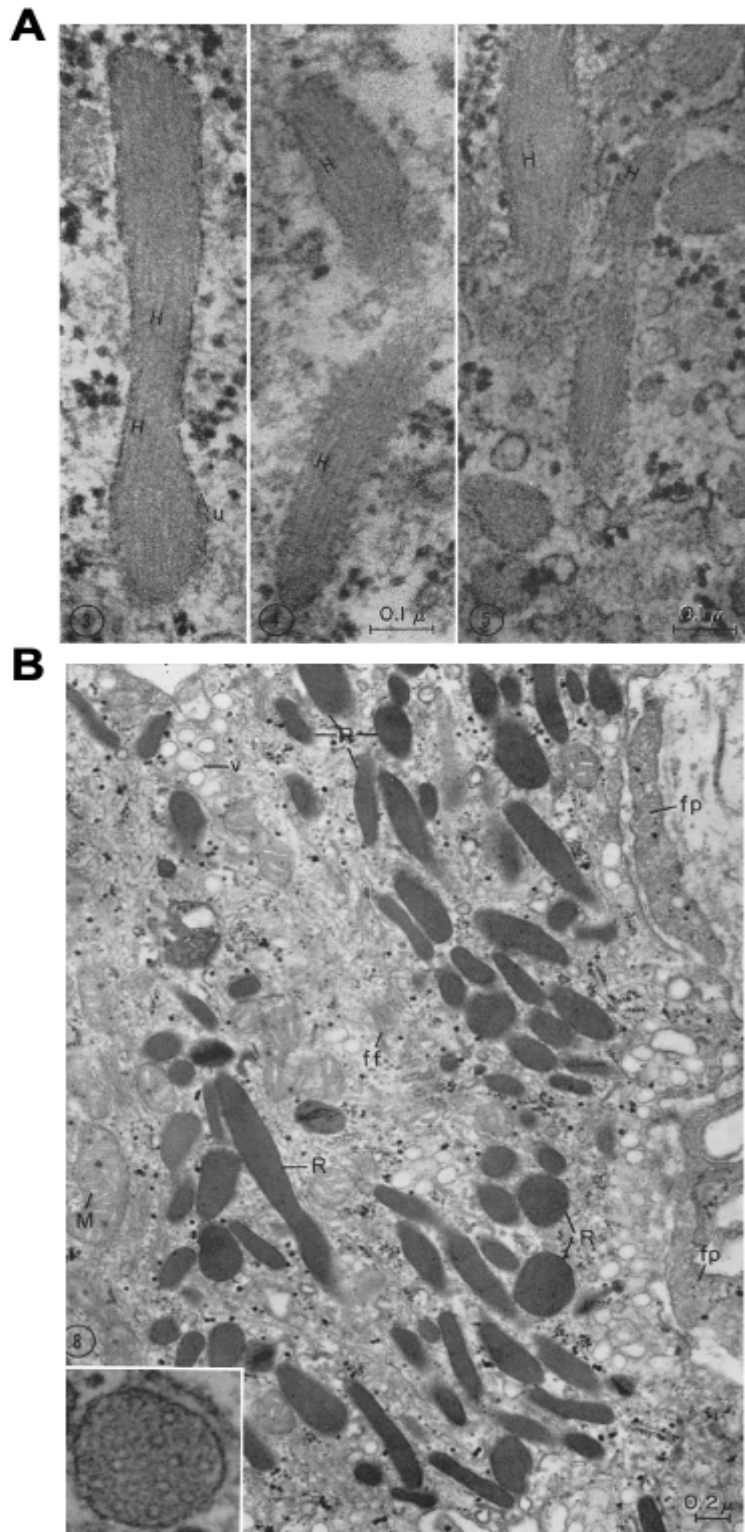


Figure 1.3 First micrograph of Weibel-Palade Bodies acquired in 1962

(A) Endothelium of a small rat pulmonary artery, showing the cluster of rod-shaped particles. The tubular structure of their content is displayed in cross-section and in oblique sections, showing parallel arrangement of internal tubules (H) tightly fitted enveloping membrane (u). (B) Rod-shaped bodies (R), mitochondria (M), plasmalemmal vesicles (v) and bundles of fine fibrils (ff) appear in the cytoplasm of an obliquely sectioned endothelial cell. Pericyte foot processes can be seen at fp. Adapted from Weibel & Palade, 1964.

1.2.1 WPB biogenesis

The main constituent of WPBs is vWF, a large haemostatic protein. Endothelial vWF is a critical requirement and a pre-requisite for WPB formation, with expression of recombinant vWF in non-endothelial cell types inducing formation of elongated WPB-like granules (Wagner et al., 1991; Voorberg et al., 1993). In addition, endothelial cells extracted from vWF-deficient transgenic animals do not possess WPBs (Denis et al., 2001; Haberichter et al., 2005). However, vWF expression in endothelial cells is not sufficient for WPB biogenesis. Porcine aortic cells lack WPBs and vWF is passively released in a constitutive manner, whereas in megakaryocytes, the only non-endothelial source of vWF, storage of vWF is within a different type of organelle called α -granules (Cramer et al., 1985; Royo et al., 2003). Nevertheless, from the substantial body of research done on the topic, it is clear that vWF is the initial trigger for WPB biogenesis in the majority of vascular beds (Michaux and Cutler, 2004; Valentijn et al., 2011).

WPB biogenesis is a complex and multi-step process, commencing with vWF synthesis (Figure 1.4). vWF is synthesised as a 350 kDa monomer, comprising a signalling sequence, propeptide and the mature vWF. The signal peptide is responsible for ensuring the newly synthesised polypeptide chain enters the ER where pro-vWF assembles into dimers in a 'tail-to-tail' fashion (Wagner, 1990). In addition to dimerisation, mature vWF undergoes glycosylation within the ER, a process required for vWF dimers to translocate to the trans-Golgi network (TGN; Wagner et al., 1986). Pro-vWF further multimerises in a 'head-to-head' manner via interchain disulfide bonds (Vischer and Wagner, 1994) and is pH-dependent, occurring at the TGN where pH is at ~ 6.2 (Wagner et al., 1986; Paroutis et al., 2004). The vWF multimers, together with the propeptide, are condensed into tubules, thus forming elongated vesicles coated with clathrin and AP-1 complexes. These are essential for the packaging vWF into tubules and WPB elongation (Lui-Roberts et al., 2005). Newly formed WPBs bud off from the TGN. Trafficking between target membranes and membrane fusion of WPBs is mediated by SNARE proteins. The SNARE complex comprises vSNARE on the vesicle membrane and t-SNARE on the acceptor membrane which together form a four-helix complex that enables the membrane fusion. The SNARE subfamily of longin-SNARE (VAMP7, YKT6 and Sec22b) regulates subset of membrane fusion events that regulate traffic from and to the TGN. Moreover, Sec22b is a determinant of WPB morphology. Loss of Sec22b also shows retention of provWF in the cells suggesting role in trafficking (Karampini et al., 2020).

Apart from vWF, WPBs can store other components, such as P-selectin and IL-8 which are recruited during initial formation of immature WPBs at the TGN, others are delivered directly to mature WPBs. For example, the P-selectin co-

factor CD63 is delivered to mature WPBs in an AP-3-dependent mechanism or fused to WPBs via intraluminal vesicles, and Rab27a, a marker of WPB maturation, is also found on elongated mature WPBs near the cell periphery (Hannah et al., 2003; Berriman et al., 2009; Valentijn et al., 2010; Valentijn et al., 2011; Streetley et al., 2019). After departure from TGN, Rab27a is recruited to WPBs and subsequently joined by MyRIP. Together, they form a complex which anchors WPBs to actin filaments at the cell periphery and prevents premature secretion of WPBs (Nightingale et al., 2009). Another method of distinguishing mature WPBs from immature WPBs is the fact that they are much more electron dense than the latter and by further decrease in pH to ~5.4 (Zenner et al., 2007; Erent et al., 2007a).

Defects in vWF tubulation or in multimerisation can result in misshaped organelles (Michaux and Cutler, 2004). Additionally, dysregulated cellular machinery including aftiphilin or Rab27a can also cause defective vWF multimerisation and disrupted trafficking of immature WPBs (Nightingale et al., 2018a). WPB biogenesis and maturation processes are highly linked to their function. Studies have shown that artificially reducing WPB size at biogenesis ablates endothelial haemostatic function by drastically diminishing platelet recruitment. This is most likely due to reduction of vWF multimerization (Ferraro et al., 2014). Furthermore, WPBs are classed under the umbrella of lysosome-related organelles (LROs). LRO biogenesis is regulated by HPS (Hermansky-Pudlak syndrome) protein associated complexes (HPACs), such as the BLOC - 1, -2, -3, AP-3 and HOPS complexes. Interestingly, mutating HPS genes in murine models or congenital mutations in humans lead to bleeding symptoms (Wei and Li, 2013). BLOC-2 is another player in the WPB biogenesis cellular machinery that has been found to affect the tubulation and secretion of vWF factor (Ma et al., 2016).

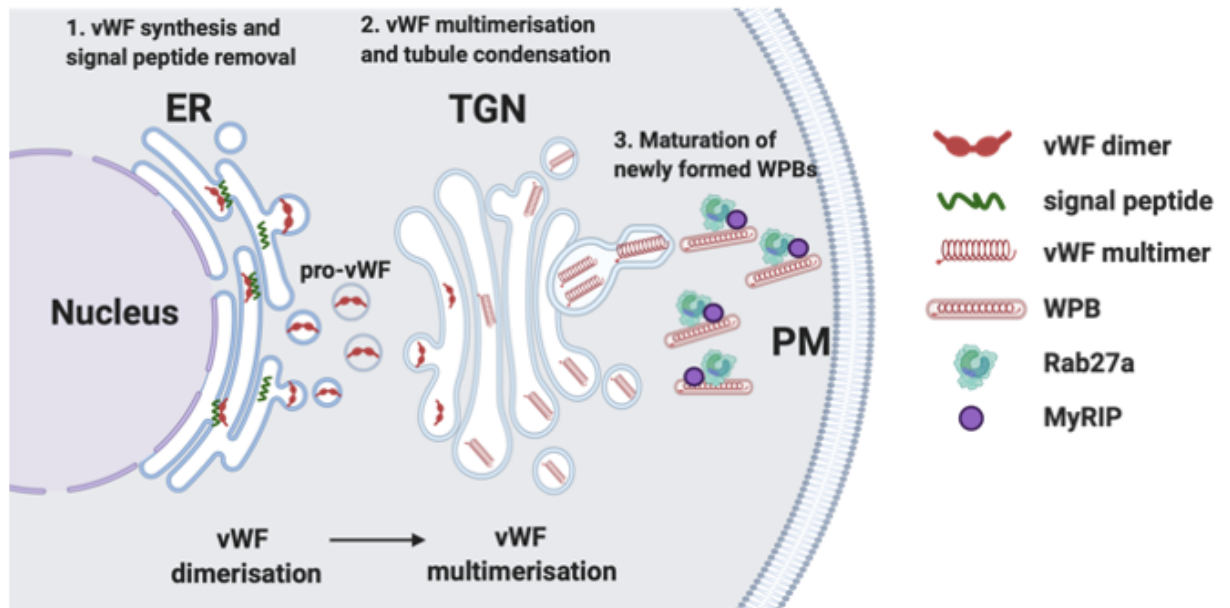


Figure 1.4 Biogenesis of Weibel-Palade bodies.

vWF expression, the driving force of WPB biogenesis, is synthesised in the endoplasmic reticulum (ER) as pre-pro-vWF (pro-vWF and its signal peptide). Upon exiting the ER, the signal peptide is cleaved and pro-vWF-containing vesicles traffic to the trans-Golgi network (TGN) for further processing (e.g. multimerization and tubule condensation) and post-translational modification. After vWF is fully processed and multimerised, it condenses into newly formed Weibel-Palade bodies (WPBs). The newly synthesised WPBs can remain at the TGN for further recruitment of other WPB cargo, such as P-selectin. Additionally, within immature WPBs, vWF continues multimerising and the immature WPBs recruit effectors Rab27a and MyRIP. These enable anchoring to the actin cytoskeleton at the plasma membrane to promote maturation.

1.2.2 WPB cargo and function

Studies have shown that ECs do not have a homogenous phenotype. Rather, they display heterogeneous characteristics between different vascular beds (Chi et al., 2003; Hirakawa et al., 2003; Hendrickx et al., 2005). It is no surprise then, that in addition to vWF, WPBs actively recruit a number of bioactive constituents at the TGN, referred to as 'WPB cargo' hereinafter. The growing list of WPB cargo (Table 1.1.1) that can reside within WPBs suggests a functional role of WPBs in several physiological processes, including haemostasis, inflammation, angiogenesis and vascular tone (Rondaij, Bierings, Kragt, Van Mourik, et al., 2006). Differential recruitment of such functionally diverse cargo to WPBs and vascular bed leads to the formation of heterogeneous WPB populations. In fact, more than one WPB population may be present within a single cell, each having different cargo and separate physiological function (Øynebråten et al., 2004; Cleator et al., 2006).

Storage of WPB cargo is not solely determined at transcriptional level or by active recruitment at the TGN during maturation. Both WPB-derived and non-WPB derived cytokines such as IL-8, IL-6, GRO- σ , MCP-1, and eotaxin-3 and tPA can be localised to WPBs. This is believed to be due to missorting of proteins at the TGN or passive absorption at the cellular surface (Knipe et al., 2010). Moreover, WPB population diversity can also be shaped by the local environment of ECs. Inflammatory mediators, such as IL-1 β , trigger synthesis and storage of the cytokine IL-8 in WPB, equipping WPBs and ECs with a rapidly releasable pool of IL-8, which is not detectable in quiescent vascular conditions (Utgaard et al., 1998).

Recent proteomic studies have identified a larger list of potential and novel proteins that may be stored in WPBs, with the majority of them to be confirmed in the future (not included herein; (Van Breevoort et al., 2012; Holthenrich et al., 2019).

Table 1.1.1 Known Weibel-Palade bodies cargo and their function

WPB Cargo	Cargo function
Von Willebrand Factor	Haemostasis
Angiopoeitin-2	Angiogenesis
P-selectin	Leukocyte adhesion
CD63	Membrane trafficking / P-selectin stabilisation
Endothelin-1	Vasoconstriction
IL-8	Inflammation
Eotaxin-3	Inflammation
Osteoprotegerin	Vascular homeostasis
Insulin-like growth factor-binding protein 7	Angiogenesis
α 1,3-fucosyltransferase VI	Inflammation
Calcitonin gene-related peptide	Vasodilation

1.2.2.1 Von Willebrand factor

Referred to as the 'Jedi Knight of the bloodstream' (Springer, 2014), vWF is a large glycoprotein that constitutes the main cargo of WPBs. Its multimerisation induces WPB biogenesis, as outlined above in Section 1.2.1. Different types of vWF multimers can be released from ECs, such as low-molecular-weight (LMW), high-molecular-weight (HMW) and ultra-large-molecular-weight (ULMW) vWF multimers (Sporn et al., 1986; Tsai et al., 1991).

Studies have shown that multimer size governs the haemostatic potential of vWF. Prevalence of smaller size multimers (i.e. LMW) is linked to vWF functional loss, while very large multimers (i.e. ULMW) are highly thrombotic, characterised by more effective binding to FVIII and platelets adhesion (Stockschlaeder et al., 2014). Upon vascular injury, ULMW multimer strings of vWF undergo exocytosis from WPBs onto the endothelial surface. Here, primary haemostatic plug formation is initiated by vWF by modulating platelet adhesion through binding to the platelet GPIb-IX-V complex, and potentiation of further platelet aggregation (Savage et al., 2001; Ruggeri, 2007; Li et al., 2010). Platelet-bearing strings are highly thrombotic, but can be cleaved into smaller vWF multimers by the metalloprotease ADAMTS-13, as a 'switch-off' mechanism (Levy et al., 2001). In addition to platelet adhesion, vWF can also bind to several types of collagen (Romijn et al., 2001), heparin (Rastegar-Lari et al., 2000) and the pro-coagulation protein, factor VIII. vWF has an important protective role, both under homeostatic conditions, and in patients with haemophilia by stabilising factor VIII in the circulation and preventing its degradation by activated protein C (Sadler, 1998; Franchini and Lippi, 2007b). During coagulation, thrombin activates FVIII by cleaving it and releasing FVIIIa, preventing further vWF binding by disrupting the vWF binding site thereafter. Overall, it can be concluded that primary haemostasis depends on the balance between biogenesis of vWF, its exocytosis from WPBs and subsequent degradation by the ADAMTS-13 metalloprotease (Peyvandi et al., 2011). Importance of vWF as a haemostatic agent is further emphasised by studies in transgenic mouse models deficient in vWF. Although, vWF-deficient mice exhibit normal embryonic development, spontaneous bleeding events can be observed, mimicking von Willebrand factor disease (Denis et al., 1998). In more recent in vivo study with mice deficient in vWF, a vWF role in angiogenesis was described (Starke et al., 2011).

1.2.2.2 P-selectin

P-Selectin (CD62P), also known as PADGEM or GMP-140, is a 140kDa single chain glycoprotein mainly expressed in ECs and platelets. P-selectin is part of the selectins protein family, a family of multi-functional adhesion receptors (P-, E-

and L-selectin) that enable interactions between leukocytes and the endothelium. Similar to vWF, P-selectin is also stored in platelet α -granules, whereas in ECs it is one of the first proteins found to co-reside with vWF in WPBs (McEver et al., 1989b; Merten and Thiagarajan, 2000). E-selectin (CD62E) is also expressed by the endothelium. However, unlike P-selectin, E-selectin is not stored in WPBs and its expression is transcriptionally regulated by signalling demand (Bevilacqua et al., 1987). P-selectin protein structure consists of a large luminal domain and short cytoplasmic tail, both participating in P-selectin targeting and incorporation into WPBs early on at the TGN (Harrison-Lavoie et al., 2006). Although vWF is stored in two types of organelles, WPBs and α -granules, vWF deficiency only disrupts P-selectin recruitment to WPBs, but has no effect on platelet storage of P-selectin in α -granules. In contrast, P-selectin-deficient mice have normal vWF biosynthesis and WPB biogenesis (Denis et al., 2001).

As noted above, the main function of P-selectin is mediating inflammation through early recruitment and adhesion of leukocytes to activated ECs. Upon activation, P-selectin is rapidly mobilised and exocytosed from WPBs and expressed on the endothelial plasma membrane, where it interacts with circulating or patrolling leukocytes (Patel et al., 2002). This is facilitated through binding of P-selectin to its ligand, P-selectin glycoprotein ligand 1 (PSGL-1; expressed on various leukocytes (Laszik et al., 1996)), which allows leukocyte entry, also known as extravasation, at the site of vascular injury. In fact, leukocytes extracted from P-selectin-deficient mice display severely impaired rolling and poor extravasation (Mayadas et al., 1993). Although robust, surface expression of P-selectin is only transient. P-selectin is rapidly internalised and degraded or repackaged into WPBs at the TGN (Straley and Green, 2000; Arribas and Cutler, 2000).

1.2.2.3 Angiopoietin-2

Angiopoietins-1 to -4 represent an important family of growth factors involved in regulation of angiogenesis, which signal through the endothelial tyrosine kinase receptors, Tie-1 and Tie-2. The best characterised of the family, and endogenous ligands of Tie-2, are Angiopoietin-1 and Angiopoietin-2 (Jones et al., 2001). Angiopoietin-1 regulates Tie-2-dependent processes such as cell survival, endothelial quiescence and maturation of newly developed vasculature (Papapetropoulos et al., 2000). Angiopoietin-2 has opposing effects, mainly through antagonism of the Tie-2 receptor. It signals in an autocrine manner, induced by a range of stimulants, including VEGF, thrombin and cancer, thereby destabilising the blood vessels and potentially promoting angiogenesis (Yancopoulos et al., 2000). Angiopoietin-2 is currently among one of the most sought after target molecules for the discovery of anti-angiogenic drugs (Huang

et al., 2010). In addition to cancer and tumorigenesis, Angiopoietin-2 was found to be involved in other inflammatory conditions, such as rheumatoid arthritis and psoriasis, suggesting that Angiopoietin-2 is an important crosslinker between angiogenesis and inflammation (Westra et al., 2011; Scholz et al., 2015). Molecular expression profiling has revealed ECs as the primary source of Angiopoietin-2, with pronounced endothelial production of Angiopoietin-2 occurring upon EC activation (Zhang et al., 2003). Indeed, Angiopoietin-2 localises to WPBs in ECs, probably due to incorporation into WPBs at the TGN. Although previously debated, Angiopoietin-2 resides only in WPB subpopulations that lack P-selectin, deeming the storage of the two proteins mutually exclusive (Fiedler et al., 2004a; van Agtmaal et al., 2012).

1.2.2.4 Other cargo

Another WPB cargo of major importance is the tetraspanin CD63 (Lamp3), which is a well-known component of the late endosomal and lysosomal systems (Fukuda, 1991; Vischer and Wagner, 1993; Escola et al., 1998). In addition to WPBs, CD63 is targeted to the endo-lysosomal membranes and in other cells types can be found in secretory lysosomes, a type of immune secretory granule (Griffiths, 1996). Unlike P-selectin and Angiopoietin-2, CD63 is not recruited to WPBs at the TGN, but is selectively delivered to mature WPBs by a mechanism that is dependent on AP3 and annexin A8, endo-lysosomal targeting adaptors and by means of intraluminal vesicles internalisation (Kobayashi et al., 2000; Harrison-Lavoie et al., 2006; Poeter et al., 2014; Streetley et al., 2019). Sorting of the endosomal protein CD63, to mature post-TGN WPBs is another characteristic of WPBs that suggests that WPBs share some similarities with lysosome-related organelles (Cutler, 2002). Outside of the endo-lysosomal system, the functional role of CD63 in the vasculature and the immune system has previously been considered redundant (Schröder et al., 2009). However, later studies have shown that CD63 acts as an essential co-factor in leukocyte adhesion by P-selectin. ECs lacking CD63 display impaired leukocyte recruitment during inflammatory responses, similar to P-selectin deficiency (Mayadas et al., 1993; Doyle et al., 2011; Poeter et al., 2014).

Endothelin (ET-1) is a 21 amino acid long peptide, originating from a prepropeptide that is converted to mature ET-1 by an endothelin-converting enzyme (ECE) (Kowalczyk et al., 2015). ET-1 is mostly known for its powerful vasoconstricting properties and its effect on blood pressure (Stauffer et al., 2008). In ECs, both ET-1 and ECE have been shown to locate at WPBs, suggesting that upon demand, WPBs may be the place of ET-1 conversion to its active form (Ozaka et al., 1997; Russell et al., 1998a; Russell et al., 1998b). Although not

shown in the literature, it is predicted that ET-1 and ECE are recruited to WPBs at the TGN (Valentijn et al., 2011). The ability to store and rapidly release ET-1 further places WPBs as primary responders to vascular injury.

Considering the fact that WPBs contain cargo involved in regulation of inflammatory processes, storage of cytokines would be unsurprising. In ECs, transient P-selectin expression mediates the initial interaction with leukocytes, as described above (Section 1.2.2.2). However, stable adhesion of leukocytes to the endothelium occurs through integrin binding (Von Andrian et al., 1991; Von Andrian et al., 1992). Such integrin recruitment and adhesion potentiation can be accomplished by cytokines, such as the chemotactic cytokine (chemokine) IL-8 (Detmers et al., 1990). Studies in ECs have shown that IL-8 localises intracellularly to WPBs, from which it can be rapidly secreted during vascular injury in order to aid leukocyte recruitment (Utgaard et al., 1998). Interestingly, IL-8 is synthesised and stored in WPBs solely after exposing ECs to inflammatory mediators, such as IL-1, independent of *de novo* synthesis. These studies suggest that storing IL-8 in WPBs may represent endothelial “memory” as an adaptation mechanism in response to inflammation (Wolff et al., 1998; Hol et al., 2009).

Overall, WPBs are indeed ‘the perfect first aid kit’ after a vascular injury, mounting powerful haemostatic and inflammatory responses (Figure 1.5) due to the fact that they are differentially equipped with cargo proteins that exert a range of endothelial functions. This also contributes to the emerging concept of WPB plasticity, meaning that WPBs orchestrate specialised exocytotic responses, governed by local stimuli context, recent history and EC location in the vascular tree.

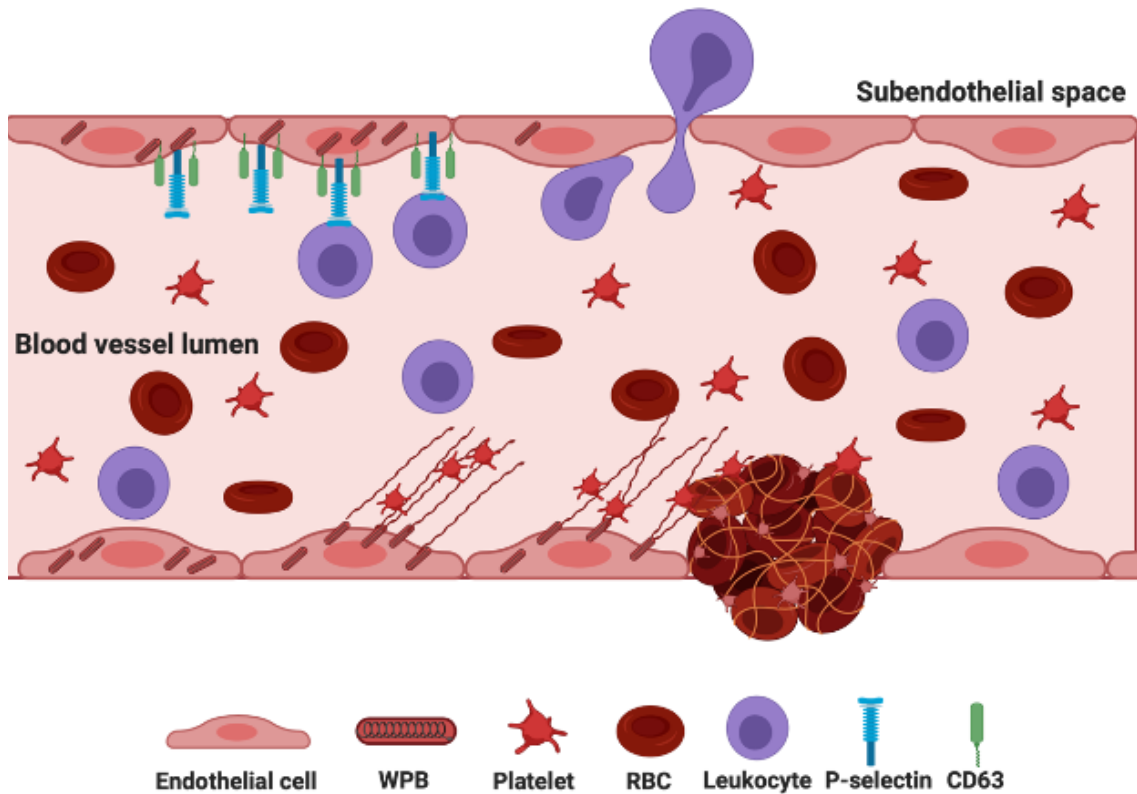


Figure 1.5 Weibel-Palade bodies in action during vascular injury

Upon vascular injury, endothelial cells are activated and release Weibel-Palade bodies (WPBs), pre-stored endothelial-specific organelles. Large Von Willebrand Factor (vWF) multimers, main cargo of WPBs, are released on the endothelial cell surface in the form of long haemostatic strings that 'trap' platelets and initiate the primary haemostatic plug, preventing further bleeding and exacerbation of the injury. In addition, P-selectin, a leukocyte adhesion molecule, and the tetraspanin CD63 are also released simultaneously from WPBs on the endothelial surface. P-selectin mediates leukocyte adhesion by binding to its ligand P-selectin glycoprotein ligand 1 (PSGL-1) on leukocytes, initiating the rolling step which is crucial for leukocyte extravasation to the site of vascular injury. P-selectin is likely to help in the formation of the platelet plug. CD63 is released together with P-selectin and promotes P-selectin stable expression on the endothelial surface. After the initial 'first-aid' WPBs can release other cargo that is likely to further promote vascular injury resolution (e.g. angiogenesis via Angiopoietin-2) and ultimately restore vascular homeostasis.

1.2.3 WPBs in clinic - When things go wrong

The historical origin of vWF dates back to 1924, when the Finnish physician Erik von Willebrand first reported patients with a serious hereditary bleeding affecting consanguineous families (Willebrand, 1999). The initial patient was a five year old girl with multiple instances of severe bleeding since birth, with another young sibling exhibiting similar symptoms. von Willebrand had thought that a platelet disorder or a defect of the vasculature were potential causes of the bleeding. Dr

von Willebrand noted several distinct characteristics of this peculiar disorder that contrasted it from what medical science knew about haemophilia at the time. First, both genders were affected. Second, there was prolonged bleeding time. Third, unlike haemophilia, where there is characteristic subcutaneous or joint bleeding, the phenotype of the new bleeding disorder was characterised mostly by mucocutaneous bleeding. Dr von Willebrand called this disease “hereditary pseudohaemophilia”. Since the original observations, the disease has been extensively studied and it was shown in the mid 1950s that the symptoms of impaired haemostasis result from disruption in the von Willebrand factor, therefore it was renamed to von Willebrand Disease (VWD; Swami and Kaur, 2017).

Today, the disease prevalence is ~1% and it is the most common inherited disorder. VWD can be split in two main forms: inherited and acquired (Sadler et al., 2006). The acquired form occurs predominantly in patients over 40 years with no prior history of bleeding disorders. It has a diverse pathology, but in the majority of patients the disease is characterised by increased vWF-targeting antibodies or elevated tumour cell adhesion, usually in patients with lymphoproliferative disease including multiple myeloma, cardiac defects and myeloproliferative disorders (Franchini and Lippi, 2007a). Hereditary forms include three major types and a platelet type. The three major types are type 1, type 2, and type 3. Type 1 comprises 60%–80% of cases. It is characterised by the fact that the clotting impairment may not be seen clearly in early stages. Bleeding tendency is mainly because of decreased levels of vWF (James et al., 2007). Furthermore, type 2 comprises 20–30% of all cases. Although there is little to no change in plasma vWF levels, type 2 is characterised by a structural and functional defects in vWF protein, which impair its functional abilities (Favaloro, 2001). Finally, type 3 accounts for > 5% of all VWD cases. It is caused by a recessive mutation, which leads to an undetectable vWF level and it is one of the most severe forms of VWD in which patients experience severe mucosal bleeding due to complete lack of detectable vWF (Eikenboom et al., 1992).

Due to its role in primary haemostasis, there has been a substantial research effort into investigating if vWF is linked to cardiovascular disease. Studies in VWD have shown that patients deficient in vWF are protected from developing acute coronary syndromes (ACS), such as myocardial infarction (MI; Sanders et al., 2013; Seaman et al., 2016). Moreover, epidemiological analysis of ACS prevalence or other cardiovascular disturbances in VWD patients is 11% lower than patients with normal vWF genetic material. Even upon consideration of age, gender, hypertension, hyperlipidaemia, diabetes mellitus, obesity, and smoking, the occurrence of ACS is 15% lower in VWD patients than in non-VWD patients.

By contrast, epidemiological studies have established a strong correlation between elevated plasma vWF (gain of function vWF mutation) and ACS occurrence (Schneppenheim et al., 2019). A causal role is suggested for vWF in both coronary thrombus formation and the associated microcirculatory dysfunction in patients with ACS. Hence, drug therapies that target vWF may represent a valuable adjunct to treatment strategies in ACS, with several anti-vWF therapies currently undergoing clinical trials (Jilma-Stohlawetz et al., 2011; Markus et al., 2011; Scully et al., 2019). In addition, increased plasma levels of not only vWF but other WPB constituents, such as P-selectin and **Angiopoietin-2**, can be utilised as clinical biomarkers of atherosclerosis and risk of future ACS, all serving as a prognostic index of future adverse cardiovascular event risk in the general population (Patel et al., 2008; Tscharré et al., 2019; Fan et al., 2020). In addition to mediating primary haemostasis, inflammation and angiogenesis, a function for vWF cancer metastasis has been described. Various patient cohorts have shown increased plasma levels of vWF. Increased levels of the proteins are localised to and within the tumor microenvironment. This correlates with advanced disease stage and poorer clinical outcome. vWF role in promoting pro-inflammatory signalling, mediation of angiogenesis and vascular permeability, is proposed to enhance tumor cell growth and invasion across the blood vessels (Patmore et al., 2020). Conversely, chronic myeloid leukemia patients have been reported to suffer from pseudo or acquired vWD (Mohri et al., 1996; Knöfler et al., 2020).

These findings place vWF, together with WPBs and other WPB constituents, on the map as key players in cardiovascular disease modulation. Moreover, the research outlined above emphasises the importance of further investigation into the complex mechanisms of WPB trafficking and exocytosis, and the pathophysiological consequences of pathway dysregulation, that may ultimately lead to the discovery of novel, more specific cardiovascular therapeutic targets

1.2.4 Mechanisms underlying WPB exocytosis

1.2.4.1 Basal and constitutive WPB exocytosis

As a specialised type of epithelial cells, ECs have two polarised membranes: the apical and basolateral, which face the vessel lumen and the subendothelial extracellular space, respectively. Interestingly, vWF can be secreted both apically and basolaterally, resulting in luminal and subendothelial vWF pools, which have different roles in haemostasis (Reininger, 2008). There are 3 known vWF exocytotic pathways: constitutive, basal and regulated. All the secretory pathways begin at the TGN, where vWF either multimerises and forms WPBs, or

is secreted directly through the constitutive pathway by anterograde carrier proteins (Sporn et al., 1986). WPBs store vWF for regulated secretion upon endothelial activation, but they can also fuse and release in the absence of any stimulation, which is termed as basal release of vWF and is independent of the constitutive pathway (Giblin et al., 2008). Another difference between the three exocytotic pathways is the types of multimers released. Constitutively released vWF is composed of mainly low thrombogenic LMW-vWF, whereas basal and regulated vWF exocytosis is composed of highly thrombotic HMW- and ULMW-vWF (Da Silva and Cutler, 2016). The existence of these three separate exocytotic pathways is evidence that the endothelium tightly regulates the pro-thrombotic activity of vWF.

1.2.4.2 WPB exocytosis on demand

The endothelium receives multiple stimuli from surrounding cell types, from molecules and cells in the blood stream and from shear force (Aird, 2005; Chistiakov et al., 2017). Such signals may be pro-inflammatory, pro-angiogenic, pro-thrombotic and fibrinolytic. Perturbation of ECs and subsequent exocytosis of WPBs may initiate haemostasis through vWF release, induce vasoconstriction to prevent unnecessary loss of blood components (ET-1 and its converting enzyme, ECE), regulate inflammatory responses (P-selectin, CD63, IL-8), and aid angiogenic processes (Angiopoietin-2; Rondaij et al., 2006). The remarkable diversity of bioactive cargo present within WPB populations is surprising and, at first sight, might even seem hazardous in terms of vascular health and homeostasis. It has been documented that even low intensity exercise of cardiovascular nature results in a rise in vWF levels in the bloodstream, with such release likely originating from WPBs (Van Mourik et al., 1999). In this scenario, excessive release of, for instance, inflammatory mediators would be undesirable and physiologically irrelevant. Similar examples of the need for agonist appropriate responses would include discrete physiological events such as immunogenic responses (e.g. histamine), or pro-thrombotic responses (e.g. thrombin), where ECs need to release WPB cargo relevant to the local blood vessel environment. This suggests that either formation and trafficking of subpopulations of WPBs with distinct cargo is tightly controlled, or that ECs regulate secretion of WPB constituents at the plasma membrane (Rondaij et al., 2006; Schillemans et al., 2019a).

1.2.4.3 WPB release at the plasma membrane

As mentioned previously, WPBs can undergo a rapid, regulated exocytosis. Multiple stimuli can trigger release of WPB cargo into the bloodstream (e.g. Angiopoietin-2), or exposure at the plasma membrane (e.g. P-selectin). In addition to diverse signalling pathways, different modes of exocytosis may enable the release of subsets of WPB constituents in response to the vast range of physiological stimuli. For example, WPBs can undergo transient fusion with the plasma membrane, forming an exocytotic pore which acts as a filter that selectively releases WPB contents based on their molecular size (Babich et al., 2008). During this “lingering kiss”, small pro-inflammatory WPB constituents such as IL-8 and eotaxin-3 are released, whereas large sized constituents (i.e. vWF and/or P-selectin) remain in the fusion pore. Another mode of WPB exocytosis at the plasma membrane is multigranular exocytosis, a process where several WPBs aggregate in a “secretory pod”, before fusing with the plasma membrane in a large pore. It has been proposed that multigranular exocytosis may facilitate the formation of large pro-thrombotic vWF strings at the EC surface by pooling the content of multiple WPBs within the secretory pod (Valentijn et al., 2010). Furthermore, actin involvement in WPB exocytosis has an opposing effect, with actin anchoring of immature WPBs preventing early exocytosis. However, studies suggest that in a more ‘conventional’ exocytosis of single WPB at the plasma membrane, formation of an ‘actin ring’ helps propel WPB contents from a fusion pore, and recruitment of such ring structure is stimulus-dependent (Nightingale et al., 2011; Nightingale et al., 2018b). Evidence on different modes of regulated WPB exocytosis at the plasma membrane provides another layer of complexity on the mechanisms for selective release of WPB cargo.

Overall, to date literature suggests that release of cargo from WPBs is tightly controlled by both integration of distinct signalling pathways activated by multiple endothelial agonists, and by diverse WPB exocytotic machinery at the plasma membrane. The presence of more than one WPB population may be present in a single cell, with each subpopulation carrying functionally different cargo. Taken together with the fact that multiple endothelial agonists can trigger WPB exocytosis, this poses many unanswered research questions. A key to unravelling the complex exocytosis of WPB subpopulations is understanding how specific endothelial stimuli are coupled to WPB trafficking. Ca^{2+} signalling pathways in the ECs have been shown to be responsible for differential trafficking and exocytosis of WPB (Zupančič et al., 2002; Lenzi, Stevens, Osborn, Matthew J. Hannah, et al., 2019). However, the exact mechanisms coupling Ca^{2+} to differential trafficking of WPBs subpopulations are not known and are to be further

addressed. The current literature on signalling pathways involved in WPB trafficking and exocytosis are described below.

1.2.5 Exocytotic machinery and signalling pathways of regulated WPB release

1.2.5.1 Mechanism of WPB exocytosis

Shortly after completion of the biogenesis step at the TGN, immature WPB are not sorted for exocytosis straight-away until they acquire the correct part of their exocytosis machinery. WPBs recruit several Rab GTPases on their way to maturation, such as Rab27a, Rab3D isoforms and Rab15 (Zografou et al., 2012). Rab GTPases are masters of cellular cargo trafficking acting as a molecular ON and OFF switch by hydrolysing GTP (described in detail below in 1.4). Most importantly, aforementioned Rabs are able to recruit specific effector proteins (MyRIP, Munc13-4 and Slp4-a) to the WPB surface (Bierings et al., 2012; Chehab et al., 2017). Acquisition of such effector proteins serves as a marker of acquiring exocytosis competence and maturation of WPB. Binding of Rab27a to MyRIP allow effective binding of the complex to actin which enables interaction with the motor protein myosin Va, tethering immature WPBs at the cell periphery awaiting exocytosis signal (Pulido et al., 2011). Actin filaments play opposing roles in WPB exocytosis; it allows for peripheral distribution WPBs at the cell periphery, which itself is dependent on another motor protein, myosin IIa. Additionally, actin filaments act a physical barrier for tethering and arrest of Rab27a-MyRIP-positive WPBs by interaction with MyRIP acting as an exocytosis stop (Conte et al., 2016). Munc13-4, another WPB exocytotic machinery effector, has the ability to bind to both Rab27a and Rab15. Munc13-4 'marks' release A2-S100A10-containing sites at the plasma membrane periphery, tethering ready to release WPBs. Slp4-a is both Rab3 and Rab27a effector which provides the important link between mature WPBs and SNARE complex (Chehab et al., 2017). Overall maturation is a long process of acquiring several Rab GTPases and their effectors which engage in a 'tug of war' battle the outcome of which is determined by signalling pathways. The final step of exocytosis is interaction with the SNARE complex which allows fusion with the plasma membrane. SNARE complex is a ternary complex that are positioned on two opposing membranes. In terms of WPBs exocytosis, there are two main types of SNARE proteins – t-SNAREs and v-SNAREs. V-SNARE consists of vesicle-associated membrane protein (VAMP) family which is located on the donor membrane, which in this case is the WPB outer surface. To achieve exocytosis, there are several t-SNAREs located on the

plasma membrane side – one SNARE composed of a type of syntaxin protein and another two SNARE from SNAP25 isoforms (Schillemans et al., 2019a). Altogether, SNAREs form a 4 helix complex which brings donor (WPB) and acceptor membrane (plasma membrane) together to enable fusion and exocytosis. Two types of VAMP proteins can be located on WPBs, VAMP3 and VAMP8, however VAMP3 is the only v-SNARE found to be responding to WPB exocytosis on demand (i.e. in response to signalling pathways). T-SNAREs found in participating in WPBs exocytosis are SNAP23, syntaxin-3, syntaxin-4 and syntaxin-2 (Schillemans et al., 2018). Due to spontaneous variations and heterogeneity of ECs, combinations of SNARE interactions exist including, but not limited to, syntaxin-3 interaction with VAMP8 and SNAP23 or syntaxin-4-interaction with VAMP3 and SNAP23. Finally, the formation of SNARE complex itself is regulated by syntaxin-binding proteins (STXBPs). Several STXBPs have been identified to be specific to WPB exocytosis. In particular, STXBP1 interacts with Slp4-a and syntaxin-2 and -3, thereby promoting vWF secretion (Schillemans et al., 2019b). Interestingly, a polymorphism N436S substitution in STXBP5 has been linked to lower circulating vWF. In healthy ECs, STXBP5 normal function has been identified as a negative regulator of WPB exocytosis that interacts with syntaxin-4 but not with SNAP23, suggesting that STXBP5 arrests the SNARE complex formation and prevents WPB exocytosis (Smith et al., 2010). Unlike other cell types, the SNARE complex variation and combinations of such are highly dynamic in the endothelium due to its ability to either promote or disable WPB exocytosis. This suggests the possibility that endothelium employs many different regulation strategies of WPBs exocytosis which when dysregulated can lead to serious pathophysiology (discussed in 1.2.3).

1.2.5.2 cAMP

A wide range of physiological stimuli/agonists (stress hormones, e.g. epinephrine; proteases, pro-thrombotic factors e.g. thrombin; biogenic amines, e.g. histamine and 5-hydroxytryptamine; and mechanical force e.g. shear stress) and pathological (bacterial toxins e.g. Shiga toxin) signals can trigger WPB exocytosis. In order to achieve specific and appropriate exocytosis of WPB cargo in response to incoming stimuli, the ECs need a rapid and versatile signalling system, hence a large number of endothelial ligand-gated receptors are coupled to intracellular second messenger signalling. These can be split in two major groups depending upon which second messenger their respective receptor is coupled to: cAMP or Ca²⁺.

cAMP-mediated stimuli, such as epinephrine and vasopressin, act systemically to increase endothelial barrier function and induce a smaller, sustained release

of WPBs (Figure 1.6). This pathway is exploited clinically to correct prolonged bleeding times in patients with mild haemophilia A or VWD through administration of the vasopressin analogue, desmopressin. It triggers vWF release through the activation of vasopressin-2 receptor (V2R), thereby restoring the patients' blood ability to clot with mild but physiologically relevant levels of vWF in the plasma. Activation of the V2R and adrenergic receptors (e.g. epinephrine) activates cAMP-dependent protein kinase A (PKA). PKA is critically involved in vWF secretion by activating a number of downstream effector pathways, such as the Ral GDS–Ral A pathway and the Annexin A2–S100A10 tethering complex, or via zyxin phosphorylation during contractile ring assembly. During cAMP-mediated stimulation, a subset of WPBs cluster around the perinuclear area, also known as the microtubule organising centre (MTOC), as a result of dynein-dependent retrograde transport. Whether this subset of WPBs avoids exocytosis, or represents a specific granule subset that are selectively set aside (e.g. by maturation), remains unclear and is an active area of research (Rondaij et al., 2006). Additionally, epinephrine stimulation of ECs leads to cAMP-mediated WPBs release but through Rap1 activation in a PKA-independent fashion. This process is mediated by the guanine nucleotide exchange factor Epac1 which activates Rap1 GTPase. Activated Epac1-Rap1 promotes downstream the activation of the Rho GTPase, Rac1. The Rap1–Rac1 interaction results in rearrangement of the actin cytoskeleton into actin rings, in proximity to the plasma membrane, allowing fusion with WPBs. Rap1 can be activated in an Epac-independent manner following stimulation of endothelium with thrombin, suggesting that common signalling pathways can converge in response to different stimuli (Van Hooren et al., 2012a).

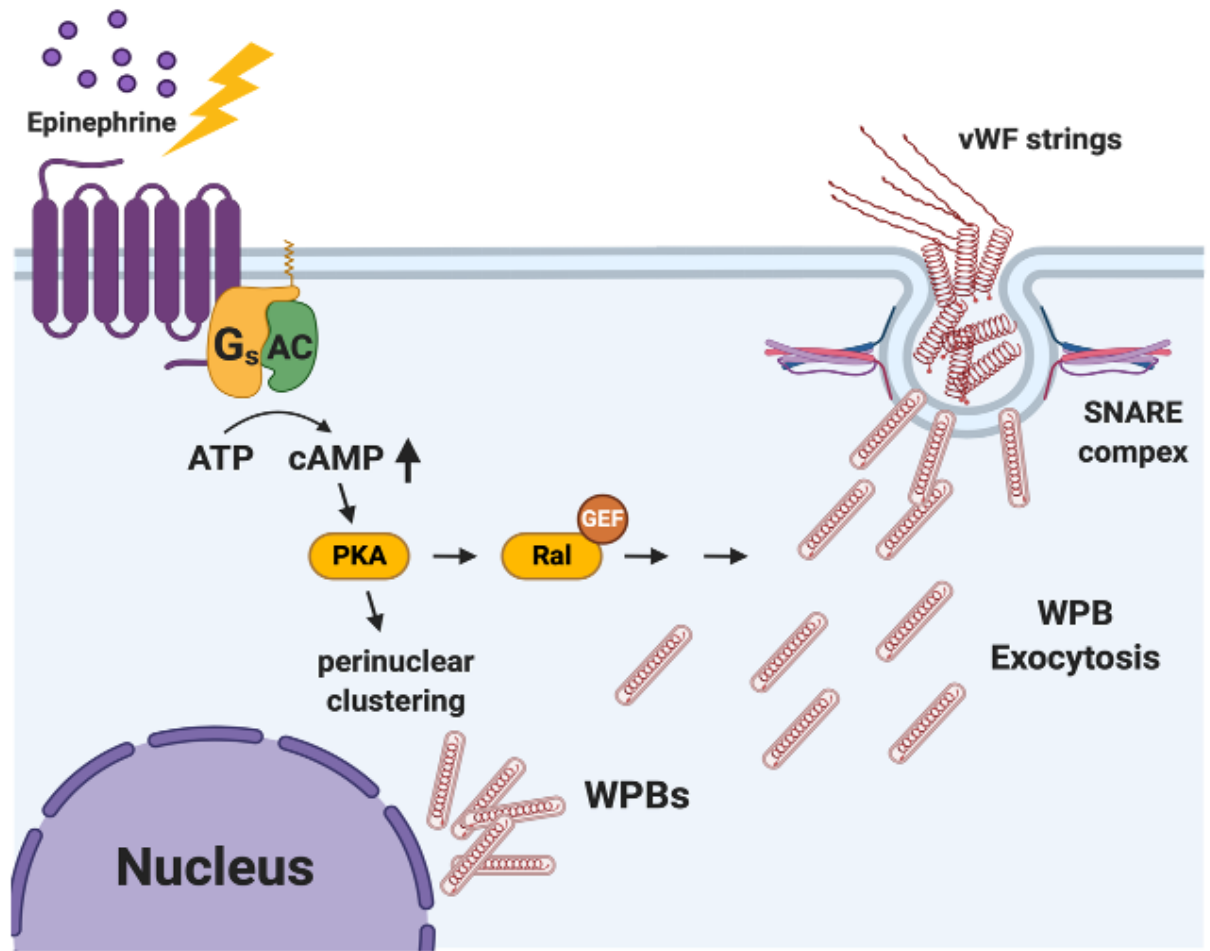


Figure 1.6 Current working model of cAMP-dependent Weibel-Palade body exocytosis pathway.

cAMP-raising agonists, such as epinephrine, act on G-protein coupled receptors (GPCRs) coupled to the G_s protein, thereby activating adenylate cyclase (AC), which produces cAMP from ATP. cAMP binds and activates protein kinase A (PKA). PKA activity leads to both perinuclear clustering and exocytosis of WPBs at the cell surface via a PKA-dependent mechanism. Epinephrine induces activation of the small GTPase, Ral, and recruitment of its guanine nucleotide exchange factors (GEFs), which promotes exocytosis of WPBs by inducing assembly of the exocytosis complex, soluble N-ethylmaleimide-sensitive factor activating protein receptor (SNARE).

1.2.5.3 Endothelial Ca²⁺ signalling and WPBs

Canonically, ligand-bound G-protein coupled receptors (GPCRs) trigger the release of intracellular Ca²⁺ from the endoplasmic reticulum into the cytoplasm via activation of phospholipase C (PLC) and inositol 1,4,5-trisphosphate (IP₃; for further details please see section 1.3.2.1). In fact, WPBs exocytosis in response to ionophores or caged Ca²⁺ is dose-dependent, suggesting that sustained elevation of cytoplasmic Ca²⁺ is a sufficient transduction signal to drive WPB fusion with the plasma membrane, independently from specific ligand-triggered

receptor signalling (Zupančič et al., 2002). In most cellular secretory systems, a Ca^{2+} sensor is responsible for coupling elevations in cytosolic Ca^{2+} to vesicle or cargo trafficking through the soluble N-ethylmaleimide-sensitive factor attachment protein receptor (SNARE) fusion machinery (Pang and Südhof, 2010). To date, several proteins that have the ability to act as Ca^{2+} sensors that participate in the WPBs exocytotic machinery, such as Annexin2-S100A10 and Synaptotagmin-5, have been identified (Wang et al., 2007; Chehab et al., 2017; Lenzi et al., 2019). From aforementioned, only synaptotagmin-5 is found to be directly colocalised with mature WPBs. In addition, synaptotagmin-5 has a lower affinity for Ca^{2+} and weaker ability to bind to SNARE complex suggesting that synaptotagmin-5 responds only to high concentration of Ca^{2+} in the cytoplasm. This reflects the fact that Ca^{2+} -dependent WPBs exocytosis under resting conditions is very low (Erent et al., 2007b) and synaptotagmin-5 plays role in limiting WPB exocytosis near the plasma membrane. Furthermore, when Ca^{2+} is associated with the Ca^{2+} -sensor CaM (see section 1.2.2.5), the Ca^{2+} -bound CaM complex binds to the N-terminus of Ral GDS, thereby unleashing its guanine exchanger factor (GEF) activity towards the small GTPase, Ral A (Rondaij et al., 2006). Activated Ral A is predicted to induce tethering by promoting Arf6-dependent phospholipase D1 (PLD1) activity. PLD1 generates plasma membrane microdomains that recruit the Ca^{2+} -binding and phospholipid-binding AnxA2-S100A10 tethering complex. This, in turn, links WPBs to plasma membrane fusion sites through the specific WPB tethering factor, Munc13-4 (Chehab et al., 2017). Furthermore, it has also been suggested that Ca^{2+} -mediated vWF secretion is also dependent on rapid changes in the actin cytoskeleton that lead to the formation of parallel stress fibers, a process mediated by Rho GTPases (Conte et al., 2016). Upon GPCR induced PLC activation, diacylglycerol (DAG) is also produced, in addition to IP_3 . DAG is a powerful activator of protein kinase C (PKC; Huang, 1989). PKC is a key signalling mediator for a number of endogenous or exogenous endothelial agonists that trigger vWF secretion. These include the phorbol ester phorbol 12-myristate 13-acetate (PMA), histamine, VEGF and Shiga toxin 1B (Stx1B; Schillemans et al., 2019a). Some studies highlight that agonists, such as histamine, can activate multiple PKC isoforms in ECs (PKC δ and PKC α ; Xiong et al., 2009). Nevertheless, several ambiguities suggest that PKC is not always essential for WPB exocytosis, as broad range PKC inhibition or specific depletion of PKC δ and PKC α fail to reduce exocytosis triggered by histamine (Lorenzi et al., 2008). Paradoxically, other studies have shown that blocking intracellular Ca^{2+} -signalling entirely abolishes vWF release induced by histamine, suggesting a difference in requirement for PKC and Ca^{2+} (Lorenzi et al., 2008; Xiong et al., 2009). This difference could perhaps, at least in part, be explained by a recent

study by Esposito and colleagues that identified another endothelial Ca^{2+} pool involved in WPB exocytosis. They showed that histamine H_1 receptor is coupled to NAADP-evoked Ca^{2+} -release from the endo-lysosomal Ca^{2+} stores. For more details on NAADP Ca^{2+} please see section (1.2.2.2). In addition, the pharmacological inhibition of NAADP-evoked Ca^{2+} release by the NAADP antagonist *trans*-Ned-19 and siRNA knockdown of the TPC2 channels (NAADP target channels) decreases vWF release in response to histamine, but not Ca^{2+} -dependent protease thrombin (Figure 1.7; Esposito et al., 2011). These findings question the historically accepted view that Ca^{2+} -dependent WPB exocytosis is operated solely by ER intracellular Ca^{2+} release, and further corroborate the existence of specific WPB Ca^{2+} sensors that can distinguish between separate Ca^{2+} signals in common EC signalling pathways. Therefore, understanding the architecture of the endothelial Ca^{2+} signalling toolkit would provide insights into the mechanisms underlying signal-coupled WPB trafficking.

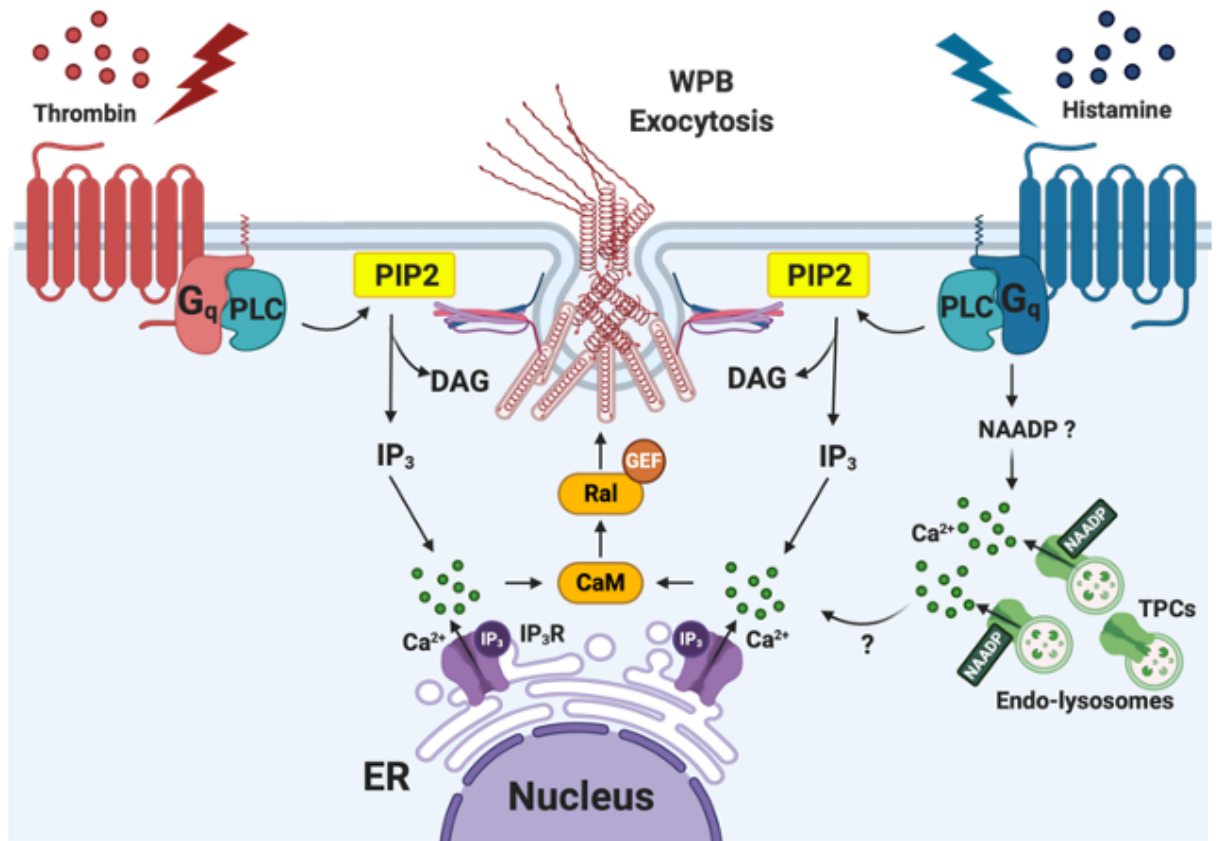


Figure 1.7 Differential Ca^{2+} -dependent Weibel-Palade body exocytosis pathways

Thrombin and histamine both act on G-protein coupled receptors (GPCRs) coupled to the Gq11 protein (PAR1 and H₁ receptor, respectively), thereby activating phospholipase C (PLC) which cleaves membrane-bound phosphatidylinositol 4,5-bisphosphate (PIP₂) into diacylglycerol (DAG) and inositol 1,4,5-trisphosphate (IP₃). IP₃ binds to IP₃ receptors located on the endoplasmic reticulum (ER), triggering an intracellular release of Ca²⁺ from the endoplasmic Ca²⁺ stores. Canonically, the working model for Ca²⁺-dependent WPB agonists described that increased [Ca²⁺]_i activates calmodulin (CaM) and Ral GTPase, promoting Weibel-Palade body (WPB) exocytosis at the endothelial cell surface by inducing assembly of the exocytosis complex, SNARE. However, recent study has revealed that the thrombin and histamine Ca²⁺ signaling pathways diverge. In fact, the H₁ receptor is coupled to NAADP which mobilises Ca²⁺ release from the endo-lysosomal Ca²⁺ stores via the two-pore channels (TPCs). WPB exocytosis is dependent on NAADP signalling. However, it is not known if NAADP serves as a 'trigger' and co-agonist of the IP₃ receptors, or NAADP-mobilized Ca²⁺ from the endo-lysosomes itself is responsible for WPB exocytosis.

1.3 Ca²⁺ toolkit in the endothelium

Changes in cytosolic Ca²⁺ concentration constitute an evolutionarily conserved and ubiquitous signalling pathway that regulates multiple cellular processes. Highly versatile, but complex, signalling pathways can be differentiated depending on the speed, amplitude and spatio-temporal patterning of the Ca²⁺ ion. Rapid kinetics of highly localised Ca²⁺ spikes modulate fast responses, whereas slower responses are controlled by large, globalised Ca²⁺ transients or Ca²⁺ waves. Ca²⁺ itself directly controls the molecular expression patterns of its systems resulting in continuous remodelling, both in health and disease. ECs possess a dynamic and varied Ca²⁺-signalling toolkit, detailed below, used to assemble signalling systems with very different spatial and temporal dynamics, enabling the endothelium to respond expertly to a plethora of stimuli from the bloodstream.

1.3.1 Ca²⁺ entry mechanisms

1.3.1.1 Store-operated Ca²⁺ entry

Store-operated Ca²⁺ entry (SOCE) is an ubiquitous, evolutionary conserved mechanism of Ca²⁺ entry (Putney, 2017). It has taken several decades of researchers to decode SOCE from hypothesis to discovery of participating proteins. In 1986, James Putney described a model of SOCE, wherein receptor-operated Ca²⁺ release from ER is followed by a direct Ca²⁺ refilling of ER store from the extracellular pool of Ca²⁺, thereby bypassing entry into the cytoplasm (Putney, 1986). This mechanistic model gained more confidence after the discovery of I_{CRAC}, a specific Ca²⁺ release-activated calcium (CRAC) current (Hoth and Penner, 1992). More than a decade later, stromal interaction molecule 1 and 2 (STIM1, STIM2) and 3 isoforms of plasma membrane ion channels, namely Orai1, Orai2 and Orai3, were described as essential contributors to I_{CRAC} and components of SOCE (Roos et al., 2005; Feske et al., 2006).

STIM1 is predominantly localised to the ER membrane (Liou et al., 2005), with a limited distribution at the plasma membrane (Zhang et al., 2005). STIM1 has several domains, including a Ca²⁺ sensing EF hand and a sterile-a motif (SAM) domain on the ER luminal side. On the cytoplasmic side, a coiled-coil (CC), ezrin-radixin-moesin (ERM), serine-proline-rich (S/P) and lysine-rich (K) domains are displayed. Orai1 is localised at the plasma membrane, with four membrane-spanning regions and intracellular N and C termini (Lewis, 2007). STIM1 EF-hands act as sensors of ER [Ca²⁺]. ER Ca²⁺ depletion following stimulation (for more details please see Section 1.3.2.1 below) triggers the dimerisation of STIM1 luminal domain. This is rapidly followed by further conformational change in the

cytosolic domains, also known as 'priming', and relocalisation of STIM1 near the plasma membrane in order to form ER-plasma membrane puncta or junctions (Hogan and Rao, 2015). At the same time, upon ER Ca^{2+} store depletion, Orai1 channels are recruited to the plasma membrane, where they overlap with ER-plasma membrane STIM1 puncta (Mercer et al., 2006). Orai1 transitions to the STIM1 puncta by diffusion in the plasma membrane and is reversibly docked by direct interaction of its C-terminus with STIM1 (Park et al., 2009; Wu et al., 2014). Further interaction between STIM1 and the Orai1 N-terminus governs gating of the Orai1 channel and completes the molecular STIM1-Orai1 coupling. This allows entry of Ca^{2+} through the channel from outside the cell into the ER via sarcoendoplasmic reticulum Ca^{2+} -ATPase (SERCA) and the cytoplasm (Figure 1.8), replenishing the $[\text{Ca}^{2+}]_{\text{ER}}$ and enables activation of downstream signalling pathways, respectively (Li et al., 2007; Bhardwaj et al., 2016). Mechanisms of STIM1-Orai1 disassembly will be described later in this chapter.

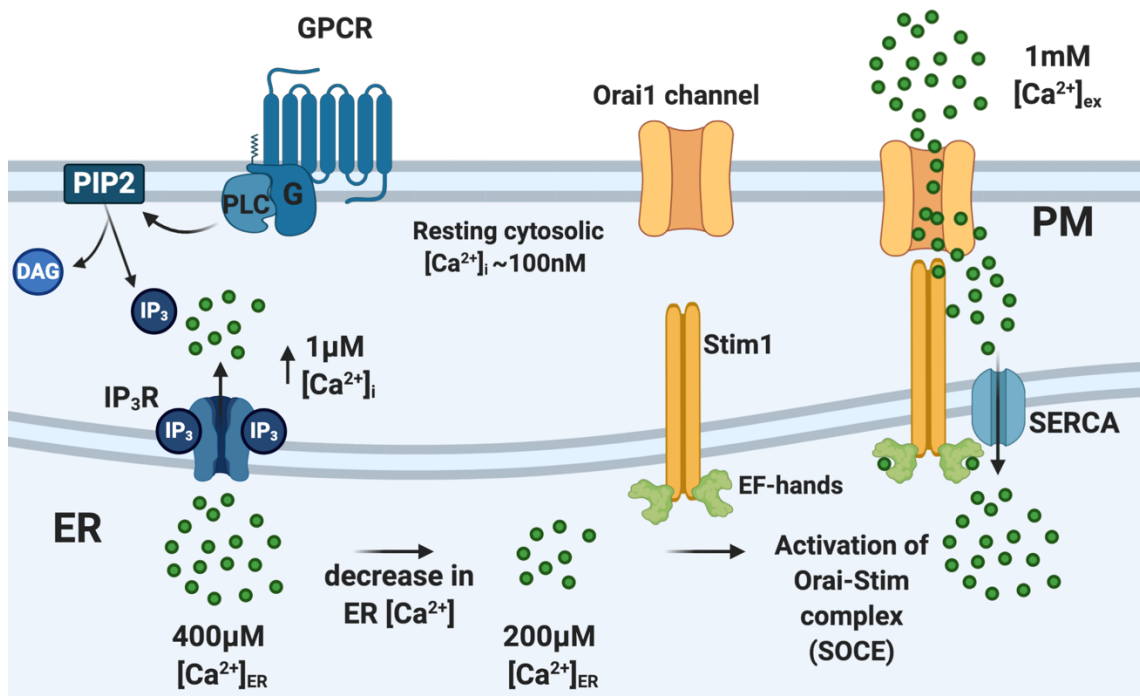


Figure 1.8 Store-operating Ca²⁺ entry

At resting endoplasmic reticulum (ER) Ca²⁺ levels (~400 μM [Ca²⁺]_{ER}), both STIM1 and Orai1 channel have diffused localisation in the ER membrane and the plasma membrane (PM), respectively. In ECs, the agonist-induced stimulation of G-protein coupled receptors (GPCRs) activates phospholipase C (PLC), resulting in hydrolysis of phosphatidylinositol 4,5-bisphosphate (PIP2) on the inner leaflet of the PM and release of diacyl glycerol (DAG) and inositol 1,4,5-trisphosphate (IP3). IP3 diffuses in the cytosol and binds to its receptor IP3R, located on the ER membrane. This causes release of Ca²⁺ from the ER via the IP3R. Upon reduction in [Ca²⁺]_{ER} (e.g. ~200 μM), STIM1 EF-hands sense the loss of local Ca²⁺. This activates STIM, triggering its translocation to ER-PM contact sites, where STIM1 and Orai1 form an activated complex, leading to influx of extracellular Ca²⁺ into the cytosol. Consequently, ER stores are refilled via Ca²⁺ influx through sarcoendoplasmic reticulum Ca²⁺-ATPase (SERCA), which is co-recruited at these ER-PM contact sites. (SOCE, store-operated Ca²⁺ entry).

Although the molecular mechanisms of SOCE are relatively well described, SOCE function to date is a topic of extensive research and academic discussion (Putney et al., 2017). In immune cells, it is known that apart from refilling the ER store and sustaining the Ca²⁺ release wave, Ca²⁺ influx from SOCE activates Nuclear factor of activated T-cells (NFAT) via calmodulin and calcineurin (Braun, 2014). NFAT is an important transcription factor responsible for *de novo* synthesis transcription of cytokines and other mediators of lymphocytes activation. Indeed, some human mutations of STIM1 and Orai1 are lethal or require **bone marrow transplantation** (Gwack et al., 2007; Feske, 2010). ECs express functional SOCE molecular machinery and intact I_{CRAC} (Abdullaev et al., 2008). Notably, Orai1 knockdown in ECs disrupts several endothelial processes, including migration and proliferation, sustained intracellular Ca²⁺ release triggered by VEGF and tube

formation, and endothelial NFAT activation (Abdullaev et al., 2008; Rinne et al., 2009; Li et al., 2011). It is well known that endogenous endothelial agonists that raise intracellular $[Ca^{2+}]$ transiently activate nitric oxide (NO) generation, which is a vital vasodilator, generated by the endothelial nitric oxide synthase (eNOS) enzyme (Blatter et al., 1995). Analysis of the Ca^{2+} signals responsible for eNOS activation in ECs revealed that SOCE, triggered by Ca^{2+} release-dependent store depletion, is Ca^{2+} signal necessary for NO generation (Dedkova and Blatter, 2002). Collective experimental evidence described above places SOCE as a key contributor in several endothelial functions and as a lucrative target for tumorigenesis due to SOCE role in VEGF-dependent endothelial migration and proliferation (Prevarskaya et al., 2014).

1.3.1.2 Trans-plasmalemmal Ca^{2+} entry channels

Voltage-gated Ca^{2+} channels (VGCCs) are ubiquitous Ca^{2+} channels in excitable cells (e.g. cardiomyocytes, neurons) (Brette et al., 2006). VGCCs are activated upon membrane depolarisation, allowing Ca^{2+} entry in response to action potentials, or subthreshold depolarisation events. Ca^{2+} entry through VGCCs serves as a primary second messenger of electrical signals in excitable cells, triggering multiple cellular downstream pathways. They comprise a five subunit complex ($\alpha 1$, $\alpha 2$, β , δ and γ) with $\alpha 1$ forming the central transmembrane pore. There are five major types of VGCCs (L, N, P/Q, R and T) and 3 subfamilies (Ca_v1 , Ca_v2 and Ca_v3). Due to variations in the $\alpha 1$ subunit, there are total of 10 known subtypes, accommodating VGCCs tissue-specific distribution and heterogeneous physiological functions (Ertel et al., 2000; Catterall, 2011). In cardiomyocytes, VGCCs play a key role in regulation of excitation-contraction coupling (L-type) and rhythmic activity (T-Type; Tevoufouet et al., 2014). ECs are generally classed as non-excitable cells. However, the presence of VGCCs in ECs has been described previously (Bossu et al., 1989; Bossu, Elhamdani and Feltz, 1992; Bossu, Elhamdani, Feltz, et al., 1992; Bkaily et al., 1993). Historically, these channels have been considered to be of little functional importance in the endothelium, because most possess small conductance capabilities and voltage-dependent Ca^{2+} influx (Lückhoff and Busse, 1990; Himmel et al., 1993). Despite the fact that GPCRs and VGCCs are known to form signalling complexes (Altier, 2012), classical VGCCs inhibitors, such as diltiazem and verapamil, have no effect on agonist-induced Ca^{2+} entry in isolated ECs (Yamamoto et al., 1995; Li et al., 1999). Exception to this has been a recent study on T-type VGCCs in whole vessels, that describes T-type channel contribution to endothelial acetylcholine signalling and pulmonary artery relaxation (Gilbert et al., 2017).

Organisms have adapted to rapidly and accurately transduce cues from their environment by utilising ion channels (Samanta et al., 2018). The superfamily of cation channels, Transient Potential Receptor (TRP) channels, plays a major role in cation, particular Ca^{2+} , entry mechanisms across the plasma membrane. TRP channels have a promiscuous mode of activation and can be activated by multiple factors, including, but not limited to, endogenous ligands, PLC-coupled intracellular pathways, voltage, heat, pH, and mechanical force (Numata et al., 2016). Twenty-seven TRP isoforms have been found in human tissues that can be classified into six subfamilies: canonical (TRPC); melastatin (TRPM); vanilloid (TRPV), ankyrin (TRPA), polycystin (TRPP) and mucolipins (TRPML). TRP channels are non-selective cation channels that can permit Ca^{2+} entry, and are critically involved in the maintenance of endothelial homeostasis and progression pathology in the vasculature (Earley and Brayden, 2015). The endothelium has been reported to express most mammalian TRP channels isoforms (at least at transcript level), including TRPC1,3–7, TRPV1,2,4, TRPP1,2, TRPA1, TRPM1–4,6-8, expression of which has been found to vary across the different vascular beds (Wong and Yao, 2011; Cao et al., 2018). TRP channels contribute to and sustain the Ca^{2+} influx induced by a number of endogenous endothelial agonists (e.g. Ang-II, bradykinin, ATP, thrombin, VEGF), which activate multiple signalling pathways and vital endothelial functions, such as endothelial-dependent vasodilation (TRPV1-4, TRPA1, TRPC3, 4), endothelial permeability (TRPC1, 4, 6, TRPV4) and angiogenesis (TRPC1, 3-6, TRPV4; Bishara and Ding, 2010; Earley and Brayden, 2015).

Shear stress is a frictional force applied by incoming blood flow to ECs in blood vessels. It is actively sensed by ECs in order to regulate vascular development and homeostasis. The endothelium possesses multiple mechanisms for detecting shear stress, in particular via the non-selective cation channel, Piezo1. Studies have shown that application of shear stress or mechanical force induces Piezo1-dependent Ca^{2+} entry in ECs. Piezo1 mutations are responsible for a number of human diseases and endothelial Piezo1 knockdown in mice has been found to be embryonically lethal (Ando and Yamamoto, 2013; Li et al., 2015).

Another class of Ca^{2+} entry ion channels that are present in the endothelium are the P2X channels. These are ligand-gated and their endogenous ligand is ATP. Studies have found the presence of several P2X channels in the endothelium, such as P2X_{1, 4-7}. Functional studies, mainly on P2X₄ channel, suggest that the channels are mostly present at the endothelial junctions and are involved in the endothelial-dependent vasodilation in response to shear stress (Ralevic, 2012). Indeed, P2X₄-specific knockdown in mice impairs their ability to vasodilate and regulate blood pressure (Yamamoto et al., 2006).

1.3.1.3 Ca²⁺ exchangers and pumps

In order to maintain cytosolic Ca²⁺ homeostasis and low resting Ca²⁺ at approximately 100 nM, cells have adopted mechanisms for Ca²⁺ extrusion out of the cytoplasm into the extracellular space. This can be achieved either via the Na⁺/Ca²⁺ exchanger (NCX) and plasma membrane ATPase (PMCA) pump, and cells express isoforms of such ubiquitously. NCX and PMCA complement the other's functions due to differences in Ca²⁺ affinity and transport capacity. PMCAs are suggested to be effective at maintaining basal Ca²⁺ and responding to modest Ca²⁺ elevations in the cytoplasm, while NCXs have the ability to respond to larger and more dynamic Ca²⁺ transients (Berridge et al., 2003; Clapham, 2007). Consistent with their complementing, but opposing, functions in regulation of intracellular Ca²⁺ homeostasis in the endothelium, NCX has been found to have a role in vasodilation and NO production (Lillo et al., 2018). Conversely, studies have shown that PMCA interacts with eNOS and downregulates NO synthesis, therefore participating in vascular tone regulation (Guibert, 2010).

1.3.2 Intracellular Ca²⁺ stores and signalling

Above, I described mechanisms of Ca²⁺ entry from the extracellular space (~1 mM [Ca²⁺]_{ex}). Cells can also store high concentrations of free, or buffered Ca²⁺, within some of their organelles. Whilst resting EC cytosolic [Ca²⁺]_i is maintained at ~ 100 nM, Ca²⁺ can be rapidly released from internal stores at high concentrations in response to a range of environmental cues from the blood, such as endogenous receptor ligands, mechanical force, membrane potential etc (Berridge et al., 2000; Tran et al., 2000). Thus, understanding the internal Ca²⁺ stores and mechanism by which Ca²⁺ signals are released is of utmost importance for understanding EC function. The ER is by far the best studied Ca²⁺ store, possessing a well-defined list of Ca²⁺ channels, pumps and buffer proteins (Berridge, 2002). Ca²⁺, however, is also contained in a variety of other cellular organelles in both prokaryotic and eukaryotic cells. This was recognised as early as the 1970s using histochemical and imaging techniques (Pozzan et al., 1994).

1.3.2.1 Endoplasmic reticulum

The ER, or sarcoendoplasmic reticulum (SR) in muscle cells, is a large organelle, comprising a network of cisternae and microtubules, expanding from the nucleus to the surface of the eukaryotic cell. The ER has two main functions: to synthesise and package newly formed proteins, and to store and sequester intracellular Ca²⁺. As a Ca²⁺ store, the ER is dynamic and versatile signalling hub due to its ability to both receive and transduce relevant signals. It is customary that, under homeostatic conditions, those two functions are carried out simultaneously, but

independent of the other (Berridge, 2002). In this thesis, only the ER role as a Ca^{2+} store and signalling organelle will be described and discussed. The ER has an immense capacity to store large amounts of Ca^{2+} . It is estimated that the ER lumen contains approximately 1–3 mM Ca^{2+} , sequestered by Ca^{2+} -binding proteins, and approximately 100–400 μM of free Ca^{2+} ions (Michalak and Opas, 2009).

ER balances its Ca^{2+} homeostasis by avoiding a net loss or gain of Ca^{2+} ion through actively pumping Ca^{2+} back into the ER lumen after a Ca^{2+} release event. This reuptake of Ca^{2+} is achieved via the SERCA pump, which stoichiometrically transports two Ca^{2+} ions for one ATP molecule. SERCA is present in all eukaryotic cell types and is encoded by three genes (SERCA 1, 2 and 3) with multiple tissue specific isoforms (Berridge et al., 2003; Periasamy and Kalyanasundaram, 2007). Studies on SERCA and the ER as a Ca^{2+} store have been aided by the discovery that thapsigargin, a non-phorboid tumour promoter, inhibits SERCA activity (Lytton et al., 1991). Both SERCA2 and SERCA3 are expressed in the endothelium and isoform distribution is vascular bed specific (Mountian et al., 1999; Khan et al., 2000).

A universal mechanism of signal transduction from the ER is achieved via Ca^{2+} release from ion channels located on ER membrane, namely IP_3 receptors (IP_3Rs) or ryanodine receptors (RyRs). IP_3R isoforms ($\text{IP}_3\text{R}1$, 2 and 3) are expressed in most types of cells (Taylor, 1997), while RyR isoforms ($\text{RyR}1$, 2 and 3) are predominantly active in excitable cells such as muscle cells, cardiomyocytes, pancreatic β -cells and neurons (Lanner et al., 2010). IP_3R is a large tetrameric ion channel (each subunit approximately 260 kDa), with multiple cytosolic regulatory sites and protein-binding domains (Prole and Taylor, 2019). IP_3Rs have both IP_3 and Ca^{2+} binding sites, and their activation is dependent on both (Marchant and Taylor, 1997; Taylor and Tovey, 2010). Interestingly, while activation of IP_3R by IP_3 and subsequent Ca^{2+} release from the receptor is dose dependent, IP_3R mobilisation by cytosolic Ca^{2+} elicits biphasic effects and bell-shaped dependence. Generally, IP_3 is synthesised upon signalling through GPCRs (Gq/11 subtypes) and tyrosine kinases receptors (TKR), which activate phospholipase $\text{C}\beta$ ($\text{PLC}\beta$) and γ ($\text{PLC}\gamma$), respectively. Thereafter, PLCs cleave membrane-bound phosphatidylinositol 4,5-bisphosphate (PIP_2) into IP_3 and DAG. Upon IP_3 binding, in order to amplify the Ca^{2+} signal and propagate a global Ca^{2+} wave, IP_3Rs form clusters with more IP_3Rs or engages in cross-talk with adjacent RyRs (Haak et al., 2001; Rahman and Taylor, 2009). IP_3Rs are often described as 'signalling hubs' due to participating in multiple signalling pathways and their interaction with many proteins, for example IRBIT (IP_3R -binding protein released with IP_3) which regulates their IP_3 sensitivity, whereas another protein,

ERp44, is involved redox signalling (Mikoshiya, 2007). In the endothelium, molecular studies in freshly isolated ECs and primary ECs suggests that ECs express heterogenous populations of IP₃Rs, switching predominantly to IP₃R3 with increasing passages (Mountian et al., 1999). In ECs, the IP₃Rs are considered to be the primary mediators of vascular agonist-induced Ca²⁺ release from the ER. Studies in porcine aortic ECs suggest that IP₃-mediated Ca²⁺ release is tightly regulated by cytosolic Ca²⁺ concentration (Carter and Ogden, 1997). Examples of endogenous vascular agonists and their receptors coupled to IP₃ signalling in the endothelium include VEGF, histamine, thrombin, ATP, bradykinin and sphingosine-1-phosphate (Tran et al., 2000). It worth noting that overall IP₃Rs on their own have a profound role in ECs function. In a study of transgenic mice lacking all three types of IP₃Rs in the endothelium researchers found that those animals have disrupted basal NO concentration and experience high levels of blood pressure (Lin et al., 2019).

The RyRs are large tetrameric channels (2.2 mDa), and their name came from a plant alkaloid called ryanodine, which, depending on its concentration, can either block or promote Ca²⁺ release from the channel. RyRs endogenous agonist is cytosolic Ca²⁺ with a bell-shaped concentration dependence, similar to IP₃Rs. In cardiac cells, Ca²⁺ influx from VGCCs triggers this Ca²⁺-induced Ca²⁺ release (CICR) and allows the amplification of local Ca²⁺ events to propagate a global Ca²⁺ wave, thus generating rhythmic activity in the heart (Zahradník et al., 2005; Lanner et al., 2010). Ca²⁺ sensitivity of RyRs is regulated by another endogenous mobiliser cyclic adenosine diphosphate–ribose (cADPR). Low cADPR concentrations require higher concentrations of cytoplasmic Ca²⁺ in order to activate the channel and vice versa (Venturi et al., 2012). Caffeine is an exogenous agonist and a useful experimental tool that promotes Ca²⁺ release from the RyRs (McPherson et al., 1991). Similarly to IP₃R, a large proportion of RyRs are cytoplasmic, which allows interaction with proteins, including calmodulin, PKA and FK-506-binding proteins (Bers and Morotti, 2014). Human mutations in RyRs cause a plethora of lethal and life threatening conditions, such as malignant hyperthermia and ventricular tachycardia (MacLennan et al., 1996; Liu et al., 2008). In non-excitable cells, such as ECs, the RyRs main function is to assist ER Ca²⁺ release from IP₃Rs. Molecular and electrophysiological investigations in ECs suggest that only RyR3 is expressed, which releases Ca²⁺ upon stimulation with low doses of ryanodine and caffeine (Köhler et al., 2000; Köhler et al., 2001).

1.3.2.2 Acidic Ca²⁺ stores

While studies on the ER Ca²⁺ stores have dominated the Ca²⁺ signalling field for decades, Ca²⁺ stored within other organelles, such as the endo-lysosomal system (also known as acidic Ca²⁺ stores) have recently gained increasing interest and importance in the research community. The endo-lysosomal system is a dynamic and heterogenous system encompassing a range of acidic organelles, including intermediate and late endosomes, primary lysosomes, early autophagosomes, and multivesicular endosomes. Some of the primary functions of this system are transport and degradation of endocytic cargo, vesicular fusion/fission, energy metabolism and apoptosis (Klumperman and Raposo, 2014). The first reports of the endo-lysosomal system as an acidic Ca²⁺ store and its contribution to cellular Ca²⁺ homeostasis date as early as the 1970s (Pozzan et al., 1994). In eukaryotic cells, in addition to the endo-lysosomal system, organelles that classify as acidic Ca²⁺ stores include lysosome-related organelles (e.g. melanosomes, lytic granules) and secretory vesicles (e.g. synaptic vesicles; Patel and Muallem, 2011). In this chapter, the only acidic Ca²⁺ store to be described is the endo-lysosomal system. As both endosomes and lysosomes mature, they undergo simultaneous active acidification (endosomes pH ~6; lysosomes pH 4-5). The harsh acidic and proteolytic environment within the endo-lysosomes makes direct measurements of their luminal Ca²⁺ content experimentally challenging. Despite this fact, it has been estimated that endosomes can store ~40 µM [Ca²⁺] (which is close to the lower concentration found in the ER), and lysosomes can carry very high concentrations of Ca²⁺, ~500 µM [Ca²⁺] (Miyawaki et al., 1997; Sherwood et al., 2007; Patel and Docampo, 2010). Similarly, deciphering the mechanisms of Ca²⁺ storage and buffering within the endo-lysosomes is also experimentally difficult, resulting in limited information in the literature. It has been suggested, however, that in the endo-lysosomal and other acidic Ca²⁺ stores, Ca²⁺ can be buffered in polyanionic matrixes, such as polyphosphates, or in cell-type specific Ca²⁺-binding proteins (e.g. melanin in melanocyte Pisoni and Lindley, 1992; Hoogduijn et al., 2003).

Endo-lysosomal Ca²⁺ uptake or refilling is a topic of debate. It is believed that the proton gradient generated during the acidification of endo-lysosomes is responsible for the Ca²⁺ uptake into the organelles, mainly due to the presence of the vacuolar ATP-ase (V-ATPase) proton pump, together with Na⁺/H⁺, Ca²⁺/H⁺ and perhaps Na⁺/Ca²⁺ exchangers, though the molecular identity of such exchangers remains controversial. This hypothesis has been mainly corroborated by pharmacological disruption of the endo-lysosomal proton gradient by inhibition of V-ATPases with specific inhibitors (e.g. bafilomycin A1), which prevent Ca²⁺ release from endo-lysosomes (Morgan et al., 2011; Brailoiu and

Brailoiu, 2016). However, these findings are challenged, at least in part, by studies on ER-lysosome contact sites. It has been shown that endo-lysosomes may acquire Ca^{2+} by means of sequestering Ca^{2+} released from the ER, independently of SOCE. In fact, IP_3Rs preferentially interact with endo-lysosomes, delivering Ca^{2+} at the contact sites between the two organelles thereafter (López-Sanjurjo et al., 2013; Garrity et al., 2016; Atakpa et al., 2018). These studies contribute to the notion that lysosomal Ca^{2+} uptake is a dynamic and versatile process, complexity of which exceeds initial hypotheses.

1.3.2.3 Acidic stores release mechanisms

The Ca^{2+} release mechanism from the endo-lysosomes was first underpinned in 2002 where researchers found that the Ca^{2+} mobiliser nicotinic acid adenine dinucleotide phosphate (NAADP) triggers Ca^{2+} from acidic stores (Churchill et al., 2002). Previously, NAADP was shown to be the most potent second messenger to trigger intracellular Ca^{2+} release, however, unlike IP_3 and cADPR, it mobilises Ca^{2+} from stores that are distinct from the ER (Hon Cheung Lee and Aarhus, 1995). Interestingly, NAADPs mode of action differs due to its ability to self-desensitise and self-inactivate, a unique mechanism best described by a bell-shaped dose-response curve and not observed by any other Ca^{2+} mobilisers (Cancela et al., 1999). For example, in pancreatic acinar cells a maximal Ca^{2+} release can be observed at concentrations as low as 10 nM and 1 μM , while at 1 mM was without effect (Figure 1.9). This phenomenon has been observed first in mammalian cells (Cancela et al., 1999), and similar mechanism of receptor desensitisation in sea urchin egg preparation (Aarhus et al., 1996). In fact, pre-incubation of sea urchin eggs, and in some mammalian cells, with sub-maximum concentration of NAADP inactivates the NAADP-evoked Ca^{2+} release that would otherwise produce a robust Ca^{2+} event. An initial, localised Ca^{2+} event is followed by a larger Ca^{2+} release wave. This bi-phasic response is readily inhibited by bafilomycin A1, whereas heparin, an IP_3R inhibitor, can specifically block the second Ca^{2+} wave (Genazzani et al., 1996; Aarhus et al., 1996). These observations helped researchers formulate the “trigger” hypothesis as one of the several characteristic modes of action for NAADP, and suggested that NAADP-evoked Ca^{2+} from the acidic stores can provide Ca^{2+} as a co-agonist enhancing IP_3Rs or RyRs Ca^{2+} release by CICR (Cancela et al., 1999; Lam and Galione, 2013; Galione, 2015a). Due to their dynamic trafficking, acidic stores can be found near the plasma membrane regions which allows for localised Ca^{2+} release that can be mobilised by NAADP in order to modulate plasma membrane channels activation. In excitable cells (e.g. neurons) that can play a significant role in membrane potential regulation (G.C. Brailoiu et al., 2009), whilst in non-excitable cells (e.g. pancreatic acinar cells), modulation of Ca^{2+} -activated plasma

membrane channels may control fluid secretion (Cancela et al., 1999). In addition, NAADP can mobilise local Ca^{2+} release forming Ca^{2+} nanodomains within the cytoplasm (Davis et al., 2020a), and therefore coupling NAADP to a plethora of cellular functions (Figure 1.10). Such functions range from house-keeping vesicular trafficking events (fusion/fission) to extracellular stimuli, wherein NAADP signalling drives physiologically important yet distinct processes, such as egg fertilization, inflammation, angiogenesis, arrhythmogenesis, autophagy and nutrient sensing (Galione, 2015b).

Although there is a clear consensus in the research community that a large proportion of Ca^{2+} release from the endo-lysosomes Ca^{2+} stores is indeed mobilised by NAADP, the identity and mechanisms of resident Ca^{2+} channels responsible for such release to date remain a contentious topic (Galione and Ruas, 2005; Jha et al., 2014). A number of candidate Ca^{2+} channels have been proposed over the years - RyRs, transient receptor potential mucolipin-1 (TRPML1) and two-pore channels (TPCs; Galione, 2011). Studies in pancreatic acinar cells and T-cells on the potential activation of RyRs by NAADP has found that only RyR1 is activated by physiological concentrations of NAADP (Guse and Wolf, 2016). Though this finding is unlikely relevant in ECs as single-cell reverse transcription-polymerase chain reaction (RT-PCR) and immunocytochemistry studies have revealed that ECs mainly express RyR3, but not RyR1 and RyR2. Some initial reports, in rodent hepatocytes and myocytes have proposed the lysosomal ion channel TRPML1 as a target Ca^{2+} release channel for NAADP signalling (Zhang and Li, 2007; Zhang et al., 2011). However, comparative studies between TRPML1 and TPCs have disputed these findings and refuted TRPML1 involvement in NAADP-trigger Ca^{2+} release from the endo-lysosomal Ca^{2+} stores (Yamaguchi et al., 2018).

Due to the substantial body of studies linking TPCs to NAADP-evoked Ca^{2+} release from the endo-lysosomes, and in particular, several articles outlining their importance in the endothelium, this chapter will primarily focus on TPCs.

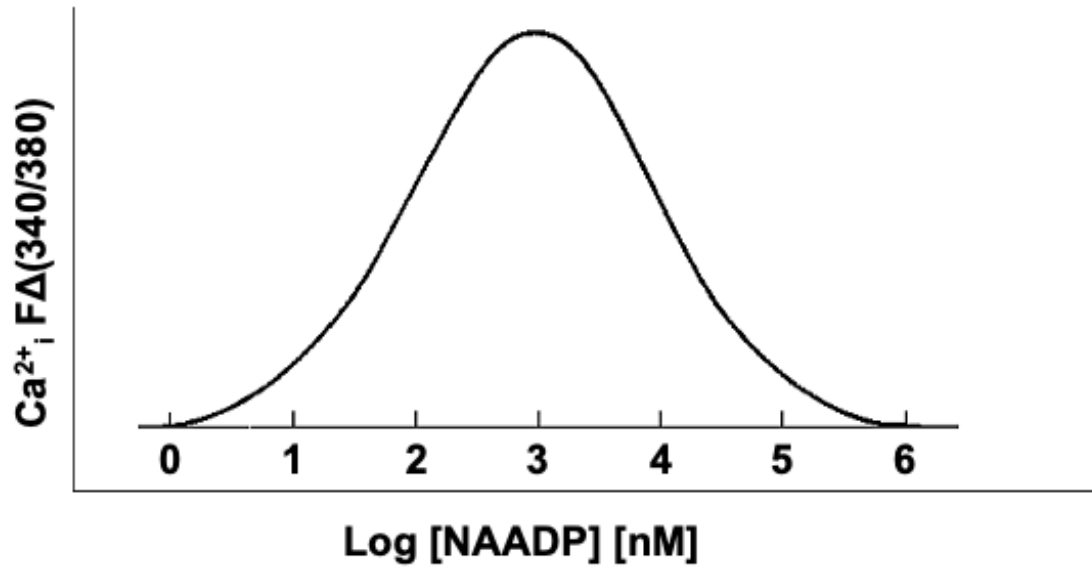


Figure 1.9 NAADP dose-response curve.

Unlike the canonical Ca^{2+} mobiliser IP_3 , intracellular Ca^{2+} release mobilized by NAADP follows a bell-shaped dose response curve. Adapted from Berg *et al.*, 2000.

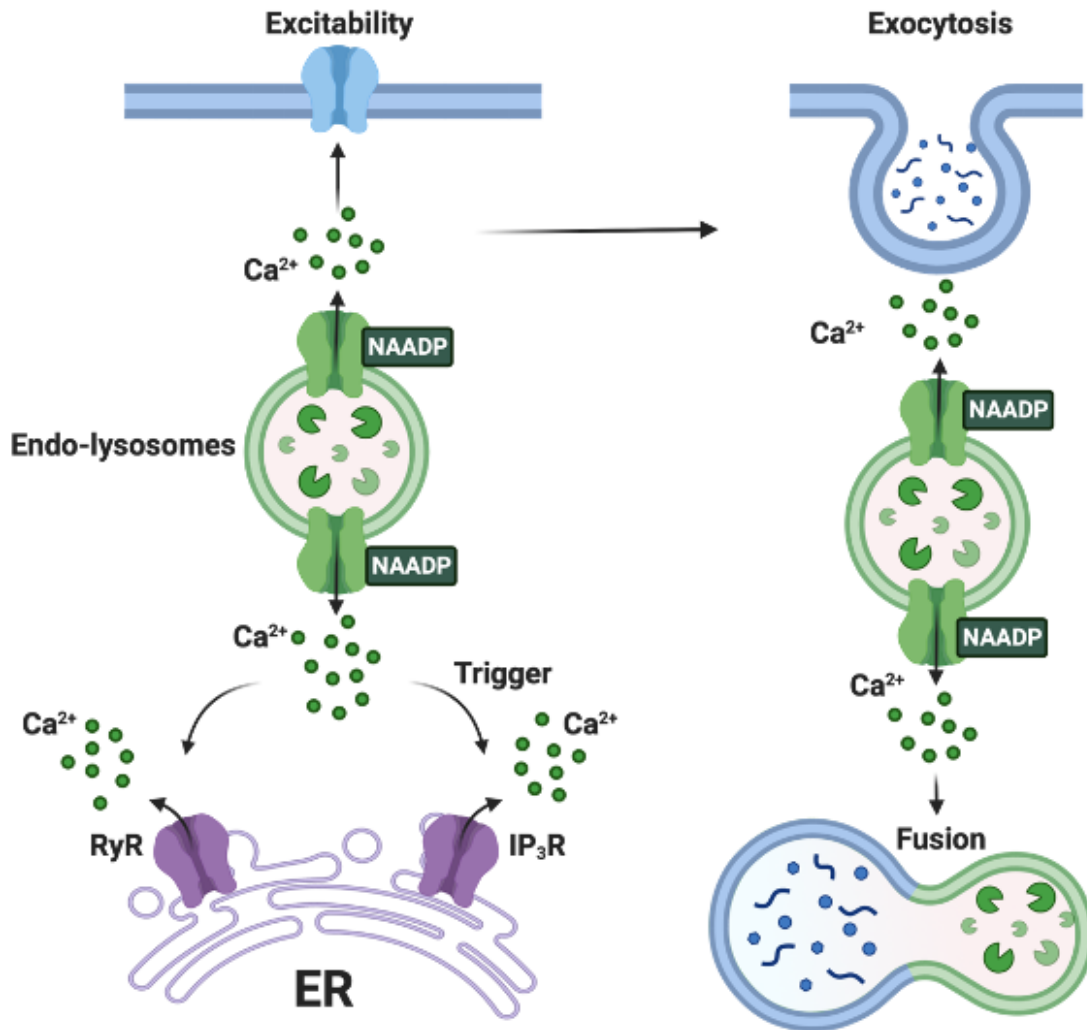


Figure 1.10 NAADP-mediated Ca^{2+} release mode of action and cellular

Endo-lysosomes or acidic stores are a small Ca^{2+} stores. Their heterologous location within the cell allows them to release Ca^{2+} in a small-scale and localised manner as opposed to global Ca^{2+} release from the endoplasmic reticulum (ER). Ca^{2+} release from the endo-lysosomal stores may also act as a 'trigger' or co-agonist for further Ca^{2+} release from the ER through IP_3Rs or RyRs resulting in a larger more global Ca^{2+} response. Depending on its cellular localisation, Ca^{2+} release can influence Ca^{2+} -dependent ion channels on the plasma membrane of excitable cells, and in non-excitable cells it can regulate other processes such as exocytosis. Local Ca^{2+} release from endo-lysosomal organelles may also promote fusion of vesicles with lysosomes or other vesicles as well as trafficking and exocytosis of vesicles. Adapted from Galione, 2015.

1.3.2.4 Two-pore channels

TPCs family are relatively newly discovered ion channels, whose founding member TPC1 was first cloned in 2000, however, TPC1s function as a Ca^{2+} release channel in the acidic Ca^{2+} store in plants (the vacuole), was not described until five years later (Ishibashi et al., 2000; Peiter et al., 2005). With two repeats

of six transmembrane segments, TPCs share a structural homology with VGCCs, some researchers propose that TPCs represent an ancestral form, which has been conserved in evolution and it gave rise to the VGCCs (Guo et al., 2016). Another two members, TPC2 and TPC3, were discovered, although only TPC2 is present in human and rodent species (Cai and Patel, 2010; Zhu et al., 2010). In mammalian cells, through series of elegant Ca^{2+} imaging and electrophysiology experiments both TPC1 and TPC2 were identified as NAADP-sensitive channels, releasing Ca^{2+} from the endo-lysosomes. High resolution imaging studies have identified that TPC1 colocalises predominantly with Lamp1-positive endosomal compartments and other unidentified compartments, while TPC2 is readily localised with Lamp2, a lysosomal marker (Calcraft et al., 2009; E. Brailoiu et al., 2009). Despite substantial evidence of TPCs as the main contestants for NAADP receptors, their modulation by NAADP and Ca^{2+} selectivity have been challenged (Wang et al., 2012; Cang et al., 2013). However, studies in primary cells where TPC2 is knockdown with a specific short hairpin RNA (shRNA) and in cells **extracted from transgenic mice** with double TPC1 and TPC2 knockout NAADP unequivocally failed to evoke Ca^{2+} from acidic stores. In fact, transient expression of TPCs in the double knockout mouse rescues NAADP-dependent Ca^{2+} signalling (Zhang et al., 2013; Ruas et al., 2015). Nevertheless, the controversy around TPCs have sparked extensive interest in TPCs which resulted in a number of discovery about the activation and inactivation mechanisms of the channels. Notably, TPCs can be modulated by the endo-lysosomal lipid $\text{PI}(3,5)\text{P}_2$, the kinases (mTOR), luminal pH of the endo-lysosomes, endo-lysosomal membrane potential and Rab GTPases (Figure 1.11).

This plethora of activation and de-activation mechanisms perhaps, in part, explains the importance of these ion channels in multiple organ systems and pathophysiology (Figure 1.12). It is worth highlighting that although NAADP selectively mobilises Ca^{2+} release from TPCs researchers have failed to locate a NAADP binding site on the channels. Many have hypothesised that this is due to presence of an intermediate NAADP-binding protein (Lin-Moshier et al., 2012; Guse and Wolf, 2016; Guse and Diercks, 2018). In 2014, in a TPC interactome study it has been found that it is very likely that, at least in some mammalian cells, the NAADP-binding protein that activates Ca^{2+} release from TPCs **is an unknown** Rab GTPase, thus placing TPCs at a converging point in multi-modal regulation of endo-lysosomal trafficking (Lin-Moshier et al., 2014; Marchant and Patel, 2015).

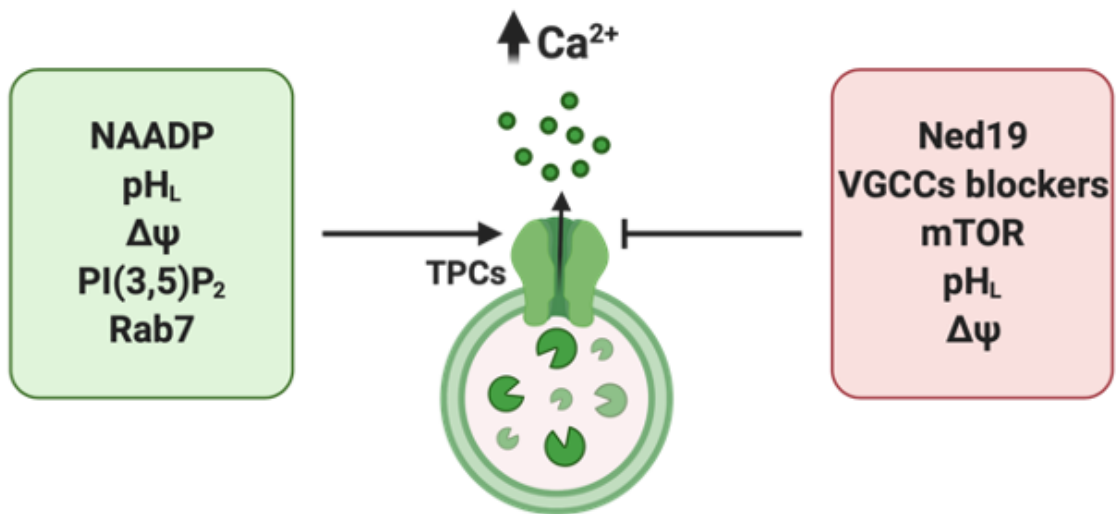


Figure 1.11 Multiple regulators of Two-pore channels affect Ca^{2+} release from the endo-lysosomes.

Positive modulators of TPC activity affecting Ca^{2+} release from the endo-lysosomes (green box) include, but not limited to, NAADP, luminal pH (pH_L), luminal membrane potential ($\Delta\psi$; only TPC1 and TPC3), the endo-lysosomal lipid $\text{PI}(3,5)\text{P}_2$, small GTPase Rab7. Negative modulators of TPCs that prevent Ca^{2+} release include the NAADP antagonist *trans*-Ned19, voltage-gated Ca^{2+} channel (VGCC) blockers, the kinase mTOR as well as pH_L and $\Delta\psi$.

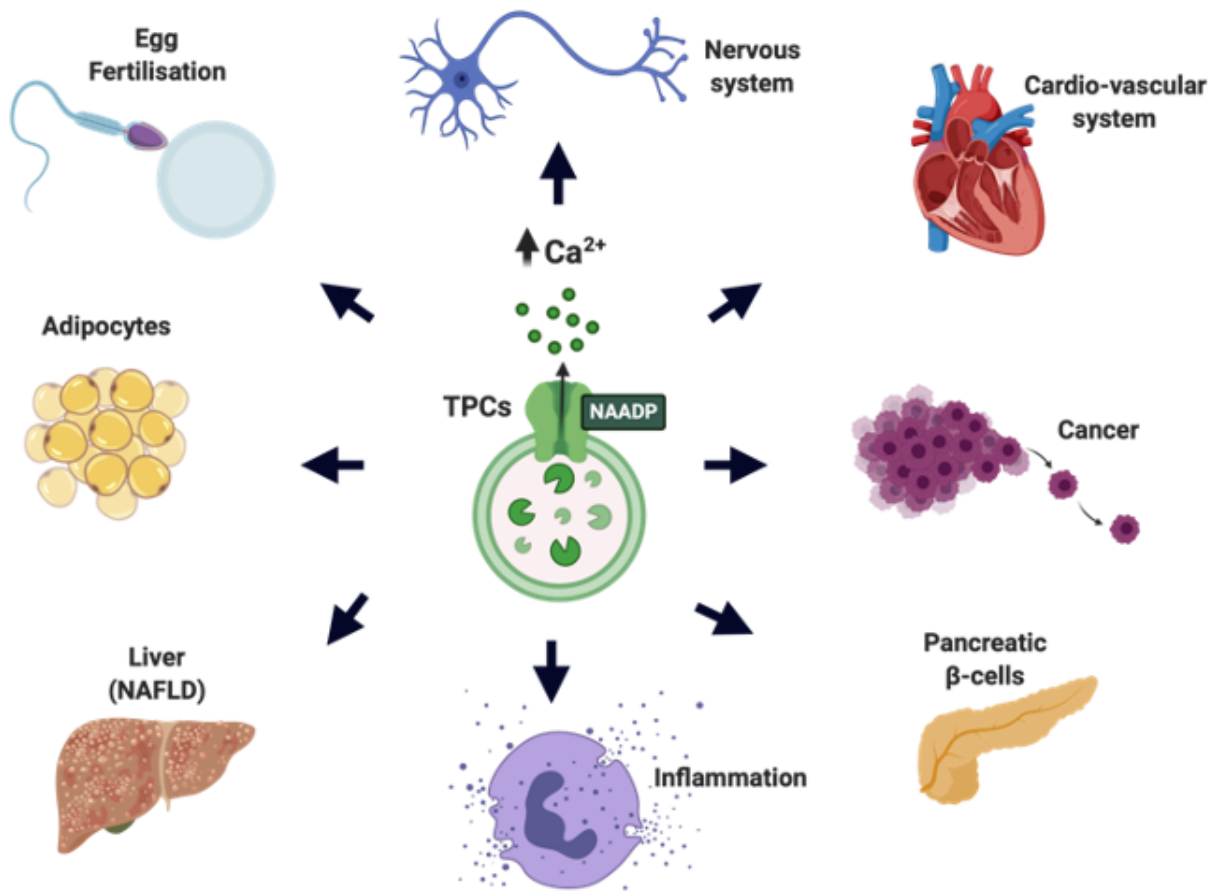


Figure 1.12 Two-pore channels function in different tissue types and role in disease.

Due to their location at the endo-lysosomal membranes, two-pore channels (TPCs) are widely and innately expressed in different cells types. In the nervous system, NAADP and TPCs are linked to crucial processes such as neurotransmitter release, membrane excitability and proliferation as well as progression of some neurodegenerative disorders (e.g. Parkinson's disease). In sperm, NAADP levels increase in the sperm head due to stimulation by egg chemo-attractant factors. At the sperm-egg contact site, NAADP is introduced into the egg, triggering electrical changes and propagating Ca^{2+} wave across the egg as part of the fertilization process. In the adipose tissue, NAADP-mediated Ca^{2+} signalling through the TPCs is involved in insulin-mediated glucose uptake in adipocytes and in the mode of action of rosiglitazone, insulin sensitizing drug used in type 2 diabetes therapy. In the hepatobiliary system, it has been shown that deletion of TPCs is a key cause of progression of non-alcoholic fatty liver disease (NAFLD) and non-alcoholic steatohepatitis (NASH). In the immune system, NAADP has been extensively studied primarily in T lymphocytes activation where NAADP is tightly coupled to IP_3 -mediated Ca^{2+} release from the endoplasmic reticulum, linking NAADP and their target channels TPCs to inflammation. NAADP and TPCs signaling has been extensively studied in pancreatic β -cells due to their important involvement in glucose-evoked depolarization and insulin secretion. Mutation or loss of TPCs can impact multiple endo-lysosomal trafficking pathways therefore linking TPCs to cancer cell migration and metastasis, particularly distinct defects in endo-lysosomal trafficking such as integrin trafficking.

Figure 1.11 Continued. Finally, in the cardio-vascular system, NAADP and TPCs are involved in cardiac cells adrenergic signaling and arrhythmogenesis. In the vascular endothelium, NAADP and TPCs have been linked to VEGF-induced angiogenesis and secretion of vWF by histamine. Additionally, studies in vascular smooth muscle cells (VSMCs) shown that NAADP and TPCs signaling may be involved in vessel relaxation.

In endothelial cells, acidic stores Ca^{2+} release has been found to modulate several important processes. For example, in aortic endothelial cells NAADP-evoked Ca^{2+} participates in regulation of the endothelial membrane potential by activating K channels and promoting NO synthesis, thereby affecting blood pressure *in vivo* (Brailoiu et al., 2010a). In the endothelium-derived cell line EA.hy926, it was found that in addition to IP_3 -mediated ER Ca^{2+} release, histamine H_1 receptors are coupled to acidic Ca^{2+} stores and NAADP signalling. The observed NAADP-dependent Ca^{2+} release from acidic stores occurs via the TPCs and it affected endothelial exocytosis of vWF (to be further described in section 1.3.3.2; Esposito et al., 2011). Furthermore, a study has shown that acidic Ca^{2+} stores and TPC2 are involved in angiogenesis and capillary network formation via VEGF receptor signalling (Faviaa et al., 2014a). The studies outlined here suggest that Ca^{2+} release from TPCs and acidic stores is crucially involved in several functionally distinct processes in the endothelium. This questions the status quo and the canonical model of endothelial Ca^{2+} signalling, paving a path for future discoveries of the potential involvement of NAADP in distinct endothelial signalling pathways.

Overall, the general consensus that remains is that TPCs play an important role in NAADP-evoked Ca^{2+} release from the acidic Ca^{2+} stores, but this is a contribution to a large NAADP signalling network with multiple sensors and binding proteins which is specialised in a cell type and tissue-dependent manner.

1.3.2.5 Other Ca^{2+} stores

Mitochondria are vital and dynamic organelles regulating cellular processes such as ATP production, metabolism and cell death (Duchen, 2004). Mitochondria take an important part of intracellular Ca^{2+} homeostasis and Ca^{2+} signalling pathways due to their ability to sequester and release Ca^{2+} . Among many, mitochondria can participate in Ca^{2+} regulation as both regulators and decoders of Ca^{2+} due to their location, interaction with other Ca^{2+} stores (e.g. ER), and ability to accumulate large amounts of Ca^{2+} in their matrix (resting state 100–200 nM [Ca^{2+}]; activated 100-200 μM [Ca^{2+}]; Giorgi et al., 2018). Mitochondrial Ca^{2+} influx is low affinity and it is mainly driven by mitochondrial membrane potential difference, generated by the respiratory chain which provides the proton electrochemical force required

for Ca^{2+} ions to enter the mitochondrial matrix, and ER-mitochondria contact sites (Finkel et al., 2015). Historically, Ca^{2+} efflux from the mitochondrial matrix is believed to be governed mainly by tissue-specific $\text{Na}^+/\text{Ca}^{2+}$ exchanger (NCX) and $\text{H}^+/\text{Ca}^{2+}$ exchanger (HCX; Jung et al., 1995). Although, the identity of said exchangers has been questioned by many opposing studies. Mitochondrial permeability pore (PTP) has been proposed as an alternative for mitochondrial Ca^{2+} release, albeit controversial (Lu et al., 2016). In the endothelium, mitochondrial Ca^{2+} studies are mainly focussed on altered mitochondrial Ca^{2+} uptake protein expression in atheroprone regions; a corollary of the high levels of oxidative stress and inflammation in those regions. In particular, ECs under high oxidative stress display a pathogenic increase of mitochondrial Ca^{2+} and reactive oxygen species (ROS) thereafter leading to decreased NO bioavailability and progression of endothelial dysfunction (Alevriadou et al., 2017). Overall, mitochondria are an important intracellular Ca^{2+} store that has the ability to buffer and shape Ca^{2+} waves due their proximity to ER and their various distribution around the cytosol. Perturbation of mitochondrial Ca^{2+} homeostasis can unequivocally lead to endothelial pathology (Duchen, 2004).

In eukaryotic cells, the Golgi apparatus is the main organelle mediating post-translational modification, sorting and packaging of macromolecules synthesised in the rough ER. The Golgi apparatus also serves the role of a large cellular Ca^{2+} store in addition to the ER, mitochondria and nucleus. Earlier studies have shown that Ca^{2+} stored within the Golgi apparatus can regulate its structure and function, and limiting Golgi $[\text{Ca}^{2+}]$ can lead to disruptions of such (Yang et al., 2015). Storage of Ca^{2+} within the Golgi is generated by the Calcium-transporting ATPase type 2C member 1 (SPCA1). Similarly to ER, Ca^{2+} storage capacity is managed and increased by Ca^{2+} binding proteins (e.g. calnuc), although the Ca^{2+} concentration in the Golgi is unevenly-distributed, ranging from 130 μM in the *trans*-Golgi to 250 μM in the *cis*-Golgi (Micaroni et al., 2010). There are limited evidence describing Ca^{2+} release from the Golgi and whether such Ca^{2+} release participates in cellular signalling cascades. It has been suggested, mainly from cell line studies, that Ca^{2+} efflux can be mediated by the IP_3R or RyRs channels (Yang et al., 2015). However, the Golgi apparatus' proximity and interaction with other large Ca^{2+} stores, the ER and the nucleus, deem the deciphering of Golgi Ca^{2+} release from aforementioned channels challenging.

The nucleus has been previously described as another functional Ca^{2+} store in cells (Echevarria et al., 2003). A general, yet contentious, consensus proposes the nuclear pore complexes (NPCs) as a major gateway for constitutive diffusion of Ca^{2+} ions from the cytosol into the nucleoplasm. The nuclear envelope is continuous and interacts with the ER, thereby contains SERCA and both IP_3Rs

and RyRs as a means of Ca^{2+} influx and efflux, respectively (Sarma and Yang, 2011). Recent studies suggest that nuclear Ca^{2+} participate in the regulation of gene transcription and cell-cycle progression, however, it is unclear how nuclear Ca^{2+} signals are generated and whether they are independent of other stores (Bootman et al., 2009). To date there are no studies defining differential role for the nuclear and Golgi apparatus Ca^{2+} stores in ECs signalling pathways.

1.3.2.6 Intracellular Ca^{2+} sensors and adaptors

It is evident Ca^{2+} stores and Ca^{2+} ions role as a second messenger are pivotal for transducing specific signals in the cell. Upon Ca^{2+} mobilisation and release from the intracellular stores, as discussed above, it is important that messages, varying in amplitude, frequency and localisation, are received and correct downstream cellular pathways are activated (Berridge et al., 2003; Clapham, 2007). For example, Ca^{2+} release from the acidic stores is localised whilst ER produces large, global Ca^{2+} events in the cytoplasm. These differences raise the necessity for presence of specialised Ca^{2+} sensors and adaptors that can not only recognise the nuance and complexity of Ca^{2+} events but to shape them too. Ca^{2+} sensors and adaptors are a large heterogenous group of proteins that have Ca^{2+} -sensing domains, C2 domains and/or EF-hand domains, that selectively and reversibly bind Ca^{2+} , the kinetics of such binding being fast and dynamic (Yáñez et al., 2012). A C2 domain comprises of approximately 120 amino acid and can simultaneously bind Ca^{2+} ions in several loops within its structure. Well-known signalling proteins that have C2 domains include Ca^{2+} -dependent PKC isoforms, synaptotagmins, Munc and annexins (Clapham, 2007; Yáñez et al., 2012; Chu et al., 2014). Specific isoforms of synaptotagmin, Munc and annexin are involved in endothelial exocytosis of WPBs, which will be described later in this chapter (see section 1.3.3.2). As outlined above, there are Ca^{2+} adaptor proteins that contain EF-hand domains in their structure. There are more than 66 families of proteins with EF-hand domains and 650 proteins with C2 domain know to date, which is a tangible evidence for the ubiquitousness and universality of binding Ca^{2+} to transduce cellular signals in cells (Nakayama and Kretsinger, 1994; Zhang and Aravind, 2010). EF-hand domain in Ca^{2+} sensor proteins is very widespread and common calcium-binding motif, and often the domain consists of adjacent pair of two EF-hand motifs (Figure 1.13). Calmodulin is the archetypal, and perhaps the most studied, Ca^{2+} sensor. Calmodulin have four EF-hand motifs, with each one having a distinct Ca^{2+} affinity, and such affinities are potentiated by phosphorylation or interaction of downstream target proteins (e.g. Ca^{2+} /calmodulin-dependent kinase; CaMK). Binding of Ca^{2+} to the EF-hand motifs of calmodulin induces a large conformational change and exposure of interacting surfaces within the other domains of calmodulin, thereby triggering its

Ca^{2+} sensing activity and further binding to its targets (Zhang et al., 2012; Halling et al., 2016). In addition to transducing signals from vascular agonists, in endothelial cells, calmodulin itself downregulates the Ca^{2+} -dependent NO synthesis by interacting with eNOS (Greif et al., 2004). Recently, atypically large Rab GTPase proteins, best known as masters of cellular traffic (Stenmark, 2009), were identified as EF-hand proteins that can integrate Ca^{2+} signals (described below). These Rab GTPases are shown to be involved in important physiological processes such as inflammation (Srikanth et al., 2017), leukocyte proliferation (Woo et al., 2018), differentiation (Yamaguchi et al., 2018) and trafficking (Miteva et al., 2019).

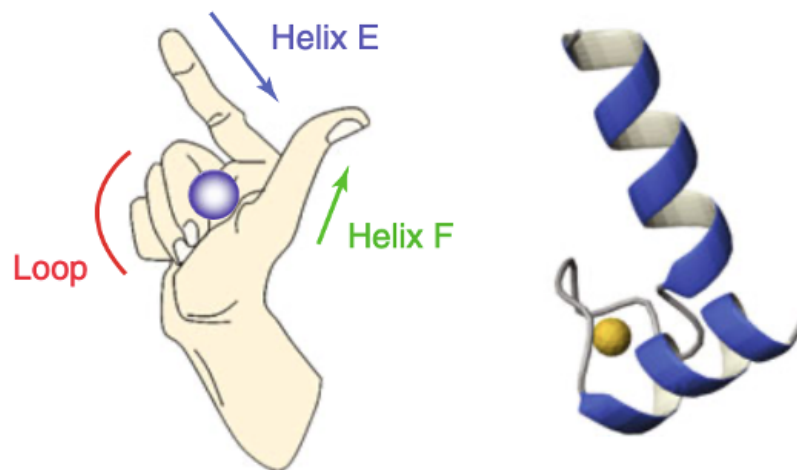


Figure 1.13 Schematic diagram of EF-hand motif.

The helix-loop-helix EF-hand Ca^{2+} -binding motif is commonly represented as a right hand due to resemblance; the index finger and thumb represent the E- and F-helices, respectively, the middle finger mimics the loop where the Ca^{2+} ions bind. Adapted from Ishida & Vogel, 2013.

Overall, the endothelium comprises a dynamic and diverse Ca^{2+} toolkit (Figure 1.14) that allows it to expertly operate numerous crucial physiological processes. It is becoming clear that the intracellular Ca^{2+} is released not only from the ER but also from other inner stores, such as the endo-lysosomes, and that the stores engage in functional cross-talk. Such diverse Ca^{2+} signals together with specific Ca^{2+} sensors are likely to be involved in the mechanisms ECs distinguish and respond to the myriad of agonists that they encounter in the blood.

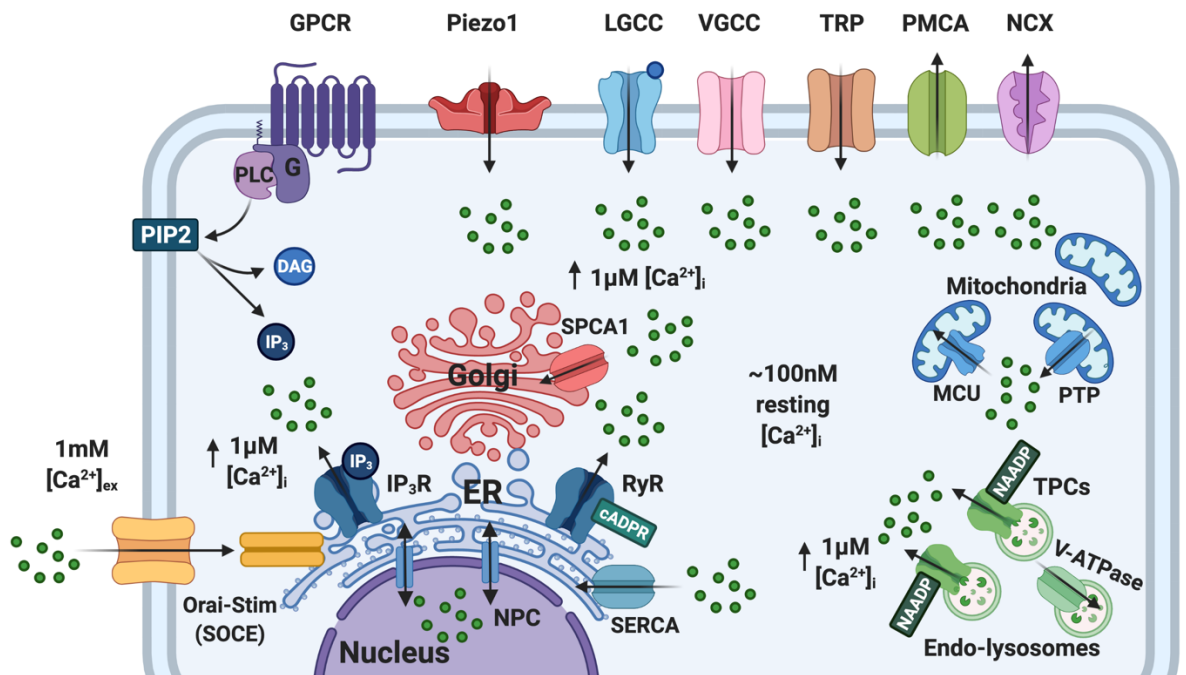


Figure 1.14 Endothelial Ca^{2+} signalling toolkit.

Endothelial cells have an extensive signalling toolkit that can be mixed and matched to create, respond or quench Ca^{2+} signals of widely different properties. G-protein coupled receptor (GPCR), Phospholipase C (PLC), Phosphatidylinositol 4,5-bisphosphate (PIP2), Diacylglycerol (DAG), Ligand-gated Ca^{2+} channel (LGCC), Voltage-gated Ca^{2+} channel (VGCC), Transient Potential Receptors (TRPs) channels Plasma membrane Ca^{2+} ATPase (PMCA), $\text{Na}^+/\text{Ca}^{2+}$ Exchanger (NCX), mitochondrial uniporter complex (MCU), mitochondrial permeability pore (PTP), Two-pore channels (TPCs), nicotinic acid dinucleotide phosphate (NAADP), Vacuolar-ATPase (V-ATPase), Sarcoendoplasmic reticulum Ca^{2+} -ATPase (SERCA), Ryanodine receptor (RyR), cyclic ADP ribose (cADPR) Inositol 1,4,5-trisphosphate receptor (IP3R), Store-operated Ca^{2+} entry (SOCE), Nuclear pore complex (NPC), Calcium-transporting ATPase type 2C member 1 (SPCA1).

1.4 Rab GTPases – masters of intracellular transport

In addition to Ca^{2+} signalling, vesicular trafficking and exocytosis is regulated by Rab GTPases. All eukaryotic cells are defined in part by their multiple and complex organelles, with some cell types even having specialised organelles (e.g. WPBs in ECs). Though valuable, this complexity of organelles requires organisation and management through active transport machinery for the exchange of messages or material between the organellar compartments. This molecular transfer is achieved through packaging of molecules into vesicles. Once produced, these vesicles are coated with a membrane containing specific binding sites to ensure accurate recognition by transport proteins (also named motor proteins). Arriving at the correct organelle vesicles are then tethered and fused with the membrane of the target organelle (Zerial and McBride, 2001; Barr, 2013). Cells coordinate this complex transport system by using Rab GTPases.

Rab GTPases constitute the largest subfamily of small GTPase proteins (20–29 kDa) in the Ras superfamily. In addition to Rabs, the Ras superfamily comprises other types of small GTPases including Ras, Rho, Ran and Arf (Colicelli, 2004). Rab GTPases proteins were first identified as Ras-related genes expressed in rat brains in 1987 (Touchot et al., 1987). More than 30 years after, researchers have identified 70 Rab GTPase family members in humans, a number that reflects the complexity of their cellular functions. Rab GTPases are often referred to as the master regulators of membrane trafficking of cellular cargo (vesicles) because they mediate a range of intracellular innate processes such as cargo sorting, motility, transport and fusion with organellar membrane targets (Stenmark, 2009).

1.4.1 Rab GTPases regulation and function

Rab GTPases are ubiquitously expressed, several Rabs (Rab1, Rab5, Rab6, Rab7 and Rab11) are found in all eukaryotic genomes suggesting their role in eukaryotic cells is vital and indispensable (Klöpffer et al., 2012). Other Rab subfamilies are expressed in cell and function specific manners. Despite major structural and biochemical similarities, Rab GTPases are involved in multiple and divergent fundamental cellular processes (Pylypenko et al., 2018). Rabs carry out these processes by localising to specific intracellular membranes and recruiting a diverse set of Rab effectors (e.g. tethering factors, molecular motors, phospholipid modulators; Hutagalung and Novick, 2011).

Generally, Rab GTPase are structured and cycle in a similar manner to typical Ras-like small GTPases. They are nucleotide dependent molecular switches that are ON in the GTP-bound (active) form and OFF in the GDP-bound (inactive)

form (Figure 1.15). This switching between GDP- and GTP-bound forms of Rab GTPases entails large conformational changes which requires recruitment of effector proteins. Exchange of GDP with GTP is catalysed by guanine nucleotide exchange factors (GEFs), which recognise specific regions in the switch regions and facilitate GDP release (Delprato et al., 2004). In the GDP-bound state, the switch regions appear to be unfolded, whereas they adopt well defined conformations when GTP is bound, allowing further binding of specific effectors. The high levels of cytosolic GTP (~1 mM) contribute to the fast exchange with GTP upon GDP release (Gabe Lee et al., 2009). Several types of specific effector molecules, including sorting adaptors, tethering factors, kinases, phosphatases and motors, can be activated or recruited by the GTP-bound Rab. Several GEFs may act on a particular Rab protein in response to a distinct upstream stimulus, providing multiple avenues for intracellular signal regulation (Müller and Goody, 2018; Rodríguez-Fdez and Bustelo, 2019). Additional conversion from the GTP- to the GDP-bound form occurs through hydrolysis of the GTP molecule, which is driven by the intrinsic GTPase activity of the Rab protein and further catalysed by GTPase-activating proteins (GAPs). To date more than 38 different human Rab GAPs have been described with the potential for more GAPs to be yet discovered (Haas et al., 2007).

Apart from GEFs and GAPs, there are other regulatory proteins that interact with the inactive, GDP-bound Rab GTPases. Initial studies identified Rab GDP dissociation inhibitors (GDIs) as proteins that prevents GDP dissociation from Rabs, thereby preferentially rendering the protein into inactive state. Subsequent research has revealed that GDIs has important supplemented roles including acting as a chaperones to geranyl-geranylated Rab GTPases in the cytosol and enabling Rab transport to its target membrane (Ullrich et al., 1993; Ullrich et al., 1994). A similar function is governed by Rab escort protein (REP); REP deliver newly synthesized, unprenylated Rab GTPases to geranylgeranyl transferase to aid membrane targeting and delivery cycle (Shen and Seabra, 1996). Overall, despite numerous studies Rab GTPase targeting to specific membranes is still a topic of debate and incompletely understood due to multiple involved factors like post-translation modification of Rabs and their interaction with GEFs, GDIs and REP.

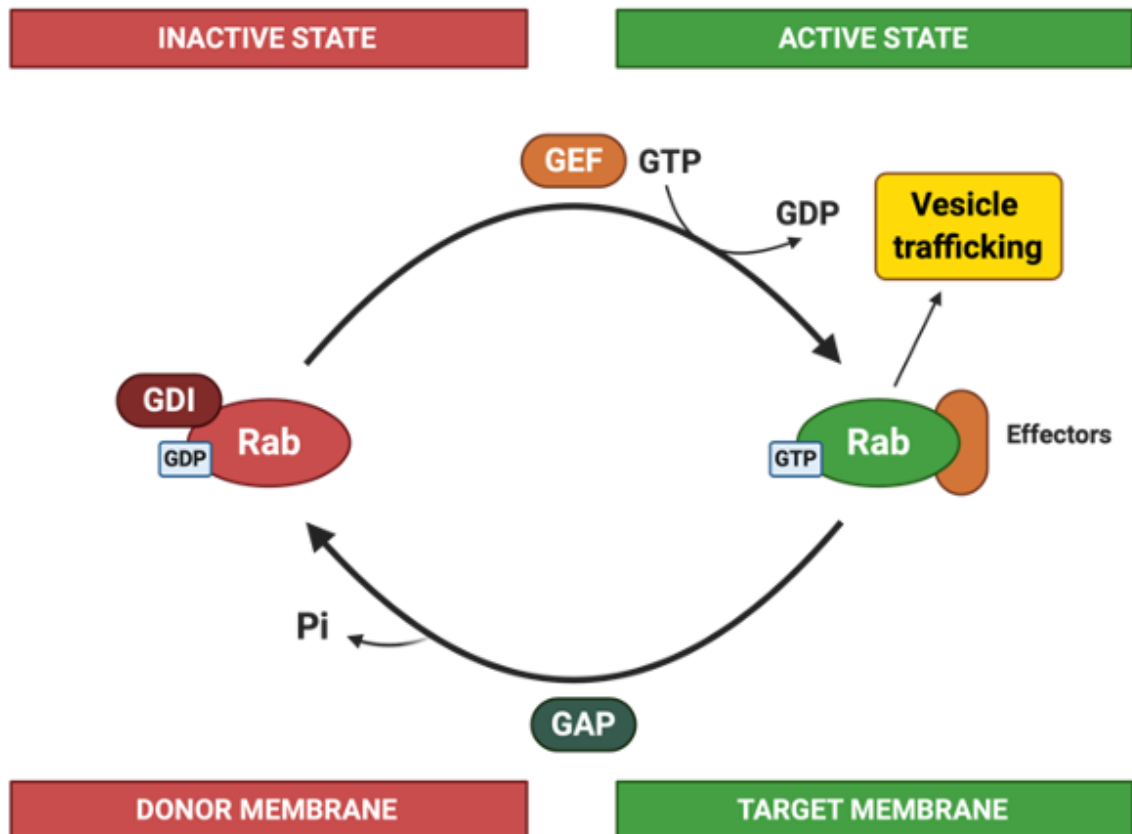


Figure 1.15 Rab GTPase cycling.

Rab GTPases switch between two conformations, an inactive GDP-bound form and an active GTP-bound form. In its inactive state, GDP-bound Rabs are translocated from a donor membrane to a target membrane. A guanine nucleotide exchange factor (GEF) catalyses conversion from GDP-bound to GTP-bound and GTP hydrolysis which leads to activation of the Rab GTPase at their target membrane. Activated Rab GTPases recruit further and type specific effectors to promote vesicle trafficking and other cellular processes. Rabs hydrolysis of GTP together with the enhancing effect of GTPase-activating protein (GAP) leads to Rab inactivation. Conversion of Rabs to the inactive state leads to binding of GDP dissociation inhibitors (GDIs) and effector dissociation from the Rab GTPase protein. The Rab GTPase then is removed from the target membrane by GDIs in preparation for the next cycle.

It is evident that by regulating all the essential steps in trafficking of cellular cargo and having multiple interacting partners, Rab GTPases are vital not only for the maintenance of cellular homeostasis but also for specialised intracellular signalling functions (Guadagno and Progidia, 2019). Rab GTPases are of a high physiological importance which is asserted by a number of pathophysiology due to acquired or inherited dysregulation of proteins of the Rab family such as:

- Neurodegenerative diseases including Alzheimer's disease, Parkinson's disease and Amyotrophic Lateral Sclerosis (ALS; Kiral et al., 2018)
- Cancer progression and metastasis (Seabra et al., 2002)

- Immune diseases and infections including Griscelli syndrome (Ménasché et al., 2000), Crohn's disease (Ohira et al., 2009) and bacterial infections (*Mycobacterium tuberculosis*, *Salmonella enterica* etc; Smith et al., 2007)

There are numerous Rab GTPases expressed in ECs (Table 1.1.2). Most of these are ubiquitously expressed in all cell types and are involved in the endo-lysosomal system trafficking. In particular, Rab3D and annexin 2 provide mechanism of selective exocytosis of vWF but not tPA (Knop et al., 2004). Additionally, a study by Zografu and colleagues, have shown that Rab27 and Rab15, and their effector Munc13-14, mediate WPB in additive manner, while Rab33a and Rab37 seem to localise to the Golgi but their function remains unknown. In addition, there are still several endothelial Rab GTPases with unidentified function (Zografu, 2012). Another endothelial Rab GTPase, Rab35, is also located on the WPB and has been found to participate in WPB exocytosis (Biesemann et al., 2017). To date there are no reports of particular endothelial Rabs involved in any vascular-related conditions. However, further defining Rab GTPases function in the endothelium remains of interest, considering their functional versatility and participation in the endo-lysosomal system, which is important not only in trafficking but in intracellular signalling.

Table 1.1.2 Endothelial Rab GTPases.

Endothelial Rab GTPases	Function
Rab1	ER-Golgi trafficking
Rab2	ER-Golgi trafficking
Rab3b,d	Biogenesis & exocytosis of WPBs
Rab4	EPCR trafficking
Rab5	Marker of early endosomes
Rab6	Golgi trafficking
Rab7	Marker of late endosomes
Rab8	Golgi trafficking
Rab9	VE-Cadherin internalisation
Rab11	Marker of recycling endosomes
Rab13	Autophagy
Rab15	Exocytosis of WPBs

Rab22	Endosomal compartments interaction
Rab27a	Maturation and exocytosis of WPBs
Rab30	Golgi trafficking
Rab33a	Localised to WPBs, unknown function
Rab35	Exocytosis of WPBs
Rab37	Localised to WPBs, unknown function

1.4.2 CRACR2A (Rab46) discovery - One gene, two isoforms

Orai1 and STIM1 are the main components forming the CRAC channels that mediate SOCE (see section 1.2.1.1). Orai1 and STIM1 co-cluster and physically interact to mediate Ca^{2+} influx through SOCE, the exact molecular identify of the cytoplasmic machinery that modulates said co-clustering remained poorly understood for several decades. In 2010 Srikanth and colleagues, using affinity protein purification identified a novel Ca^{2+} -sensing EF-hand protein, CRACR2A (also commonly referred to as CRAC regulator 2A, Cracr2a-c, EFCAB4B or FLJ33805)(Srikanth et al., 2010). They showed that in their model system, T cells, CRACR2A interacts directly with Orai1-STIM1 and forms a ternary complex. Upon Ca^{2+} influx through the CRAC channel, CRACR2A senses the elevated Ca^{2+} concentrations and disperses the Orai1-STIM1 clusters thereafter. siRNA knockdown and mutagenesis showed that CRACR2A has an important role and SOCE does not occur in T-cells void of CRACR2A or in T-cells expressing inactive CRACR2A mutant.

SOCE has a positive role in ECs cell migration induced by VEGF, hence several years later in 2015 Lesley Wilson and Lynn McKeown in Leeds sought to investigate CRACR2A's relevance in endothelial CRAC channels assembly and SOCE. Unexpectedly, CRACR2A siRNA depletion in HUVECs failed to inhibit SOCE or to detect CRAC2A protein band (~45 kDa) with anti-CRACR2A antibody(Wilson et al., 2015). However, they observed a double protein band at ~95 kDa that was labelled by the antibody, wherein the lower was depleted by two different siRNAs targeted to CRACR2A (Figure 1.16). Furthermore, it was found that the gene encoding CRACR2A, *efcab4b*, is predicted to undergo alternative splicing into two CRACR2A isoforms that were different in length.

Alignment of the predicted protein sequences of the short (CRACR2A-S) and long (CRACR2A-L) isoforms revealed that the N-terminal components (Ca²⁺ EF-hand domain) are identical but that CRACR2A-L contains a distinct long C-terminus. They predicted that this may explain the discrepancies they observed described above. Full-length cloning and sequencing in HUVEC showed that the long isoform, CRACR2A-L, is the only CRACR2A isoform in ECs. Analysis of the long C-terminus of CRACR2A-L indicated conserved sequences characteristic of Rab GTPase proteins and suggested that CRACR2A-L is a previously unrecognised member of the large Rab GTPase protein family. Rab GTPases are primarily a family of small proteins (20–29 kDa) and it is rather unusual that Rabs contain Ca²⁺-sensing EF hands. The group renamed CRACR2A-L to Rab46 in order to distinguish from the short non-Rab isoform CRACR2A-S. In this thesis, CRACR2A-L will be referred to as Rab46 hereinafter.

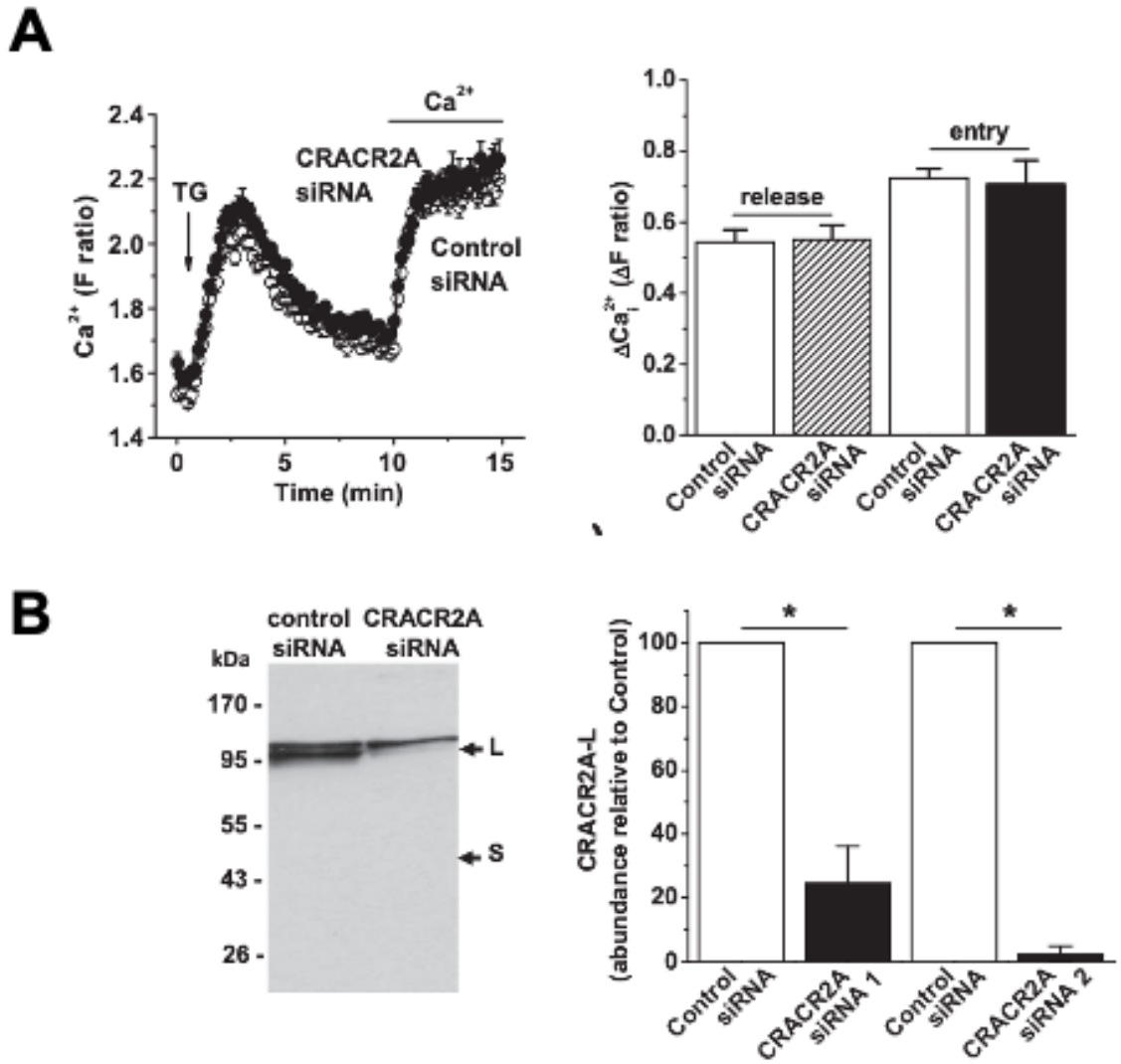


Figure 1.16 CRACR2A in endothelial cells.

(A) No effect of CRACR2A siRNA on CRAC channels in endothelial cells. Representative FlexStation intracellular Ca^{2+} trace for human umbilical vein endothelial cells (HUVECs) transfected with control siRNA or CRACR2A siRNA. (B) Detection of long but not short CRACR2A in endothelial cells. Western blot probed with anti-CRACR2A antibody for HUVECs transfected with control or CRACR2A siRNA. S indicates the expected mass for CRACR2A (short isoform). L indicates a larger protein (long isoform) which was depleted by CRACR2A siRNA. Adapted from Wilson *et al.*, 2015.

1.4.2.1 Rab46 – a large Rab in a small GTPase world

As mentioned above, Rab46 is an unusually large GTPase due to the fact that it has the extra EF-hand domain in addition to its conserved Rab GTPase domain. Before the discovery of Rab46 as a novel Rab GTPase with EF-hand domain, in literature there are only two Rab GTPases that are similar in size and structure to Rab46. Rab44 (108kDa) and Rab45 (83kDa), also contain Ca²⁺-sensing EF-hand domains (Figure 1.17). Two studies have reported that Rab44 EF-hands are important in sensing and transducing Ca²⁺ signals leading to differentiation via NFATc in osteoclasts and IgE-mediated degranulation in mast cells (Yamaguchi et al., 2018; Kadowaki et al., 2020). Rab45 was first characterised in 2007 as a self-associating Rab GTPase that primarily resides at the perinuclear area in HeLa cells (Shintani et al., 2007), whereas more recent report suggests Rab45 as a mediator of p38 activation in chronic myeloid leukaemia progenitor cells (Nakamura et al., 2011). The functional significance or potential binding partners of the EF-hand domain of Rab45 are undetermined. Similarly to Rab46, Rab44 and Rab45 are equally not very well described but aforementioned reports suggest that the presence of extra Ca²⁺ sensing EF-domain adds another layer of complexity in the regulation of Rab GTPases and their cellular functions.

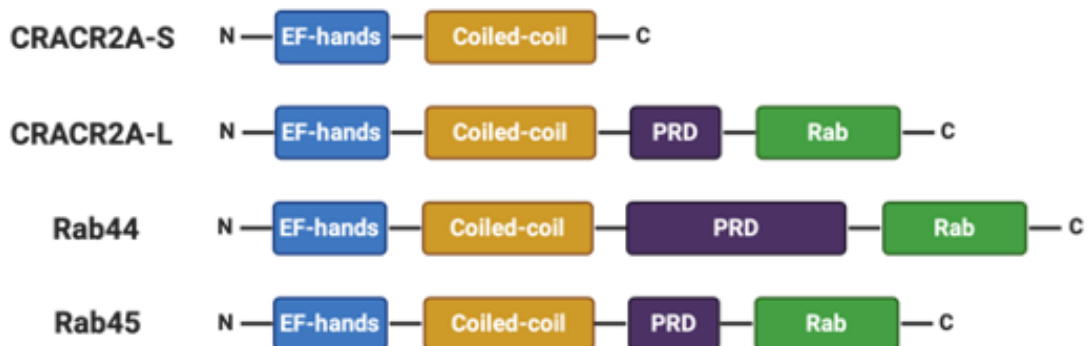


Figure 1.17 Structural similarities between CRACR2A isoforms and other EF-hand proteins.

At the N-terminal, All CRACR2A-S, CRACR2A-L (Rab46), Rab44 and Rab45 have all in common Ca²⁺ -binding EF-hand domains and protein-protein interaction coiled-coil domains. Rab44 and Rab45 have a very high similarity in their overall structure with CRACR2A-L (Rab46) further comprising highly conserved Rab GTPase domains and proline-rich domains (PRD) at their C terminal.

In 2016, in addition to CRACR2A-S, Srinath and colleagues reported the presence of Rab46 in human and murine T cells (Srikanth et al., 2016). In their study they referred to CRACR2A-S as *cracr2a-c* and Rab46 as *cracr2a-c*. In this study, they validated Rab46's GTPase domain activity by directly showing its ability to hydrolyse GTP. Nucleotide binding mutants (T559, Q604, and N658) showed an altered GTPase due to defects in GTP binding (T559N and N658I mutants) and GTP hydrolysis (Q604L). Imaging experiments revealed that in the absence of stimulation in T cells GFP-tagged WT Rab46 is localised to the TGN which is dependent on GTP binding and prenylation of the Rab domain. Upon T-cell receptor (TCR) activation, Rab46 translocates from TGN to the immunological synapse (IS) followed by subsequent activation of downstream signalling pathways resulting in phosphorylation of c-Jun N-terminal kinase (JNK). Whether this could be a potential role for Rab46 in ECs is currently unclear and it needs to be investigated. In addition to activation of the pathway, in T-cells Rab46 is also necessary for SOCE and NFATc1, as opposed to in ECs. Another study by the same group showed that *in vitro* deficiency of Rab46 decreases TCR signalling activation, thereby altering T-cells transcriptional program and differentiation. *In vivo*, an inducible *cracr2a*^{-/-} ameliorated T cells responses in acute autoimmune disease (Woo et al., 2018). These findings place Rab46 as important regulator of the immune system in health and in disease states.

Recently, Ron Vale's group has expressed an interest in Rab46 and further described its role in T-cells (Wang et al., 2019). The group provided evidence that both Rab45 and Rab46 are unusual adaptor proteins that activate the motility of the retrograde motor protein dynein. Previously, Rab GTPases have been shown to bind directly to dynein adaptor proteins such as Rab6 and Rab11FIP3. In these Rabs, the Rab binding domains **do not directly** bind to dynein, instead they primarily recruit specific adaptors (McKenney et al., 2014; Huynh and Vale, 2017). Conversely, Vale's group data indicates that Rab46 and Rab45 are indeed the first described Rab GTPase dynein adaptors. Furthermore, they showed that Rab46 interaction with dynein is Ca²⁺-dependent and that TCR-induced Ca²⁺ release triggers Rab46–dynein–mediated trafficking. Consistent with previous findings about dynein-dependent retrograde trafficking, it was shown that upon TCR activation, Rab46 traffics from the IS to the microtubule organising centre (MTOC), suggesting that Rab46 interacts with dynein in order to regulate endocytic transport in T-cells.

Alongside aforementioned studies in T cells, our group in Leeds has further characterised Rab46 role in ECs. In our joint study (K. T. Miteva et al., 2019) and Dr Lucia Pedicini thesis, we showed that endothelial Rab46 localises to WPBs (Figure 1.18A, B). Our lab has shown that in ECs Rab46 mediates retrograde

trafficking of WPBs towards the MTOC at the perinuclear area, dependent on the GTP-binding of Rab46's Rab domain (Figure 1.18A, B). Considering the nature of this unusually large Rab GTPase protein that has the capabilities to sense intracellular Ca^{2+} and our current findings, it is evident that Rab46 has a significant, perhaps selective, role in WPB trafficking. How is Rab46 involved in WPB trafficking requires further investigation, details on such are described in the following chapters of this thesis.

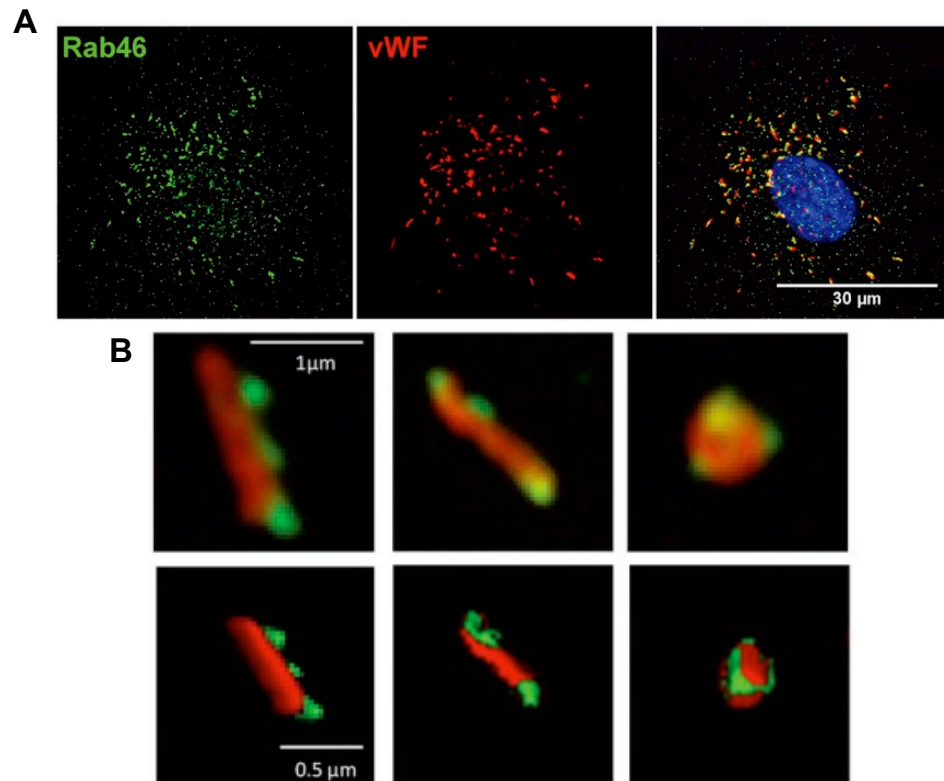


Figure 1.18 Rab46 localises to WPBs.

(A) Immunofluorescent images showing subcellular localization of endogenous Rab46 (green) and vWF (red) in HUVECs. Maximum-intensity projections from DeltaVision or confocal microscopy z stack are shown. Scale bar = 30 μm. (B) High-resolution Airyscan imaging (top panels) and 3D reconstruction (bottom panels) showing single WPBs (vWF, red) where Rab46 (green) is juxtaposed to vWF. Scale bar = 0.5 μm. Adapted from Miteva *et al.*, 2019.

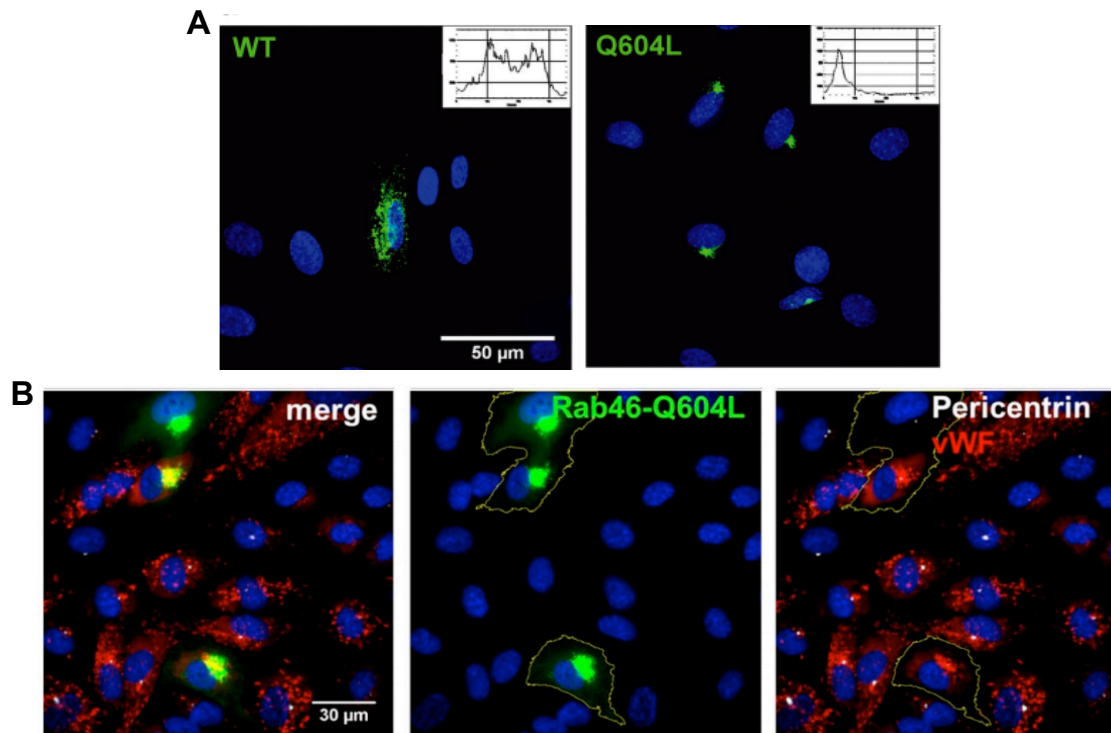


Figure 1.19 Rab46-dependent trafficking of WPBs to the MTOC.

(A) Representative image of HUVECs expressing WT Rab46 and a representative intensity plot with a random distribution (top left). Representative image of constitutively active form of Rab46 (Q604L) with its intensity plot where the peak indicates clustering (top right). Maximum-intensity projections from DeltaVision or confocal microscopy z stack are shown. Scale bar = 50 μm . (B) Constitutively active (Q604L) Rab46 localises vWF to the MTOC in the absence of stimulation. DeltaVision images of HUVECs immunostained for Rab46 Q604L (green), vWF (red), and pericentrin (white) as a marker of the MTOC in control cells. Scale bar = 30 μm . Adapted from Miteva *et al.*, 2019.

1.4.2.2 CRACR2A and disease

In the previous section it became clear that CRACR2A-L or Rab46 is a protein of functional importance in ECs and T-cells. A genome-wide association study (GWAS) revealed that in CRACR2A gene (*efcab4b*) located on Chromosome 12 in humans, there is a link between a SNP and hepatic inflammation in non-alcoholic fatty liver disease (NAFLD; Speliotes *et al.*, 2011). Another GWAS study also showed *efcab4b* association with hypertension which may explain the genetic bases of hypertension as a comorbidity in NAFLD (Newton-Cheh *et al.*, 2009). Interestingly, a recent study identified *efcab4b* gene as a novel candidate gene involved in pulmonary arterial hypertension, a rare and severe disease affecting small pulmonary arteries and caused by abnormal proliferation of their smooth muscle cells and endothelial cells leading to an increase in pulmonary

vascular resistance and heart failure. The authors of the study suggest that disruptive variants at *efcab4b* gene could interfere with Ca^{2+} homeostasis of smooth muscle cells and/or endothelial cells in which intracellular levels are finely regulated to control vascular tone (Barozzi et al., 2019). Furthermore, single nucleotide variations in the *efcab4b* gene have been associated with the complex autoimmune condition, rheumatoid arthritis (Mitsunaga et al., 2013). Recently, another GWAS study identified associations between variants in *efcab4b* gene and the chronic periodontitis suggesting a possible role of this gene in the inflammatory response underlying pathogenesis of periodontal disease (Bevilacqua et al., 2018).

The research outlined above suggest that genetic variations in *efcab4b* gene may lead to the pro-inflammatory environment necessary for development of many human diseases which have a prevailing theme of chronic inflammation. Considering the pro-inflammatory role of some of WPB constituents, further investigations are required to fully understand the relationship between Rab46 and WPB trafficking, and their potential role in the molecular mechanisms driving the onset and progression of the aforementioned conditions.

1.5 Summary

In summary, once thought to be merely a physical barrier between the blood and the tissues, the endothelium is a dynamic monolayer lining our vasculature that can respond to variety of signals from the blood and in response regulate vital, but at times distinct, physiological processes (e.g. primary haemostasis, inflammation, angiogenesis, vascular tone).

The storage of WPBs armours ECs with pre-stored bioactive molecules and factors, such as vWF, P-selectin, Angiopoietin-2 and ET-1, and allows ECs to urgently respond to acute vascular emergencies, earning WPBs the title of 'the perfect vascular first aid kit'. One of the major intracellular pathways that mobilises WPBs exocytosis is Ca^{2+} release from the intracellular stores. However, the presence of multiple agonists sharing common downstream Ca^{2+} signalling pathways suggests that there are unidentified players in those pathways which distinguish signals in agonist-specific manner, allowing the ECs to tightly regulate and differentially secrete WPB subpopulations to deliver an accurate physiological response. Additionally, recent discoveries (Brailoiu et al., 2010b; Esposito et al., 2011; Faviaa et al., 2014b) has shed more light on the fact that the endothelial Ca^{2+} signalling is a very complex network of inner stores, ion channels and Ca^{2+} sensors, exact mechanisms of which we do not yet fully understand.

A novel large Rab GTPase, CRACR2A-L (Rab46) was identified in ECs and it was found that it colocalises with WPBs. Unlike the canonical role of small Rab GTPases, Rab46 contains multiple functional domains including a Ca^{2+} -sensing EF-hand domain. The localisation of this large GTPase on WPBs raises the possibility that Rab46 could selectively couple agonist-evoked Ca^{2+} signals to differential trafficking and/or exocytosis of WPBs.

1.6 Hypothesis, Aim and Objectives

Aim

Novel Rab GTPase Rab46 is colocalised with WPBs in ECs. In addition to Rab domain, Rab46 has a Ca^{2+} sensing EF-hand domain which raises the possibility that Rab46 may play a role in the coupling cytosolic Ca^{2+} elevation in response to stimulus in the endothelium. This demonstrates that Rab46 is a potential candidate in regulation of WPB trafficking and exocytosis.

Understanding mechanisms of stimuli-coupling and the signalling pathways of this novel endothelial Rab GTPase in the endothelium could lead to discovering new endothelial trafficking mechanism and new targets to rescue WPBs exocytosis dysfunction in diseases of the cardiovascular system.

Hypothesis

Rab46 is a Ca^{2+} -regulated Rab GTPase that couples incoming endothelial stimuli to selective WPB trafficking.

Objectives

1. Establish the role of Rab46 in trafficking of WPB subpopulations in response to the endothelial stimuli, histamine and thrombin; and
2. Investigate the signalling pathways of Rab46-dependent differential WPB trafficking in response to histamine;

Chapter 2 Methods

2.1 Reagents

Chemicals and reagents were obtained from Sigma Aldrich (Germany) unless indicated otherwise. Epinephrine, isobutylmethylxanthin (IBMX) and Bafilomycin A1 were obtained from Cayman Chemical USA). *Trans*-Ned19, 2-Pyridylethylamine dihydrochloride, 4-Methylhistamine dihydrochloride, H-89 dihydrochloride and cAMPS-Rp triethylammonium salt were obtained from Tocris Bioscience (UK).

2.2 Cell culture

2.2.1 HUVECs

Pooled human umbilical vein endothelial cells (HUVECs) were obtained commercially (Lonza Inc) and grown in endothelial basal cell medium 2 (EBM-2) supplemented with EGM-2 Singlequot endothelial growth supplements (Lonza) or EBM-2 supplemented with Endothelial Cell Growth Medium 2 SupplementPack (PromoCell GmbH). HUVECs were maintained in a standard cell culture incubator at 37°C in a humidified atmosphere of 5% CO₂ and used between passages 1-5. Grown to approximately 80-90% confluency HUVECs were briefly washed in Ca²⁺ free PBS and detached via 0.05% trypsin (Gibco). HUVECs were re-seeded onto cell culture plastics at cell density appropriate to each experimental setup. All cell culture treated plastic ware was provided by Corning Inc.

2.3 Transfection

2.3.1 Short-interfering RNA (siRNA) transfection

Control siRNA (UGGUUUACAUGUCGACUAA), EFCAB4B (Rab46) siRNA Silencer® Select (GUGUGAAGGUCAAAAAGAGAtt) and Angiopoietin-2 siRNA (CCUCCAAACUUGAACGGAAAtt) were obtained from Ambion Inc. Pooled P-selectin siRNA (GCUGAGAGGAGCCGAUUAUA, GCUGAGAACUGGGCUGAUA, GUAAAGCUGUGCAGUGUCA, CUAGAGGGCCAGUUACUUA) was obtained from Dharmacon. HUVECs used at 80-90% confluence for transfection. Transfection performed using a 1:3 ratio of 50 nmol/l siRNAs with Lipofectamine™ 2000 reagent (Invitrogen) diluted in Opti-MEM® medium (Gibco) as per manufacturer instructions. Cells incubated with the transfection solution for 6 hours before the transfection media was exchanged with fresh

EBM-2 media. Knockdown assessed via Western blotting or RT-qPCR. All experiments performed at 48 and 72 hours post-transfection.

2.3.2 cDNA transfection

HUVECs plated into Ibidi μ -slide 8 well (7×10^4 cells/ml, 300 μ l per well) transfected after either 6 or 24 hours using LipofectamineTM 2000 (Invitrogen) in Opti-MEM[®] medium (Gibco). A 1:3 ratio between cDNA (100 ng) and LipofectamineTM 2000 was used. Rab46 sequence was cloned from HUVECs and Rab46 mutant plasmids were made in-house by Dr Lynn McKeown. Plasmids were sequenced via GeneWiz to ensure sequence accuracy. Plasmid sequences can be found in Table 2.1.

Table 2.1 Plasmid sequences of Rab46 mutants.

Solutions	Composition
EF-hand mutant	<p>Ggccagctagtcatgctgaggaaggcacaggagtctttcagacctgtgctgctgctg tgcaggCaagggctcatcgccaggaaggatgagcagaggctgcataagga gctaccgctcagcCtggaggaactggaggatgtgtttgatgccctggatgctg atggcaatggctatctgacccacaggagttcactactggatttagtcacttcttc ttcagccagaataac</p>
Q604L Rab domain mutant	<p>Cctgaccggctctcaagattgtgttcgtgggcaattccgcggtggggaagac atccttcTgaggagattctgtgaggaccggttctcccaggcatggcggcca ctgtgggcattgattacCgtgtgaagacgttgaatgtggacaactctcaggtgg ccctgcagctgtgggacacggctgGgctggagaggtaccggtgcatcaccca gcagttctcagaaaggcagatgggtcatcgtCatgtacgatctcacagacaag cagtcggtcctgtcgggtccggcggtggctgagcagcgtgGaggaagctgtggg agaccgggtgcctgttctctgctgggtaataagcttgacaacgagaaGgagcg ggaagtccccggggcctcggagagcagcttgccacggagaacaatctgatct tctatgaatgcagcgcctactctggtcacaacaccaaagagtccctgctccatctg gccaggtcctcaaggagcaagaagacacagtgagagaggacaccattca ggtcggc</p>

2.4 ELISA

2.4.1 Angiopoietin-2 ELISA

HUVECs grown for 72 hours in 6-well plates until formation of confluent monolayers with daily media exchange. Prior to experiments, cells were starved in serum-free M199 (Gibco) supplemented with 10 mM HEPES (Gibco) for 60 minutes. The medium was fully removed and cells were treated with compounds, all diluted in fresh M199 supplemented with 10mM HEPES. Only M199 supplemented with 10 mM HEPES or vehicle solvent was applied on control cells. Cell supernatants were collected at room temperature and stored at - 20°C for later analysis. Angiopoietin-2 concentration in cell supernatant was measured using Human Angiopoietin-2 Quantikine ELISA Kit (R&D Systems). ELISA was performed according to manufacturer instructions.

2.4.2 P-selectin surface ELISA

HUVECs were seeded in 96-well plates at cell density 5×10^4 /well and grown to confluency for 72 hours with daily media exchange. HUVECs were serum starved for 60 minutes prior to control serum-free M199 supplemented 10mM HEPES or compound treatment. All reagents were brought to room temperature prior to the experiment. After respective treatments were terminated, cells were washed with PBS and incubated with 4% paraformaldehyde for 5 minutes, followed by blocking step with bovine serum albumin (BSA). Incubation with P-selectin primary antibody (Santa Cruz) and horse radish peroxidase-conjugated secondary antibody (Jackson ImmunoResearch) solution was performed at room temperature. Tetramethylbenzidine (TMB) substrate was added for 5 minutes with gentle agitation until characteristic colour change was obtained (Figure 2.1). The reaction was terminated with an equal amount of 0.5 M of H₂SO₄ and read 450nm on a multi-modal microplate reader Flexstation II 384 (Molecular Devices).

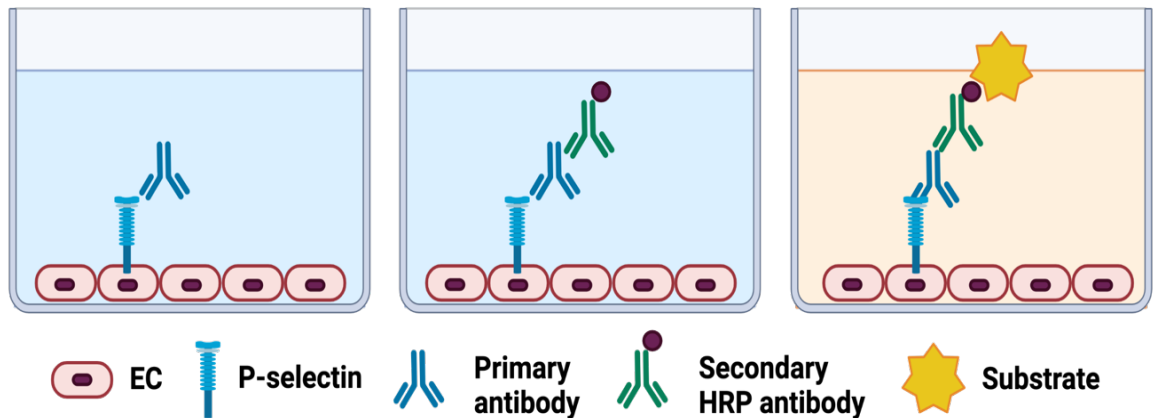


Figure 2.1 P-selectin cell surface ELISA.

The endothelial monolayer was stimulated with relevant treatments and fixed. P-selectin primary antibody was used to recognise P-selectin released on the cell surface of the monolayer. HRP-bound secondary antibody was used to attach to the primary antibody. Addition of substrate (TMB) causes a reaction with the HRP secondary antibody and characteristic colour change.

2.5 Western blot

Cells were seeded onto 6-well plates at cell density 4×10^5 /well and grown to confluency for 72 hours. Cells were then serum starved in serum-free M199 supplemented with 10mM HEPES for 60 minutes prior to treatment. Cells were first washed in cold PBS and 100 μ l NP-40 lysis buffer solution (including protease and phosphatase inhibitors cocktails; Sigma) was added to each well. Cell lysate was left on ice for 30 minutes to allow for sufficient lysis and then centrifuged at 12,000 rpm at 4°C for 10 minutes. Protein concentration of supernatants was determined via comparison to a BSA standard curve using DC Protein Quantification assay (BioRad) according to manufacturer instructions. Samples containing 10-20 μ g of protein mixed with 4x sodium dodecyl sulphate (SDS) loading sample buffer and were heated to 95°C for 5 minutes on dry heat block. Samples were loaded onto 7.5% or 4-20% TGX gels and resolved by electrophoresis in two stages - Stage 1 60V for 30 mins; Stage 2 120 minutes at 120V in running buffer.

Protein samples were then transferred onto a PVDF membrane (BioRad) at constant voltage 100V for 60 minutes for wet transfer and at constant current of 50 mA per membrane for 90 minutes for semi-dry transfer. Post-transfer the membrane was incubated for 60 minutes in 5% w/v milk or 2% BSA diluted in TBS-T for 60 minutes. Membrane was labelled overnight at 4°C with corresponding primary antibodies. Next day membranes were washed 4x 10 minutes in TBS-T, followed by 1 hour incubation with horse radish-peroxidase

(HRP) conjugated secondary antibody. Immediately after secondary antibody incubations, membranes were washed 4x 10 minutes in TBS-T and chemiluminescence imaging was performed using SuperSignal Femto (Pierce) or Super Sensitivity ECL (BioRad) detection reagents. Membranes were imaged using a G:BOX (Syngene) with genesis software. Band intensity were determined using ImageJ Fiji software measuring the mean grey intensity of each band and normalising it to that of protein loading control from the same sample (GAPDH or Vinculin). If membranes were re-probed with a different primary antibody, stripping buffer (ThermoFisher) was applied for 15 minutes at room temperature and the protocol was performed from the membrane blocking step. All buffer compositions used for Western blot are outlined below in Table 2.2.

Table 2.2 Western blot buffers

Solutions	Composition
4x SDS loading sample buffer	200 mM Tris pH 6.8, 8% SDS, 40% glycerol, 8% mercaptoethanol, 0.1% bromophenol blue
Running buffer	25 mM Tris, 192 mM glycine and 0.1% SDS, pH 8.3
Transfer buffer	48 mM Tris, 39 mM glycine, 0.5% SDS and 20% methanol
TBS-T	145 mM NaCl, 20 mM Tris-base, 0.5% Tween 20, pH 7.5

2.6 Immunoprecipitation

HUVECs plated in 10 cm Petri-dishes at cell density 1×10^6 /dish and were grown to confluency for 72 hours. Before harvesting, cells were washed 1x with PBS and protein cross-linking was achieved by application of 1% PFA (diluted in PBS) for 1 minute. This was followed by another wash with ice-cold PBS once and harvested with NP-40 lysis buffer. Lysates were left on ice for 30 minutes and then centrifuged at 12,000 g for 10 minutes at 4°C. Supernatant was quantified (as described above in Section 2.5) and 0.5 mg of total lysate was used to incubate with 2 µg of respective antibody or control IgG from the same species of the primary antibody for 4 hours at 4°C at continuous rotation. 40 µl of Protein G-Sepharose beads (washed) were added to the lysate/antibody mix and

incubated overnight rotating at 4°C. The following day the beads were pelleted, washed 3 times with ice-cold lysis buffer and then eluted with 4x SDS loading sample buffer. The samples were boiled at 95°C for 3 minutes on dry heat block and the immunoprecipitated fraction was analysed by Western blot (as described above in 2.5)

2.7 qRT-PCR

2.7.1 mRNA isolation

RNA was extracted using a phase-separation technique using TRI-reagent. 300 µl of ice-cold TRI-reagent was added to cells (plated in 6-well plate) in the end of respective experiments and then transferred in a sterile 1.5 ml eppendorf tube. 200 µl phenol-chloroform was added to all samples. The samples were briefly vortexed before undergoing centrifugation (12,000 rpm, 4°C for 15 minutes) to allow separation of the phases – RNA found in the top aqueous layer, DNA found in the middle layer and protein in the bottom layer. The RNA-containing phase was transferred to another sterile eppendorf tube and RNA was precipitated with the addition of 500 µl ice-cold isopropanol. Samples were left to incubate at 4°C for 15 minutes. The sample was then centrifuged again (12,000 rpm, 4°C, 15 minutes). RNA pellets were washed twice with 1ml of cold 75% ethanol and centrifuged (8,000 rpm, 4°C, 5 minutes). Ethanol was removed and the RNA pellet was air-dried at room temperature. The RNA pellet was briefly heated at 60°C and was dissolved in 10 µl nuclease-free water. RNA was also extracted using High Pure RNA Isolation kit (Roche). Protocol was performed according to manufacturer instructions. All RNA samples were stored at -80°C.

2.7.2 Reverse transcription

Complimentary DNA (cDNA) was synthesised using a High Capacity RNA-to-cDNA RT kit (Applied Biosystems). 1 µg of RNA was mixed with 5 µl 2x RT buffer, 1 µl 20x enzyme mix and nuclease-free water to make a 10µl total reaction volume. Non-reverse transcribed (-RT) control solutions were prepared and tested in parallel for each repeat. The solutions were mixed, centrifuged and incubated for 1 hour at 37°C followed by 5 minutes at 95°C. The cDNA was stored at -20°C or tested by real-time qPCR using SYBR green.

2.7.3 qRT-PCR

RT-qPCR was performed using SYBR Green I (BioRad) on a LightCycler 480 (Roche). Experiments were performed on 384 well plates (Corning). Each reaction well had a 10 µl total volume and contained the following: 5 µl of 2x

iTaq™ Universal SYBR® Green Supermix (containing antibody-mediated hot-start iTaq DNA polymerase, dNTPs, MgCl₂, SYBR® Green I dye, enhancers and stabilizers), 0.75 µl of forward primer (0.375µM), 0.75µl of reverse primer (0.375 µM), 1 µl cDNA and 2.5 µl nuclease-free water. Primer sequences and information are displayed in Table 2.3. DNA amplification started with 10 minutes at 95°C, followed by 40 cycles with 10 seconds at 95°C and 60 seconds at 60°C. The relative abundance of target genes amplified by RT-qPCR were calculated relative to two tested housekeeping gene, GAPDH and β-actin via the 2- $\Delta\Delta C_t$ method(Livak and Schmittgen, 2001).

Table 2.3 qPCR primers.

Target		Cargo function
Von Willebrand Factor	Forward	TTCCCGACAAGGTGTGTGTC
	Reverse	GCCTTCATGCAGAACGTAAGTG
Angiopoietin-2	Forward	CAAATGCTAACAGGAGGCTGGT
	Reverse	CAGGTGGACTGGGATGTTTAGA
Rab46	Forward	GGTCATCCTTGCCTACG
	Reverse	GCTCGCATGAGATCAAGT
H1R	Forward	TCTCTCTTTTCTGTGGGTTATTCC
	Reverse	CAGCTTAATTTCTGAGAAGGAAGG
H2R	Forward	ATACCACCTCTAAGTGCAAAGTCC
	Reverse	GATGGCTTCTAACACCTCATTGAT
H3R	Forward	CTGACTACTGGTACGAAACCTCCT
	Reverse	CTCCTCAGCAATTTTGTCTCTCTT
H4R	Forward	TGATCCCAGTCATCTTAGTCGCTTATTC
	Reverse	GGAGAAGGAACCCATTTTGGGAAGCAA
TPC1	Forward	TGGCTTTGAAAGGGAGCTCAAAC
	Reverse	CCGCCATTTTGTCTAGGTAGCTC
TPC2	Forward	GGTTGCTTGGGTTGTGCATT
	Reverse	CTCACTGCAGGTAGACAGCC

TRPML1	Forward	AGTGCCTGTTCTCGCTCATC
	Reverse	CCGGGATGCTTGATGGTGTC
TRPML2	Forward	AAAAATACCGAGCCAGACGC
	Reverse	AACGAACAAGCTGTGTGGTG
TRPML3	Forward	CGAGGCTGCTGGAGTCG
	Reverse	GATCTGCCATCTCTGGGGGA

2.8 Intracellular Ca²⁺ measurement

Intracellular Ca²⁺ was measured using multi-modal microplate reader Flexstation II 384 (Molecular Devices). The change (Δ) in intracellular Ca²⁺ concentration above baseline shown by the ratio of Fura-2-AM fluorescence emission for 340 and 380 nm excitation (Figure 2.2). The fluorescence ratio of ΔF 340/380 was utilised as an analysis measure. HUVECs were seeded (2.5×10^4 cells/well) onto clear-bottomed Nunc 96-well plates (ThermoFisher) and allowed to reach confluency for 24 hours. Cells incubated with a 2 μ M fura-2-AM loading solution containing 0.01% pluronic acid in Standard Bath Solution (SBS) for 60 mins at 37°C. SBS contained (mM): NaCl 134, KCl 5, MgCl₂ 1.2, CaCl₂ 1.5, HEPES 10, D- Glucose 8. pH was titrated to 7.4 with 4 M NaOH. Ca²⁺ free SBS had the same components but lacked CaCl₂ and contained 0.4 mM EGTA. From this point forward experimental plates were protected from light. Cells were incubated in SBS for 30 mins at room temperature and washed 3x with SBS prior to recordings to allow the de-esterification of the fura-2-AM. For experiments examining the effect of the pre-treatment of compounds, following fura-2-AM loading cells underwent incubation in 1.5 mM Ca²⁺ SBS containing the compound or its solvent at room temperature for 30 minutes or more.

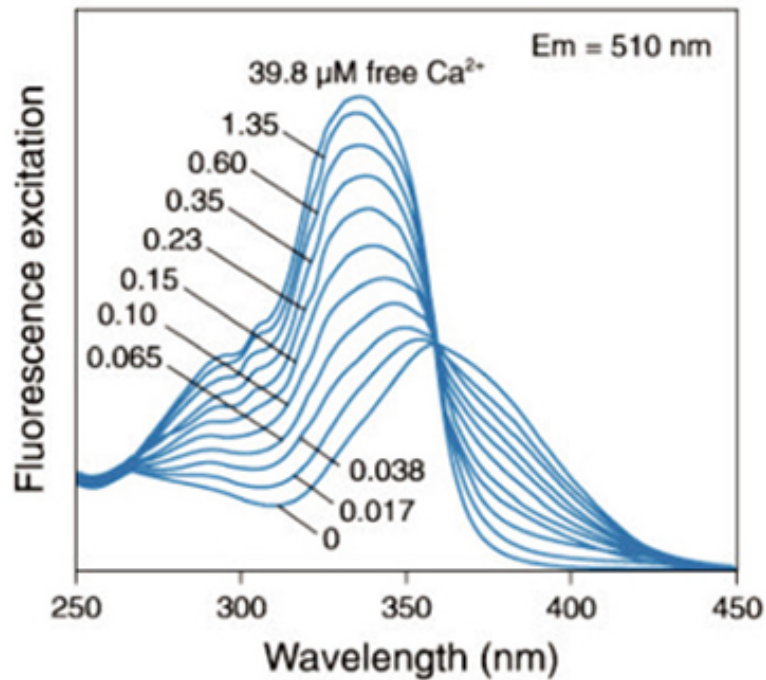


Figure 2.2 Fluorescence excitation spectra for Fura-2 in solutions containing increasing concentrations of free Ca^{2+} .

Increasing Ca^{2+} concentrations will cause the emission intensity at 510nm to rise at excitation wavelength 340nm and decrease at 380nm. Image taken from www.moleculardevices.com.

2.9 Immunocytochemistry

Cells seeded 8×10^4 cells/ml into Ibidi μ -slide 8 well. HUVECs were grown until confluency for 72 hours. Cells were starved in serum-free M199 plus 10 mM HEPES medium for 1 hour before treatments. Histamine was used at 30 μM unless otherwise stated, epinephrine hydrochloride was used at 100 μM in solution with 100 μM IBMX and thrombin used at 2.5 U/ml. Cells pre-treated with respective compounds for 30 minutes in related experiments before histamine stimulation unless stated otherwise. Cells fixed with 4% PFA for 10 minutes, washed 1x with PBS, permeabilised with 0.1% Triton-X solution. Cells incubated with a primary antibody (in PBS) for 60 minutes followed by fluorescently labelled appropriate species secondary antibodies for 30 minutes (Table 2.4, Table 2.5). Cells briefly incubated in Hoechst solution (1:1000) before being mounted with Ibidi mounting medium.

Table 2.4 Primary antibodies

Primary antibodies	Species	Dilution	Supplier & Cat Number
Anti-human vWF	Mouse	1:200	Dako M01616
Anti-human EFCAB4B	Rabbit	1:200	Proteintech 15206-1-AP
Anti-human EFCAB4B (Western blot)	Rabbit	1:800	Proteintech 15206-1-AP
Anti-pericentrin	Rabbit	1:100	Abcam ab4448
Anti-Angiopoietin-2	Goat	1:100	R&D Systems AF623
Anti-Angiopoietin-2 (Western blot)	Goat	1:1500	R&D Systems AF623
Anti-P-selectin	Mouse	1:100	Santa Cruz sc-271267
Anti-P-selectin (Western Blot)	Rabbit	1:1000	Proteintech 13304-1-AP
Anti-TPC1	Rabbit	1:100	Abcam ab94731
Anti-TPC2	Rabbit	1:100	Abcam ab119915
Anti-pCREB-1	Mouse	1:1000	Santa Cruz sc-81486
Anti-CREB-1	Rabbit	1:1000	Santa Cruz sc-377154
Anti-GAPDH	Rabbit	1:1000	GeneTex GTX100118
Anti-Vinculin	Mouse	1:2000	BioRad MCA465GA

Table 2.5 Secondary antibodies

Secondary antibodies	Dilution	Species
Alexa Fluor 488 anti-rabbit IgG	1:300	Jackson ImmunoResearch Labs 711-545-152
Alexa Fluor 594 anti- mouse IgG	1:300	Jackson ImmunoResearch Labs 115-584-003

Alexa Fluor 647 anti-mouse IgG	1:300	Jackson ImmunoResearch Labs 115-605-003
Alexa Fluor 594 anti-goat IgG	1:300	Jackson ImmunoResearch Labs 705-585-147
HRP anti-mouse IgG	1:5000	Jackson ImmunoResearch Labs 115-035-003
HRP anti-rabbit IgG	1:10000	Jackson ImmunoResearch Labs 111-035-144
HRP anti-goat IgG	1:10000	Jackson ImmunoResearch Labs 705-035-033

2.9.1 Microscopy

2.9.2 DeltaVision wide-field deconvolution microscopy

Cells visualised on an Olympus IX-70 inverted microscope using 20x/0.75 and 40x/1.35 oil objectives supported by a DeltaVision deconvolution system (Applied Precision LLC) with SoftWorx image acquisition and analysis software. 10 focal planes at 0.2 μm per z-stack were taken using a Roper CoolSNAP HQ CCD camera. The filter sets used were DAPI, FITC, and TRITC.

2.9.3 High-resolution Airyscan microscopy

High-resolution microscopy performed using an inverted confocal laser-scanning microscope Zeiss LS880 with Airyscan system (Figure 2.3). Images were captured using a 63x/1.4 oil objective and 405 nm Diode; Argon/2 (458, 477, 488, 514 nm); HeNe 543 nm and HeNe 633 nm lasers. All the images acquired and processed with Zen software.

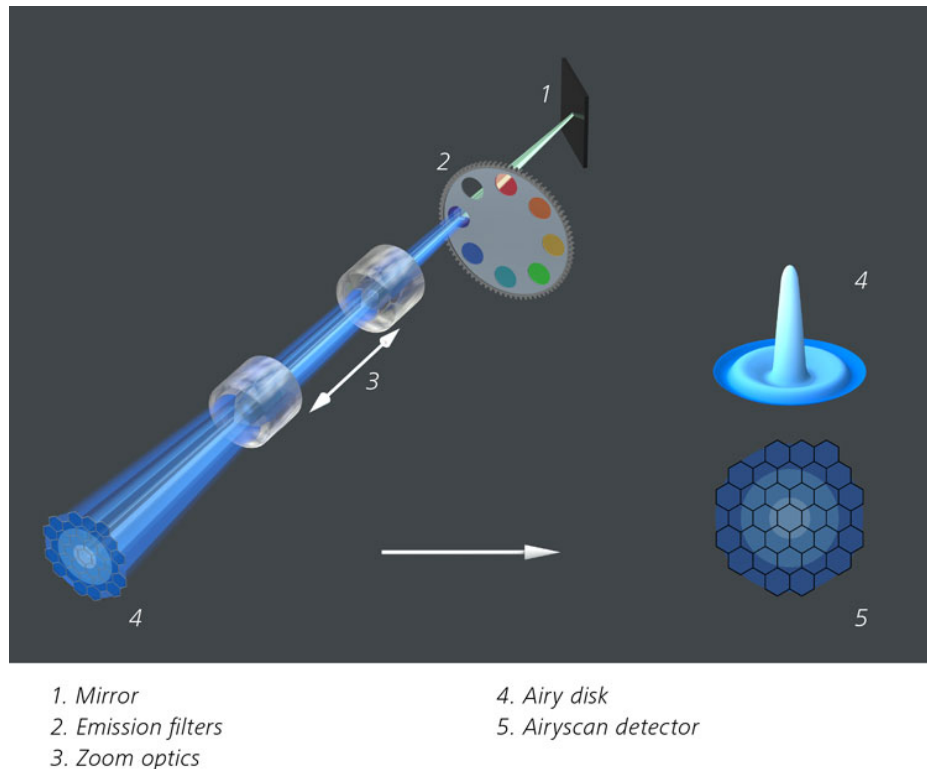


Figure 2.3 AiryScan imaging principle.

Light from samples is projected onto 32 channel GaAsP detector and the hexagonal design (5) allows to detect the Airy orders in one snap without losing any signal. A better signal-to-noise, resolution and speed is achieved (www.zeiss.com).

2.9.4 Image analysis

Maximum intensity projections and 3D surface rendering images performed using DeltaVision Softworx or Zen accordingly and analysed in ImageJ Fiji. In ImageJ the channels split, then vWF and Rab46 channels subjected to background subtraction depending of the noise level. The noise estimated using a region of interest in the background for measurement and the mean subtracted to the entire image. Pixels whose intensity values are similar to the background replaced with the mean background intensity value.

WPBs counting. For WPBs counting segmentation of WPBs was then applied. A local threshold algorithm (Bernsen method) with 15 radius applied and a binary image was created. The numbers of objectives calculated according to their size in every image and normalized to the numbers of nuclei per image. Number of vWF positive cells and the number of nuclei determined using cell counter plugin.

2.9.5 Rab46 and WPB distribution

Cellular distribution and particle intensity was determined using Fiji. Images were blinded prior to analysis. A customised macro designed to automate the analysis.

Briefly, a 16-bit image was loaded in Fiji. The channels split and a binary mask created using a Default threshold on the DAPI channel. Noise reduced using a median filter (value 2) and if required adjacent nuclei were split using the watershed algorithm to allow for accurate segmentation and distance map measurements. A distance map was generated. Green and red channels duplicated to sample the original pixel intensities of WPBs and Rab46 structures. Each channel segmented using a threshold algorithm (Max Entropy) and the distance and intensity of each particles from the nucleus was measured. Particles at the nucleus were given pixel value 0 and particles at the edge of the distance map were given value of 255. The macro automatically exports, unbiased raw data results tables with distance and intensity values per each particle, binary images of the distance map and .tiff images of each channel per analysed image. 5 to 10 widefield images (40x) were analysed per experimental group. Distance (Min) and integrated intensity (IntDen) values imported in OriginPro as X and Y values respectively. Distance values range from 0 px (nucleus) to 255 px (Periphery). This list of numerical values was binned into three areas: Perinuclear ($x < 2 \mu\text{m}$) – Intermediate ($2 \mu\text{m} < x < 5 \mu\text{m}$) – Periphery ($x > 5 \mu\text{m}$) where x is the distance from the nucleus to cells periphery (Figure 2.4). The integrated intensity normalized by the total fluorescence intensity of the image. The mean values were calculated for each area and averaged among all analysed images. The mean values averaged among all the biological repeats were presented as bar-plots with mean \pm SEM where Y-axis denoting “Normalized (integrated) intensity” and the X-axis denoting the distance from the nucleus indicated the average distribution of the analysed signal based into the three areas in the analysed cell population.

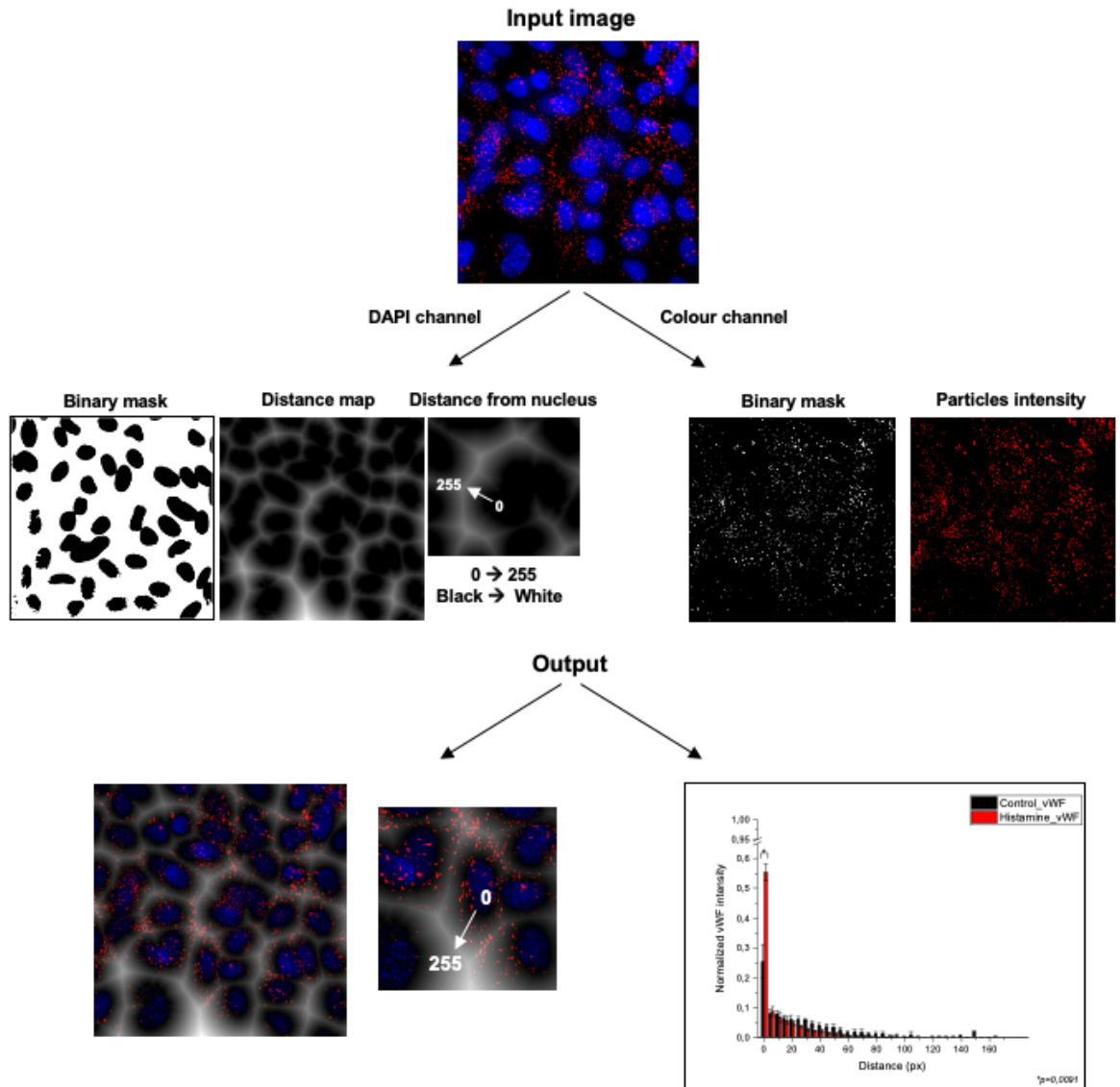


Figure 2.4 Quantification of vWF and Rab46 cellular distribution.

Raw unprocessed images were uploaded on Fiji as input. All channels were separated and binary masks were generated. A distance map was generated on the DAPI channel where each pixel is replaced with a grey value equal to that pixel distance from the nearest background pixel (nucleus: black = 0, white = 250). Distance from the nucleus of each segmented particle on the red or green channel, with their respective intensities was measured. Therefore, the outputs (distance and intensity measurements) of the summarised workflow were analysed and plotted in OriginPro. The distance is on the x-axis and the mean normalized intensity is on the y-axis.

2.9.6 P-selectin/Angiopoietin-2 colocalisation

P-selectin and Angiopoietin-2 colocalisation with Rab46 was quantified using the spot colocalisation ImageJ plugin ComDet on raw images acquired by DeltaVision. ([https://imagej.net/Spots_colocalization_\(ComDet\)](https://imagej.net/Spots_colocalization_(ComDet))).

2.10 Statistical analysis

All average data is represented by mean \pm S.E.M. Paired t-test performed as appropriate when comparison among two data groups was sought. For comparison among three or more mean values, one- or two-way ANOVA performed to determine whether significant differences exist amongst groups, coupled with Bonferonni post hoc test. Statistical significance was considered to exist at probability (p) < 0.05 (* < 0.05 , ** < 0.01 , *** < 0.001). Where comparisons lack an asterisk, they were not significantly different and/or marked as not significant, n.s. OriginPro 2017 software (USA) used for data analysis and presentation. n/N represents number of independent biological repeats/number of technical repeats.

Chapter 3 Stimuli-coupled differential trafficking of Weibel-Palade bodies regulated by Rab46

3.1 Introduction

WPBs have been named ‘the sentinels’ of the vasculature due to their ability to store and rapidly release an armour of bioactive proteins that participate in multiple processes such as primary haemostasis, regulation of vascular tone, inflammation and angiogenesis (Goligorsky et al., 2009). The functional diversity of these proteins enables WPBs to respond to a plethora of acute physiological demands in order to maintain vascular homeostasis.

As described in chapter 1, WPBs exocytosis can be triggered by multiple agonists that can be divided into two groups defined by their ability to evoke either Ca^{2+} or cAMP signals (although these are not necessarily mutually exclusive; Rondaij, Bierings, Kragt, Van Mourik, et al., 2006). WPB trafficking and exocytosis via the cAMP-PKA axis have been relatively well described in literature (Vischer and Wollheim, 1997; Rondaij et al., 2004a; Rondaij, Bierings, Kragt, Gijzen, et al., 2006; Van Hooren et al., 2012a; Li et al., 2018; Schillemans et al., 2018). Hence, the focus on studying the effects of Ca^{2+} -dependent agonists of WPB trafficking and exocytosis herein. Given the high number of WPB Ca^{2+} -dependent secretagogues and the functional diversity of WPB constituents, the topic of differential trafficking of distinct populations of WPBs has long been hypothesised (Rondaij, Bierings, Kragt, Van Mourik, et al., 2006; Babich et al., 2008), yet remain elusive. For example, WPBs can store both the leukocyte adhesion molecule, P-selectin (McEver et al., 1989b), and the angiogenic cytokine angiopoietin-2 (Fiedler et al., 2004b); two proteins that have not only been shown to regulate seemingly distinct physiological processes, but have been found to reside in mutually exclusive WPB populations (Fiedler et al., 2004b). In contrary, a later study (van Agtmaal et al., 2012) questioned this finding and reported colocalization of P-selectin and Angiopoietin-2 in endothelial progenitor cells.

Here, I demonstrate that differential trafficking of cargo restricted populations of WPBs is coupled to stimuli in HUVECs. In addition, Wilson *et al.*, 2015 described a novel endothelial Ca^{2+} -sensing Rab GTPase, CRACR2A-L, that comprises multiple functional and protein-interacting domains, now known as Rab46. My supervisor Lynn McKeown previously found that Rab46 is colocalised with WPBs. Considering Rab46’s ability to sense Ca^{2+} via its EF-hand domain suggests the possibility that Rab46 may a novel WPB Ca^{2+} sensor protein that has a regulatory role in stimuli-coupled WPB trafficking. Super-resolution imaging was used for detailed localisation of P-selectin and angiopoietin-2, and their relationship with

endogenous Rab46. Targeted RNA silencing methods and single point mutations were introduced into the Rab domain to study the effect of Rab46 depletion and the GTPase activity on P-selectin and angiopoietin-2 trafficking and exocytosis, respectively. This chapter reveals that endogenous Rab46 is primarily residing at a subpopulation of WPBs which is devoid of P-selectin and suggests a role of Rab46 in regulating angiopoietin-2 recruitment to WPBs.

3.2 Histamine evokes perinuclear clustering of Weibel-Palade Bodies

To determine if Ca^{2+} -dependent secretagogues evoke differential trafficking of WPBs, I used two well-studied Ca^{2+} -dependent agonists that have been shown to trigger WPB exocytosis but have different physiological functions: the prothrombotic factor thrombin (Birch et al., 1992) and the proinflammatory amine histamine (Hamilton and Sims, 1987).

First, it was necessary to confirm that in our hands both histamine and thrombin indeed evoke mobilisation of intracellular Ca^{2+} in HUVECs. Range of histamine (0.1-300 μM) and thrombin (0.07 U/ml) doses were added to the cells at 60 seconds and the subsequent responses were recorded for additional 240 seconds. Dose responses to histamine and thrombin were quantified by measuring changes in fluorescence in Fura-2-AM loaded cells using a FlexStation (see Chapter 2 for methods details). The recordings were obtained in an extracellular buffer containing physiological Ca^{2+} concentration. The fluorescence measurements were used to construct dose-response curves. EC_{50} values for both agonists were generated by curve fitting using the Hill1 equation in OriginPro 2018 software (Figure 3.1A, B). These results allowed selection of doses that evoke maximum Ca^{2+} concentrations of histamine (30 μM) and thrombin (2.5 U/ml).

Although both thrombin and histamine evoke release of intracellular Ca^{2+} I sought to determine if they had equivalent effects on WPB trafficking. HUVECs were grown for 72 hours into Ibidi μ -slides prior to fixation and immunostained for vWF, as a marker of WPBs, in control and treated conditions. Reasoning that WPBs are the 'emergency' pre-stored organelles of the vasculature, I observed WPB trafficking in response to 30 μM of histamine and 2.5 U/ml of thrombin at time points ranging from 5 minutes (time frame relevant to the intracellular Ca^{2+} mobilisation that mimics acute, on-demand WPB exocytosis) to 60 minutes (histamine Figure 3.2, thrombin Figure 3.3).

From image quantification (represented by distance from nucleus) of HUVECs treated with histamine, a distinct perinuclear clustering of WPBs was observed

from 5 minutes to 15 minutes that started declining at 30 minutes and was not present in cells treated with histamine for 60 minutes (Figure 3.2A). In contrast, with thrombin 15 minutes and 60 minutes (Figure 3.3A), vesicular-like pattern characteristic of WPBs can be observed and a number of cells exhibited a more typical vWF patches on the cell surface, indicating vWF exocytosis. Quantification of WPBs cellular distribution in response to thrombin and histamine at all tested time points reveals that significant clustering of WPBs at the perinuclear area was unique to histamine stimulation, with peak clustering occurring at 15 minutes (histamine Figure 3.2B, thrombin Figure 3.3B).

These results suggest that differential WPB trafficking occurs in response to two functionally distinct Ca^{2+} -dependent physiological stimuli.

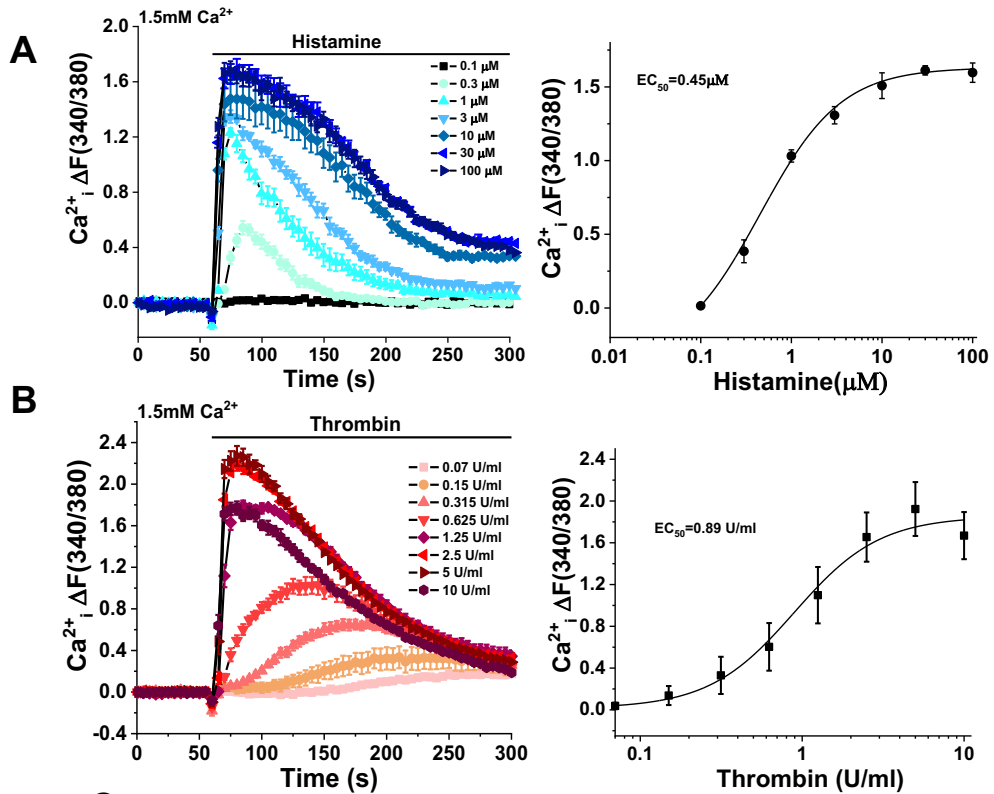


Figure 3.1 Histamine and thrombin evoke intracellular Ca²⁺ rise in ECs.

(A) Representative trace (top left) of Ca²⁺ rise in HUVECs evoked by histamine (0.1-100 μM) for 5 minutes. Mean data (top right) of HUVECs treated with histamine (0.1-100 μM) displayed as a concentration-response curve. (B) Representative trace (bottom left) of Ca²⁺ rise in HUVECs evoked by thrombin (0.07-10 U/ml) for 5 minutes. Mean data (bottom right) of HUVEC treated with thrombin (0.07-10 U/ml) are displayed as a concentration-response curve. Recordings were obtained in 1.5 mM Ca²⁺ SBS buffer. Fitted curves are plotted using a Hill Equation indicating the 50 % maximum effect (EC₅₀; n/N = 3/9, error bars represent SEM).

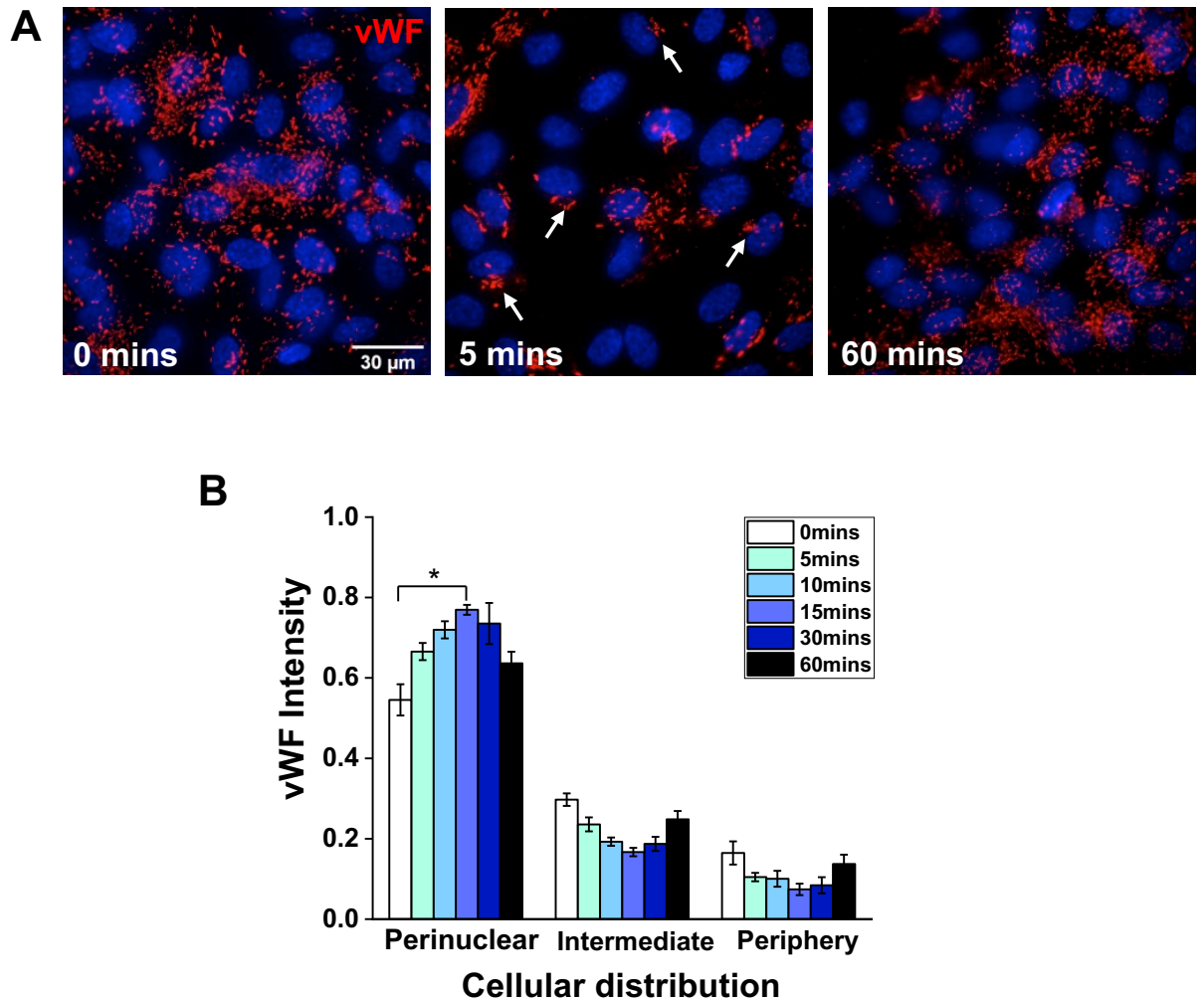


Figure 3.2 Histamine evokes time-dependent perinuclear trafficking of WPBs.

(A) Representative immunofluorescent images of HUVECS treated with 30 μ M histamine for 5 and 60 minutes (left and right, respectively), and then fixed and stained for vWF (red; marker of WPBs). Blue (DAPI) = nucleus. Scale bar = 30 μ m. (B) Mean data showing the cellular distribution of vWF in response to 30 μ M histamine at 0, 5, 10, 15, 30 and 60 minutes. Results were grouped into three areas: perinuclear, intermediate and periphery. The plots quantify vWF signal intensity in the respective area where the mean (\pm SEM) was noted as percentage of the total signal intensity ($n/N = 3/24$, * p -value < 0.05 following One-way ANOVA).

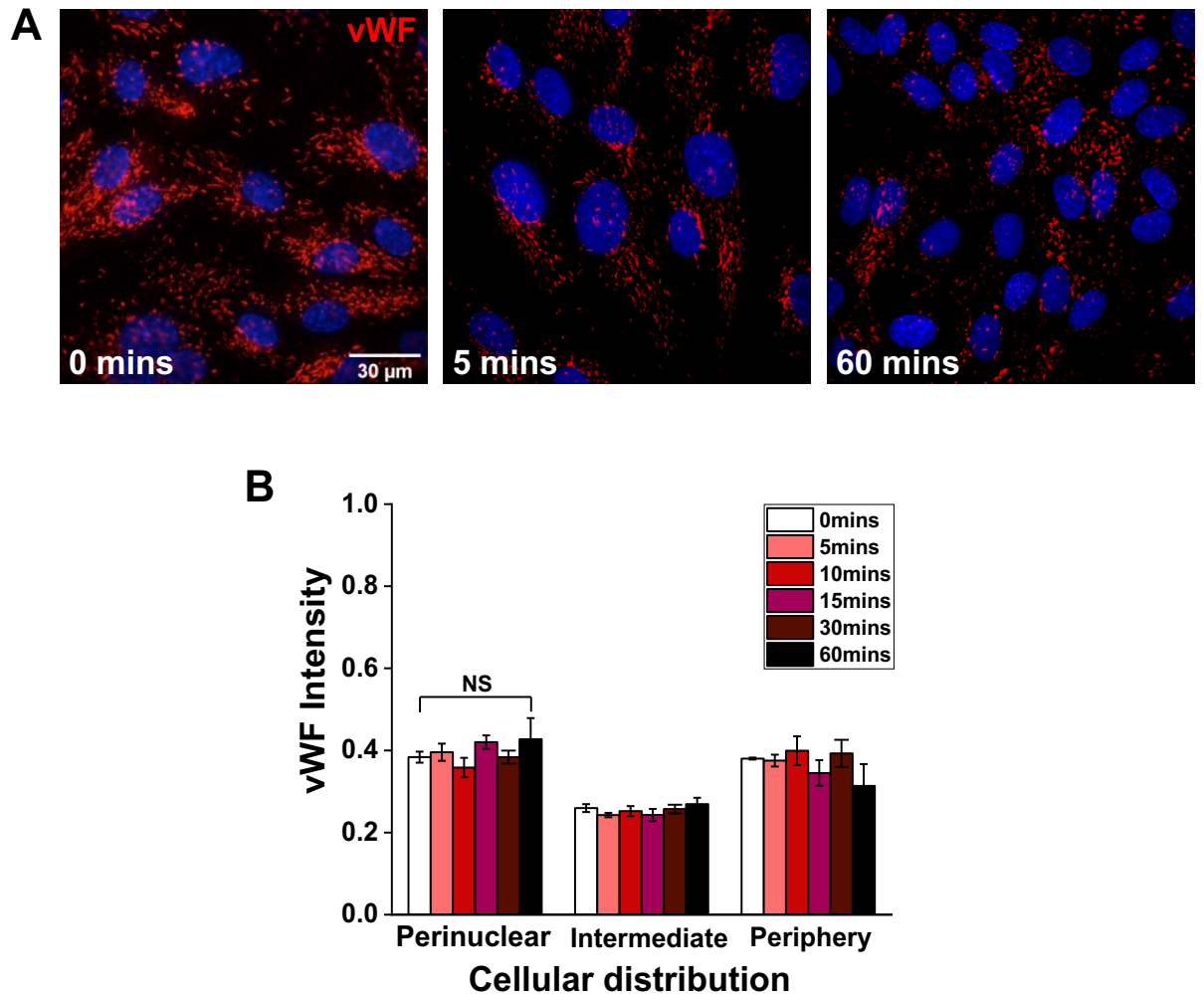


Figure 3.3 Thrombin does not evoke perinuclear trafficking of WPBs.

(A) Representative immunofluorescent images of HUVECs treated with 2.5 U/ml thrombin for 5 and 60 minutes (left and right, respectively), fixed and stained for vWF (red; marker of WPBs). Blue (DAPI) = nucleus. Scale bar = 30 μ m. (B) Mean data showing the cellular distribution of vWF in response to 30 μ M histamine at 0, 5, 10, 15, 30 and 60 minutes. Results were grouped into three areas: perinuclear, intermediate and periphery. The plots quantify vWF signal intensity in the respective area (see methods) where the mean (\pm SEM) was noted as percentage of the total signal intensity (n/N = 3/24, NS, not significant following a One-way ANOVA).

3.3 Histamine induces differential trafficking of Weibel-Palade bodies

3.3.1 P-selectin and angiopoietin-2 reside in mutually exclusive Weibel-Palade body populations

To understand the physiological relevance of histamine-evoked WPB perinuclear trafficking, I considered whether WPBs store proinflammatory and proangiogenic constituents (P-selectin and Angiopoietin-2, respectively) in mutually exclusive WPB subpopulations and are these heterogeneous subpopulations coupled to selective agonist-evoked signalling pathways (Øynebråten et al., 2004; Rondaij, Bierings, Kragt, Van Mourik, et al., 2006). First, from representative images of HUVECs immunostained for angiopoietin-2 (green) and P-selectin (red), (Figure 3.4A: DeltaVision) and (Figure 3.4B: Zeiss AiryScan), it can be observed that WPBs contain either angiopoietin-2 or P-selectin forming distinct subpopulations in HUVECs. Anomalies conferred by antibody specificity were verified by western blot detection of Angiopoietin-2 and P-selectin in cells that had been specifically targeted with siRNAs. (Figure 3.5A, B).

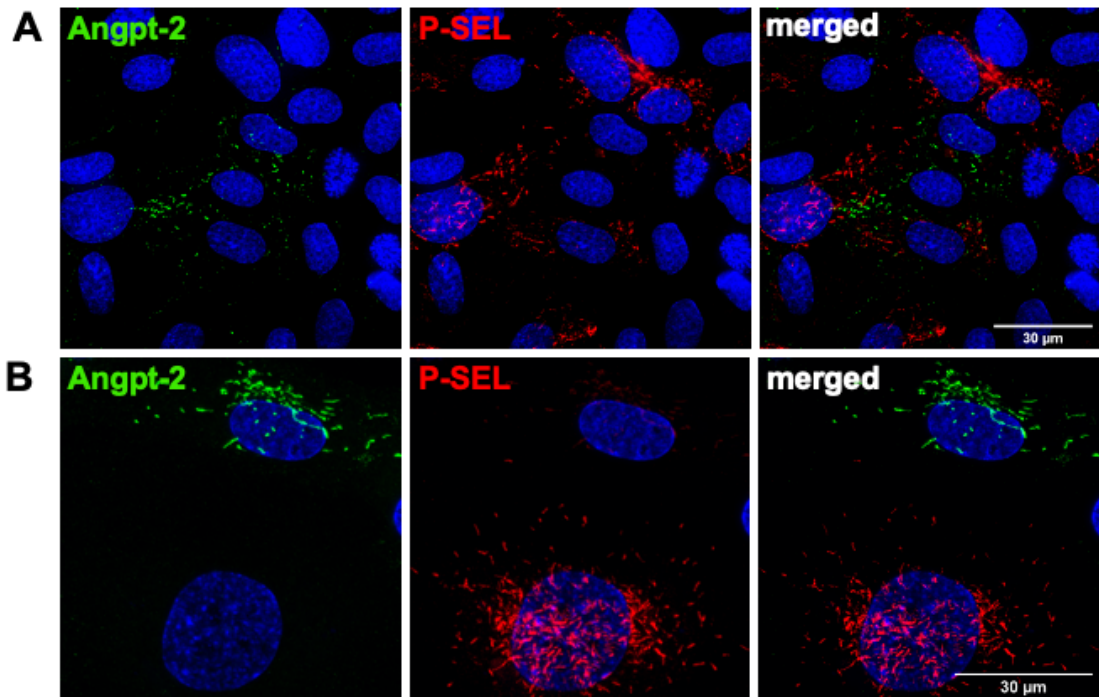


Figure 3.4 Angiopoietin-2 and P-selectin reside in mutually exclusive WPBs.

(A) Immunofluorescent images showing subcellular localisation of endogenous angiopoietin-2-2 (green; Angiopoietin-2) and P-sel (red; P-selectin) in HUVECs. DAPI (blue) shows nuclei. Merged images on the right to show the lack of colocalisation of angiopoietin-22 with P-sel. Maximum intensity projections from DeltaVision z-stack are shown. Scale bar = 30 µm. (B) High resolution AiryScan imaging showing subcellular localisation of endogenous Angiopoietin-2-2 (green; Angiopoietin-2) and P-sel (red; P-selectin) in HUVECs. DAPI (blue) shows nuclei. Merged images on the right to show the lack of colocalisation of angiopoietin-22 with P-sel. Maximum intensity projections from AiryScan z-stack are shown. Scale bar = 30 µm.

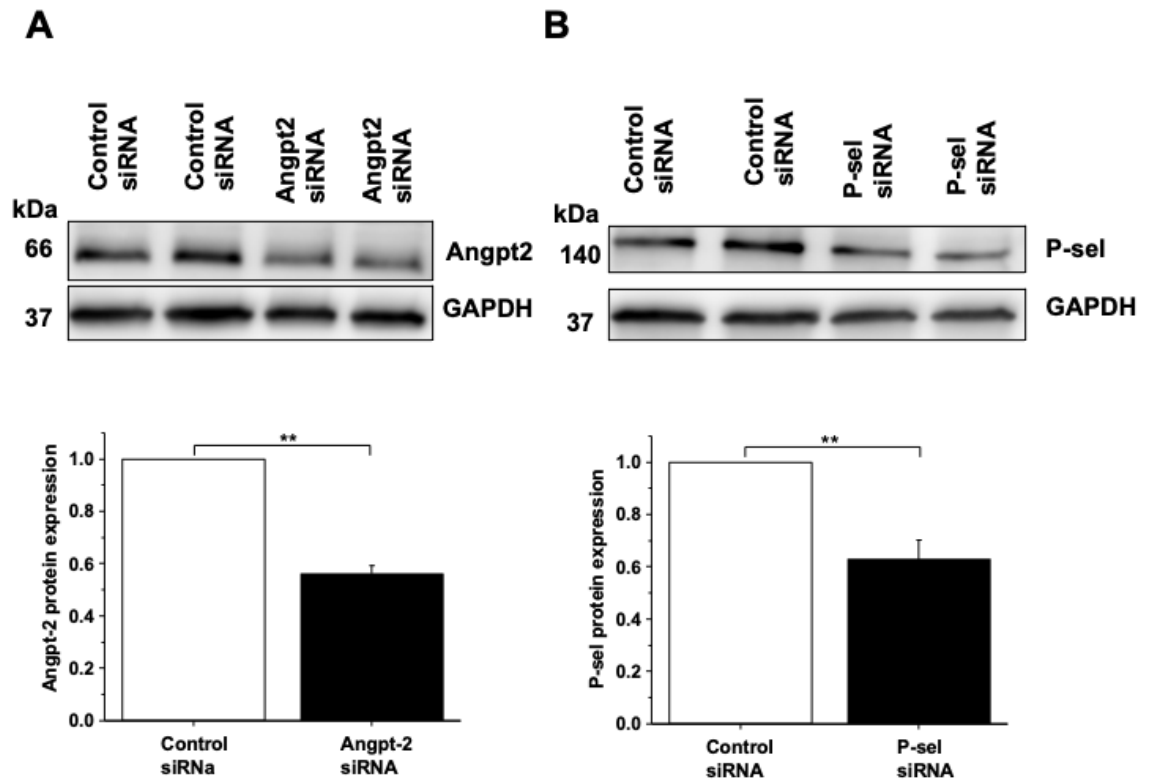


Figure 3.5 Angiopoietin-2 and P-selectin primary antibodies specificity

(A) Representative immunoblot (top left) for anti-Angiopoietin-2-2 in HUVECs transfected with scrambled control sequence or Angiopoietin-2-2 siRNA. Mean data (bottom left) of Angiopoietin-2-2 band intensity is shown as fold change relative to GAPDH ($n=3$, error bars represent SEM). (B) Representative immunoblot (top right) for anti-P-sel in HUVECs transfected with scrambled control sequence or P-sel siRNA. Mean data (bottom left) of P-sel band intensity is shown as fold change relative to GAPDH ($n = 3$, error bars represent SEM, ** p -value < 0.01 by t -test). GAPDH used as a housekeeping loading control.

3.3.2 Histamine-evoked perinuclear-localized Weibel-Palade Bodies are devoid of P-selectin

Rab46 is necessary for the histamine evoked trafficking of WPBs to the MTOC (K. T. Miteva et al., 2019). Histamine is an inflammatory hormone involved in immune responses (András and Merétey, 1992), and a key event required for the recruitment of neutrophils to sites of inflammation is the histamine-triggered exocytosis of P-selectin at the surface of ECs (Burns et al., 1999). In contrast, Fiedler and colleagues have reported that histamine does not trigger angiotensin-2 exocytosis in ECs (Fiedler et al., 2004b). Therefore, I questioned whether the WPBs clustered at the perinuclear area by histamine stimulation contained either P-selectin and Angiotensin-2, and if those are colocalised with Rab46.

In control cells immunostained for endogenous P-selectin (red) and Rab46 (green), high-resolution confocal imaging with AiryScan revealed that P-selectin localised to a WPB population that is distinct from Rab46-positive WPBs (Figure 3.6A). Therefore, to demonstrate that Rab46-dependent clusters of WPBs at the MTOC are devoid of P-selectin, I observed the localisation of P-selectin and angiotensin-2 in cells treated with histamine. Representative imaging of HUVECs treated with histamine demonstrated that Rab46-positive WPBs clustered at the MTOC, while P-selectin-positive WPBs either remained dispersed within the cytoplasm or recruited to the cell surface (Figure 3.6A) suggesting that P-selectin positive WPBs are not regulated by Rab46. In comparison, imaging analysis of HUVECs immunostained with Rab46 (green) and Angiotensin-2 (red; Figure 3.6B). Furthermore, ImageJ colocalisation analysis (Figure 3.6C) revealed that Rab46 does not localise to WPBs that contain P-selectin (control, $8.32 \pm 0.38\%$; histamine, $7.38 \pm 1.87\%$) but localises both in control and histamine-treated HUVECs to WPBs containing Angiotensin-2 (control, $27.58 \pm 1.48\%$; histamine, $32.27 \pm 1.52\%$). These results were further substantiated by imaging analysis of HUVECs immunostained with Rab46 and Angiotensin-2 or Rab46 and P-selectin and treated with histamine. It can be observed that angiotensin-2 is significantly increased at the MTOC upon histamine stimulation whilst that was not case with quantification of P-selectin immunostaining in the same conditions (Figure 3.6D). In addition, in the absence of histamine stimulation, Angiotensin-2 is residing at the MTOC, colocalised with Rab46 in HUVECs overexpressing constitutively active Q604L mutant of Rab46 (Figure 3.7A,B).

To further determine that trafficking and exocytosis of WPBs containing P-selectin was independent of Rab46, I measured histamine evoked cell surface

P-selectin expression in HUVECs transfected with control or Rab46 targeted siRNA using ELISA. Upon histamine treatment there was no significant difference in P-selectin surface exocytosis in response to histamine suggesting that histamine-evoked surface exocytosis of P-selectin is independent of Rab46 (Figure 3.8). Considering previous findings in the literature (Fiedler et al., 2006), it was hypothesised that full-blown exocytosis of Angiotensin-2 would be in juxtaposition to a specific, acute immune response triggered by histamine, and that Rab46-dependent diversion of Angiotensin-2-positive WPBs to the MTOC could participate, to an extent, in moderating exocytosis. The effect of acute histamine treatment on Angiotensin-2 secretion was evaluated (Figure 3.9). Acute stimulation in HUVECs with a lower physiological concentration (0.3 μM) of histamine (Chapter 6 – this concentration does not trigger WPB trafficking to the MTOC), evoked exocytosis of Angiotensin-2 as measured by ELISA (blue column; Figure 3.9). However, stimulating cells with a higher, but physiological relevant, concentration of histamine (30 μM) failed to augment secretion (red column; Figure 3.9). These results suggest that clustering of Angiotensin-2 at the MTOC triggered by histamine can avert further exocytosis, and raises the question whether Rab46 depletion, that would prevent perinuclear WPB clustering, would enhance Angiotensin-2 exocytosis levels. Surprisingly, Angiotensin-2 protein levels in supernatants from acutely treated HUVECs are not increased despite Rab46 siRNA-mediated knockdown (hatched columns; Figure 3.9). In HUVECs stimulated with PMA, a similar effect was observed where Rab46 depletion significantly decreased the exocytosed Angiotensin-2 levels.

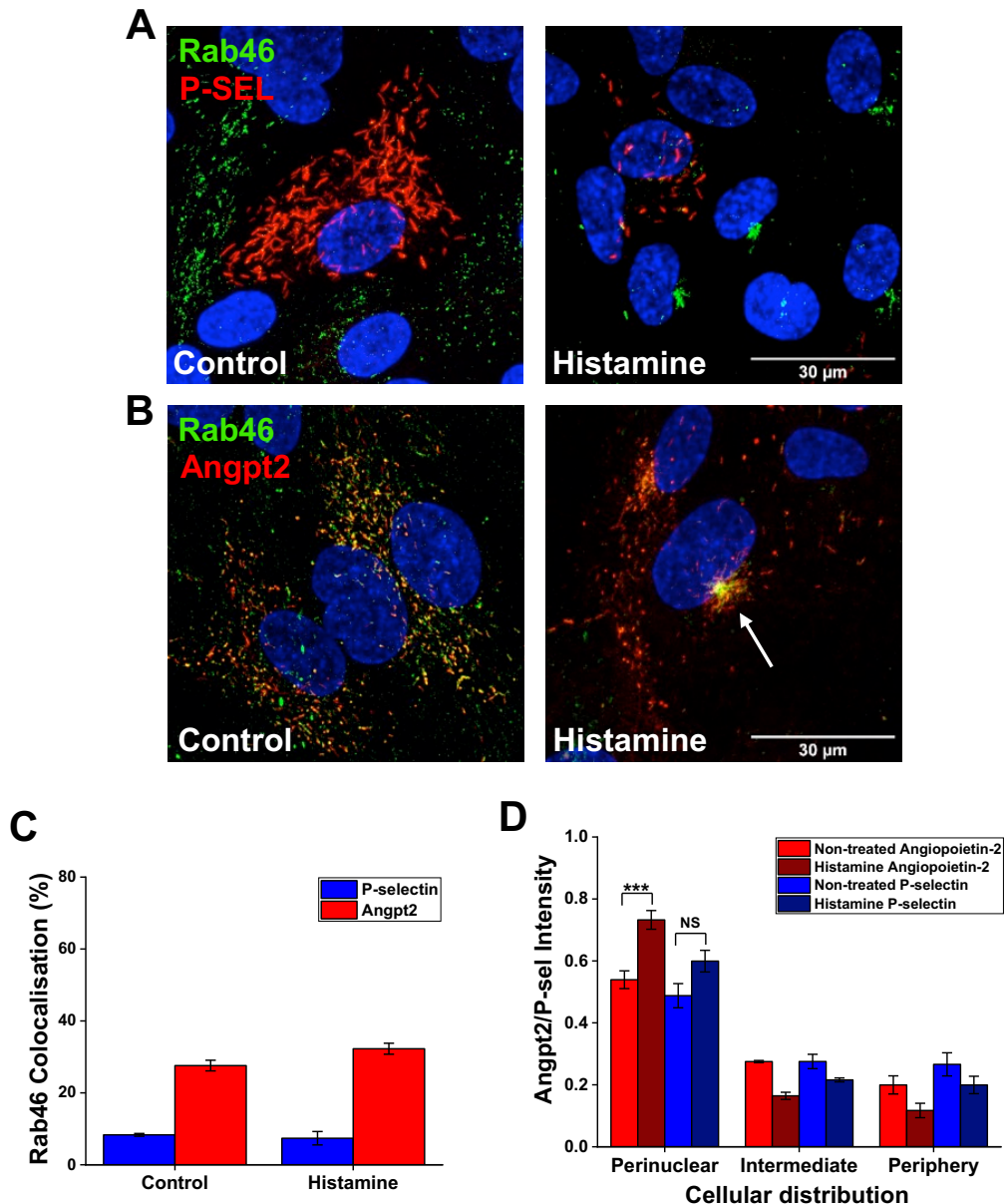


Figure 3.6 Histamine induces differential trafficking of P-selectin–negative WPBs that contain Angiopoietin-2.

(A) High resolution Airyscan imaging showing subcellular localisation of endogenous Rab46 (green) and P-sel (red; P-selectin) in control and 30 μ M histamine-treated HUVECs for 5 minutes. (B) High resolution Airyscan imaging showing subcellular localisation of endogenous Rab46 (green) and Angiopoietin-2-2 (red; Angiopoietin-2) in control and 30 μ M histamine treated HUVECs. DAPI (blue) shows nuclei. Maximum intensity projections from Airyscan z-stack are shown. Scale bar = 30 μ m. (C) Quantification of percentage Rab46 colocalisation to P-selectin and angiopoietin-22-positive WPBs in control and 30 μ M histamine treated HUVECs. The plot indicates the mean \pm SEM; number of independent biological repeats/technical repeats = 3/18–30. (D) Mean data showing the cellular distribution of Angiopoietin-2-2 and P-sel upon treatments from (A) and (B). Results were grouped into three areas: perinuclear, intermediate and periphery. The plots quantify Angiopoietin-2-2 and P-sel signal intensity in the respective area where the mean (\pm SEM) was noted as percentage of the total signal intensity (n/N=5/28-40, NS, not significant, ***, p-value < 0.001 by Two-way ANOVA).

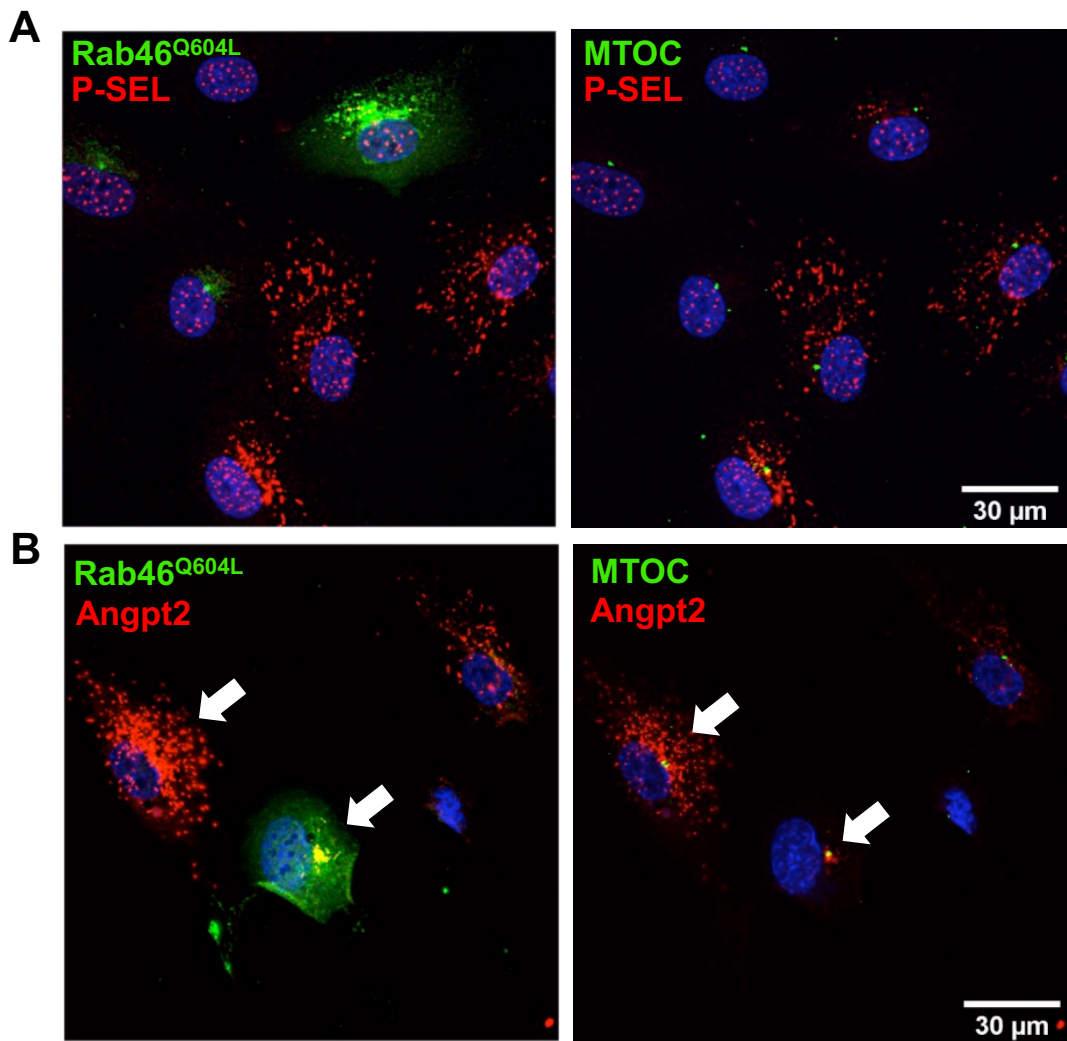


Figure 3.7 Angiopoietin-2 localizes to MTOC in the absence of stimulation with histamine in cells overexpressing Q604L Rab46 mutant.

(A) Immunofluorescent images showing subcellular localisation of constitutively active Q604L Rab46 mutant (green) and P-sel (red; P-selectin; top left) and pericentrin (green; marker of MTOC) and P-sel (red; P-selectin; top right) in HUVECs. (B) Immunofluorescent images showing subcellular localisation of constitutively active Q604L Rab46 mutant (green) and Angiopoietin-2-2 (red; Angiopoietin-2; bottom left) and pericentrin (green; marker of MTOC; bottom right) and Angiopoietin-2-2 (red; Angiopoietin-2-2; top right) in HUVECs transfected with plasmids for 24 hours. DAPI (blue) shows nuclei. Maximum intensity projections from DeltaVision z-stack are shown. Scale bar = 30 μm. Small arrows indicate a cell expressing Rab46^{Q604L}, big arrows indicates a cell for comparison.

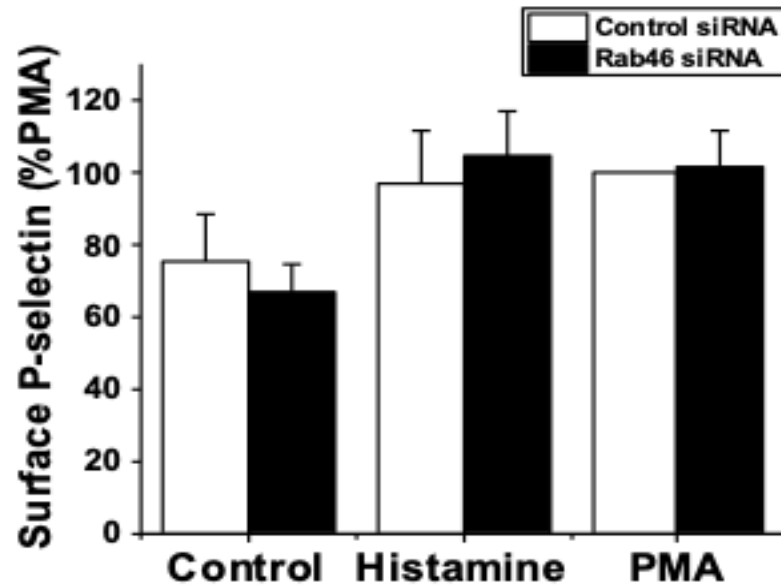


Figure 3.8 Rab46 depletion does not affect P-selectin surface expression.

ELISA measurements of cell surface P-selectin expression in HUVECs transfected with either control or Rab46 siRNA for 72 hours. HUVECs were stimulated with vehicle, 30 μ M histamine, or 1 μ M PMA. Plot indicates mean \pm SEM percentage of maximal control siRNA response (PMA; n/N= 3/9).

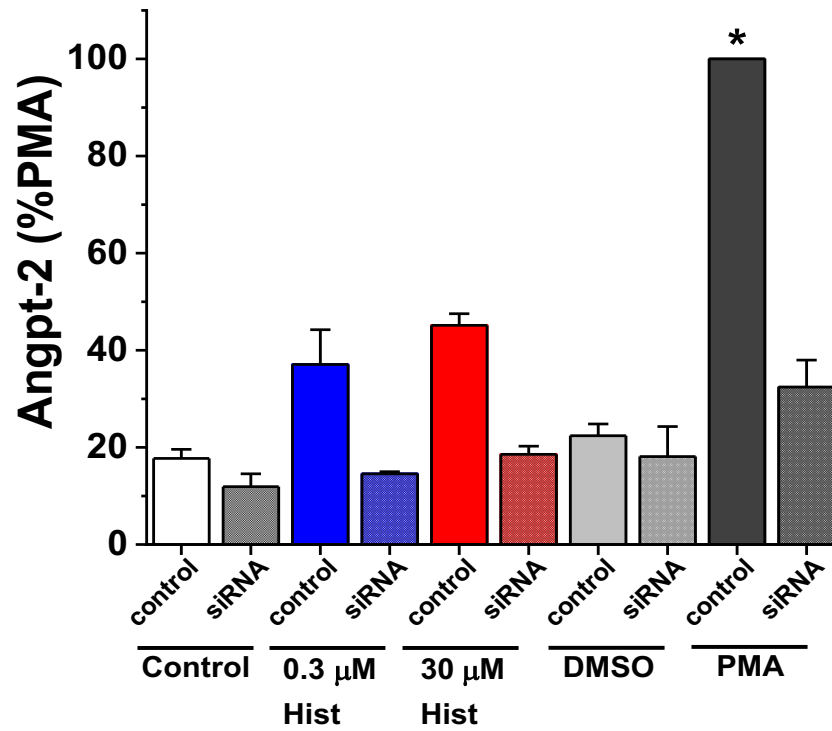


Figure 3.9 Rab46 depletion prevents histamine- and PMA-evoked Angiopoietin-2 secretion.

ELISA measurements of Angiopoietin-22 (Angiopoietin-2) secretion shown as a percentage of the PMA response in cells treated with siRNA control or Rab46 siRNA for 72 hours prior to sample collection. Quantification was performed on supernatants collected from HUVECs treated with vehicle, 0.3 μ M histamine, 30 μ M histamine, or 1 μ M PMA for 10 minutes. Plot indicates mean \pm SEM percentage of maximal control siRNA response (PMA). n/N = 3/6, * p-value < 0.05 by two-way ANOVA.

3.3.3 Angiotensin-2-positive WPBs are mis-localised in Rab46 depleted ECs

The presenting findings in the previous sections of this chapter showed that upon histamine treatment Angiotensin-2 positive subpopulation of WPBs traffics to the MTOC, dependent on Rab46. Surprisingly, in the absence of endogenous Rab46, Angiotensin-2 secretion was significantly reduced. Therefore, it was important to question the relationship between Rab46 and Angiotensin-2, for example Angiotensin-2 biosynthesis. HUVECs were transfected with Rab46 targeted siRNA and western blot was performed on the collected lysates (Figure 3.10A). Significant decrease in Angiotensin-2 protein levels were observed (Figure 3.10C). In addition, despite approximately 75% Rab46 knockdown efficiency (Figure 3.11A), Angiotensin-2 mRNA levels (Figure 3.11B) in HUVECs depleted of Rab46 remained unchanged. These data suggest that Rab46 does not play a role in Angiotensin-2 transcription. Immunofluorescent images of HUVECs immunostained for Rab46 (green), vWF (white) and Angiotensin-2 (red) where Rab46 was depleted and treated with histamine (Figure 3.12). This data further corroborated previous ELISA (Figure 3.9) and Western blot (Figure 3.10) findings. Low number of Angiotensin-2 vesicles was observed in Rab46-depleted HUVECs, suggesting that this may be due to reduced recruitment to WPBs. It is important to note that the number of cells per field of view does not change after Rab46 knockdown or histamine treatment, confirming that siRNA transfection or histamine treatment had no significant effect on the number of cells, as shown in Miteva *et al.*, 2019 (control NT 15.9 ± 1.3 ; control histamine 16.6 ± 1.4 ; Rab46 siRNA NT 15.4 ± 1 ; Rab46 siRNA histamine 15.5 ± 1.2 ; K.T. Miteva *et al.*, 2019). Taken together, these data support the concept that Rab46 couples inflammatory stimuli to differential WPB trafficking to divert irrelevant WPB constituents and potentially limit exocytosis according to the present physiological context, and Rab46 may be necessary for Angiotensin-2 recruitment. Further studies are needed in order to fully map the complex role of Rab46 and the signalling pathways governing differential trafficking of WPB subpopulations with distinct physiological functions in the vasculature.

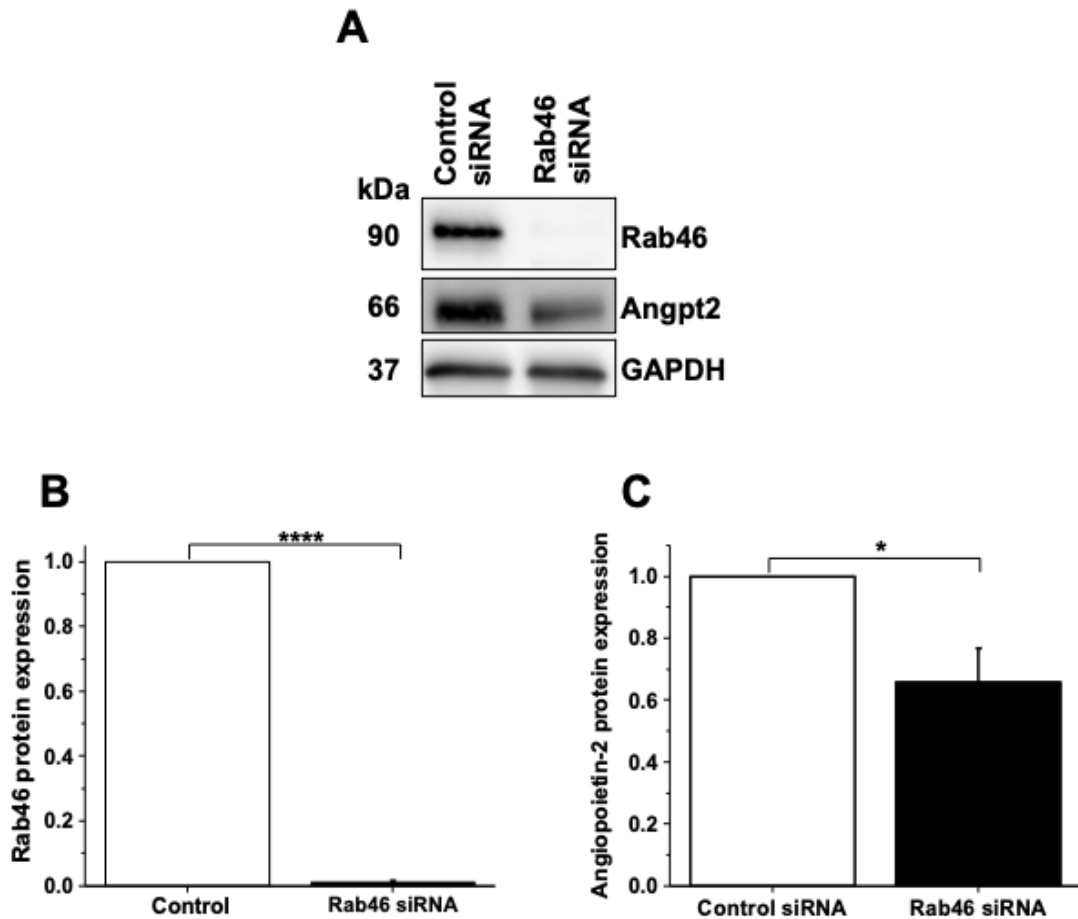


Figure 3.10 Rab46 depletion decreases total Angiopoietin-2 protein levels.

(A) Representative immunoblot for anti-Rab46, anti-Angiopoietin-2-2 and anti-GAPDH in HUVECs transfected with scrambled control sequence or Rab46 siRNA. (B) Mean data of Rab46 band intensity is shown as fold change relative to GAPDH (n=3, error bars represent SEM). (C) Mean data of Angiopoietin-2-2 band intensity is shown as fold change relative to GAPDH (n=4, error bars represent SEM, * p-value < 0.05, **** p-value < 0.0001 by t-test).

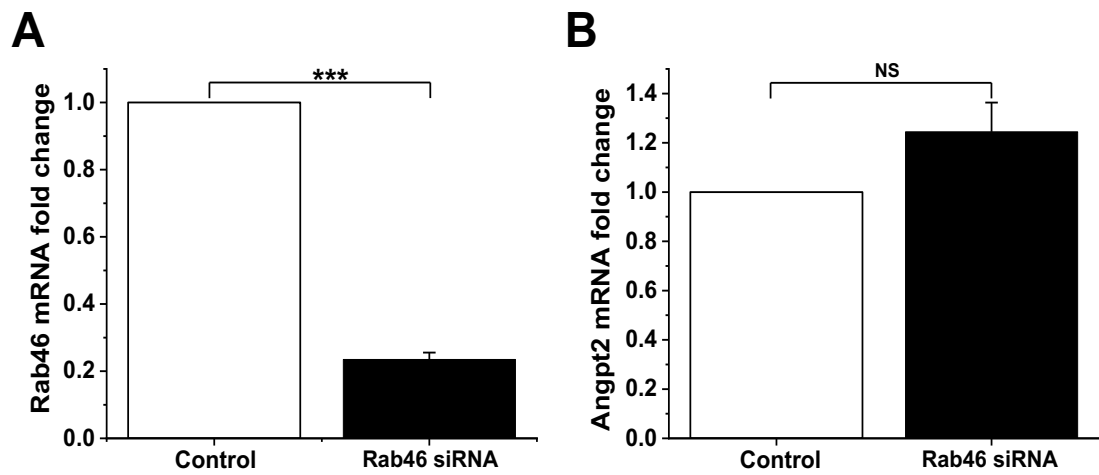


Figure 3.11 Rab46 depletion does not affect mRNA levels of Angiopoietin-2 .

(A) qPCR Δ CT analysis of Rab46 mRNA levels HUVECs transfected with scrambled control sequence or Rab46 siRNA for 72 hours (B) qPCR Δ CT analysis of Angiopoietin-2-2 mRNA levels HUVECs transfected with scrambled control sequence or Rab46 siRNA for 72 hours (n = 3, error bars represent SEM, NS, not significant, *** p-value < 0.001 by t-test).

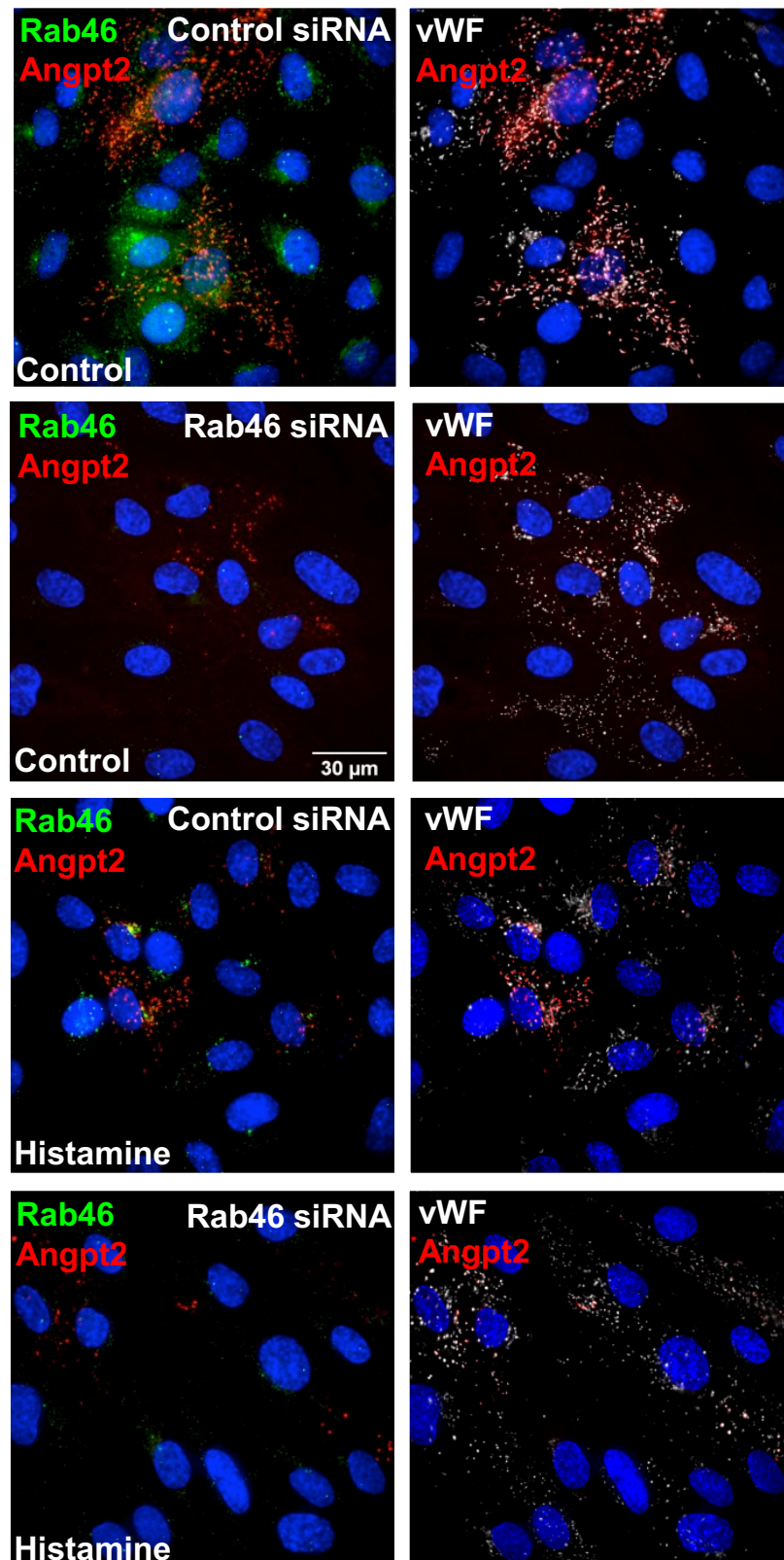


Figure 3.12 Rab46 depletion causes a loss of Angiopoietin-2 localization to WPBs.

Representative immunofluorescent images showing subcellular localisation of constitutively active Rab46 (green), Angiopoietin-2-2 (red; Angiopoietin-2) and vWF (white) in HUVECs.

Figure 3.12 continued Cells were transfected with scrambled control sequence or Rab46 siRNA and stimulated with 30 μ M histamine for 5 minutes prior to fixation. DAPI (blue) shows nuclei. Maximum intensity projections from DeltaVision z-stack are shown. Scale bar = 30 μ m. n/N = 3/18

Chapter 4 Rab46 -dependent trafficking of WPBs to the MTOC is independent of cAMP signalling

4.1 Introduction

Bidirectional transport of organelles has been well studied (Bryantseva and Zhapparova, 2012; Hancock, 2014). Briefly, organelles or other cellular cargo are transported by motor proteins along the microtubules and actin filaments of the cell. The two main types of trafficking are retrograde trafficking, towards the nucleus, and anterograde trafficking, towards the periphery of the cell. Previous studies have suggested that Ca^{2+} -dependent stimuli evoke anterograde trafficking of WPBs with subsequent release of cargo at the plasma membrane. In contrast, cAMP-dependent agonists, such as epinephrine and forskolin, mediate retrograde trafficking of WPBs which is dependent on dynein, Epac and several GTPase proteins (Rondaij et al., 2004a; Rondaij, Bierings, Kragt, Gijzen, et al., 2006; Van Hooren et al., 2012a).

In Miteva *et al.* (2019), for the first time, it was revealed that the Ca^{2+} -raising agonist, histamine, acutely induced retrograde trafficking and perinuclear clustering of a subpopulation of WPBs, and this was dependent on Rab46 (K. T. Miteva et al., 2019). It was also shown that histamine-evoked retrograde trafficking of WPBs can be pharmacologically modulated by using a dynein inhibitor, or by disruption of microtubule integrity. Pedicini *et al.* (2021) have described dynein as an effector of Rab46, in and together in Miteva *et al.* (2019) it was demonstrated dynein and Rab46 co-immunoprecipitation (Miteva et al., 2019; Pedicini et al., 2021).

In contrast, other studies have not detected histamine-induced perinuclear clustering of WPBs. The aim of this chapter was to verify and extend the observations of our aforementioned published findings.

First I sought to investigate whether cAMP, or the downstream cAMP-activated kinase PKA (Walsh et al., 1968), are involved in the histamine signalling pathway in ECs using the cAMP analogue Rp-cAMPs and the well described PKA inhibitor, H89 (Murray, 2008). Next I used siRNA specifically targeted to Rab46 to investigate if Rab46 was necessary for the cAMP-dependent retrograde trafficking evoked by epinephrine. My results suggest neither cAMP, nor its downstream pathways, were necessary for histamine signalling and WPB trafficking in ECs. Additionally, cAMP-induced perinuclear clustering of WPBs was independent of endogenous Rab46, suggesting that our original findings reveal a novel pathway for WPB retrograde trafficking in ECs.

4.2 Histamine-evoked perinuclear clustering of WPBs is independent of cAMP

I sought to determine if cAMP and PKA (cAMP-activated downstream kinase (Walsh et al., 1968) was necessary for histamine-induced trafficking of WPBs to the MTOC. First I confirmed the activity of the PKA inhibitor, H89, by measuring the phosphorylation of CREB-1. HUVECs received co-treatment with the cAMP-raising agonist epinephrine, and IBMX (IBMX is a phosphodiesterase inhibitor, and so preserves cAMP levels in the cells). As shown in the representative immunoblot and quantification (Figure 4.1A, B), application of epinephrine with IBMX together induces phosphorylation of CREB-1, a protein phosphorylated downstream of PKA (Murray, 2008). When HUVECs were pre-treated with H89, as expected, the phosphorylation of CREB-1 was inhibited, indicating positive compound activity of H89.

Preincubation of HUVECs with H89 for 30 minutes before histamine stimulation had no effect on histamine-evoked intracellular Ca^{2+} rise (Figure 4.2A, B), indicating that in the presence of H89 histamine-dependent Ca^{2+} signalling is intact. Similarly, in high-resolution representative images showing HUVECs, preincubated with H89 prior to histamine stimulation, perinuclear trafficking of vWF (red) and Rab46 (green; Figure 4.3A) remained unaffected by PKA inhibition. Quantitative analysis of perinuclear trafficking in Figure 4.3B, C further confirmed the aforementioned findings, suggesting that histamine pathway does not depend on PKA in ECs.

Historically, H89 is the most commonly used PKA inhibitor. However, it displays a broad range of kinase inhibition (Davies et al., 2000; Lochner and Moolman, 2006). Hence, it does not exclude the presence of other PKA-independent kinases downstream of cAMP, such as in the signalling cascade cAMP–Epac–ERK–CREB. The cAMP antagonist Rp-cAMP was used to further question the potential cAMP involvement in histamine-evoked perinuclear trafficking of Rab46-positive WPBs in ECs. The compound activity of Rp-cAMP was also validated via immunoblot where Rp-cAMP reduces CREB-1 phosphorylation levels activated by epinephrine and IBMX treatment (Figure 4.4A, B).

Preincubation of HUVECs with Rp-cAMP for 30 minutes before histamine stimulation had no effect on histamine-evoked intracellular Ca^{2+} release (Figure 4.5A, B). High-resolution representative images of HUVECs, preincubated with Rp-cAMP, reveal intact perinuclear trafficking of vWF (red) and Rab46 (green; Figure 4.6) in response to histamine treatment, regardless of cAMP antagonism of Rp-cAMP. Thus, our findings further corroborate that histamine-induced Rab46 and WPB clustering is cAMP-independent in ECs.

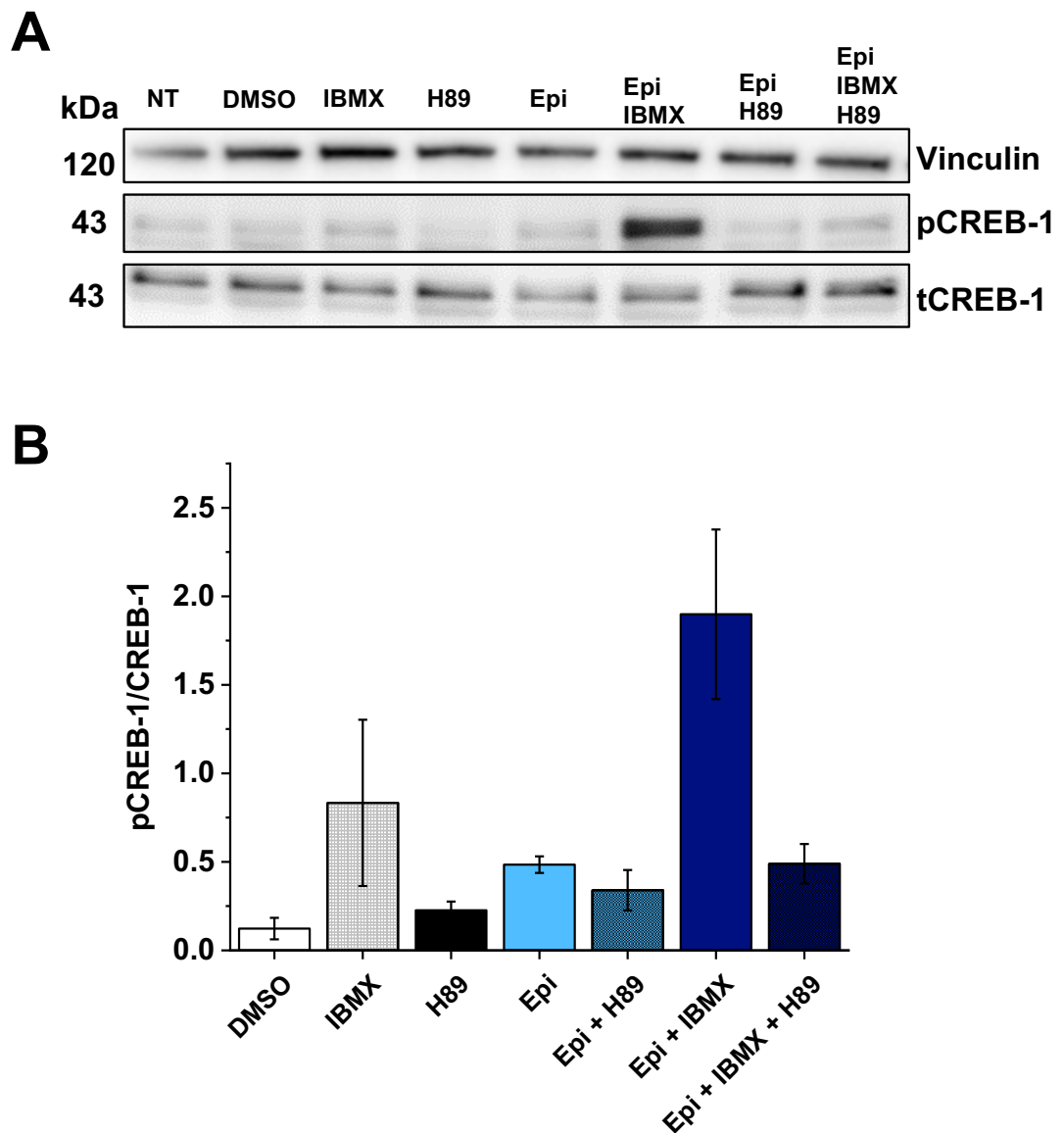


Figure 4.1 H89 inhibits PKA-induced CREB-1 phosphorylation.

(A) Representative immunoblot for -phosphorylated CREB-1 (using an anti-phosphorylation specific CREB-1 antibody: pCREB-1), total CREB-1 (tCREB-1) and anti-Vinculin in HUVECs pre-treated for 30 minutes with vehicle or 10 μ M H89, followed by treatments with epinephrine (Epi), 100 μ M Epi + 100 μ M IBMX or 100 μ M IBMX alone for 15 minutes. (B) Mean data of pCREB-1/tCREB-1 band intensity ($n=3$, error bars represent SEM).

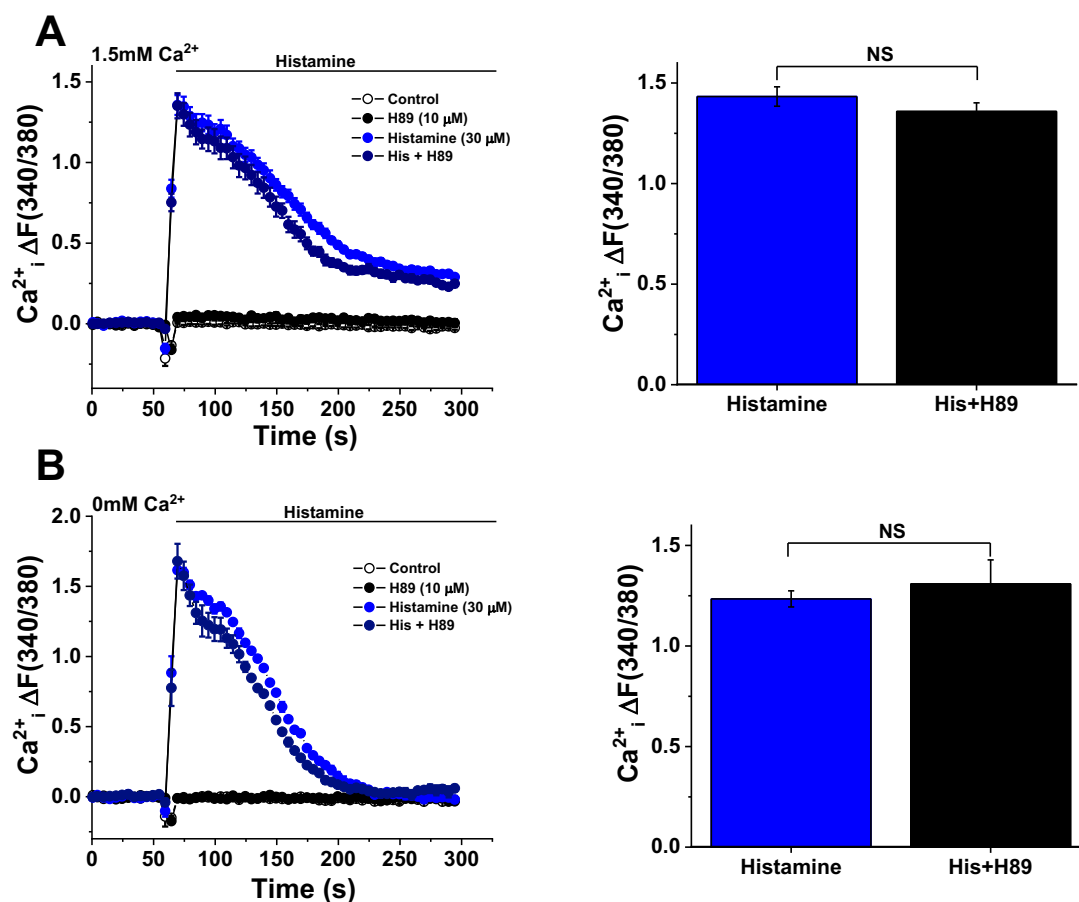


Figure 4.2 PKA inhibition does not affect histamine-induced intracellular Ca²⁺ release.

(A) Representative trace (top left) and mean data (top right) of Ca²⁺ rise in HUVECs for 5 minutes evoked by application of 30 μM histamine at 60 seconds, cells were pre-treated with 10 μM H89 for 30 minutes. Recordings were obtained in 1.5 mM Ca²⁺ SBS buffer. (B) Representative trace (bottom left) and mean data (bottom right) of Ca²⁺ release in HUVECs evoked by application of 30 μM histamine at 60 seconds, cells were pre-treated with 10 μM H89 for 30 minutes. Recordings were obtained in Ca²⁺ free buffer (n/N = 3/9, error bars represent SEM, NS, not significant by One-way ANOVA).

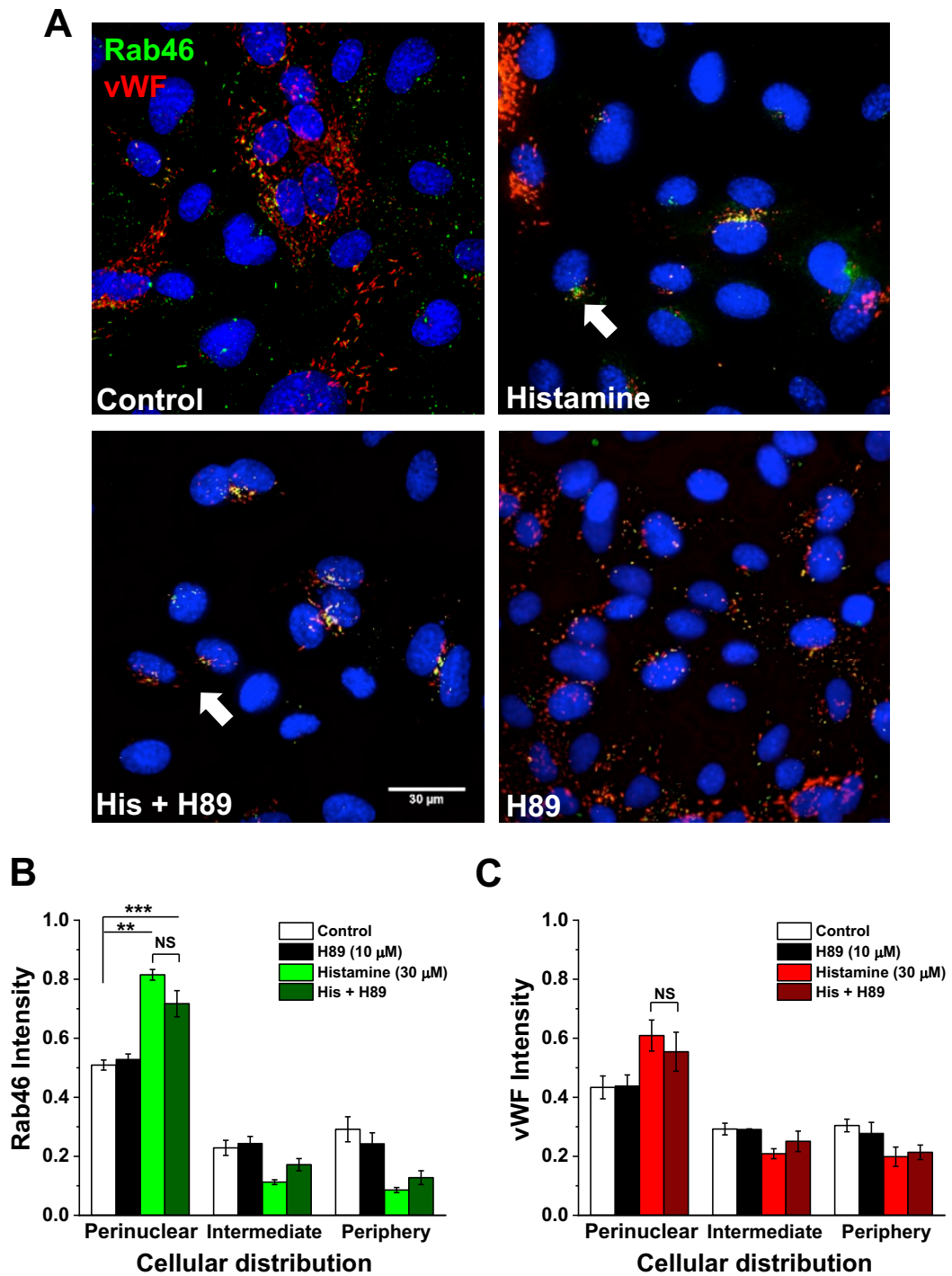


Figure 4.3 Histamine-evoked perinuclear trafficking of Rab46-positive WPBs is PKA-independent.

A) Representative immunofluorescent images of HUVECs pre-treated with vehicle or 10 μ M H89 for 30 minutes, followed by treatment with 30 μ M histamine for 15 minutes. Cells were then fixed and stained for Rab46 (green) and vWF (red; marker of WPBs). DAPI (blue) shows nuclei. Maximum intensity projections from DeltaVision z-stack are shown. Scale bar = 30 μ m. (B,C) Mean data showing the cellular distribution of Rab46 and vWF, respectively, upon treatments from (A).

Figure 4.3 (continued). Results were grouped into three cellular areas: perinuclear, intermediate and periphery. The plots quantify Rab46 and vWF normalised signal intensity in the respective area where the mean (\pm SEM) was noted as percentage of the total signal intensity (n/N = 3/24, NS, not significant, **p-value < 0.01, ***p-value < 0.001 following a Two-way ANOVA).

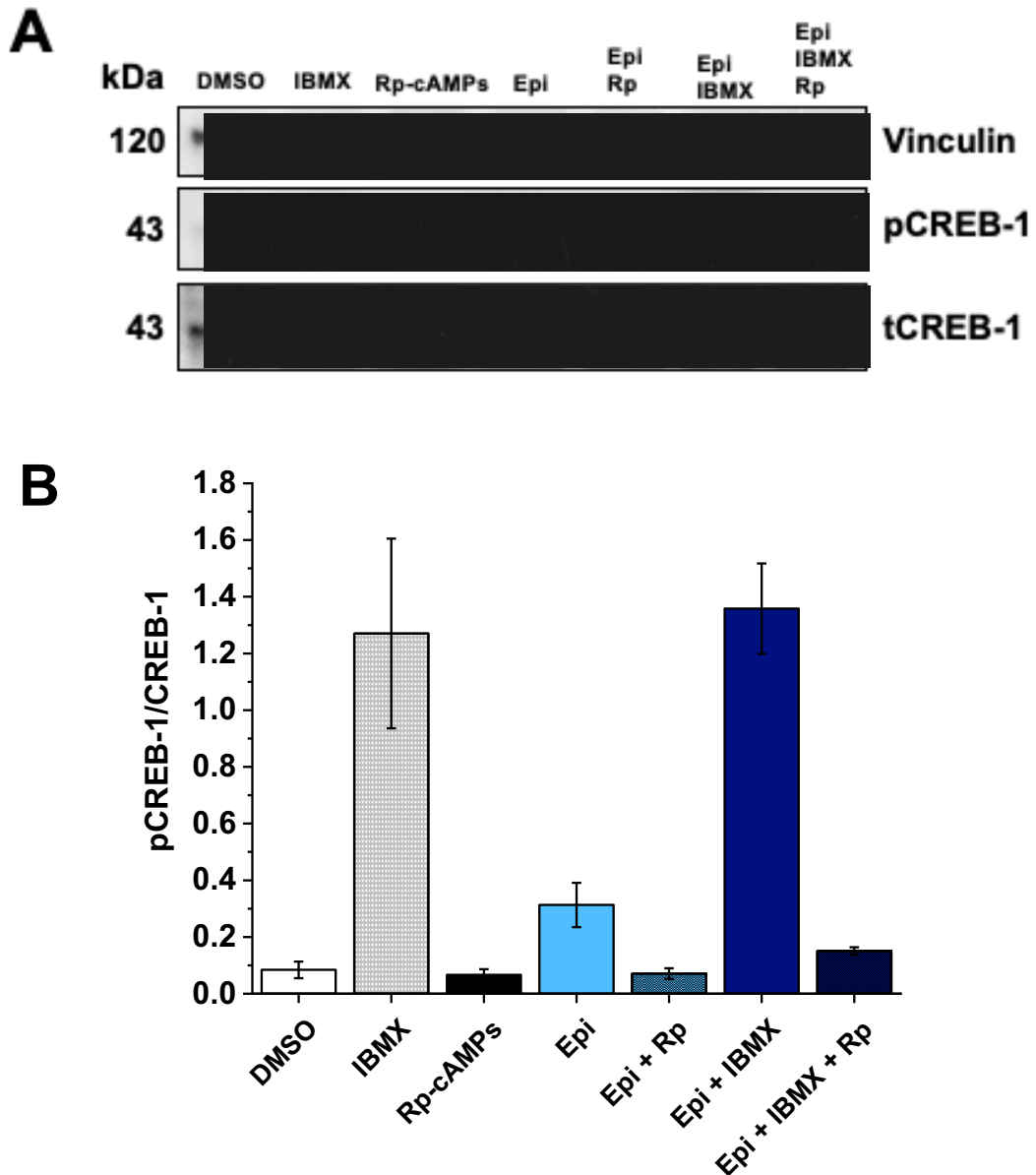


Figure 4.4 Rp-cAMP inhibits PKA-induced CREB-1 phosphorylation.

(A) Representative immunoblot for phosphorylated CREB-1 (pCREB-1), total CREB-1 (tCREB-1) and anti-Vinculin in HUVECs pre-treated for 60 minutes with vehicle or 20 μ M Rp-cAMP, followed by treatments with 100 μ M epinephrine (Epi), 100 μ M Epi + 100 μ M IBMX, or 100 μ M IBMX alone for 15 minutes. (B) Mean data of pCREB-1/tCREB-1 band intensity (n=3, error bars represent SEM).

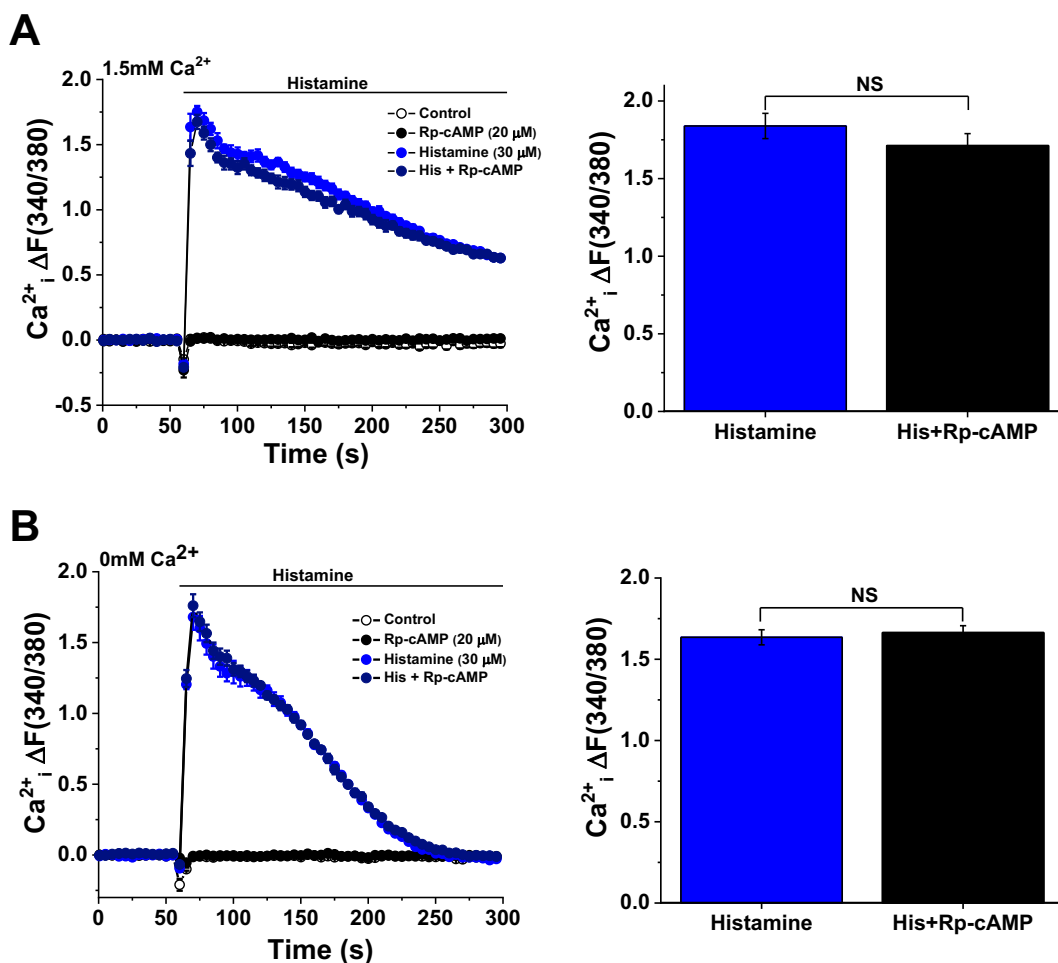


Figure 4.5 cAMP inhibition does not affect histamine-induced intracellular Ca²⁺ release.

(A) Representative trace (top left) and mean data (top right) of Ca²⁺ rise in HUVECs for 5 minutes evoked by application of 30 μM histamine at 60 seconds, cells were pre-treated with 20 μM Rp-cAMP for 60 minutes. Recordings were obtained in 1.5 mM Ca²⁺ SBS buffer. (B) Representative trace (top left) and mean data (top right) of Ca²⁺ release in HUVECs evoked by application of 30 μM histamine at 60 seconds, cells were pre-treated with 20 μM Rp-cAMP for 30 minutes. Recordings were obtained in Ca²⁺ free buffer (n/N=3/9, error bars represent SEM, n.s., not significant by One-way ANOVA).

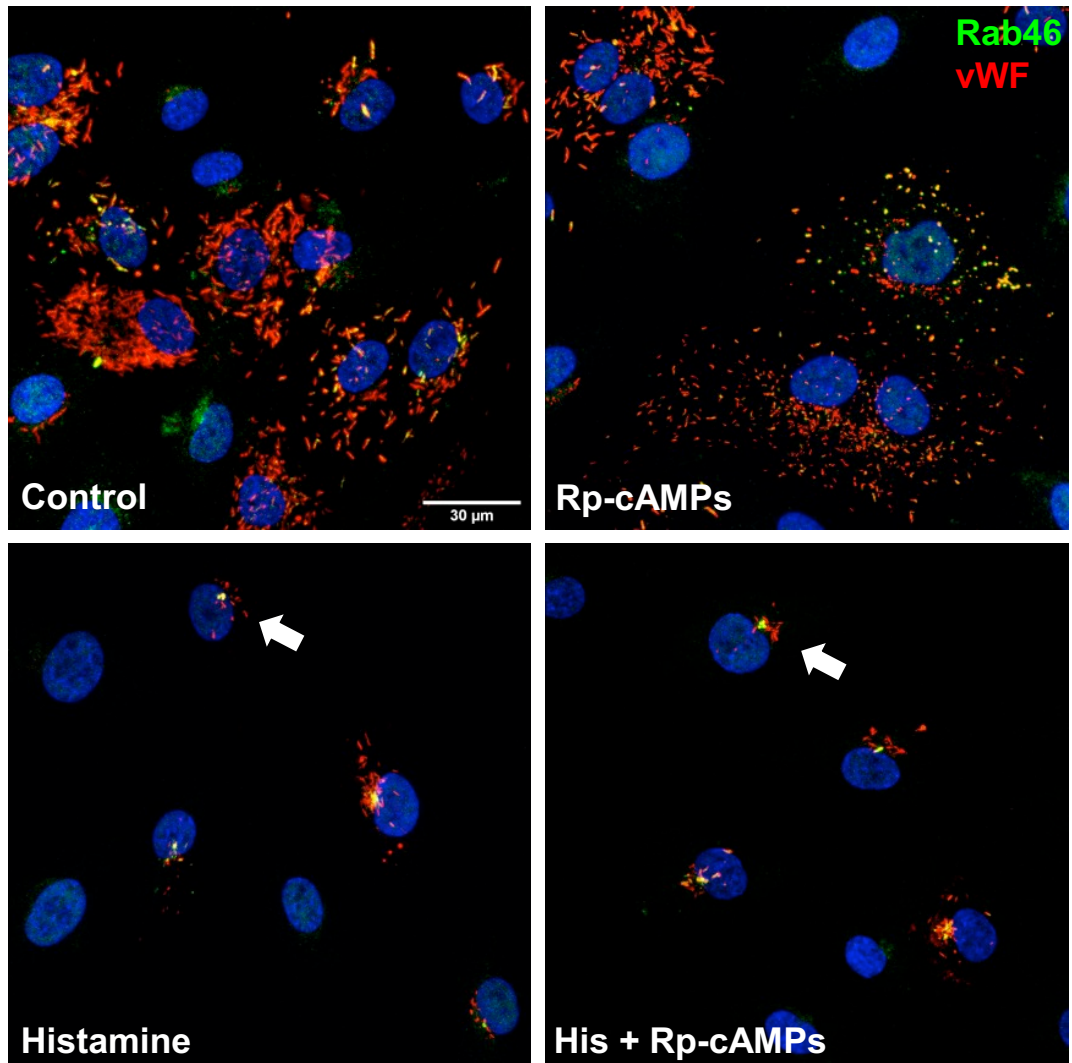


Figure 4.6 Histamine-evoked perinuclear trafficking of Rab46-positive WPBs is cAMP-independent.

Representative images of HUVECs pre-treated with vehicle or 20 μ M Rp-cAMP for 60 minutes, followed by treatment with 30 μ M histamine for 15 minutes. Cells were then fixed and stained for Rab46 (green) and vWF (red; marker of WPBs). DAPI (blue) shows nuclei. Maximum intensity projections from DeltaVision z-stack are shown. White arrows show Rab46-positive WPBs clusters. Scale bar = 30 μ m.

4.3 Epinephrine-induced perinuclear clustering of WPBs is independent of Rab46

As a novel Rab GTPase in the endothelium, I sought to determine if Rab46 played a role in cAMP-dependent perinuclear trafficking of WPBs.

Here, I used high-resolution microscopy to observe the effect of PKA inhibition on epinephrine induced retrograde trafficking of Rab46-positive WPBs. HUVECs were pre-treated with either a vehicle control or H89 prior to stimulation and then immunostained for vWF (red) and Rab46 (green). In high-resolution representative images, perinuclear clustering of Rab46-positive WPBs was only observed after acute stimulation of HUVECs with application of epinephrine and IBMX, (Figure 4.7). When HUVECs were preincubated with H89, unlike histamine-treated cells, perinuclear clustering of Rab46-positive WPBs was undetected upon epinephrine and IBMX co-treatment. This data confirms previous reports of PKA-dependent cAMP-induced perinuclear clustering of WPBs. However, in contrast to previous reports, I observed that IBMX alone induced clustering of Rab46-positive WPBs, suggesting that the potentiation of cAMP levels by IBMX is crucial for the appearance of WPB perinuclear clusters. Measurement of intracellular Ca^{2+} fluorescence confirmed that treatment of HUVECs with epinephrine and IBMX failed to evoke Ca^{2+} release from intracellular Ca^{2+} stores, indicating that in ECs, epinephrine induces cAMP as a 2nd messenger and its downstream signalling pathways, which is independent of Ca^{2+} (Figure 4.8).

As other endothelial GTPase proteins have been reported in cAMP-dependent perinuclear clustering of WPBs (Rondaij et al., 2004b; Van Hooren et al., 2012b), it was necessary to define the potential role of Rab46. HUVECs were transfected with a Rab46 specific siRNA and treated acutely with a combination of epinephrine and IBMX. Epinephrine-induced WPB clusters were still observed in cells depleted of endogenous Rab46 (Figure 4.9).

Taken together the findings in this chapter support that in ECs, histamine-induced perinuclear clustering of WPBs is independent of cAMP and PKA signalling, and Rab46 does not participate in the downstream signalling pathway of cAMP-raising agonists.

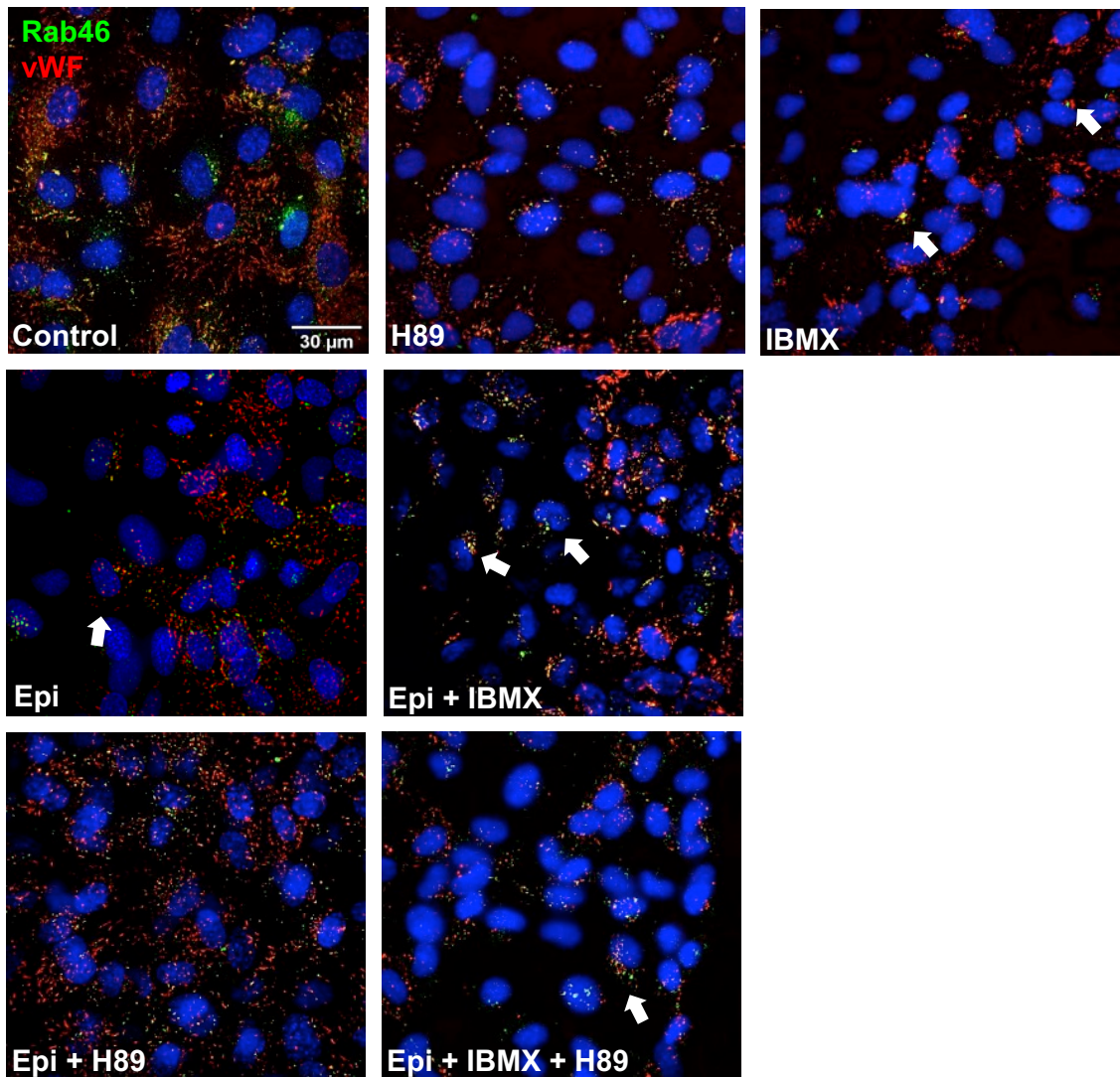


Figure 4.7 Epinephrine induces perinuclear clustering of Rab46 and WPB solely in the presence of phosphodiesterase inhibitor.

Representative immunofluorescent images of HUVECs pre-treated with vehicle control and 10 μ M H89 for 30 minutes, followed by treatment with 100 μ M epinephrine, 100 μ M epinephrine together with 100 μ M IBMX, or 100 μ M IBMX on its own for 15 minutes. Cells were then fixed and stained for Rab46 (green) and vWF (red; marker of WPBs). DAPI (blue) shows nuclei. Maximum intensity projections from DeltaVision z-stack are shown. White arrows show cells of interest. Scale bar = 30 μ m.

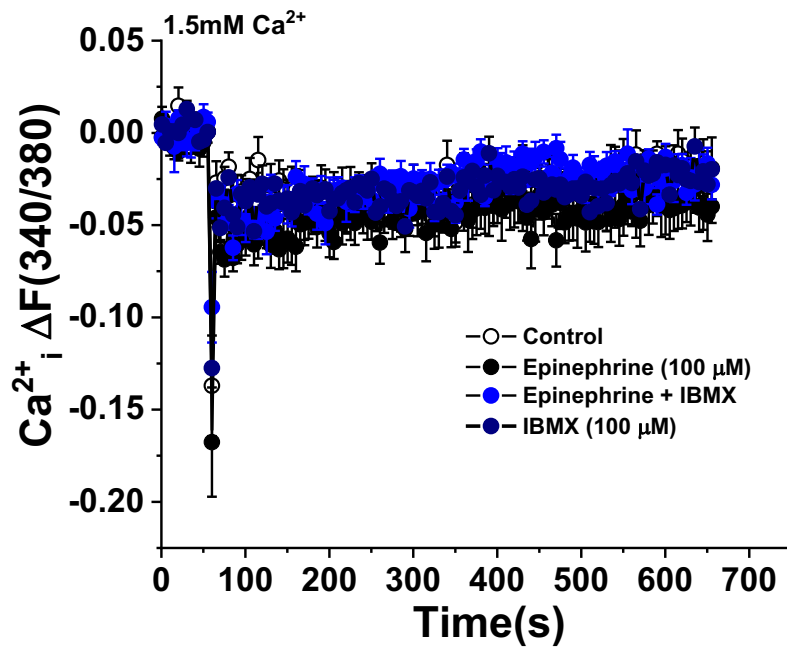


Figure 4.8 Epinephrine does not evoke intracellular Ca^{2+} release from ECs.

Representative trace of Ca^{2+} fluorescence in HUVECs for 5 minutes evoked by application of vehicle control, 100 μM epinephrine, 100 μM epinephrine together with 100 μM IBMX, or 100 μM IBMX on its own at 60 seconds. Recordings were obtained in 1.5 mM Ca^{2+} SBS buffer (n/N=3/9, error bars represent SEM).

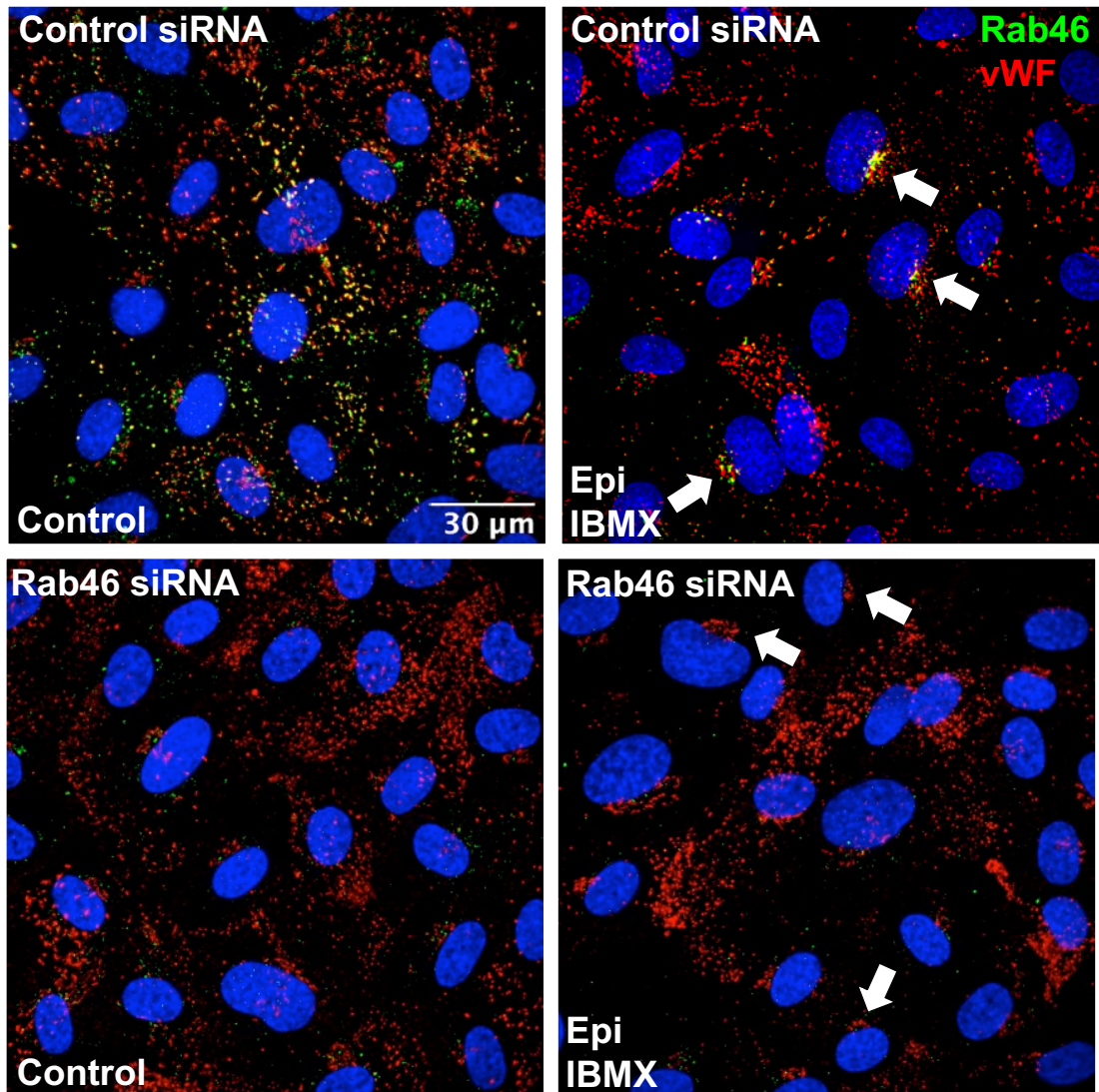


Figure 4.9 Rab46 is not necessary for cAMP-dependent trafficking of WPBs

Immunofluorescent images showing subcellular localisation of vWF (red; as a marker of WPBs) in HUVECs. Cells were transfected with scrambled control sequence or Rab46 siRNA for 72 hours. Prior to fixation, cells were treated with 100 μ M epinephrine (Epi) + 100 μ M IBMX for 15 minutes. DAPI (blue) shows nuclei. Maximum intensity projections from DeltaVision z-stack are shown. White arrows show cells of interest. Scale bar = 30 μ m (n/N = 3/18)

Chapter 5 The role of Ca^{2+} in Rab46-dependent WPB trafficking

5.1 Introduction

It is known that WPBs trafficking and exocytosis can be triggered by either cAMP- or Ca^{2+} -dependent pathways (see Chapter 1 for more detail). In Chapter 4, I presented data describing that histamine signalling in HUVECs is independent of cAMP, therefore, here, I investigate whether Ca^{2+} is necessary for the histamine-evoked WPB trafficking to MTOC that it was previously shown is dependent on Rab46 (Miteva et al., 2019).

Ca^{2+} is an ubiquitous signalling ion that regulates a wide range of intracellular signalling pathways and processes including the formation, trafficking, vesicle fusion and exocytosis of various cellular cargo (Berridge et al., 2003). WPB exocytosis is triggered by a wide range of physiological signals (e.g. histamine, VEGF, thrombin, sphingosine-1 phosphate) that use Ca^{2+} as second messenger. Global release of Ca^{2+} from intracellular Ca^{2+} stores, downstream of aforementioned physiological stimuli, is a potent trigger for WPB trafficking and exocytosis. In fact, ionophores (e.g. ionomycin) prove that a sustained, global elevation of intracellular Ca^{2+} is sufficient to drive WPB exocytosis independently of receptor-mediated signalling (Zupančič et al., 2002; Erent et al., 2007b), though further studies are needed to describe the exact mechanisms of WPB trafficking patterns governed by Ca^{2+} signals. Indeed regulation of differential, signal-selective WPB trafficking and exocytosis in response to the range of Ca^{2+} -dependent triggers and the potential of several involved Ca^{2+} -sensors has been hypothesised previously but remained elusive (Zupančič et al., 2002; Rondajij, Bierings, Kragt, Van Mourik, et al., 2006; Babich et al., 2008). More recently, Synaptotagmin-5 has been described as a Ca^{2+} sensor regulating WPBs exocytosis near the plasma membrane (Lenzi, Stevens, Osborn, Matthew J. Hannah, et al., 2019). Ca^{2+} sensors are necessary to couple transient elevations of intracellular Ca^{2+} to the majority of vesicle transport and secretion processes (Pang and Südhof, 2010). However, the identity or mechanisms of likely multiple Ca^{2+} -sensors involved in transducing acute release of Ca^{2+} from ER stores in response to physiological signals (e.g. histamine) into WPB trafficking and exocytosis remain insufficiently defined (Lenzi, Stevens, Osborn, Matthew J. Hannah, et al., 2019).

The aim of this chapter is to investigate the role of Ca^{2+} in Rab46-dependent WPBs trafficking in response to histamine. Firstly, using RT-qPCR, intracellular Ca^{2+} measurement and high-resolution imaging, I established the histamine receptor subtype mediating the Rab46-dependent perinuclear clustering of

WPBs. Secondly, chelation of Ca^{2+} and pharmacological inhibitors of Ca^{2+} entry were used to question whether histamine-induced Ca^{2+} signalling was necessary to drive the retrograde trafficking of WPBs to the MTOC. Finally, the role of Rab46 as a novel Ca^{2+} sensor in the endothelium was investigated.

5.2 Histamine-evoked WPB trafficking is mediated by the H₁ receptor

Histamine exerts its function by binding to four different G protein-coupled receptors (H₁–H₄; (Parsons and Ganellin, 2006; Haas and Panula, 2016). Histamine receptors operate via different downstream pathways. For example, H₁R is coupled to G_{q/11} which is coupled to PLC and Ca^{2+} release from the intracellular Ca^{2+} stores while H₂R are coupled to G_s and adenylyl cyclase resulting in cytoplasmic cAMP raise. H₃R and H₄R are coupled to G_{i/o} signalling which enhances Ca^{2+} signalling by inhibiting cAMP production (Jutel et al., 2005). Molecular investigations in previous studies in several types of ECs show opposing evidence on the presence of histamine receptors in HUVECs (Gantner et al., 2002; Li et al., 2003). Hence, using RT-qPCR analysis, I identified that the receptor with highest expression in the pooled HUVECs was H₁R, with only trace levels of H₄R observed (Figure 5.1A; presence of H₂R and H₃R could not be confirmed due to the high cycle values). mRNA from human brain was used as a control mRNA pool to validate the primer efficiency of the H₁₋₄R primers (Figure 5.1B; primer efficiency curves performed but not shown).

To further investigate the receptor subtype responsible for histamine-induced perinuclear trafficking of WPBs, selective agonists to H₁R (2-pyridylethylamine dihydrochloride [2-PY]) or H₄R (4-methyl- histamine dihydrochloride [4-Met]) were used in Ca^{2+} measurement assays. Dose responses were quantified by measuring changes in fluorescence in Fura-2 loaded cells using a FlexStation (see Chapter 2 for details). Dose-response curve was constructed and EC₅₀ values for H₁ agonists was generated (Figure 5.2A). H₄R agonist, 4-Met, appeared to raise Ca^{2+} fluorescence only at concentrations as high as 100 μM and 300 μM (Figure 5.3A, B). Several considerations may be underpinning this results such as poor efficacy of the agonist for its receptor, low expression of the receptor, also shown above RT-qPCR analysis in Figure 5.2A, or low recruitment of Ca^{2+} entry channels at the plasma membrane (typical for G_{i/o} coupled receptors). 2-PY EC₅₀ value (EC₅₀=18.04 μM) suggests lower potency for H₁R activation compared to histamine (EC₅₀=0.73 μM ; see Chapter 3). Hence, a higher working concentration of 2-PY (100 μM) than histamine was selected and

used hereinafter. High-resolution images of HUVECs immunostained for Rab46 (green) and vWF (red) and treated with 2-PY showed that 2-PY induced perinuclear clusters of Rab46-positive WPBs at the MTOC (Figure 5.2B). HUVECs treated with 4-Met did not induce any distinctive trafficking or clustering of neither WPB, nor Rab46 (Figure 5.3B).

Additionally, to solidify the current evidence that H₁R is indeed responsible for histamine-induced Rab46 and WPB perinuclear clustering, mepyramine (mep) was used as a well-established anti-histamine agent that selectively targets the H₁ as an inverse agonist (Fitzsimons et al., 2004). Pre-treating HUVECs with mepyramine completely abolished intracellular Ca²⁺ release triggered by 2-PY in a FlexStation assay (Figure 5.4A). Ca²⁺ measurements were performed on cells in Ca²⁺-free extracellular buffer supplemented with the Ca²⁺ chelator EGTA, in order to solely observe intracellular Ca²⁺ release events and limit extracellular Ca²⁺ entry from plasma membrane channels. High-resolution images from HUVECs immunostained with Rab46 (green) and vWF (red) revealed that mepyramine action on H₁R prevents perinuclear clustering of Rab46-positive WPBs induced by 2-PY (Figure 5.4B). Similar results were observed on intracellular Ca²⁺ release recordings in response to histamine of HUVECs pre-treated with mepyramine (Figure 5.5A). Mepyramine also abolished histamine-induced perinuclear clustering of Rab46 and WPB (Figure 5.5B). Taken together, these data provide evidence that histamine-evoked Ca²⁺ release and WPB trafficking in HUVECs is mediated by the H₁R.

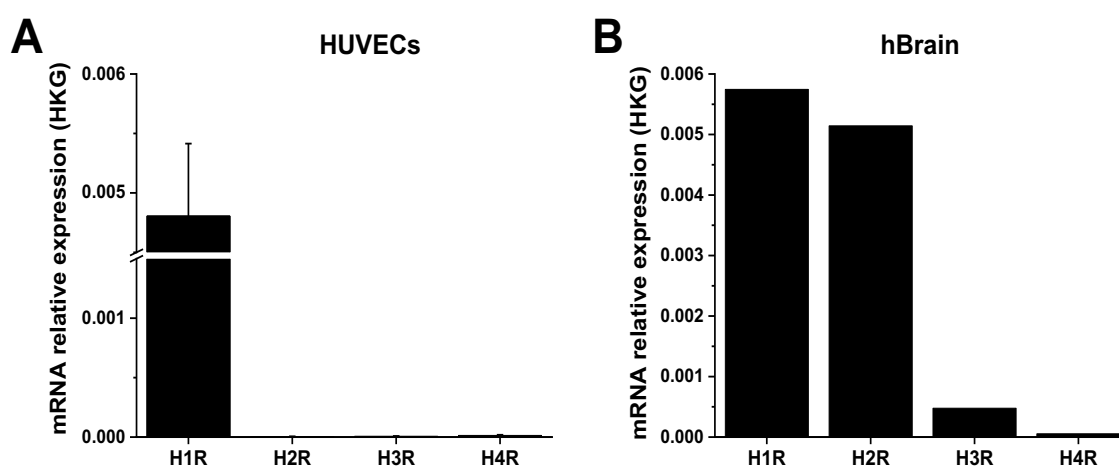


Figure 5.1 HUVECs express histamine H₁ receptors.

(A) qPCR Δ Ct analysis of *hrh1*, *hrh2*, *hrh3* and *hrh4* mRNA expression in HUVECs relative to housekeeping genes (HKG: GAPDH and β -actin; n=3, error bars represent SEM) (B) qPCR Δ Ct analysis of *hrh1*, *hrh2*, *hrh3* and *hrh4* mRNA expression in human Brain mRNA relative to housekeeping genes (HKG: GAPDH and β -actin; n=1).

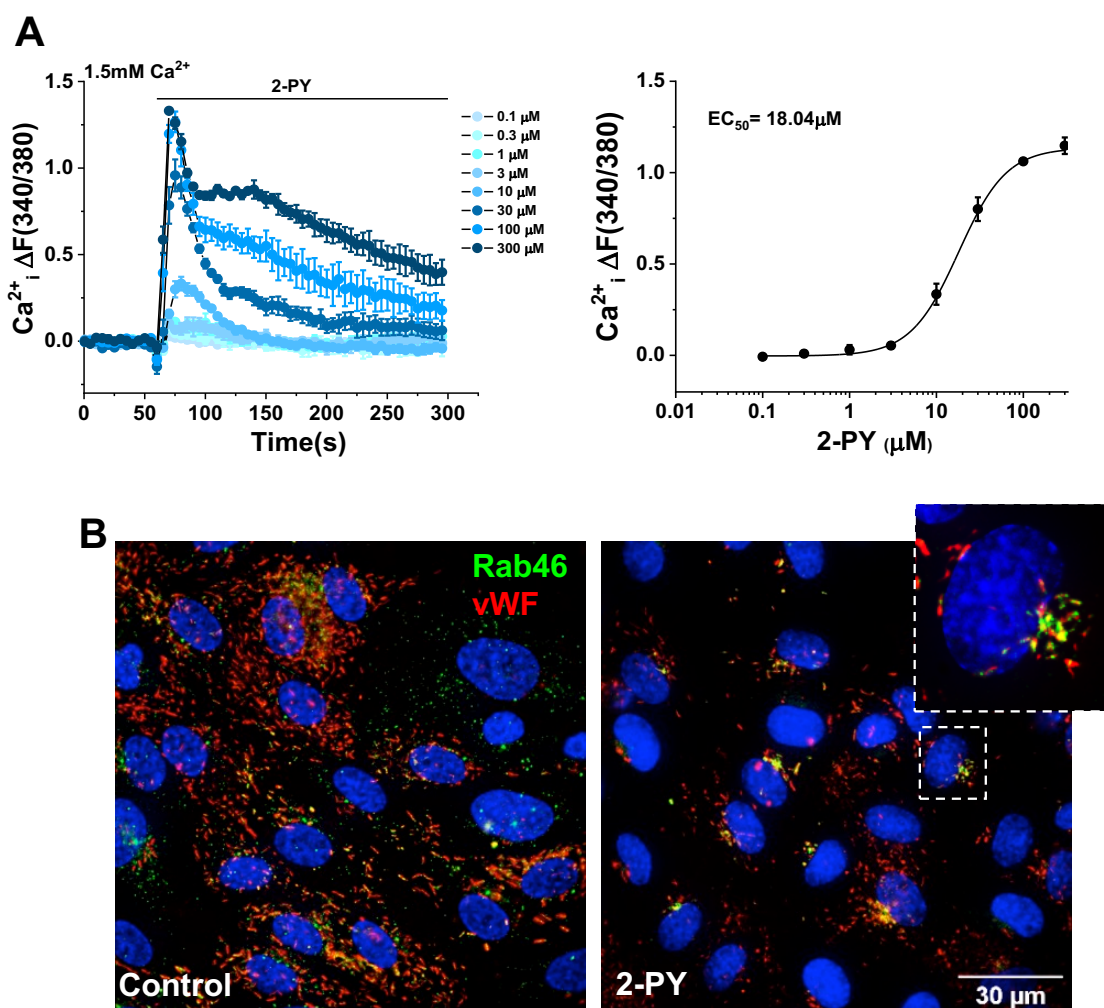


Figure 5.2 Histamine H₁ receptor selective agonist, 2-PY, evokes intracellular Ca²⁺ release and Rab46 and WPB perinuclear clustering.

(A) Representative trace (left) of Ca²⁺ rise in HUVECs for 5 minutes evoked by application of 2-PY ranging doses 0.1 – 300 μM. Recordings were obtained in 1.5 mM Ca²⁺ SBS buffer. Mean data (right) of HUVEC treated with 2-PY ranging doses 0.1-300 μM are displayed as a concentration-response curve and the fitted curve is plotted using a Hill Equation indicating the 50 % maximum effect (EC₅₀; n/N=3/9, error bars represent SEM). (B) Immunofluorescent images showing subcellular localisation of Rab46 (green) and vWF (red; as a marker of WPBs) in HUVECs treated with 100 μM 2-PY for 5 minutes. DAPI (blue) shows nuclei. Maximum intensity projections from DeltaVision z-stack are shown. Scale bar = 30 μm.

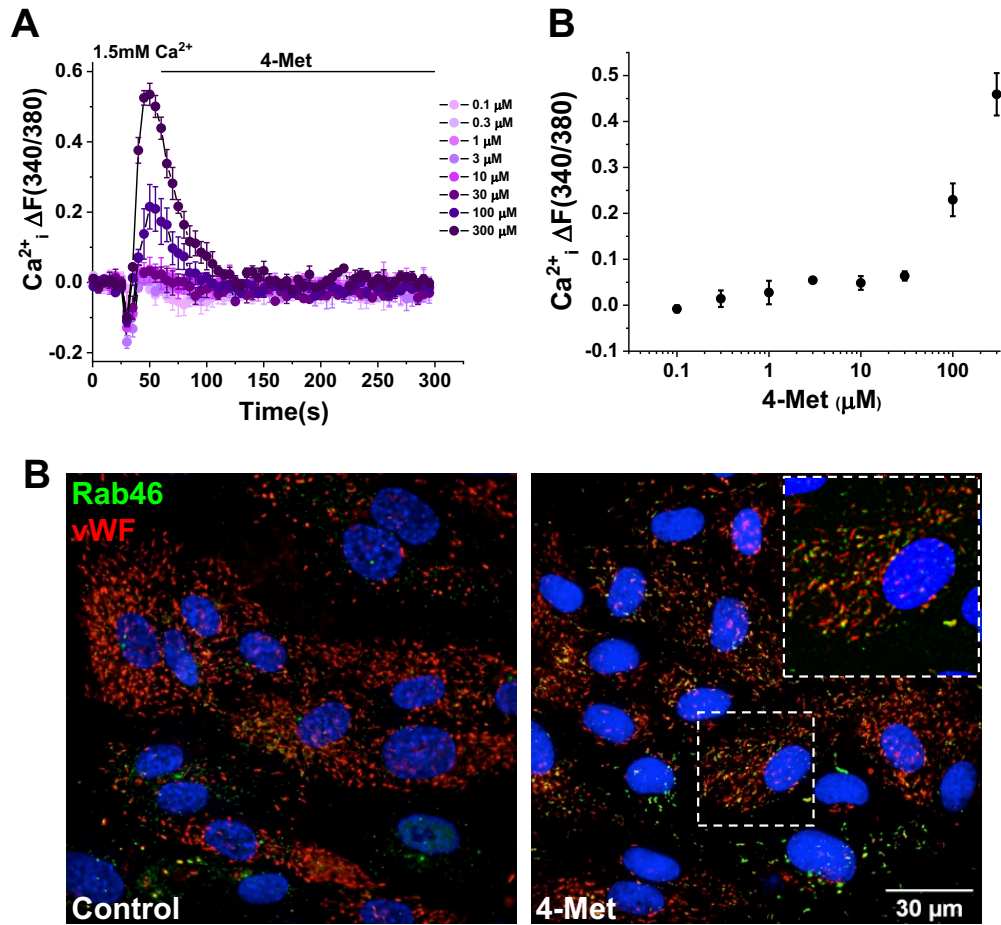


Figure 5.3 Histamine H₄ receptor agonist does not trigger perinuclear clustering of Rab46-positive WPBs.

(A) Representative trace (left) of Ca²⁺ rise in HUVECs for 5 minutes evoked by application of 4-Met ranging doses 0.1 – 300 μM. Recordings were obtained in 1.5 mM Ca²⁺ SBS buffer (n/N=3/9, error bars represent SEM). (B) Immunofluorescent images showing subcellular localisation of Rab46 (green) and vWF (red; as a marker of WPBs) in HUVECs treated with 100μM 4-Met for 5 minutes. DAPI (blue) shows nuclei. Maximum intensity projections from DeltaVision z-stack are shown. Scale bar = 30 μm.

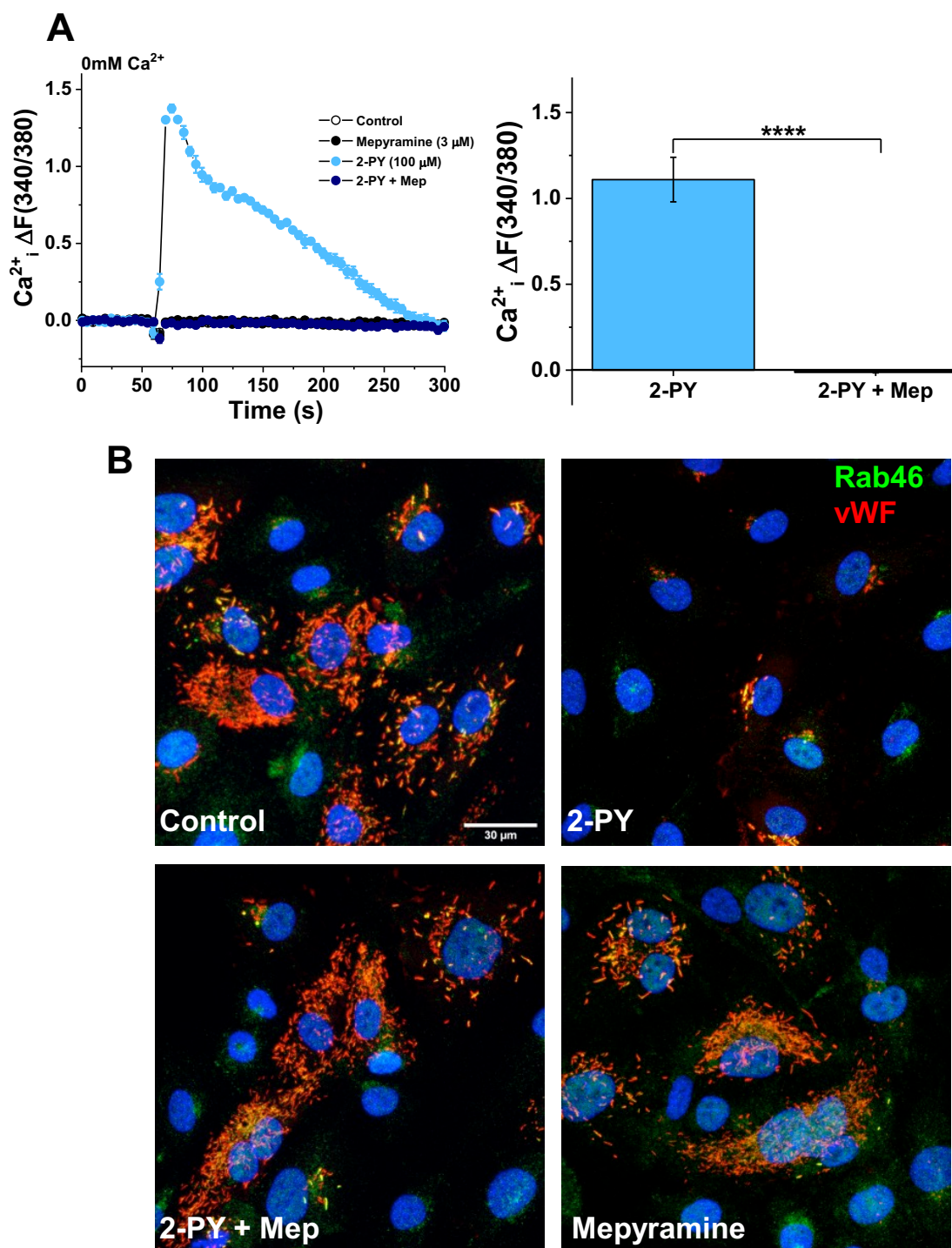


Figure 5.4 H₁R selective inverse agonist inhibits 2-PY evoked intracellular Ca²⁺ release.

(A) Representative trace (left) and mean data (right) of Ca²⁺ release in HUVECs for 5 minutes evoked by application of 100 μ M 2-PY at 60 seconds, cells were pre-treated with 3 μ M mepyramine for 30 minutes. Recordings were obtained in Ca²⁺ free buffer. (n/N=3/18, error bars represent SEM, n.s., not significant, **** p-value < 0.0001 by One-way ANOVA). (B) Immunofluorescent images showing subcellular localisation of Rab46 (green) and vWF (red; as a marker of WPBs) in HUVECs pre-treated with 3 μ M mepyramine for 30 minutes. Prior to fixation cells were treated with 100 μ M 2-PY for 5 minutes. DAPI (blue) shows nuclei. Maximum intensity projections from LSM 700 z-stack are shown. Scale bar = 30 μ m.

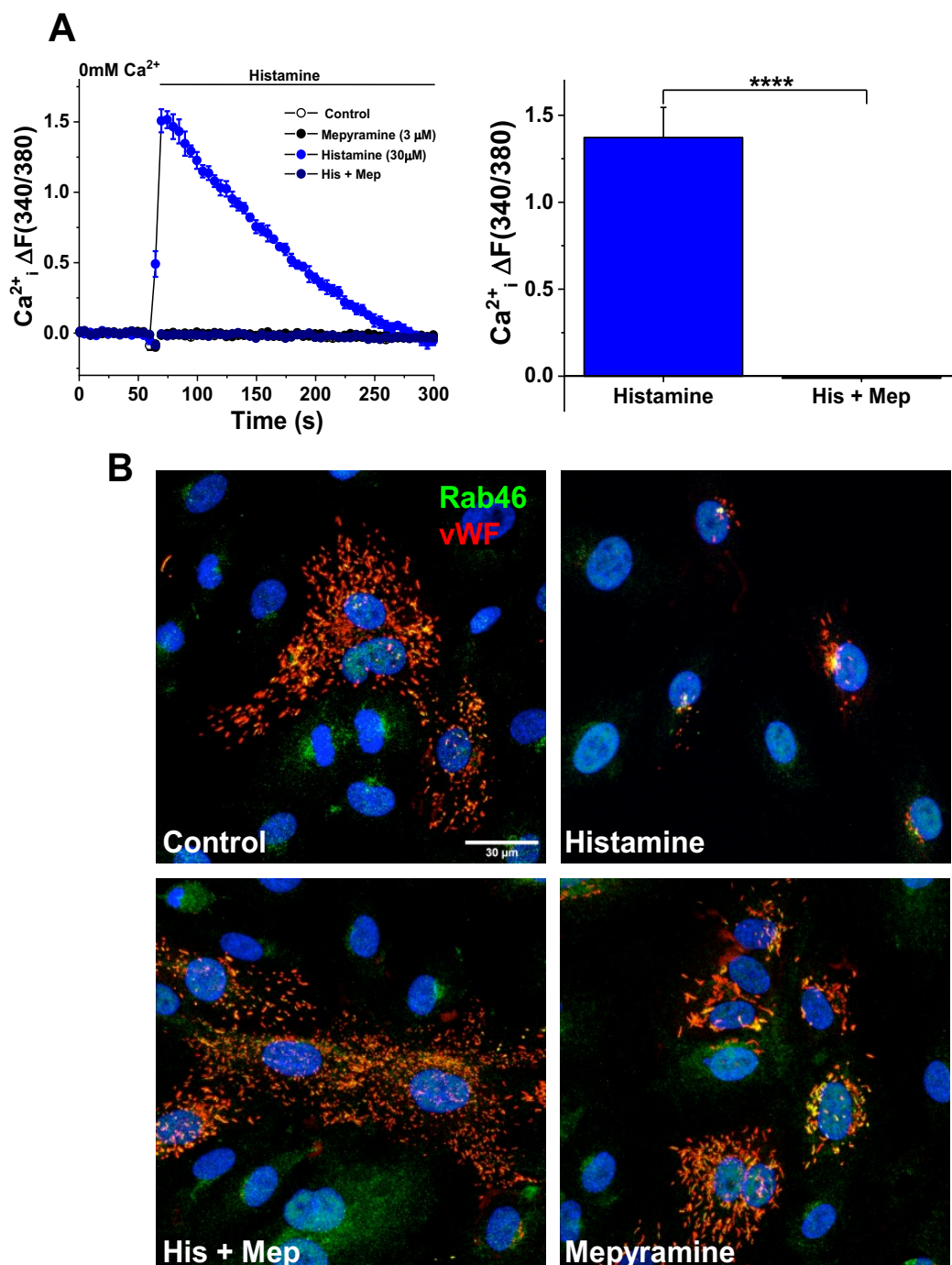


Figure 5.5 H₁R inverse agonist inhibits histamine-evoked intracellular Ca²⁺ release.

(A) Representative trace (left) and mean data (right) of Ca²⁺ release in HUVECs for 5 minutes evoked by application of 30 μM histamine at 60 seconds, cells were pre-treated with 3 μM mepyramine for 30 minutes. Recordings were obtained in Ca²⁺ free buffer. (n/N=3/18, error bars represent SEM, n.s., not significant, **** p-value < 0.0001 by One-way ANOVA). (B) Immunofluorescent images showing subcellular localisation of Rab46 (green) and vWF (red; as a marker of WPBs) in HUVECs pre-treated with 3 μM mepyramine for 30 minutes. Prior to fixation cells were treated with 30 μM histamine for 5 minutes. DAPI (blue) shows nuclei. Scale bar = 30 μm. Maximum intensity projections from confocal microscope Zeiss LSM 700 z-stack are shown.

5.3 Histamine-evoked retrograde trafficking of WPBs is independent of intracellular Ca²⁺

5.3.1 Store-operated Ca²⁺ entry is not involved in histamine-evoked perinuclear clustering of Rab46-positive WPBs

Several studies have implicated that the Ca²⁺ influx from SOCE via the Orai1 channel is involved in several intracellular signalling pathways (Capiod, 2011; Dubois et al., 2016). Additionally, Noy and colleagues have described a link between Orai1 (SOCE channel) and vWF release (Noy et al., 2019). Although Rab46 does not participate in the SOCE in endothelial cells (Wilson et al., 2015), it is necessary to investigate whether Ca²⁺ influx from histamine-activated (via the H₁R) SOCE itself is the trigger for perinuclear trafficking of Rab46-positive WPBs.

In FlexStation assay, HUVECs were stimulated with histamine and then physiological concentration of Ca²⁺ was added back to the cells as a measure of SOCE through the Orai channels (Figure 5.6A). Ca²⁺ fluorescence recordings were performed in Ca²⁺ free buffer. Histamine induced a peak response after 10 seconds, demonstrating a characteristic Ca²⁺ release from intracellular stores. Transient Ca²⁺ entry was observed upon addition of Ca²⁺ to the recording buffer. Pre-treatment of HUVECs with Orai1 channel inhibitor RO2959 completely abolished this Ca²⁺ entry (Figure 5.6B, C). Next, HUVECs were again pre-treated with RO2959 and immunostained for Rab46 (green) and vWF (red; Figure 5.7). High-resolution imaging in replicating the conditions used in Figure 5.6 revealed that histamine stimulation on its own induced perinuclear trafficking of Rab46-positive WPBs to the MTOC as previously shown. However, Orai1 inhibition did not appear to affect this trafficking, suggesting that Ca²⁺ influx from histamine-triggered SOCE does not participate in the perinuclear trafficking of Rab46-positive WPBs.

Taken together data from Ca²⁺ chelation and SOCE inhibition experiments show that perinuclear trafficking of Rab46-positive WPBs to the MTOC is independent of histamine-induced intracellular Ca²⁺ entry via Orai1 during SOCE.

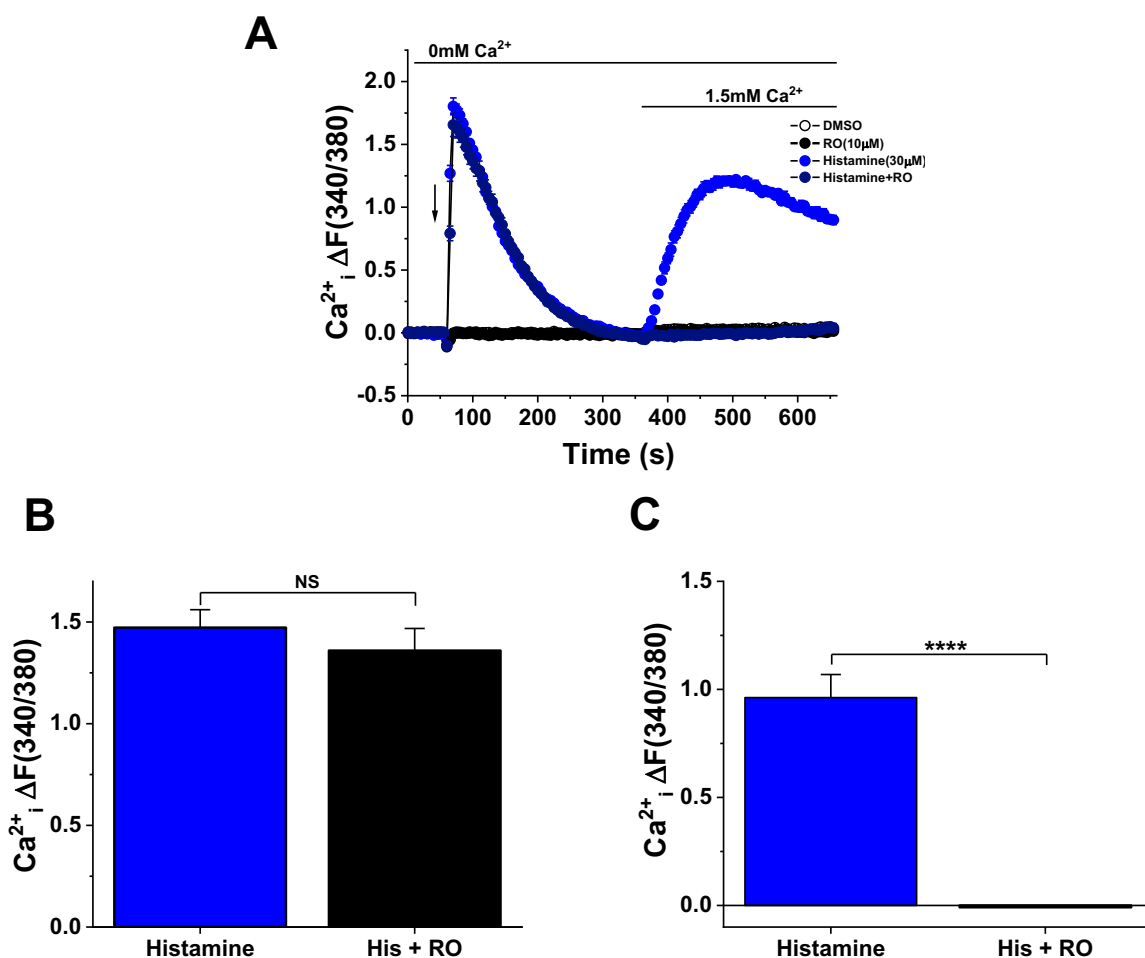


Figure 5.6 Inhibition of SOCE through Orai channels does not inhibit histamine-induced Ca²⁺ release from intracellular stores.

(A) Representative trace of Ca²⁺ release and entry in HUVECs for 10 minutes. Release from stores evoked by application of 30 μM histamine to cells incubated in 0 calcium at 60 seconds. SOCE is evoked by adding back 7.5 mM Ca²⁺ at 360 seconds. Cells were pre-treated with control or 10 μM RO2959 for 30 minutes to inhibit Orai1. (B) Mean data of Ca²⁺ release in HUVECs evoked by application of 30 μM histamine at 60 seconds, cells were pre-treated with 10 μM RO2959 for 30 minutes. (C) Mean data of Ca²⁺ entry in HUVECs evoked by application of 7.5mM Ca²⁺ SBS buffer at 360 seconds. Recordings were obtained in Ca²⁺ free buffer prior to Ca²⁺ at 360 seconds. (n/N=5/15, error bars represent SEM, *** p value < 0.001 by One-way ANOVA).

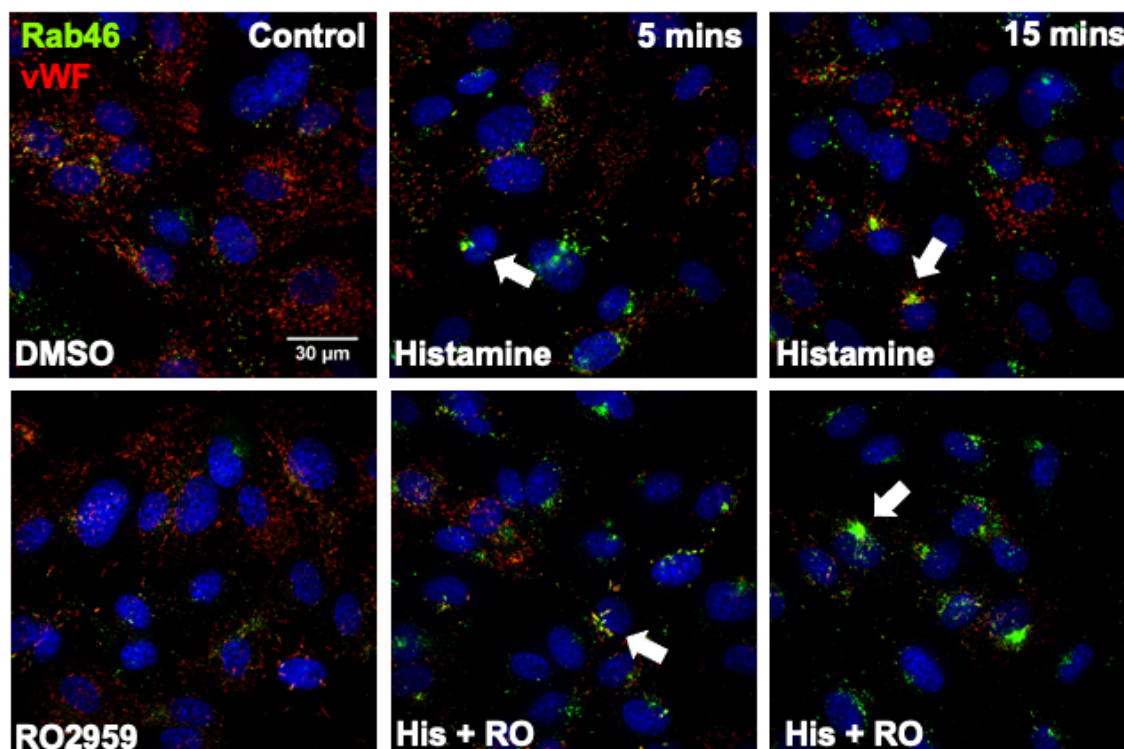


Figure 5.7 Inhibition of store-operated Ca^{2+} -entry does not prevent histamine-induced Rab46 and WPB perinuclear clustering.

Representative immunofluorescent images of HUVECs pre-treated with vehicle or 10 μM RO2959 for 30 minutes followed by treatment with 30 μM histamine for 5 and 10 minutes, and then fixed and stained for Rab46 (green) and vWF (red; marker of WPBs). DAPI (blue) shows nuclei. Arrows show Rab46 and WPB clustering in selected cells. Maximum intensity projections from DeltaVision z-stack are shown. Scale bar = 30 μm .

5.3.2 Chelation of intracellular Ca^{2+} does not prevent histamine-evoked perinuclear clustering of Rab46-positive WPBs.

Canonically activated H_1R signals through $\text{G}\alpha\text{q}/11$, which triggers $\text{PLC}\beta$ and subsequent IP_3 -mediated Ca^{2+} release from the ER stores (Parsons and Ganellin, 2006; Haas and Panula, 2016). Previously I have shown that H_1R signalling evokes Ca^{2+} release and trafficking of WPBs to the perinucleus and we have published that this retrograde trafficking is dependent on Rab46. Since Rab46 is an unusual Rab GTPase because, along with its GTPase domain, it has Ca^{2+} sensing EF-hand domains (Wilson et al., 2015), here I first evaluated the need for intracellular Ca^{2+} mobilisation in histamine-evoked retrograde trafficking of WPBs. I used AM-BAPTA as a well-established cell permeable Ca^{2+} chelator with fast Ca^{2+} binding kinetics (Naraghi, 1997; Dargan and Parker, 2003). First, to validate AM-BAPTA activity, Fura-2 loaded HUVECs were pre-incubated with 10

μM AM-BAPTA, and Ca^{2+} measured upon histamine stimulation. Ca^{2+} fluorescence recordings were performed on cells incubated in an extracellular buffer supplemented with either physiological concentrations of Ca^{2+} or Ca^{2+} free buffer with EGTA. Histamine-triggered Ca^{2+} release was significantly decreased in HUVECs pre-treated with $10 \mu\text{M}$ AM-BAPTA (Figure 5.8A, B). Although significantly decreased, HUVECs stimulated with histamine displayed prolongation of weak and global Ca^{2+} transients, a hallmark characteristic of Ca^{2+} chelation with AM-BAPTA (Dargan and Parker, 2003). Next, HUVECs were loaded with AM-BAPTA, stimulated with histamine and subsequent immunostaining with Rab46 (green) and vWF (red; Figure 5.9A) was performed. Quantification of high-resolution images revealed that Ca^{2+} chelation did not inhibit histamine-evoked perinuclear clustering of Rab46 or WPBs (Figure 5.9B, C respectively). These data indicate that although histamine signalling in HUVECs is coupled to Ca^{2+} release from stores, the perinuclear clustering of Rab46-positive WPBs triggered by histamine is independent of Ca^{2+} release.

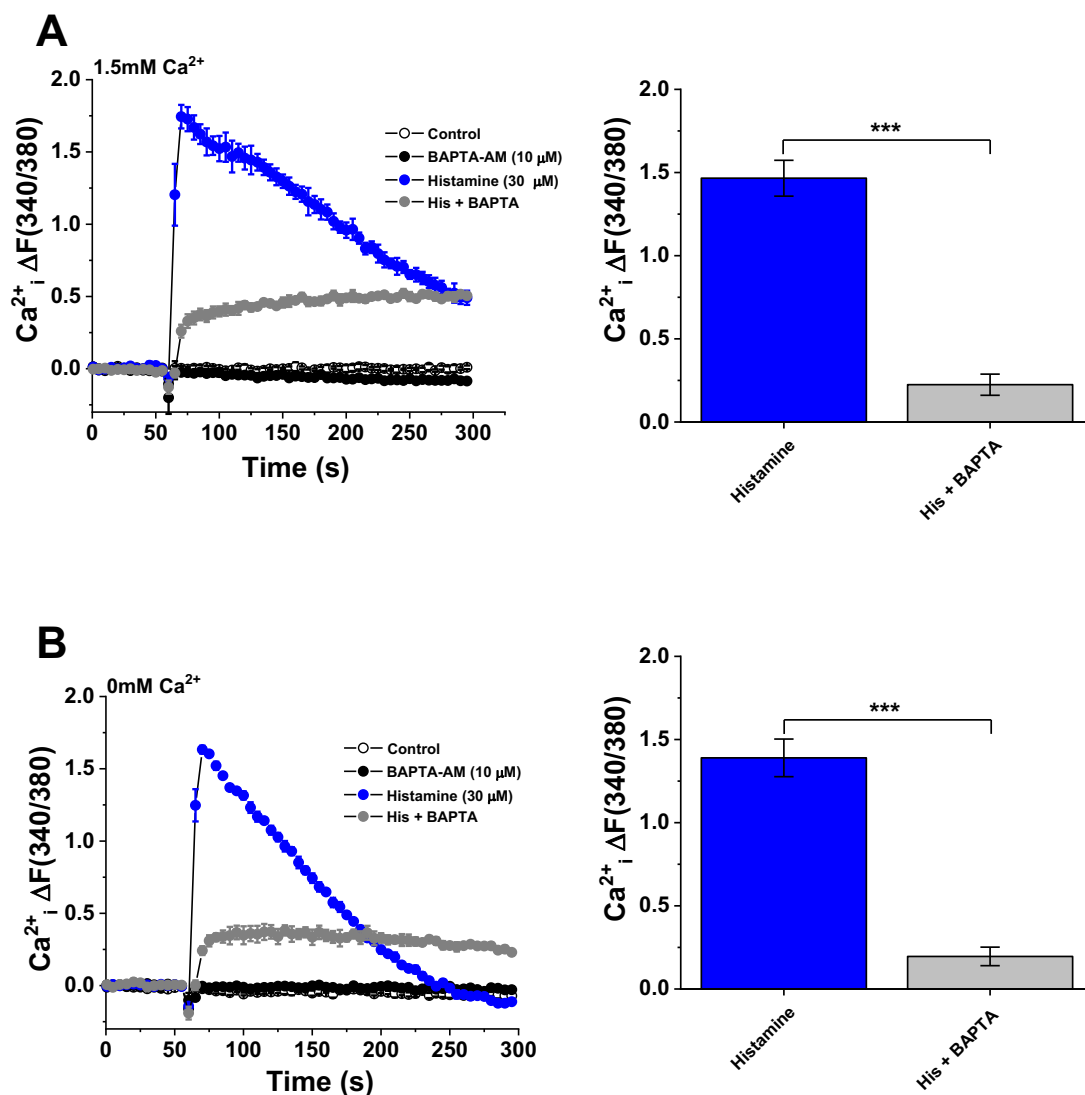


Figure 5.8 BAPTA-AM chelates histamine-evoked intracellular Ca²⁺ release.

(A) Representative trace (top left) and mean data (top right) of Ca²⁺ release in HUVECs for 5 minutes evoked by application of 30 μM histamine at 60 seconds, cells were pre-treated with 10 μM AM-BAPTA for 20 minutes. Recordings were obtained in 1.5 mM Ca²⁺ SBS buffer. (B) Representative trace (top left) and mean data (top right) of Ca²⁺ release in HUVECs evoked by application of 30 μM histamine at 60 seconds, cells were pre-treated with 10 μM AM-BAPTA for 20 minutes. Recordings were obtained in Ca²⁺ free buffer (n/N=3/9, error bars represent SEM, *** p value < 0.001 by One-way ANOVA).

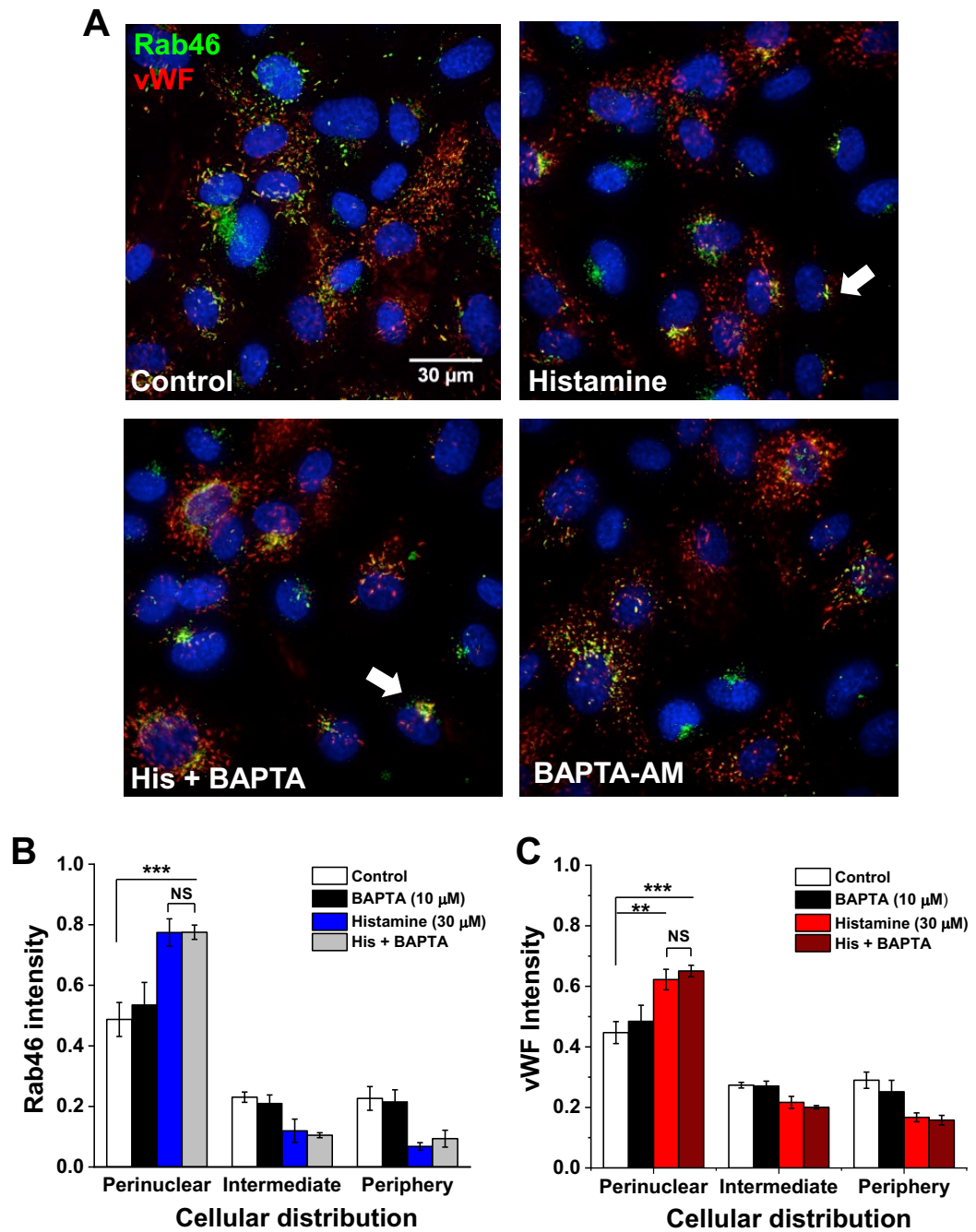


Figure 5.9 Acute histamine-evoked perinuclear trafficking of WPBs is independent of intracellular Ca^{2+} release.

A) Representative immunofluorescent images of HUVECs pre-treated with vehicle and 10 μ M AM-BAPTA for 20 minutes followed by treatment with 30 μ M histamine for 5 minutes, and then fixed and stained for Rab46 (green) and vWF (red; marker of WPBs). White arrows show Rab46-positive WPBs clusters. DAPI (blue) shows nuclei. Maximum intensity projections from DeltaVision z-stack are shown. Scale bar = 30 μ m.

Figure 1.9 continued (B, C) Mean data showing the cellular distribution of Rab46 and vWF, respectively, upon treatments from (A). Results were grouped into three areas: perinuclear, intermediate and periphery as described in methods. The plot quantifies Rab46 and vWF normalised signal intensity in the respective area where the mean (\pm SEM) was noted as percentage of the total signal intensity (n/N=3/24, NS, not significant, ** p-value < 0.01, *** p-value < 0.001 following a Two-way ANOVA).

5.4 Intracellular Ca²⁺ evokes Rab46-dependent dispersal of WPB clusters from the MTOC

In the previous section, I showed that histamine-evoked WPB trafficking to the MTOC is Ca²⁺-independent. Those results raised the question of what is the function of the Ca²⁺-sensing domains (EF-hands) in Rab46. From previous studies it is known that there is a short isoform of the Rab46 gene (CRACR2A-S), which does not have the Rab GTPase domain but has functional EF-hand domains (Srikanth et al., 2010; Srikanth et al., 2016). Endothelial cells do not express this shorter form of Rab46 (Wilson et al., 2015), however, CRACR2A-S is a vital protein in T cells. Srikanth and colleagues have demonstrated that Ca²⁺ from SOCE binds to the EF-hands of CRACR2A-S, and this triggers the dispersal of Orai1 channel and Stim1 clusters at the plasma membrane. Hence, it was hypothesised that Ca²⁺ binding to the EF-hand is necessary for dissociation of Rab46 and WPB perinuclear clusters formed at the MTOC by histamine stimulation.

Firstly, to investigate the hypothesis outlined above, HUVECs were transfected with a Rab46 mutant that is unable to bind Ca²⁺, Rab46^{EF} (EF-hand), and expression was monitored at either 6 or 24 hours. Transfected cells were immunostained for Rab46 (green) and vWF (red). High-resolution images, shown in Figure 5.10, suggest that the Rab46^{EF} mutant becomes localised to the perinuclear area in the absence of histamine stimulation. Interestingly, at the earlier timepoint (6 hours), it can be observed that the Rab46^{EF} mutant is correctly localised to WPBs, suggesting that Ca²⁺ binding to Rab46 is not necessary for recruitment of Rab46 to WPBs or Rab46-dependent trafficking to the perinuclear area over time.

Secondly, to investigate the role of free cytosolic Ca²⁺ ions on the trafficking of WPBs, HUVECs were stimulated with histamine to induce perinuclear trafficking of WPB, then global intracellular Ca²⁺ was released by treating the cells with the ER Ca²⁺-ATPase pump inhibitor, thapsigargin, resulting in dispersal of Rab46-positive WPBs perinuclear clusters (Figure 5.11A). Treated cells were immunostained for Rab46 (green) and vWF (red) at the end of the experiment.

Quantification of the cellular distribution of vWF and Rab46 from high-resolution images, show that thapsigargin treatment alone does not affect the trafficking of WPBs but triggered a significant dispersal of the histamine-evoked perinuclear clusters of endogenous Rab46 (Figure 5.11B).

These data indicate that Ca^{2+} binding to the EF hand domain of Rab46 triggers Ca^{2+} -dependent dispersal of Rab46-positive WPBs perinuclear clusters. To investigate this hypothesis, dispersal experiments with the same protocol as above were performed in HUVECs overexpressing Rab46^{WT} or Rab46^{EF} (Figure 5.12A). HUVECs were transfected with Rab46^{WT} or Rab46^{EF} mutant for 24 hours. Quantification of high-resolution images revealed that thapsigargin induced the dispersal of Rab46^{WT}, but not Rab46^{EF} mutant, suggesting that it is indeed Ca^{2+} binding to the EF-hand domains of Rab46 that is necessary for dispersal of Rab46 from the perinuclear clusters (Figure 5.12B C). Taking into consideration that perinuclear clustering of WPBs in response to histamine is Rab46-dependent (Miteva et al., 2019), it can be presumed that this is the endogenous mechanism for dispersal of WPBs in HUVECs.

Taken altogether, the data from this chapter evaluate the role of Ca^{2+} in trafficking of WPBs. It can be concluded that perinuclear trafficking to the MTOC is independent of SOCE and intracellular Ca^{2+} , and on the contrary Ca^{2+} binding to the EF-hand domains of Rab46 is necessary for dispersal of Rab46-positive WPBs from the MTOC.

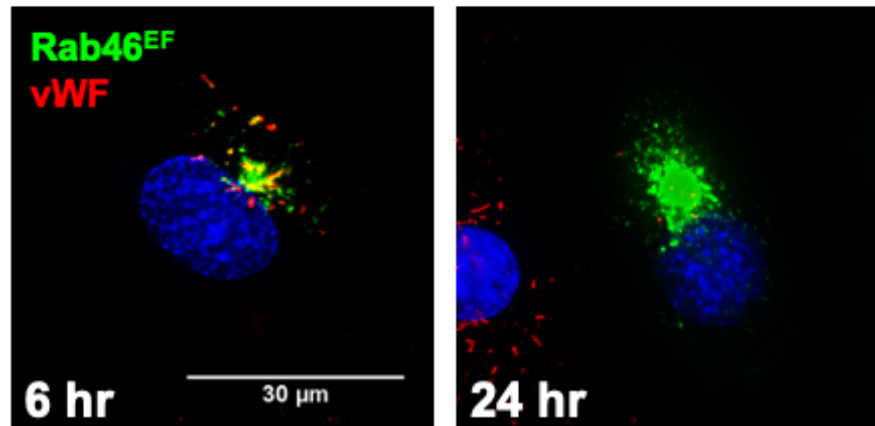


Figure 5.10 Rab46 EF-hand mutant is located at the MTOC in absence of stimulation.

Representative immunofluorescent images showing subcellular localisation of vWF (red; marker of WPBs) and Rab46^{EF} mutant (green) transfected for 6 hours (left) and 24 hours (right). DAPI (blue) shows nuclei. Maximum intensity projections from DeltaVision z-stack are shown. Scale bar = 30 μm.

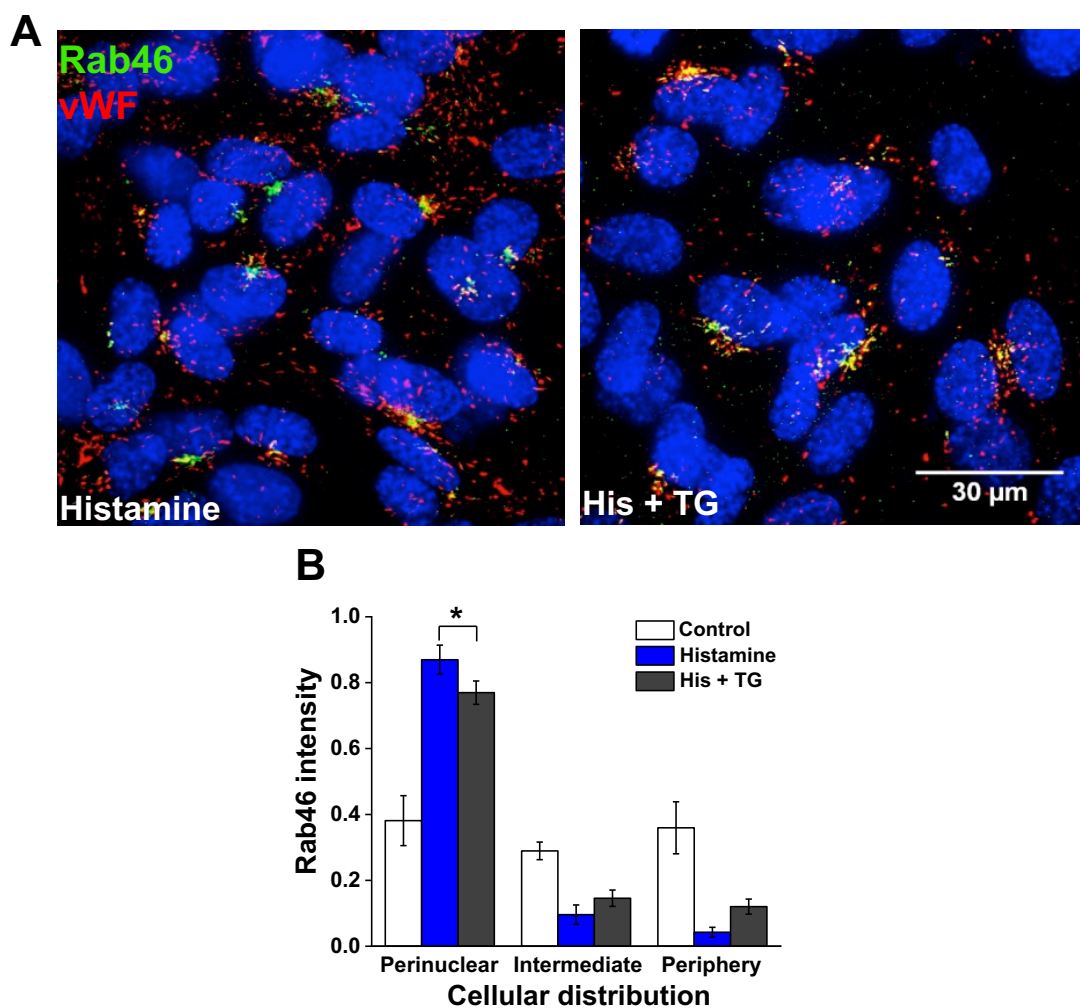


Figure 5.11 Intracellular Ca^{2+} evokes Rab46-dependent WPB dispersal from the MTOC.

A) Representative immunofluorescent images of HUVECs treated with 30 μM histamine for 10 minutes alone or histamine 10 minutes followed by 1 μM thapsigargin, and then fixed and stained for Rab46 (green) and vWF (red; marker of WPBs) after 5 minutes of thapsigargin. DAPI (blue) shows nuclei. Maximum intensity projections from DeltaVision z-stack are shown. Scale bar = 30 μm . (B) Mean data showing the cellular distribution of Rab46 upon treatments from (A). Results were grouped into three areas: perinuclear, intermediate and periphery as described in methods. The plot quantifies Rab46 signal intensity in the respective area where the mean (\pm SEM) was noted as percentage of the total signal intensity ($n/N=3/24$, * p-value < 0.05 following a Two-way ANOVA).

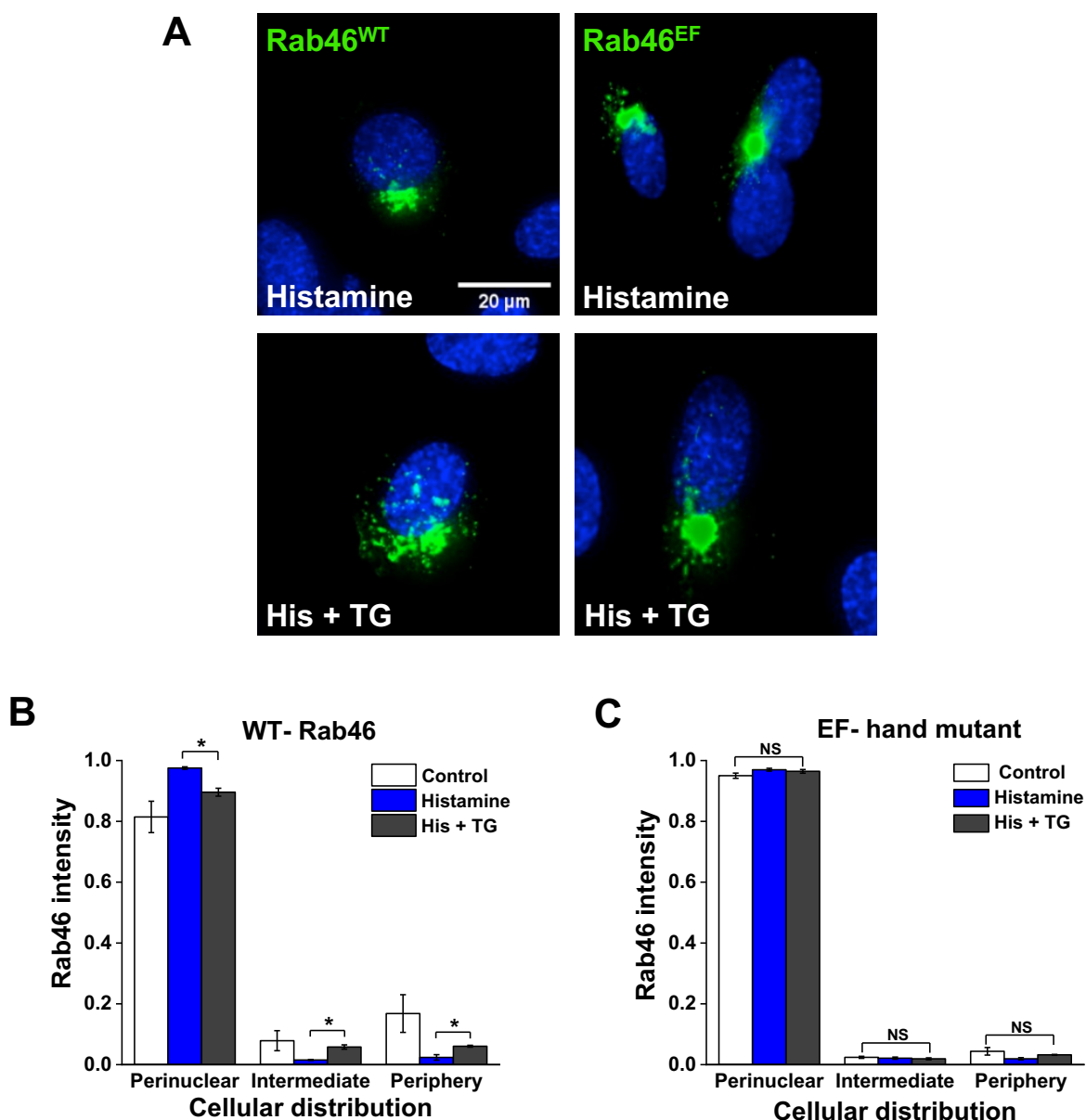


Figure 5.12 Rab46 EF-hand is necessary for Ca^{2+} -dependent WPB dispersal from the MTOC

A) Representative immunofluorescent images of HUVECs transfected with with Rab46^{WT} (left) and Rab46^{EF} mutant (right) treated with 30 μ M histamine for 10 min alone or followed by 1 μ M thapsigargin for 5 minutes, and then fixed and stained for Rab46 (green) and vWF (red; marker of WPBs). Mutants were transfected for 24 hours prior to treatments. DAPI (blue) shows nuclei. Maximum intensity projections from DeltaVision z-stack are shown. Scale bar = 20 μ m. (B, C) Mean data showing the cellular distribution of Rab46 WT mutant (B) and Rab46 EF-hand mutant (C) upon treatments from (A). Results were grouped into three areas: perinuclear, intermediate and periphery. The plot quantifies Rab46 signal intensity in the respective area where the mean (\pm SEM) was noted as percentage of the total signal intensity (n/N=3/24, * p-value < 0.05 following a Two-way ANOVA).

Chapter 6 NAADP-sensitive Ca^{2+} pool regulates Rab46-dependent Weibel-Palade body trafficking

6.1 Introduction

There are 3 major messengers that can mobilise Ca^{2+} from the intracellular stores: IP_3 , cADPR and NAADP. Major research effort in the past two decades has shown that the mode of action of NAADP differs from the canonical IP_3 -ER release axis. Instead, produced in response to various receptor-agonists, NAADP triggers Ca^{2+} release from thapsigargin-insensitive stores (thereby excluding the ER), that have since been identified as the endo-lysosomal Ca^{2+} stores in many cell types (Galione, 2015b). Due to the varied and dynamic localisation of the endo-lysosomes around the cell, the Ca^{2+} released is small but highly localised. In some cell types this NAADP-dependent Ca^{2+} release on its own is sufficient to mediate a cellular function such as phagocytosis in macrophages (Davis et al., 2020b) or stimulus-coupled secretion in T cells (Davis et al., 2012). However, in other cases such as pancreatic acinar cells (Cancela et al., 1999), the Ca^{2+} released from NAADP-sensitive stores serves as a co-agonist, or a trigger, to the IP_3R (also known as 'the trigger hypothesis') thereby modulating the global Ca^{2+} response. Another functional distinction of NAADP Ca^{2+} signalling is that it exhibits a bell-shaped dose-response relationship; meaning that nM concentrations of intracellular NAADP, evokes Ca^{2+} release but release is not detectable at μM concentrations of NAADP (Morgan and Galione, 2008). Although NAADP signalling is present in multiple cell types, there are only a couple of studies investigating the function of NAADP signalling in the endothelium. What can be extrapolated from these studies is that although several agonists are coupled to NAADP, their function in the endothelium is distinct (i.e. VEGF, histamine; G Cristina Brailoiu et al., 2010; Esposito et al., 2011; Faviaa et al., 2014). In particular, Esposito and colleagues showed that in ECs histamine H_1R is coupled to NAADP and inhibition of NAADP signalling decreases vWF release evoked by H_1R agonism.

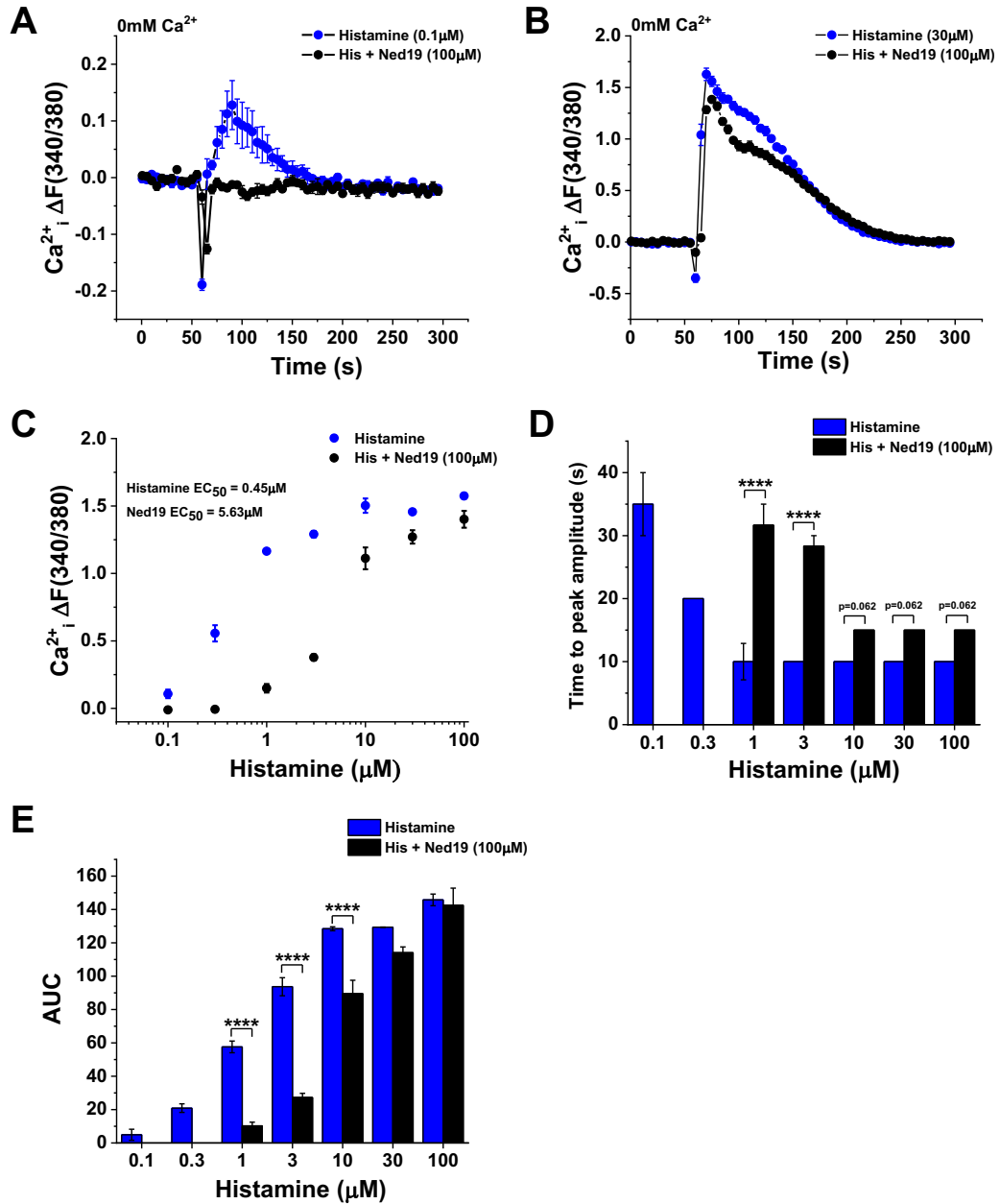
In the previous chapters of this thesis, I have described differential trafficking of subpopulations of WPBs (the major store of vWF) that is dependent on Rab46, a novel Ca^{2+} -sensing Rab GTPase. In the endothelium, Rab46-dependent trafficking is coupled to histamine but not thrombin. High concentrations of histamine trigger WPB and Rab46 clustering at the MTOC (also described here as the perinuclear area) in a Ca^{2+} - independent manner, however, dispersal of those clusters from the MTOC depends on binding of Ca^{2+} to the EF-hand of Rab46. Given the intricacies of both NAADP signalling and WPBs trafficking, it is

important to gain more insight on their potential relationship. Therefore, the aim of this chapter is to investigate the role of NAADP signalling in histamine-evoked trafficking of WPBs. In the following pages, Ca^{2+} imaging techniques are used to investigate NAADP coupling to the histamine response. Immunofluorescent imaging and image quantification methods decipher the role of NAADP in WPB trafficking. In addition, molecular biology and high resolution imaging reveal the presence and the endogenous localisation of endo-lysosomal channels in ECs. Preliminary data in this chapter suggests that Rab46 interacts with TPCs and proposes Rab46 as a sensor of NAADP-evoked Ca^{2+} signalling in ECs.

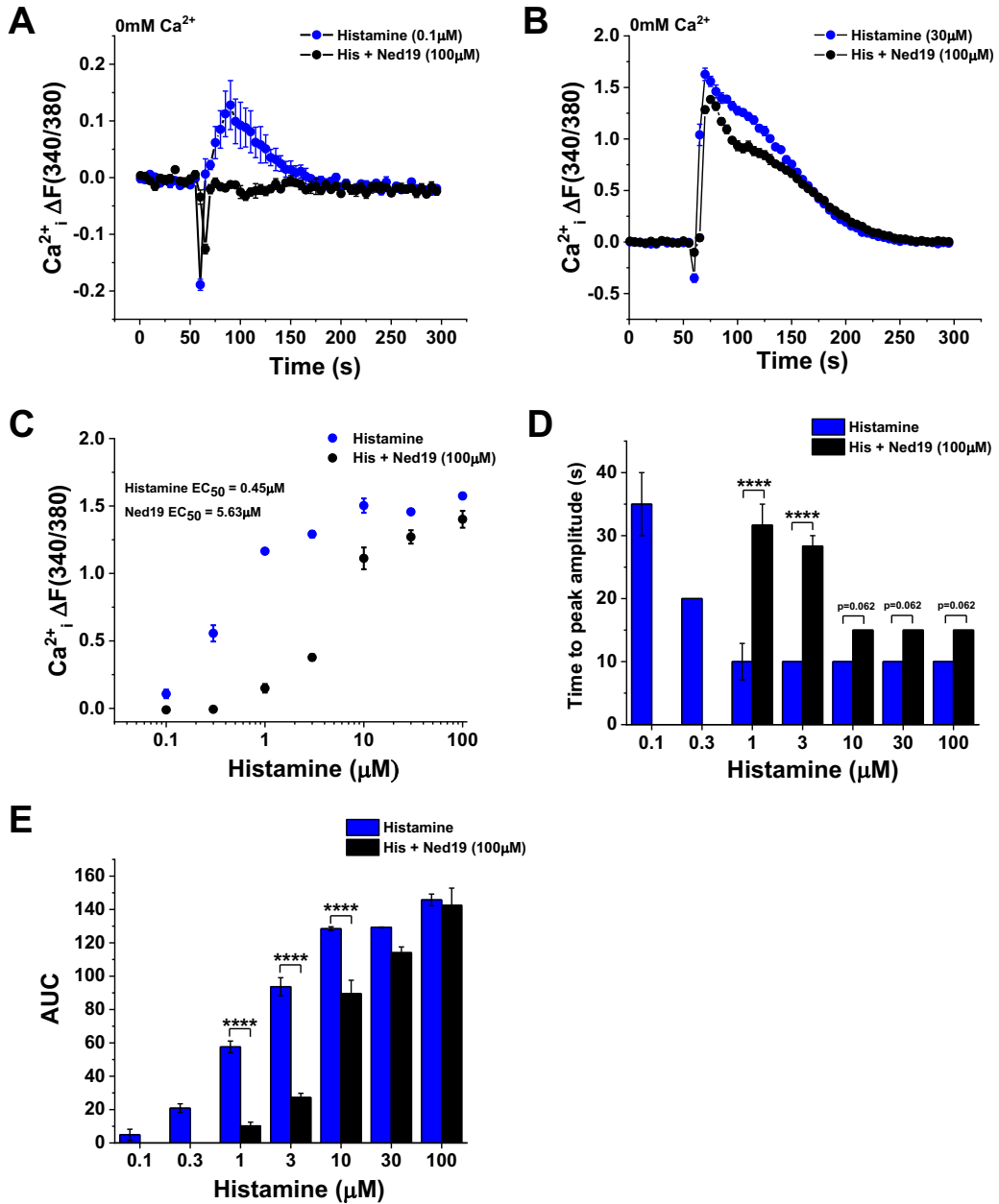
6.2 Histamine-evoked intracellular Ca^{2+} release is coupled to NAADP in endothelial cells

In 2015 Esposito and colleagues showed that the endothelial cell line EA.hy926 expresses two histamine receptors – H_1R and H_2R . Through further investigation of the H_1 receptor in the cell line their team confirmed that, in addition to release of intracellular Ca^{2+} via IP_3 -dependent route, the receptor activation also triggers Ca^{2+} release from NAADP-sensitive Ca^{2+} stores (Esposito et al., 2011). Taking into consideration that I use a different endothelial model system (HUVECs), it was important to first confirm that the same stands true in HUVECs.

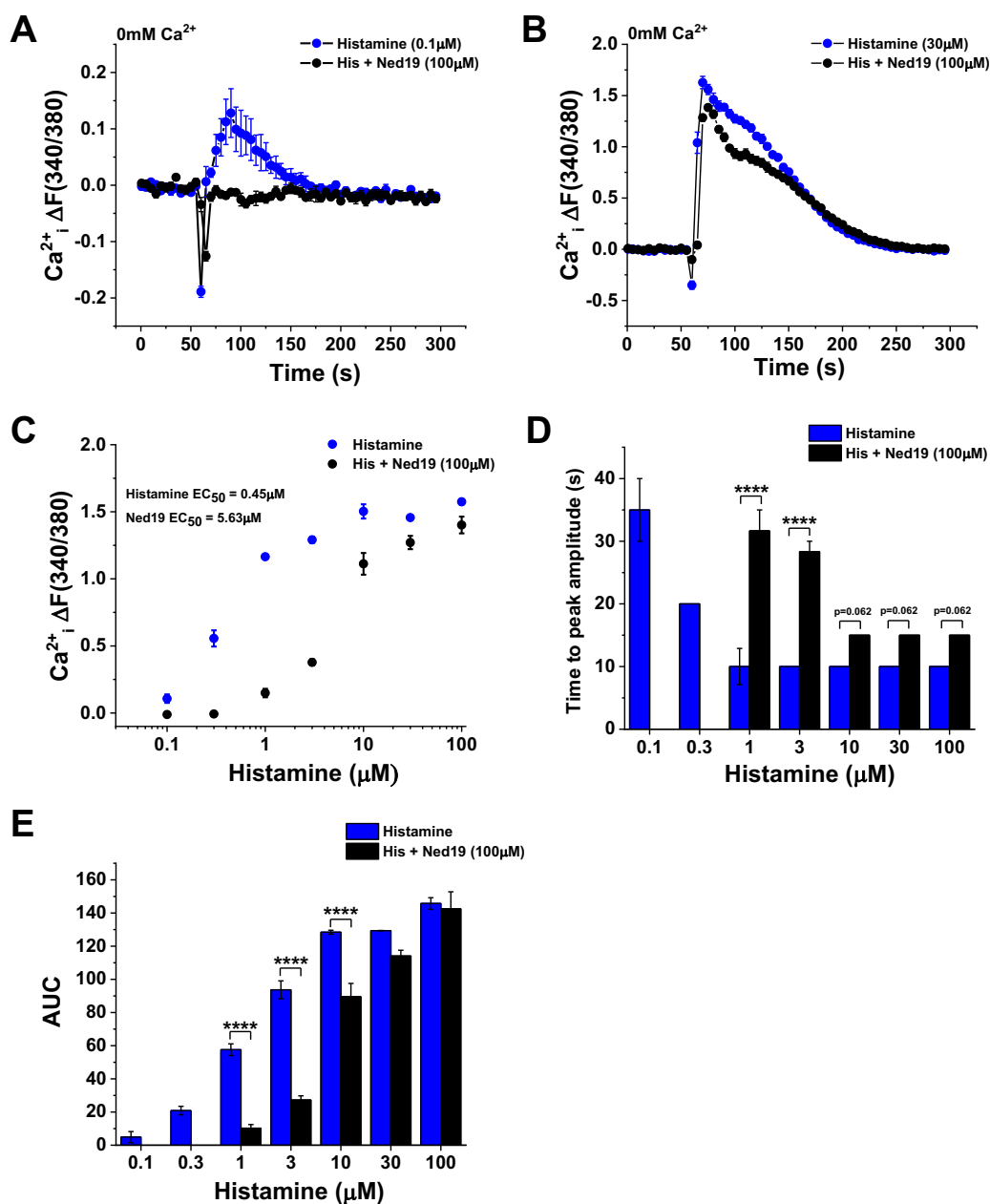
I evaluated endothelial Ca^{2+} dynamics in response to either histamine a H_1R -selective agonist or thrombin (as a control) (Figures 6.1 - 6.6). Firstly, using FlexStation-based Ca^{2+} imaging I generated a dose-response curve, (histamine concentrations 0.1-100 μM) where histamine was applied to HUVECs that were either pre-treated with vehicle control (in this case DMSO) or 100 μM of the NAADP antagonist *trans*-Ned19 (Ned19;



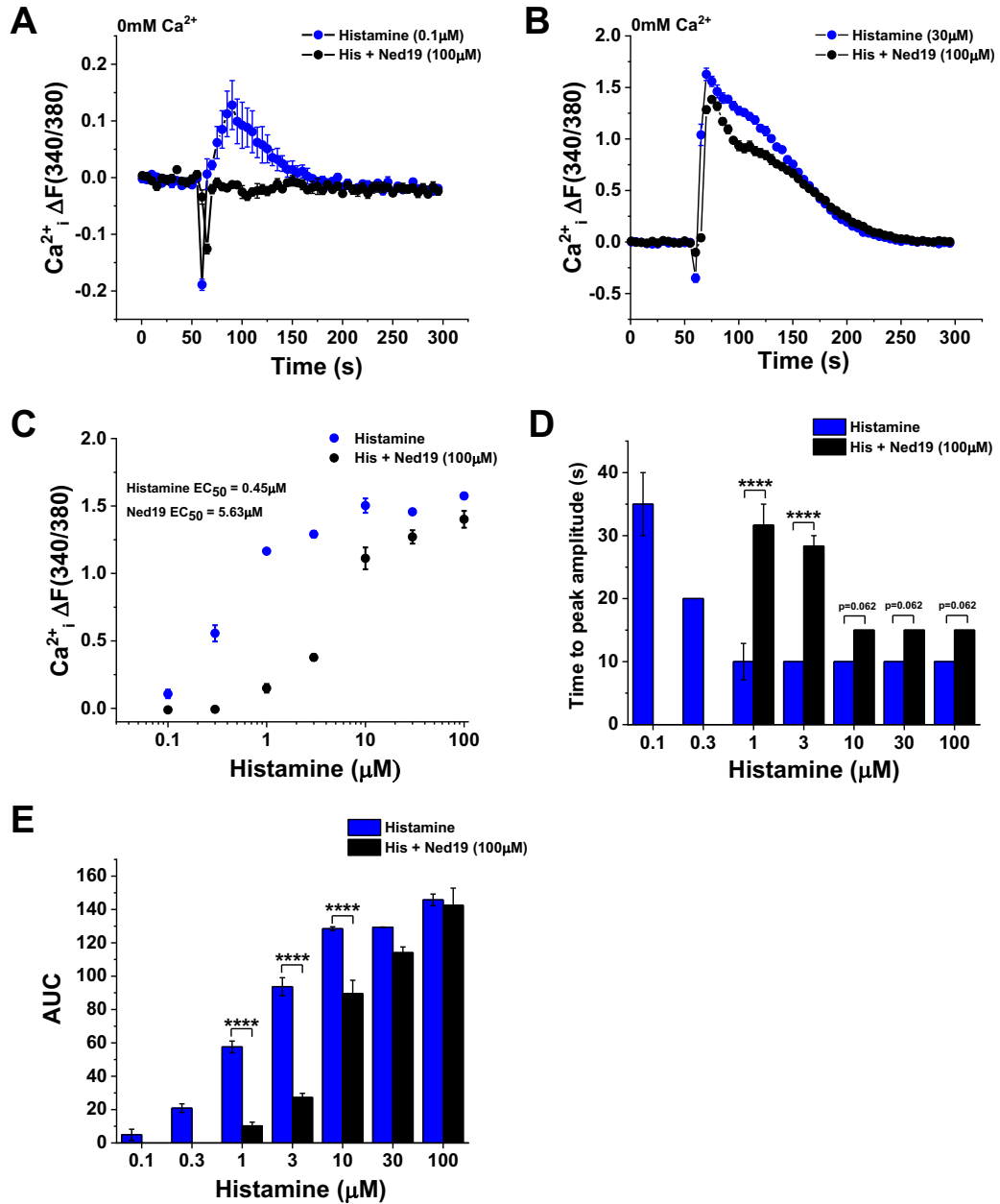
A-E). The fluorescence recordings were performed in the absence of extracellular Ca^{2+} in order to study whether NAADP antagonism reduced Ca^{2+} release from NAADP-sensitive stores. In cells treated with low doses of histamine (e.g. 0.1 μM or 0.3 μM), the observed Ca^{2+} release is completely inhibited by pre-treatment with Ned19 and no fluorescence was recorded above baseline (



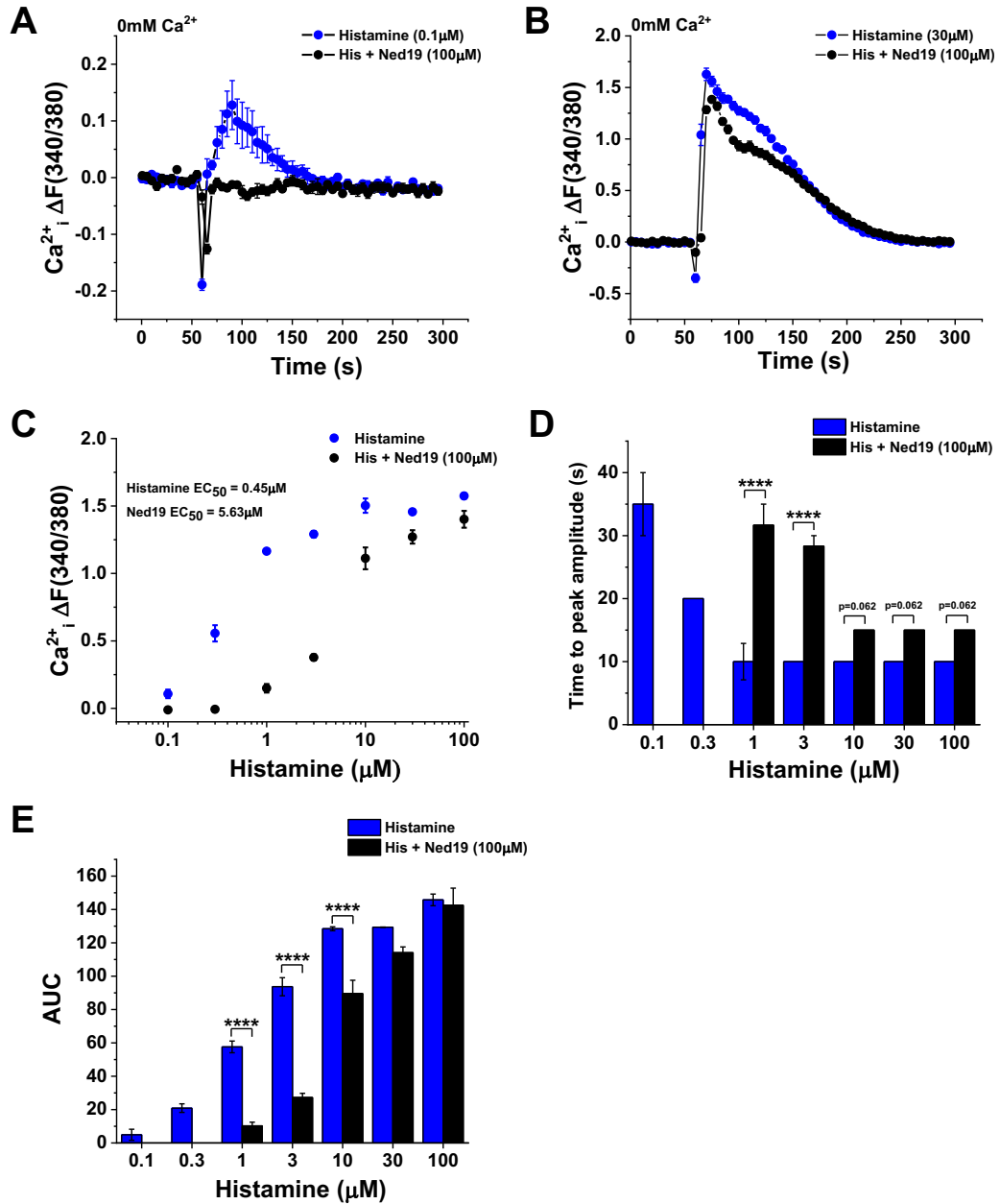
A, C), suggesting that low, but physiological concentrations, of histamine trigger Ca²⁺ release solely from NAADP-sensitive intracellular Ca²⁺ stores. Conversely, at 30 μM or 100 μM concentrations, NAADP antagonism significantly decreased the peak amplitude of the histamine-evoked Ca²⁺ release, but not completely inhibiting it, suggesting that the peak Ca²⁺ release response in high concentrations of histamine is a combination of Ca²⁺ from both NAADP and IP₃-sensitive stores (



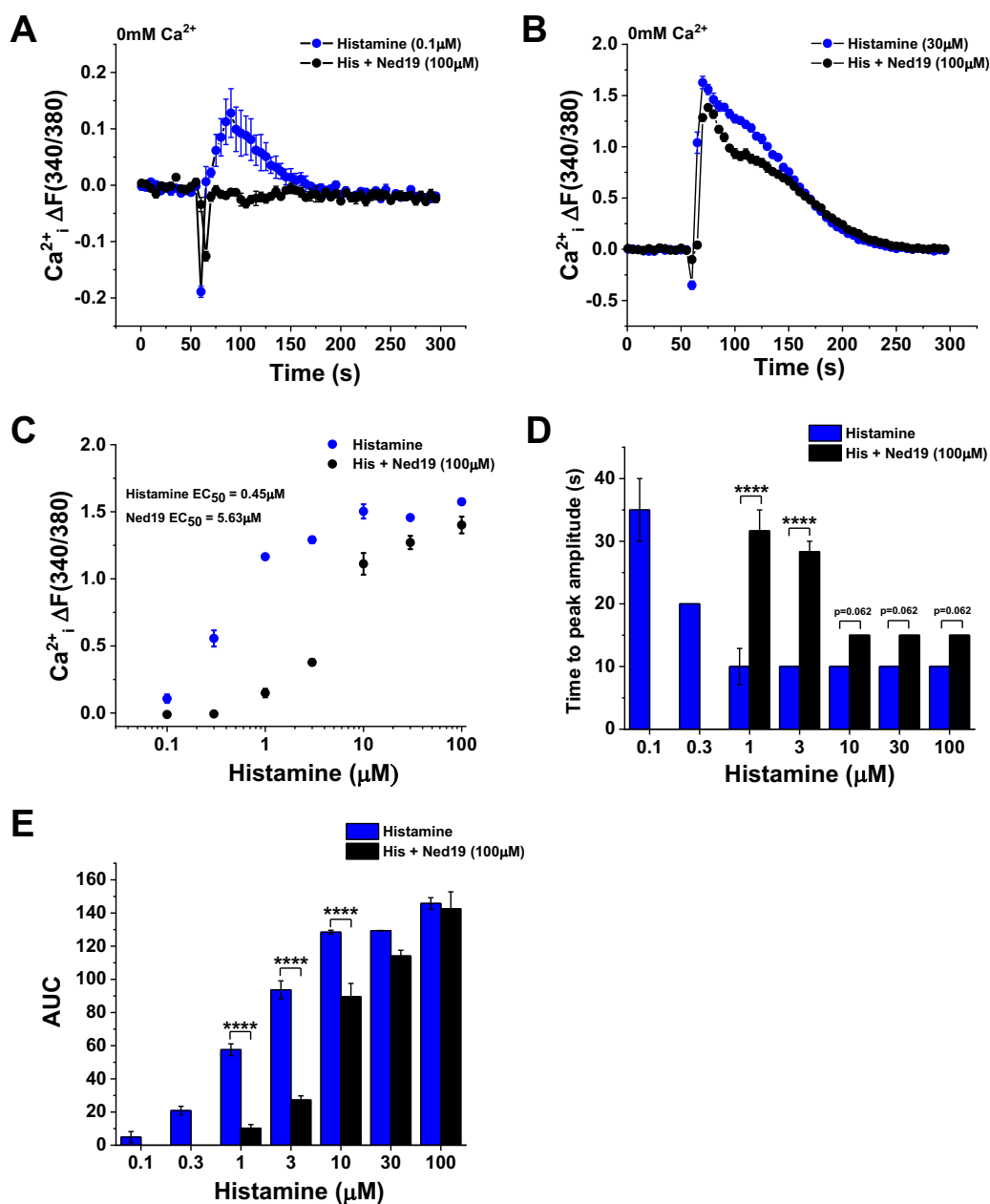
B, C). Overall, dose-response curve fitting analysis showed that Ned19 pre-treatment shifted the doses response curve and increased the EC₅₀ value of histamine in HUVECs from 0.45 μM to 5.45 μM. This data suggests that NAADP antagonism lowers histamine's efficacy of Ca²⁺ release (



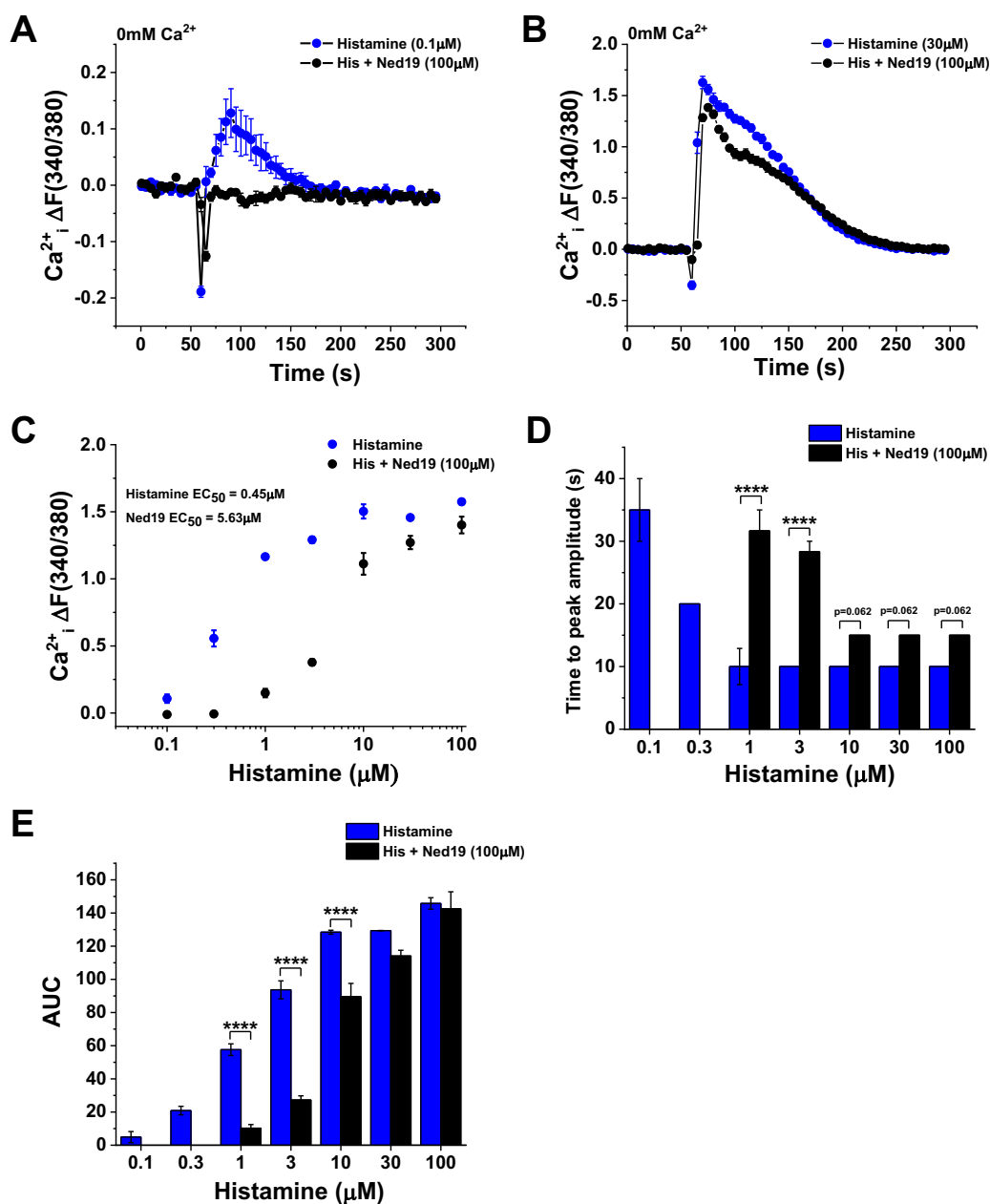
C). In HUVECs pre-treated with Ned19, time to peak (TTP) amplitude values are significantly increased by histamine, consistent with the NAADP 'trigger hypothesis' and further corroborating that histamine mobilises Ca²⁺ from NAADP-sensitive intracellular Ca²⁺ stores (



D). Additionally, measurements of total area under the curve (AUC) showed that Ned19 significantly decreases the AUC in response to histamine, indicating that less Ca²⁺ has been released as opposed to histamine treatment on its own (



E). To control for any non-specific effects of Ned19 treatment on the Ca²⁺ response evoked by histamine (which includes both Ca²⁺ release and Ca²⁺ entry), experiments were repeated in the presence of physiologically relevant extracellular Ca²⁺ (Error! Reference source not found.A-E). Similarly to



C, Ned19 reduces histamine's ability to release Ca²⁺ from the intracellular stores with an increase in EC₅₀ from 0.31 μM to 4.04 μM (**Error! Reference source not found.C**). In addition, the histamine-evoked TTP significantly increased and the AUC decreased, when the cells were pre-treated with Ned19. These comparable data suggest that pre-treatment with Ned19 does not appear to have nonspecific effects on the extracellular components participating in the overall Ca²⁺ response evoked by histamine (**Error! Reference source not found. D, E**). Secondly, I tested a H₁R-selective agonist, 2-(3-trifluoromethyl) phenyl histamine dimaleate (TMPH) described by Esposito and colleagues on the endothelial cell line EA.hy926. However, in HUVECs, TMPH evoked an inconsistent and small Ca²⁺ release, both in low and high concentrations, which is not comparable to the histamine Ca²⁺ response amplitude and also not dose-dependent (data not shown), therefore generation of a dose-response curve was not possible.

Additionally, TMPH has been shown to have a higher affinity for H₁R in guinea pig in comparison to human cells (Seifert et al., 2003), therefore I selected and validated in HUVECs via Ca²⁺ measurements another commercially available selective H₁R agonist, 2-PY (previously described in Chapter 5). Here, HUVECs were treated with, 2-PY (0.03 μM to 300 μM) with and without Ned19 pre-treatment. The recordings were obtained both in absence (**Error! Reference source not found.A-E**) and presence (**Error! Reference source not found.A-E**) of extracellular Ca²⁺. Pre-treatment of HUVECs with Ned19 had a significant effect on Ca²⁺ release in response to 2-PY; 2-PY at 0.03 μM to 10 μM Ned19 completely abolished the Ca²⁺ response (**Error! Reference source not found.A, C; Error! Reference source not found.A, C**) and at high concentrations, the Ca²⁺ was significantly reduced (**Error! Reference source not found.B, C; Error! Reference source not found.B, C**). Moreover, after dose-response curve fitting analysis, the EC₅₀ values increased when cells were pre-treated with Ned19 (Ca²⁺_{ex} free recordings 2-PY EC₅₀ = 7.2 μM vs 2-PY + Ned19 EC₅₀ = 50.9 μM, **Error! Reference source not found.C**; Ca²⁺_{ex} recordings 2-PY EC₅₀ = 10 μM vs 2-PY + Ned19 EC₅₀ = 111 μM, **Error! Reference source not found.C**). These data indicate that, similar to histamine, Ned19 decreased the potency of the Ca²⁺ release response evoked by 2-PY. Furthermore, Ned19 pre-treatment evoked a significant increase in TTP values and significant reduction of the AUC in response to 2-PY (**Error! Reference source not found.D, E; Error! Reference source not found.D, E**). Next, as a negative control, I used thrombin which is an endothelial agonist known to evoke intracellular Ca²⁺ release and evoke vWF release in HUVECs (Hallam et al., 1988). In Figure 6.5A-E, HUVECs were pre-treated with Ned19 and thrombin at concentrations ranging from 0.07 to 2.5 U/ml was applied to the cells. Fluorescence recordings were obtained in Ca²⁺ free buffer in order to solely measure intracellular Ca²⁺ release in response to thrombin. In low doses of thrombin (i.e. 0.07 U/ml) pre-treatment with Ned19 has a small but insignificant effect on the intracellular Ca²⁺ release peak amplitude (Figure 6.5A, C), whilst at higher concentrations of 1.25 U/ml and 2.5 U/ml, Ned19 pre-treatment has no impact on the Ca²⁺ released evoked by thrombin (Figure 6.5B, C). In fact, NAADP antagonism by Ned19 does not alter thrombin's potency to release intracellular Ca²⁺ as shown by dose-response curve fitting analysis and EC₅₀ values calculations (thrombin EC₅₀ = 0.34 U/ml vs thrombin + Ned19 EC₅₀ = 0.36 U/ml, Figure 6.5C). In addition, Ned19 pre-treatment does not alter TTP values in response to thrombin and AUC measurements (Figure 6.5D, E), indicating that intracellular Ca²⁺ release by thrombin is not coupled to NAADP-sensitive Ca²⁺ stores. Similarly, when recordings in response to thrombin and Ned19 pre-treatment were performed in physiological extracellular Ca²⁺ concentrations, it can be similarly observed that there is no effect of Ned19 on

the overall Ca^{2+} response evoked by thrombin. Finally, SOCE is an integral part of the endothelial Ca^{2+} toolkit and it is initiated by intracellular Ca^{2+} release from ER Ca^{2+} stores by endothelial agonists (as discussed in Chapter 1 and Chapter 5). A Ca^{2+} addback assay was used (Figure 6.7A; for detailed Ca^{2+} addback assay description see Chapter 2 Methods) to control for any effects of NAADP antagonism by Ned19 on SOCE. In short, HUVEC ER Ca^{2+} stores were pharmacologically 'released' and depleted by application of thapsigargin (ER SERCA pump inhibitor) which induces a large increase in cytosolic Ca^{2+} . Physiologically relevant Ca^{2+} concentration is then added back to the cells which allows Ca^{2+} entry into the cytosol via the Orai channels. Measurement of peak amplitude of both Ca^{2+} release and Ca^{2+} entry (Figure 6.7B,C) in the presence and absence of Ned19 pre-treatment showed no effect of NAADP antagonism on SOCE in HUVECs. Overall, the data in this section revealed that in HUVECs NAADP antagonism by Ned19 is specific to histamine via the H_1R and not thrombin.

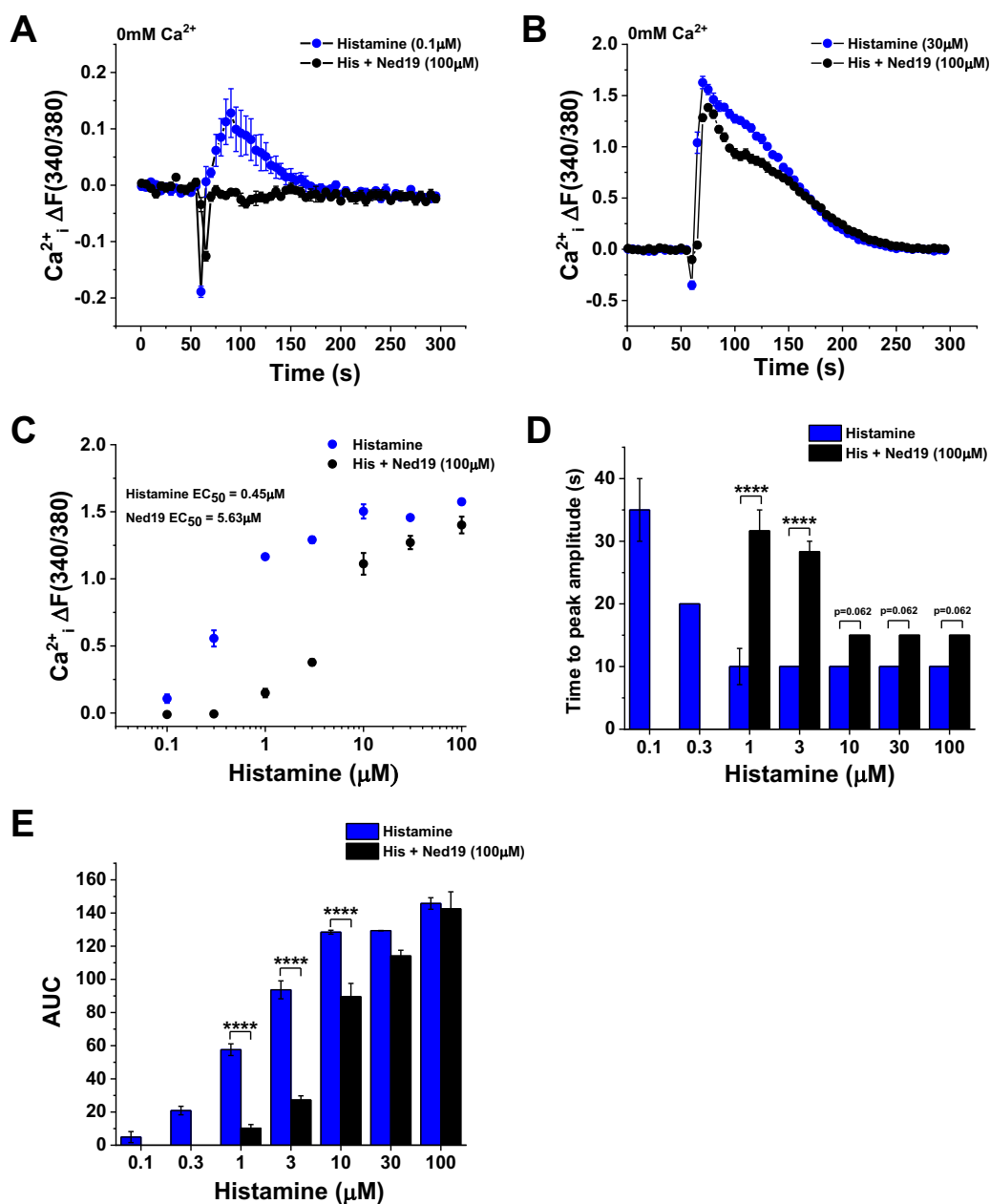


Figure 6.1 Histamine-evoked intracellular Ca²⁺ release is coupled to NAADP-sensitive Ca²⁺ stores in HUVECs.

(A) Representative trace of Ca²⁺ release in HUVECs for 5 minutes evoked by application of 0.1 μM histamine at 60 seconds, cells were pre-treated with 100 μM Ned19 for 30 minutes. Recordings were obtained in Ca²⁺-free buffer. (B) Representative trace of Ca²⁺ release in HUVECs evoked by application of 30 μM histamine at 60 seconds, cells were pre-treated with 100 μM Ned19 for 30 minutes. Recordings were obtained in Ca²⁺-free buffer. (C) Peak amplitude mean data of HUVEC treated with histamine ranging from 0.1 to 100 μM are displayed as a concentration-response curve and the fitted curve is plotted using a Hill Equation indicating the 50 % maximum effect (EC₅₀) of either in the presence or absence of 100 μM Ned19. (D) Mean data of time to peak amplitude of treatments from (C) (E) Mean data of area under the curve (AUC) of treatments from (C) (n/N = 3/9, error bars represent SEM, **** p value < 0.0001 by One-way ANOVA).

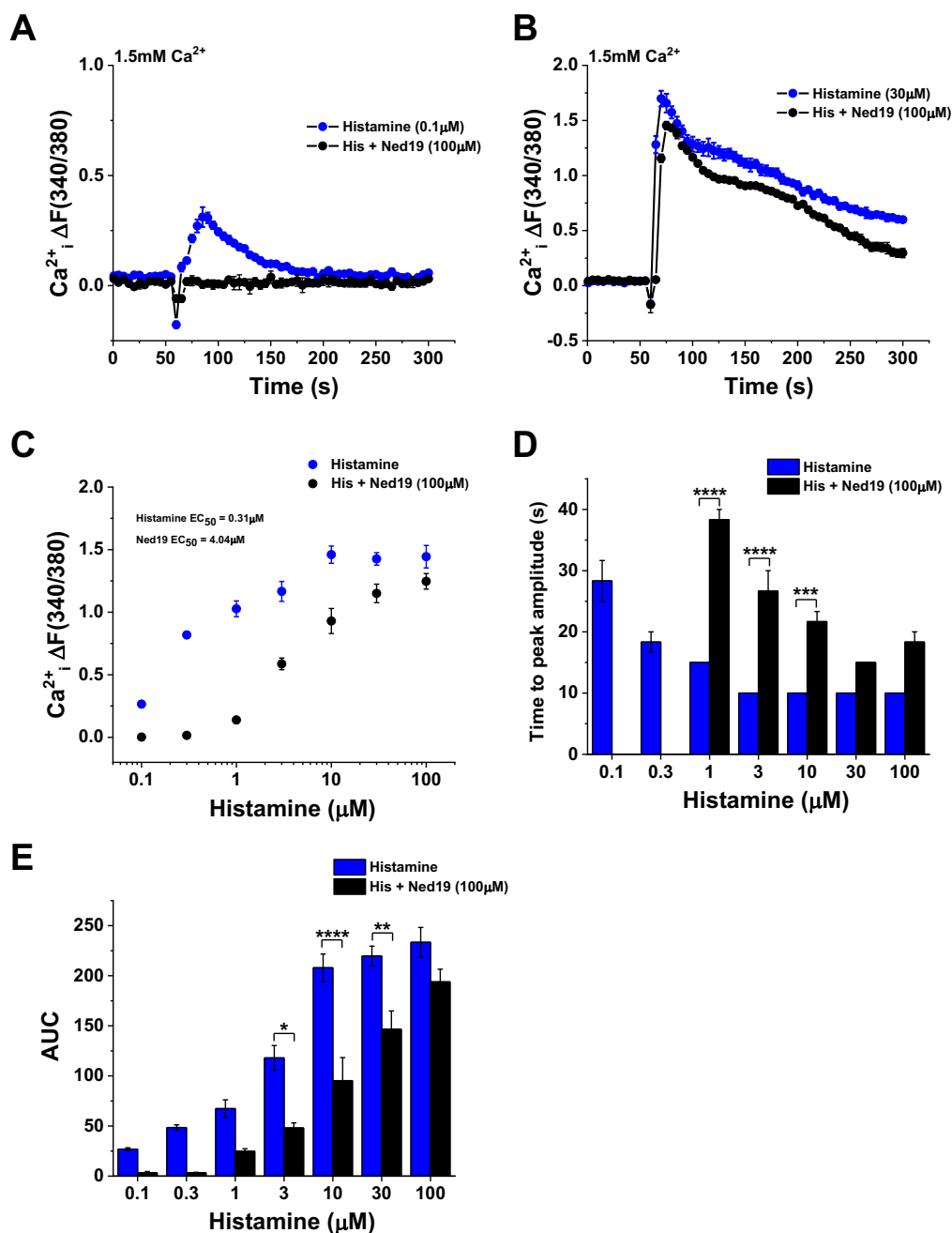


Figure 6.2 Histamine-evoked Ca²⁺ release is coupled to NAADP-sensitive Ca²⁺ stores in HUVECs.

(A) Representative trace of Ca²⁺ release in HUVECs for 5 minutes evoked by application of 0.1 μM histamine at 60 seconds, cells were pre-treated with 100 μM Ned19 for 30 minutes. Recordings were obtained in 1.5 mM Ca²⁺ buffer. (B) Representative trace of Ca²⁺ release in HUVECs evoked by application of 30 μM histamine at 60 seconds, cells were pre-treated with 100 μM Ned19 for 30 minutes. Recordings were obtained in 1.5 mM Ca²⁺ buffer. (C) Peak amplitude mean data of HUVEC treated with histamine ranging doses 0.1-100 μM are displayed as a concentration-response curve and the fitted curve is plotted using a Hill Equation indicating the 50 % maximum effect (EC₅₀) of either in the presence or absence of 100 μM Ned19. (D) Mean data of time to peak amplitude of treatments from (C) (E) Mean data of area under the curve (AUC) of treatments from (C) (n/N=3/9, error bars represent SEM, *** p value < 0.001, **** p value < 0.0001 by One-way ANOVA).

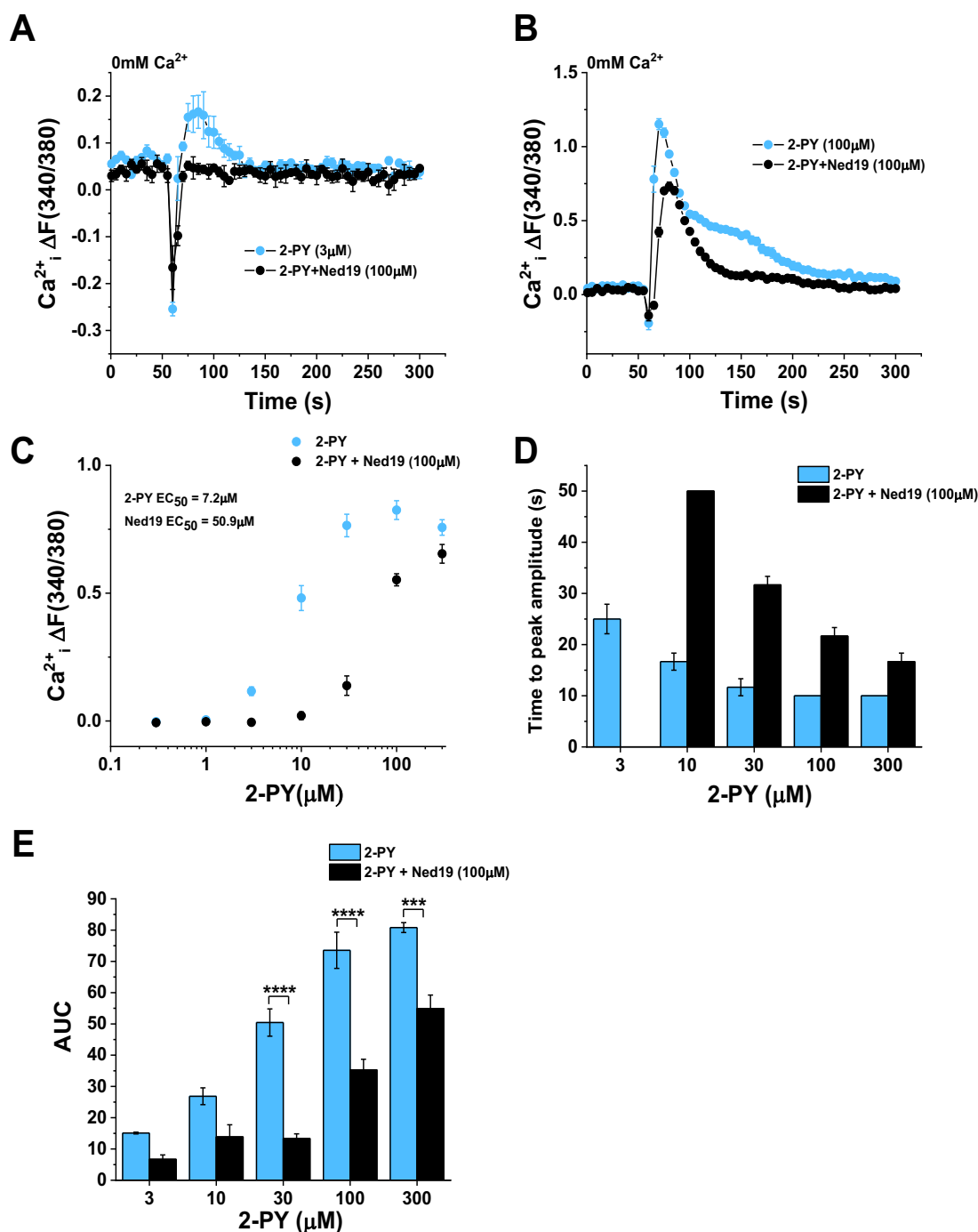


Figure 6.3 H₁ receptor triggers intracellular Ca²⁺ release from NAADP-sensitive Ca²⁺ stores.

(A) Representative trace of Ca²⁺ release in HUVECs for 5 minutes evoked by application of 3 μM 2-PY at 60 seconds, cells were pre-treated with 100μM Ned19 for 30 minutes. Recordings were obtained in Ca²⁺ free buffer. (B) Representative trace of Ca²⁺ release in HUVECs evoked by application of 100 μM 2-PY at 60 seconds, cells were pre-treated with 100μM Ned19 for 30 minutes. Recordings were obtained in Ca²⁺-free buffer. (C) Peak amplitude mean data of HUVEC treated with 2-PY ranging doses 0.3-300 μM are displayed as a concentration-response curve and the fitted curve is plotted using a Hill Equation indicating the 50 % maximum effect (EC₅₀) of either in the presence or absence of 100 μM Ned19. (D) Mean data of time to peak amplitude of treatments from (C) (E) Mean data of area under the curve (AUC) of treatments from (C) (n/N=3/9, error bars represent SEM, *** p value < 0.001, **** p value < 0.0001 by One-way ANOVA).

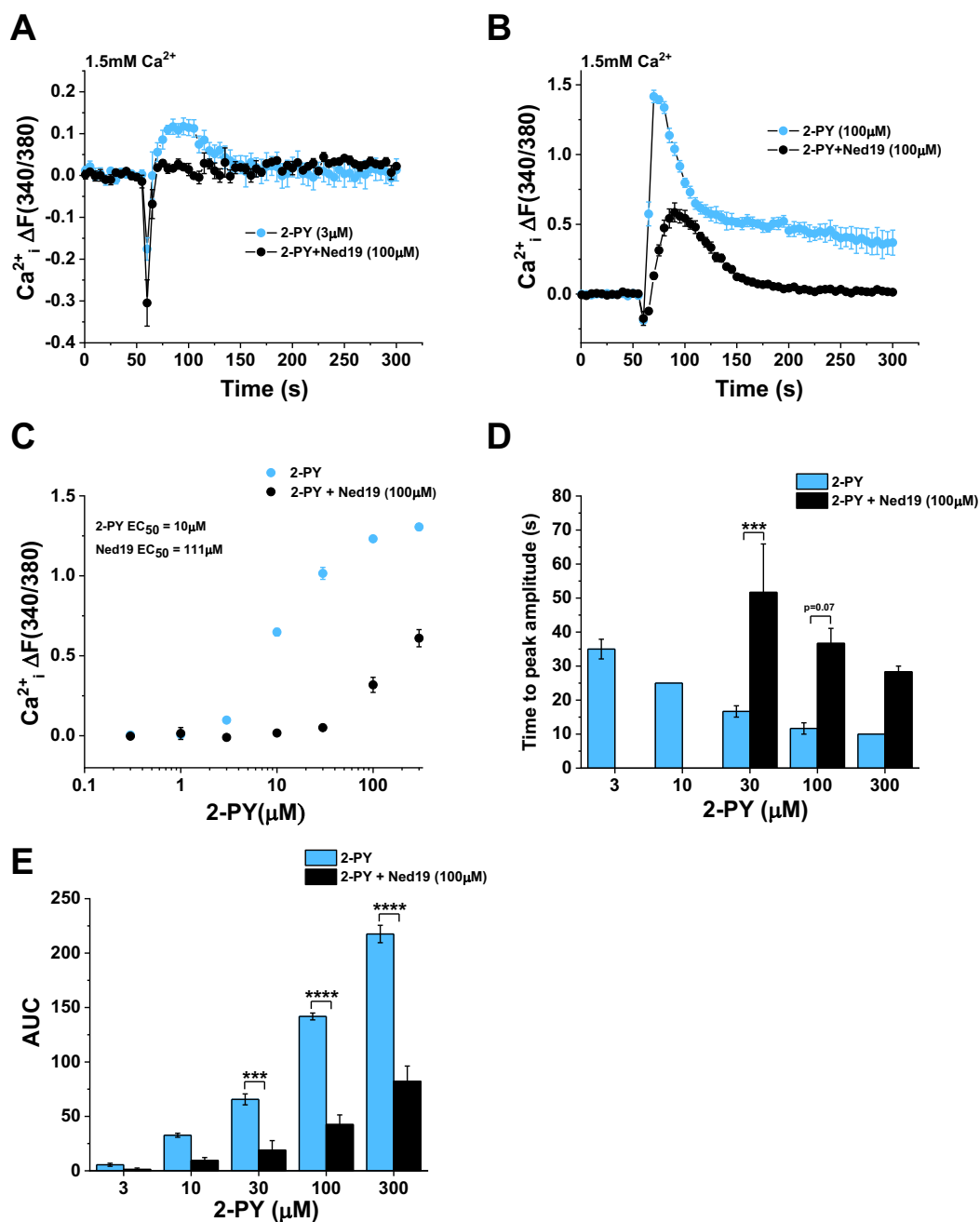


Figure 6.4 H₁ receptor is coupled to NAADP-sensitive Ca²⁺ stores.

(A) Representative trace of Ca²⁺ release in HUVECs for 5 minutes evoked by application of 3 μM 2-PY at 60 seconds, cells were pre-treated with 100 μM Ned19 for 30 minutes. Recordings were obtained in 1.5 mM Ca²⁺ buffer. (B) Representative trace of Ca²⁺ release in HUVECs evoked by application of 100 μM 2-PY at 60 seconds, cells were pre-treated with 100 μM Ned19 for 30 minutes. Recordings were obtained in 1.5 mM Ca²⁺ buffer. (C) Peak amplitude mean data of HUVEC treated with 2-PY ranging doses 0.3-300 μM are displayed as a concentration-response curve and the fitted curve is plotted using a Hill Equation indicating the 50 % maximum effect (EC₅₀) of either in the presence or absence of 100 μM Ned19. (D) Mean data of time to peak amplitude of treatments from (C) (E) Mean data of area under the curve (AUC) of treatments from (C) (n/N=3/9, error bars represent SEM, *** p value < 0.001, **** p value < 0.0001 by One-way ANOVA).

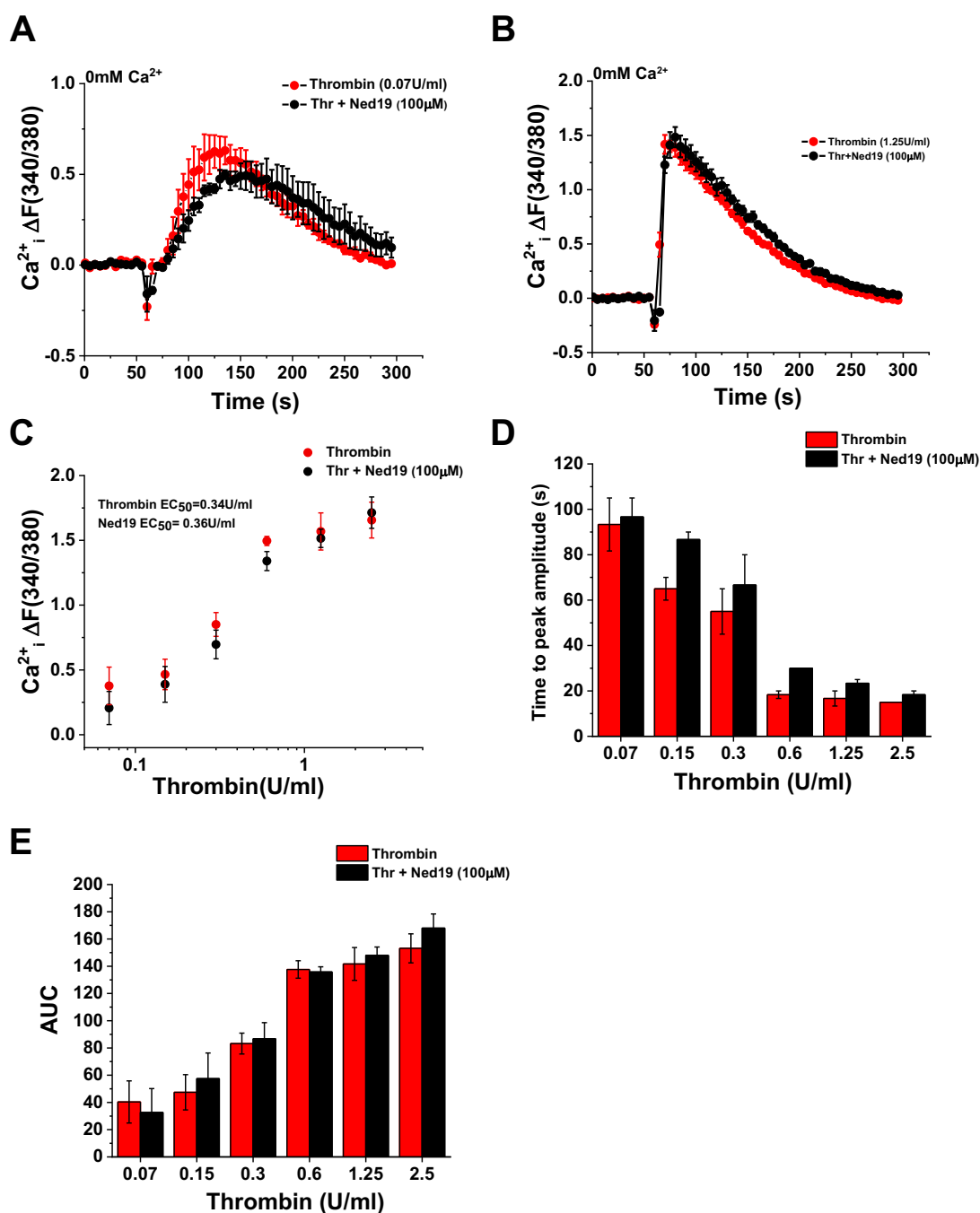


Figure 6.5 NAADP antagonism does not affect intracellular Ca²⁺ release evoked by thrombin.

(A) Representative trace of Ca²⁺ release in HUVECs for 5 minutes evoked by application of 0.07 U/ml at 60 seconds, cells were pre-treated with 100 μM Ned19 for 30 minutes. Recordings were obtained in Ca²⁺ free buffer. (B) Representative trace of Ca²⁺ release in HUVECs evoked by application of 1.25 U/ml at 60 seconds, cells were pre-treated with 100 μM Ned19 for 30 minutes. Recordings were obtained in Ca²⁺-free buffer. (C) Mean data of HUVEC treated with thrombin ranging doses 0.07-2.5 U/ml are displayed as a concentration-response curve and the fitted curve is plotted using a Hill Equation indicating the 50 % maximum effect (EC₅₀) of either in the presence or absence of 100 μM Ned19. (D) Mean data of time to peak amplitude of treatments from (C) (E) Mean data of area under the curve (AUC) of treatments from (C) (n/N = 3/9, error bars represent SEM).

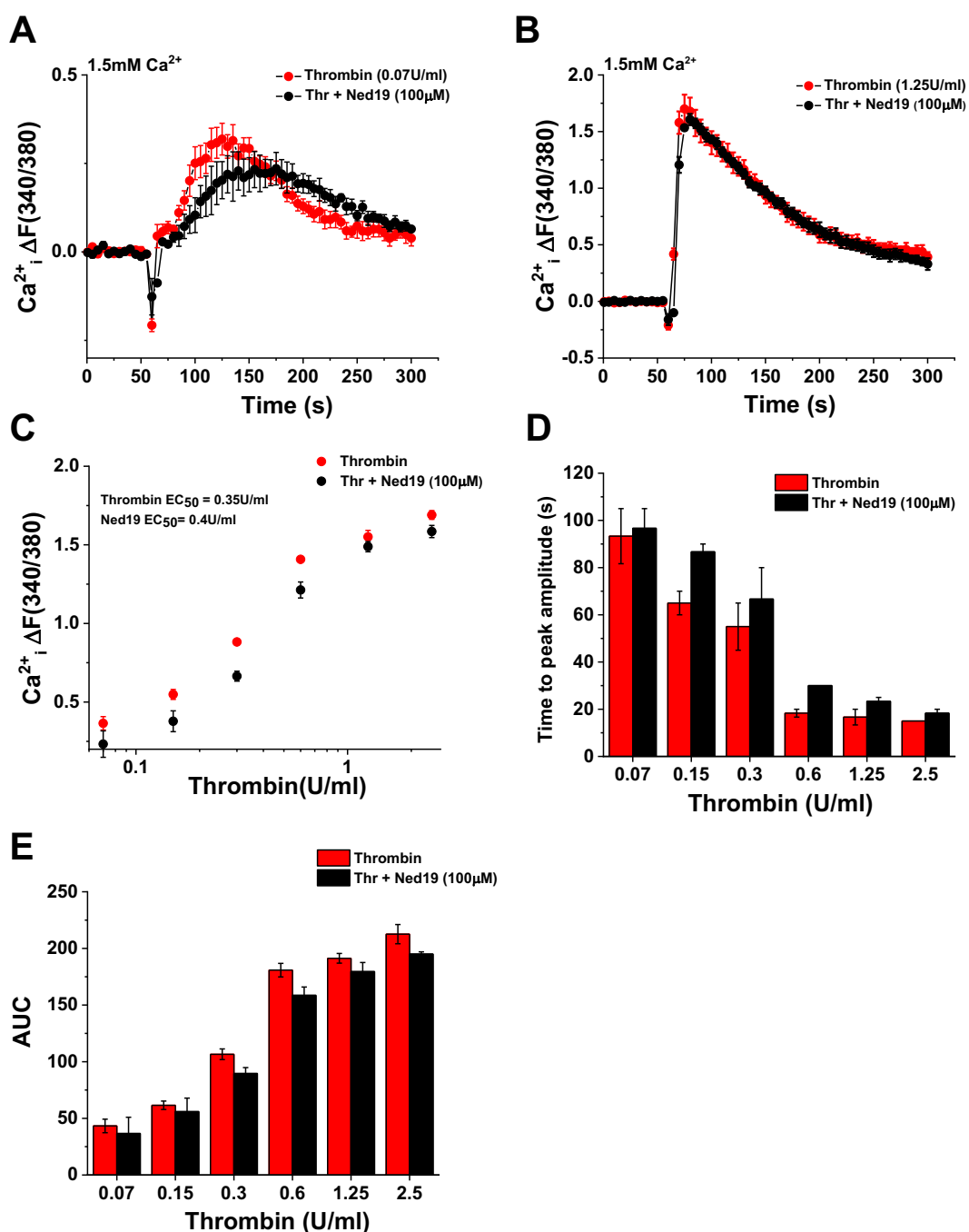


Figure 6.6 NAADP antagonism does not affect Ca²⁺ release evoked by thrombin.

(A) Representative trace of Ca²⁺ release in HUVECs for 5 minutes evoked by application of 0.07 U/ml at 60 seconds, cells were pre-treated with 100 μM Ned19 for 30 minutes. (B) Representative trace of Ca²⁺ release in HUVECs evoked by application of 1.25 U/ml at 60 seconds, cells were pre-treated with 100 μM Ned19 for 30 minutes. Recordings were obtained in 1.5 mM Ca²⁺ buffer. (C) Mean data of HUVEC treated with thrombin ranging doses 0.07-2.5 U/ml are displayed as a concentration-response curve and the fitted curve is plotted using a Hill Equation indicating the 50 % maximum effect (EC₅₀) of either in the presence or absence of 100 μM Ned19. (D) Mean data of time to peak amplitude of treatments from (C) (E) Mean data of area under the curve (AUC) of treatments from (C) (n/N=3/9, error bars represent SEM).

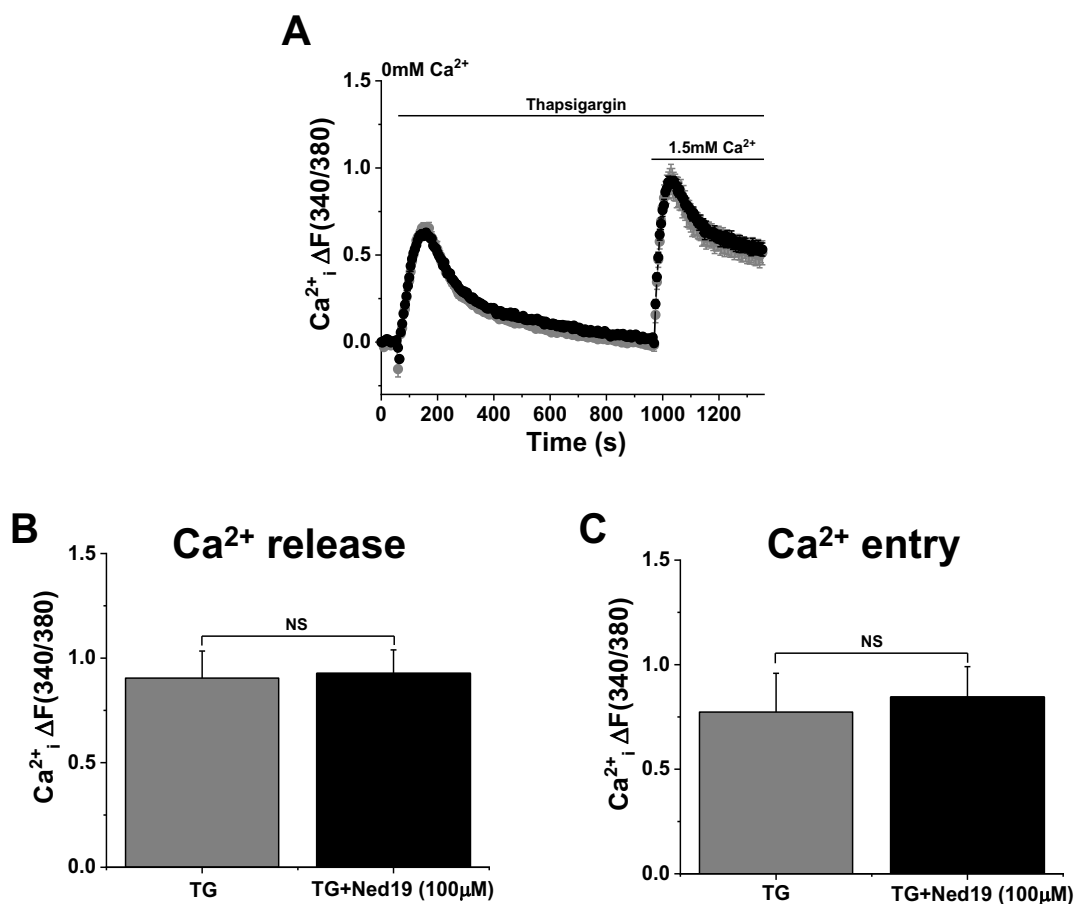


Figure 6.7 NAADP antagonism does not affect store-operated Ca²⁺ entry in HUVECs.

(A) Representative trace of Ca²⁺ release and entry in HUVECs evoked by application of 5 μM thapsigargin (TG) at 60 seconds and Ca²⁺ addback (7.5 mM Ca²⁺ buffer) at 960 seconds, cells were pre-treated with 100 μM Ned19 for 30 minutes. Recordings were obtained in Ca²⁺-free buffer. (B), (C) Mean data of peak amplitude (B) Ca²⁺ release and (C) Ca²⁺ entry response (n/N=5/15, error bars represent SEM, NS, not significant by One-way ANOVA).

6.3 The role of NAADP store in Rab46 trafficking

In the previous chapters of this thesis and in my first author publication (K. T. Miteva et al., 2019), I showed that Rab46 regulates trafficking of selective WPB populations in an agonist-appropriate manner. It was observed that histamine induced trafficking of Rab46-positive WPBs towards the perinuclear area where they formed clusters at the MTOC. I also showed that this perinuclear trafficking, also known as retrograde trafficking, is both cAMP- and Ca^{2+} -independent, with inhibition of cAMP signalling pathway and intracellular Ca^{2+} failing to prevent Rab46 and WPB clustering. Furthermore, in Chapter 5, I showed that although retrograde trafficking of Rab46 and WPB is independent of global Ca^{2+} events in the cytosol, the dispersal of Rab46 and WPB from the MTOC is indeed dependent on Ca^{2+} binding to the EF-hand domain of Rab46. This Ca^{2+} necessary for said dispersal must be from a highly localised Ca^{2+} release event in close proximity (due to limited diffusion of Ca^{2+}) to the perinuclear area where Rab46-positive WPBs congregate. From the literature, it is known that NAADP evokes small, highly localised pockets of Ca^{2+} release from the endo-lysosomal Ca^{2+} stores, forming Ca^{2+} nanodomains therein, that have the ability to fine tune cellular responses (Galione, 2015a). Therefore, it was hypothesised that the origin of the Ca^{2+} necessary for dispersal of Rab46 and WPB clusters from the perinuclear area is indeed released from the endo-lysosomal (or acidic) Ca^{2+} stores. In Section 6.2 of this chapter, I showed in detail that using Ned19 as a pharmacological tool to antagonise NAADP, in HUVECs the histamine-evoked Ca^{2+} release is coupled to NAADP in addition to IP_3 mediated Ca^{2+} release from the ER, which corresponded to the current evidence in literature (Esposito et al., 2011). Interestingly, the data revealed that at a low concentration of histamine (i.e. 0.1 μM) Ned19 evoked a complete inhibition of Ca^{2+} release, which suggested that at such low doses of histamine the Ca^{2+} recordings may be representing small NAADP-dependent Ca^{2+} release events from the endo-lysosomal stores.

6.3.1 NAADP-sensitive Ca^{2+} pool is necessary for dispersal of histamine-induced Rab46-positive WPBs clusters

Firstly, pharmacological tools were used to confirm whether there are functional endo-lysosomal Ca^{2+} stores in HUVECs. Although debated recently, dipeptide glycyl-L-phenylalanine 2-naphthylamide (GPN), a substrate for the endo-lysosomal enzyme cathepsin C, was used in order to rupture endo-lysosomal membranes and release the Ca^{2+} stored therein. A study have shown evidence that GPN evokes solely ER Ca^{2+} release and does not target the lysosomal membranes, unlike previous studies that have shown that GPN- and ER-evoked

Ca^{2+} inhibit each other. Further research into establishing the exact GPN mode of action is needed, however due to overwhelming evidence by peer reviewed articles on its action on lysosomal membranes here GPN is used as an important control for studies of lysosomal Ca^{2+} (Morgan et al., 2015; Atakpa et al., 2019; Morgan et al., 2020). Using a FlexStation assay, GPN and TG (as an ER Ca^{2+} stores release control) were added to HUVECs and the fluorescence was measured (Figure 6.8A, B). A large release of Ca^{2+} can be observed in response to GPN, reaching a peak amplitude at ~150 seconds. All recordings were obtained in Ca^{2+} free extracellular buffer in order to observe solely the intracellular Ca^{2+} release of the inner stores. In addition, nigericin (NG), an electroneutral ionophore that exchanges K^+ and H^+ typically utilised to target lysosomal Ca^{2+} stores by increasing their luminal pH (pH_L ; Katsnelson et al., 2016), was used as another pharmacological agent to disrupt the endo-lysosomal Ca^{2+} stores and subsequently release Ca^{2+} . Upon addition to the cells, NG induced slow sustained Ca^{2+} release, though smaller in amplitude than GPN and TG (Figure 6.8B, C). These Ca^{2+} measurements confirm that HUVECs have intact and functional endo-lysosomal Ca^{2+} stores.

Secondly, to observe whether NAADP-dependent Ca^{2+} release has a role in Rab46 and WPB trafficking, HUVECs were pre-treated with Ned19 and then a low dose of histamine ($0.1 \mu\text{M}$) was applied to the cells for 5 minutes. HUVECs were then immunostained for Rab46 (green) and vWF (red; as a marker of WPBs). Notably, at $0.1 \mu\text{M}$, histamine did not induce any of the characteristic perinuclear clustering of Rab46-positive WPBs that it is observed at high histamine concentrations (i.e. $30 \mu\text{M}$), described in the previous chapters of this thesis. However, when the cells were pre-treated with Ned19 prior to stimulation with $0.1 \mu\text{M}$ histamine Rab46-positive WPBs clustered at the perinuclear area (Figure 6.9A). Image quantification analysis showed that Ned19 pre-treatment followed by acute stimulation with $0.1 \mu\text{M}$ histamine (5 minutes) markedly increased both Rab46 and vWF distribution at the perinuclear area (Figure 6.9B). Interestingly, this effect of Ned19 was lost when the cells were treated with higher concentration of histamine ($30 \mu\text{M}$; Figure 6.10A, B). Taken together the data described thus far suggest that at low histamine concentrations, Rab46 has the ability to sense small Ca^{2+} release events localised at the perinuclear area evoking rapid dispersal of Rab46-positive WPBs, unless said Ca^{2+} release is inhibited by Ned19, where Rab46-positive WPBs then cluster because Rab46 cannot detect Ca^{2+} . At high concentrations of histamine, we suggest that the NAADP generated is self-inhibitory and therefore Rab46-positive WPBs cluster at the perinuclear region and Ned19 has no further affect.

Lastly, bafilomycin A1 (BA1) is an inhibitor of the lysosomal proton V-ATPase pump that depletes endo-lysosomal Ca^{2+} concentration and it is commonly utilised in literature to disrupt NAADP-induced Ca^{2+} signalling (Li et al., 2016). In a FlexStation assay, HUVECs were pre-treated with BA1 for 1 hour followed by addition of histamine or thrombin (as a control). BA1 failed to decrease histamine Ca^{2+} release (as opposed to Ned19) and it actually enhanced Ca^{2+} release in both histamine and thrombin treated HUVECs (Figure 6.11A), suggesting the presence of non-specific effects in these cells. Moreover, in representative immunofluorescent images of HUVECs treated with BA1 and immunostained for Rab46 (green) and vWF (red), it can be observed that BA1 treated HUVECs have a reduced population of WPBs compared to control (Figure 6.11B). These findings suggest that in HUVECs BA1 is not a suitable pharmacological tool to study endo-lysosomal Ca^{2+} signalling mobilised by NAADP and its effects on Rab46-positive WPBs, raising the need for alternative pharmacological intervention targeting the Ca^{2+} release mobilised by NAADP in HUVECs.

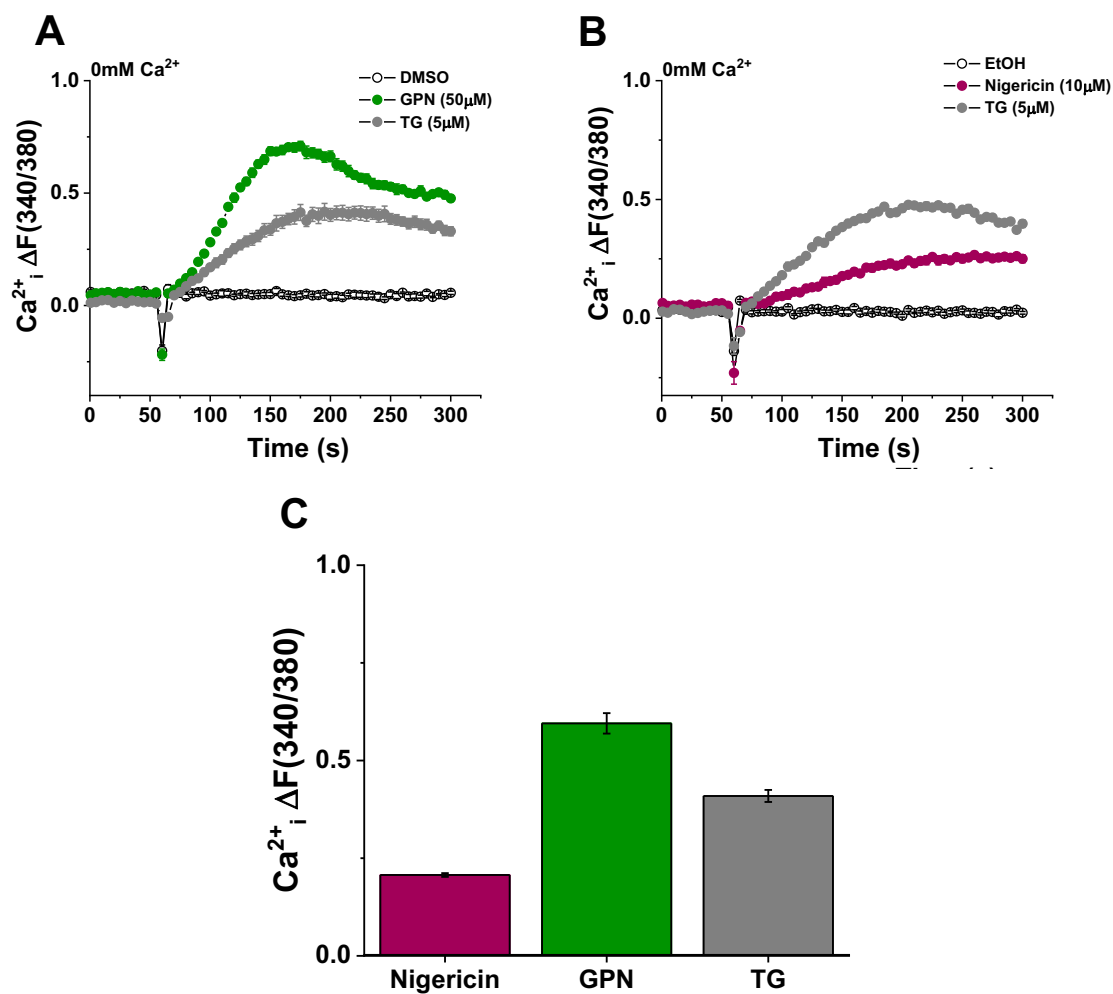


Figure 6.8 HUVECs have functional endo-lysosomal Ca²⁺ stores.

(A) Representative trace of acidic store Ca²⁺ release in HUVECs for 5 minutes evoked by application of 50 μM GPN and 5 μM thapsigargin (TG) at 60 seconds. Recordings were obtained in Ca²⁺ free buffer. (B) Representative trace of acidic store Ca²⁺ release in HUVECs evoked by application of 10 μM Nigericin and 5 μM thapsigargin (TG) at 60 seconds. Recordings were obtained in Ca²⁺ free buffer. (C) Mean data of peak acidic store Ca²⁺ release of (A) and (B) (n/N=3/9, error bars represent SEM).

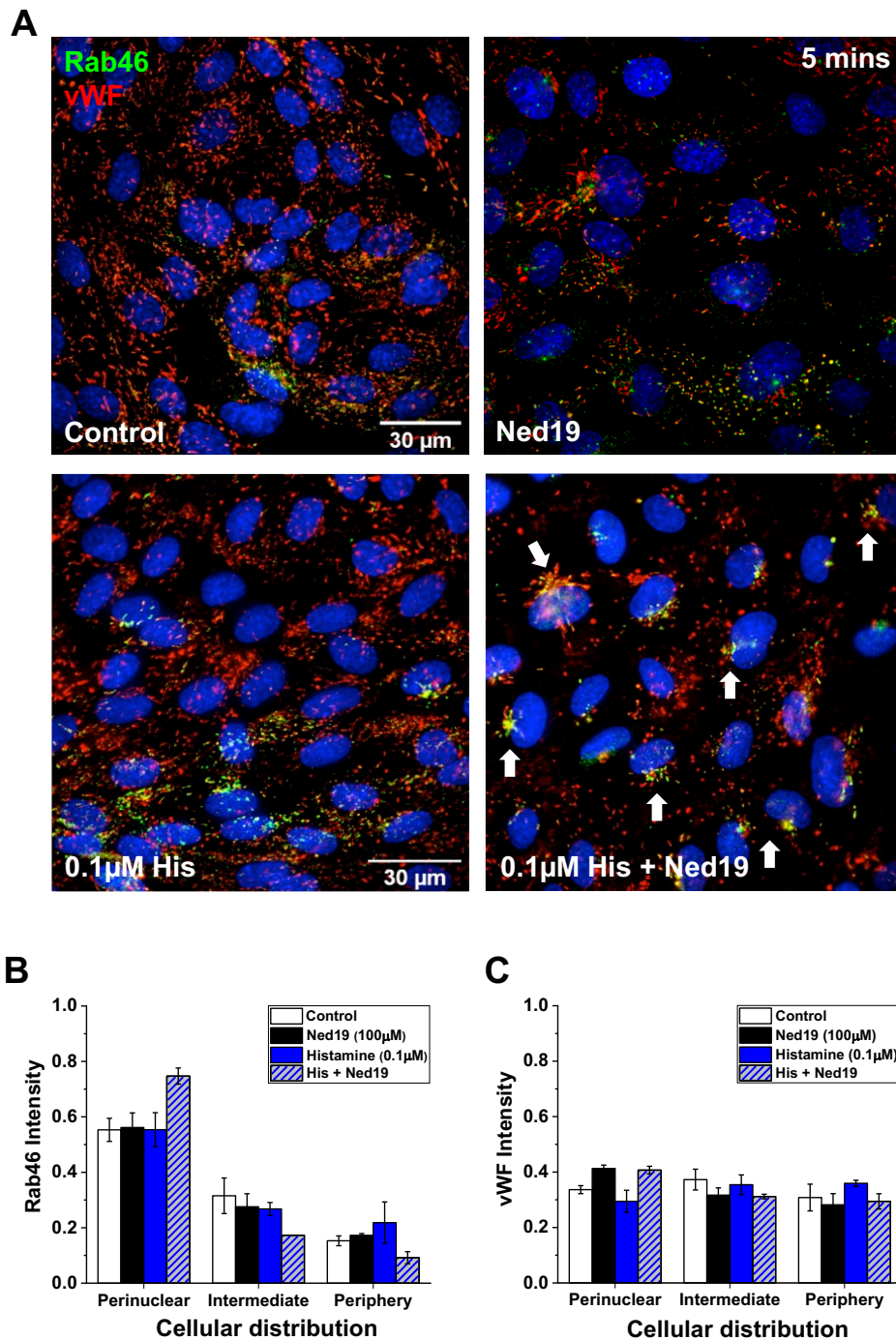


Figure 6.9 Ca^{2+} release from NAADP-sensitive Ca^{2+} stores governs histamine-induced Rab46 and WPB clusters dispersal from the MTOC.

(A) Representative immunofluorescent images of HUVECs cells pre-treated for 30 minutes with 100 μM Ned19, stimulated with 0.1 μM histamine for 5 mins and then fixed and stained for vWF (red) and Rab46 (green). DAPI (blue) shows nuclei. Maximum intensity projections from DeltaVision z-stack are shown. White arrows indicate perinuclear clusters of vWF and Rab46 Scale bar = 30 μm . (B) Mean data showing the cellular distribution of Rab46 upon treatments from (A). (C) Mean data showing the cellular distribution of vWF upon treatments from (A). Results were grouped into three areas: perinuclear, intermediate and periphery. The plots quantify normalised Rab46 (B) and vWF (C) signal intensity in the respective area where the mean (\pm SEM) was noted as percentage of the total signal intensity ($n/N=2/16$).

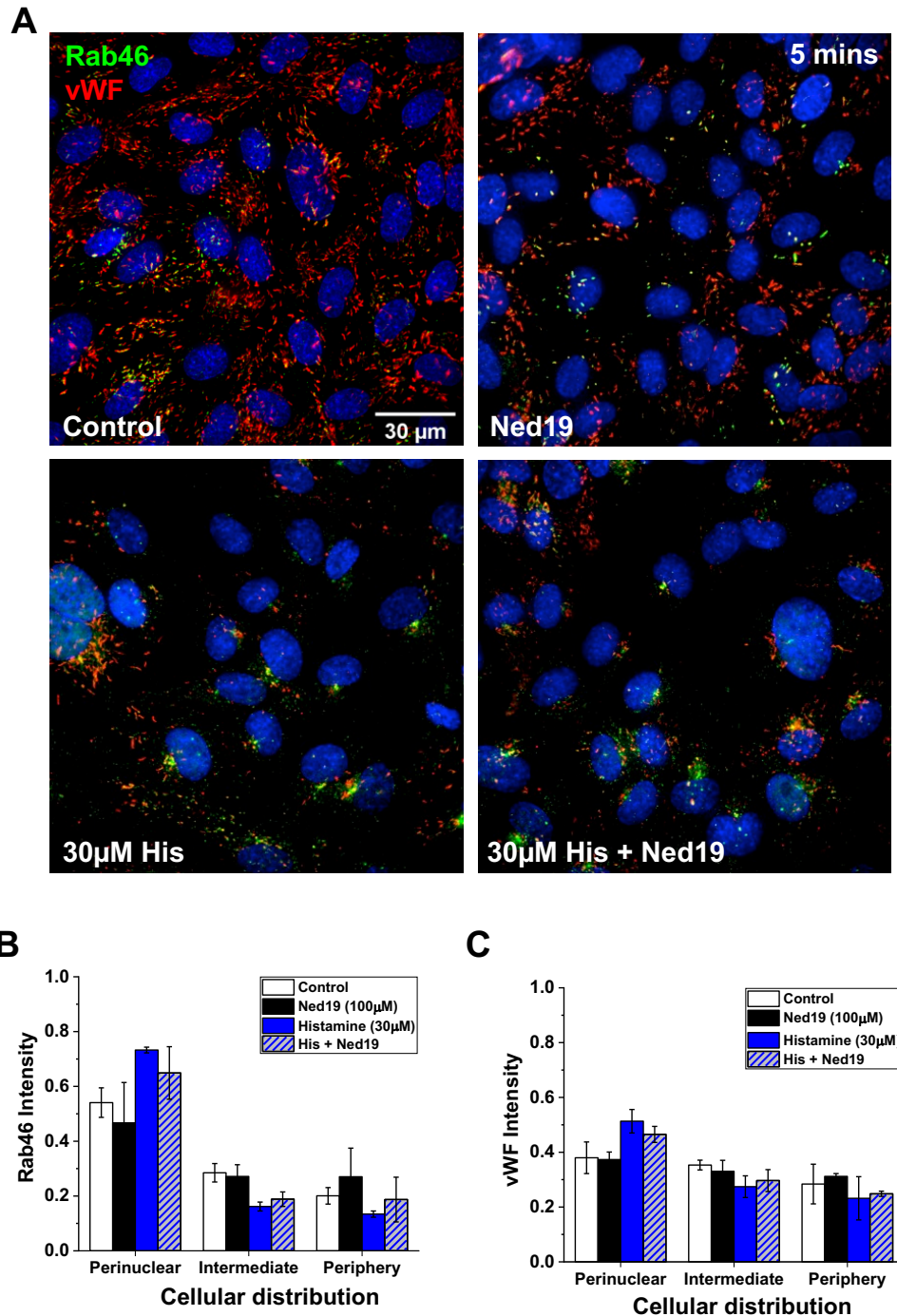


Figure 6.10 High concentrations of histamine does not induce Rab46 and WPB clusters dispersal from the MTOC.

(A) Representative immunofluorescent images of HUVECs pre-treated for 30 minutes with 100 μM Ned19, stimulated with 30 μM histamine for 5 minutes and then fixed and stained for vWF (red) and Rab46 (green). DAPI (blue) shows nuclei. Maximum intensity projections from DeltaVision z-stack are shown. Scale bar = 30 μm . (B) Mean data showing the cellular distribution of Rab46 upon treatments from (A). (C) Mean data showing the cellular distribution of vWF upon treatments from (A). Results were grouped into three areas: perinuclear, intermediate and periphery. The plots quantify normalised Rab46 (B) and vWF (C) signal intensity in the respective area where the mean (\pm SEM) was noted as percentage of the total signal intensity (n/N=2/16).

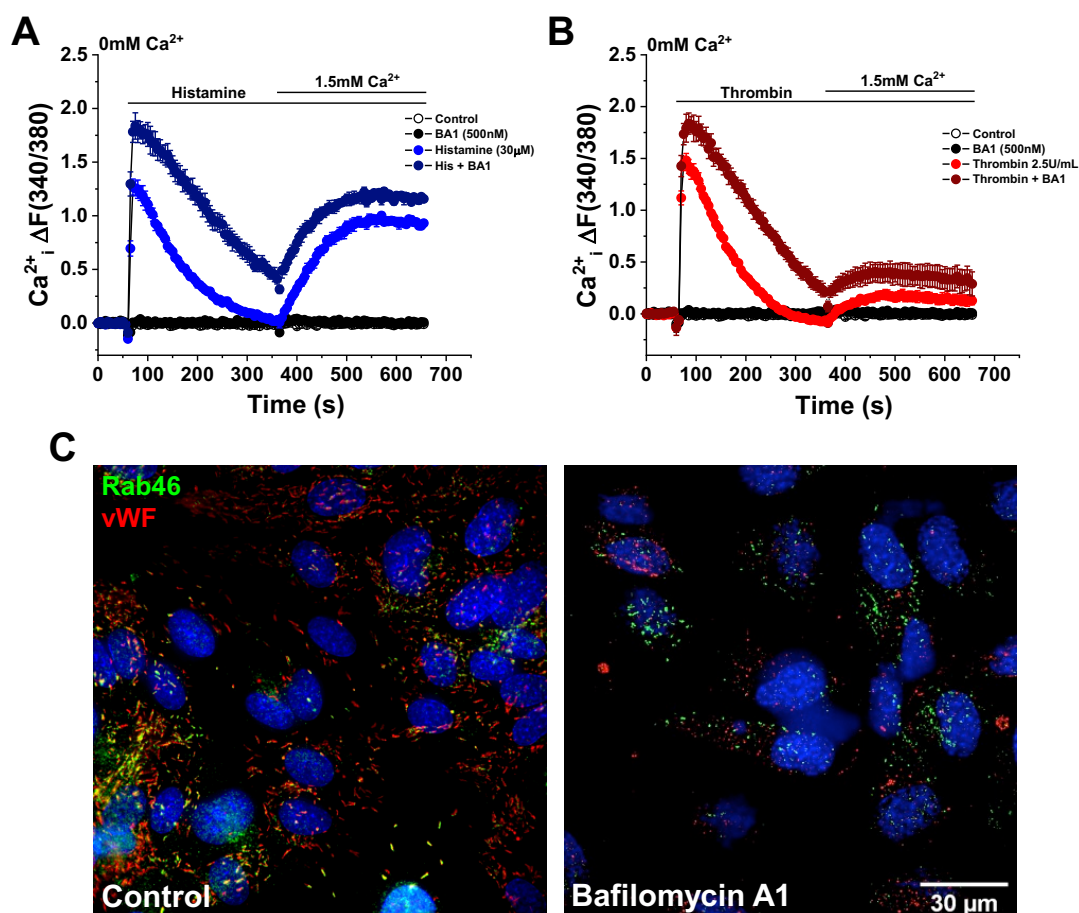


Figure 6.11 Bafilomycin A1 inhibition of V-ATPase activity is not a suitable pharmacological tool to study endo-lysosomal Ca²⁺ signalling in HUVECs.

(A) Representative trace of Ca²⁺ release and entry in HUVECs evoked by application of 30 μM histamine at 60 seconds and Ca²⁺ addback (7.5 mM Ca²⁺ buffer) at 360 seconds, cells were pre-treated with 500 nM Bafilomycin A1 (BA1) for 60 minutes. Recordings were obtained in Ca²⁺-free buffer (n/N=3/9, error bars represent SEM). (B) Representative trace of Ca²⁺ release and entry in HUVECs evoked by application of 2.5 U/ml thrombin at 60 seconds and Ca²⁺ addback (7.5 mM Ca²⁺ buffer) at 360 seconds, cells were pre-treated with 500 nM Bafilomycin A1 (BA1) for 60 minutes. Recordings were obtained in Ca²⁺-free buffer (n/N=3/9, error bars represent SEM). (C) Representative immunofluorescent images of HUVECs treated with vehicle control and 500 nM BA1 for 60 minutes and then fixed and stained for vWF (red) and Rab46 (green). DAPI (blue) shows nuclei. Maximum intensity projections from DeltaVision z-stack are shown. Scale bar = 30 μm.

6.3.2 TPCs are NAADP target channels in ECs

As discussed previously, a large body of research literature has identified TPCs as the Ca^{2+} release channels targeted by NAADP (Calcraft et al., 2009; Galione, 2015a). To begin with, it was imperative to assess the presence of endo-lysosomal Ca^{2+} release channels in HUVECs. Measurement of endo-lysosomal channels gene expression in mRNA extracted from HUVECs showed a marked expression of TPC1 (Figure 6.12). TPC2 was also expressed, though at lower level than TPC1. In addition, other endo-lysosomal channels such as TRPML1 and TRPML2 channels, part of the mucopilin TRP channels family, were expressed. This qPCR data indicates that ECs have diverse endo-lysosomal channels expression.

The VGCCs inhibitor tetrandrine has been previously identified as a potent inhibitor of TPCs (Kilpatrick et al., 2017; Gunaratne et al., 2018). Therefore, HUVECs were pre-treated with tetrandrine and the histamine response was explored using a FlexStation Ca^{2+} imaging assay. Two different doses of histamine were tested, a low dose of histamine 0.1 μM (Figure 6.13A) and a high dose of histamine 30 μM (Figure 6.13C). All Ca^{2+} measurements recordings were obtained in Ca^{2+} free extracellular buffer in order to observe intracellular Ca^{2+} signalling. Similarly to NAADP antagonism by Ned19, TPCs inhibition by tetrandrine completely abolished Ca^{2+} release in response to 0.1 μM of histamine (Figure 6.13B). Moreover, tetrandrine pre-treatment significantly decreases Ca^{2+} peak evoked by 30 μM histamine (Figure 6.13D). Consistent with previous observations, AUC calculations show that tetrandrine treatments decreases the total amount of released Ca^{2+} at both histamine concentrations (Figure 6.13E, F). As a negative control, thrombin was added to tetrandrine pre-treated cells in a FlexStation assay. Tetrandrine treatment had a small but significant effect on the total Ca^{2+} released by thrombin, as per AUC calculations however, tetrandrine had no effect on , the mean Ca^{2+} peak (Figure 6.14). All Ca^{2+} measurements data described herein are consistent with above data described in this chapter and further corroborate the coupling of NAADP signalling to histamine-evoked Ca^{2+} release in HUVECs.

In section 6.3, I showed that a NAADP-sensitive Ca^{2+} pool is necessary for dispersal of histamine-induced Rab46-positive WPBs clusters located at the perinuclear area by using the NAADP antagonist Ned19. It was important to further investigate this finding by targeting TPCs as the Ca^{2+} release channels mobilised by NAADP, whose presence and role in histamine-evoked Ca^{2+} signalling, I have confirmed in this section. In Figure 6.15, HUVECs were pre-treated with tetrandrine followed by treatment with either 0.1 μM or 30 μM histamine. Cells were immunostained for Rab46 (green) and vWF (red). In

representative immunofluorescent images, it can be observed that in response to 0.1 μM histamine, Rab46-positive WPBs are not located at the perinuclear area. However, when cells were pre-treated with tetrandrine, similar to imaging experiments utilising Ned19 described above, Rab46-positive WPBs were notably located at the perinuclear area (Figure 6.15). This finding was also not observed when cells were treated with 30 μM histamine (Figure 6.16). Overall, these data suggest that in response to a low dose of histamine, NAADP mobilises a small but localised Ca^{2+} release event from TPCs, with Ca^{2+} release being necessary for the dispersal of Rab46-positive WPBs at the perinuclear area.

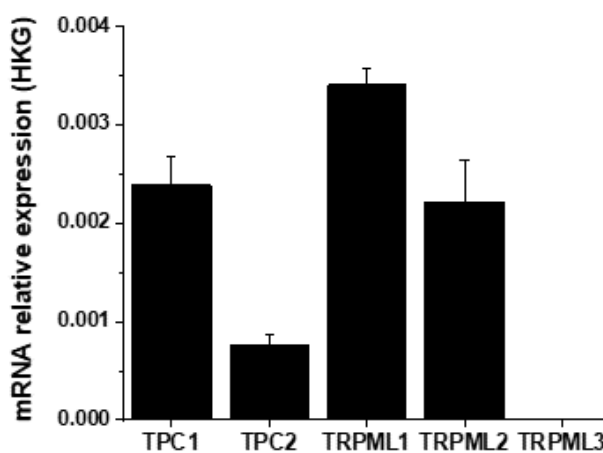


Figure 6.12 Relative mRNA expression of endo-lysosomal cation channels in HUVECs.

qPCR ΔCt analysis of *tpcn1*, *tpcn2*, *mcoln1*, *mcoln2* and *mcoln3* gene expression relative to housekeeping genes (HKG: GAPDH and β -actin; $n = 3$, error bars represent SEM).

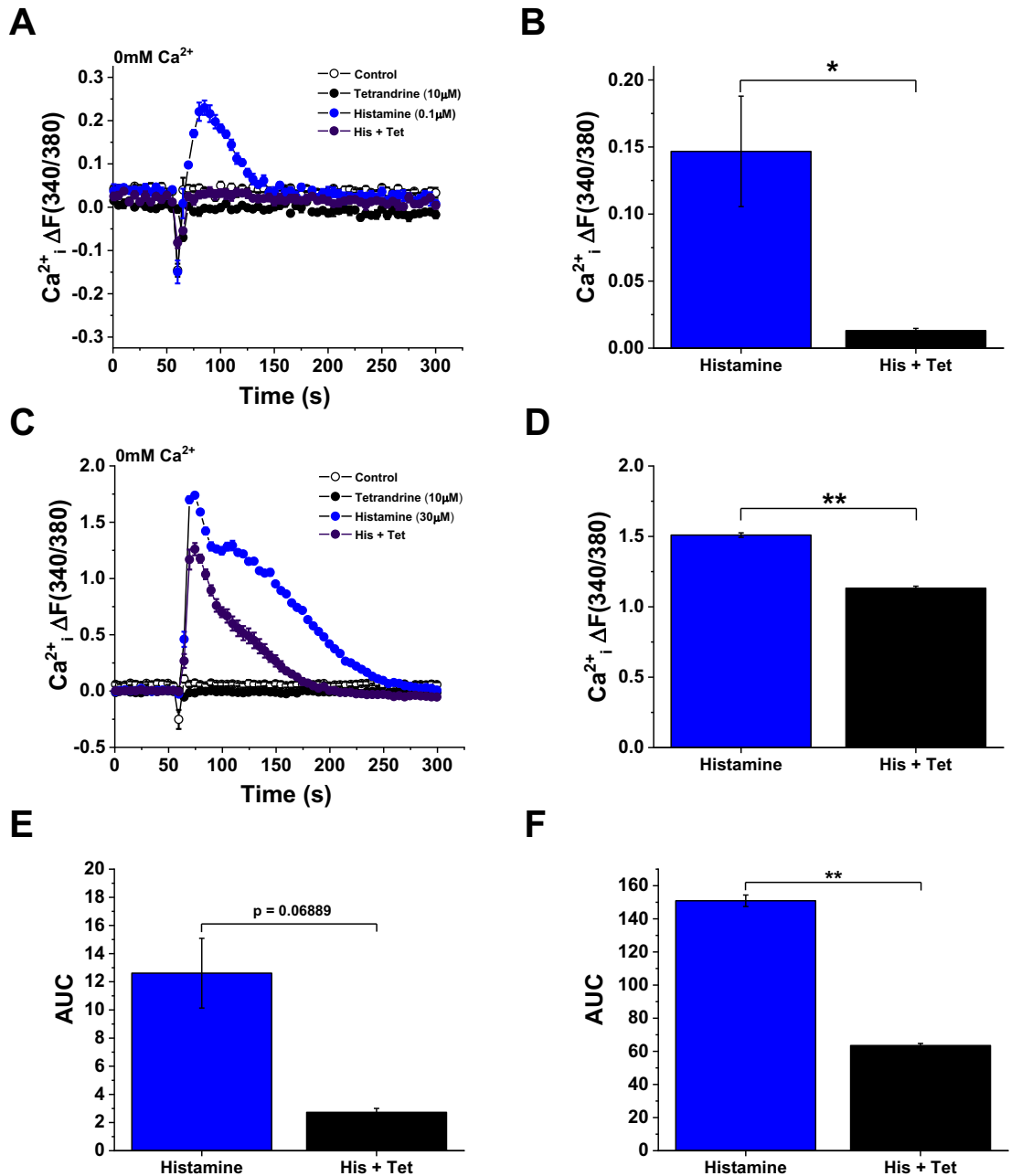


Figure 6.13 TPCs inhibition by tetrandrine decreases histamine-evoked intracellular Ca²⁺ release.

(A) Representative trace of Ca²⁺ release in HUVECs for 5 minutes evoked by application of 0.1 μM histamine at 60 seconds, cells were pre-treated with 10 μM Tetrandrine (Tet; TPCs inhibitor) for 30 minutes. (B) Peak amplitude mean data of treatments from (A). (C) Representative trace of Ca²⁺ release in HUVECs evoked by application of 30 μM histamine at 60 seconds, cells were pre-treated with 10 μM Tetrandrine for 30 minutes. (D) Peak amplitude mean data of treatments from (C). (E) Mean data of area under the curve (AUC) of treatments from (A). (F) Mean data of area under the curve (AUC) of treatments from (C). Recordings were obtained in Ca²⁺-free buffer. (n/N=3/15, error bars represent SEM, * p value < 0.05, ** p value < 0.01 by One-way ANOVA).

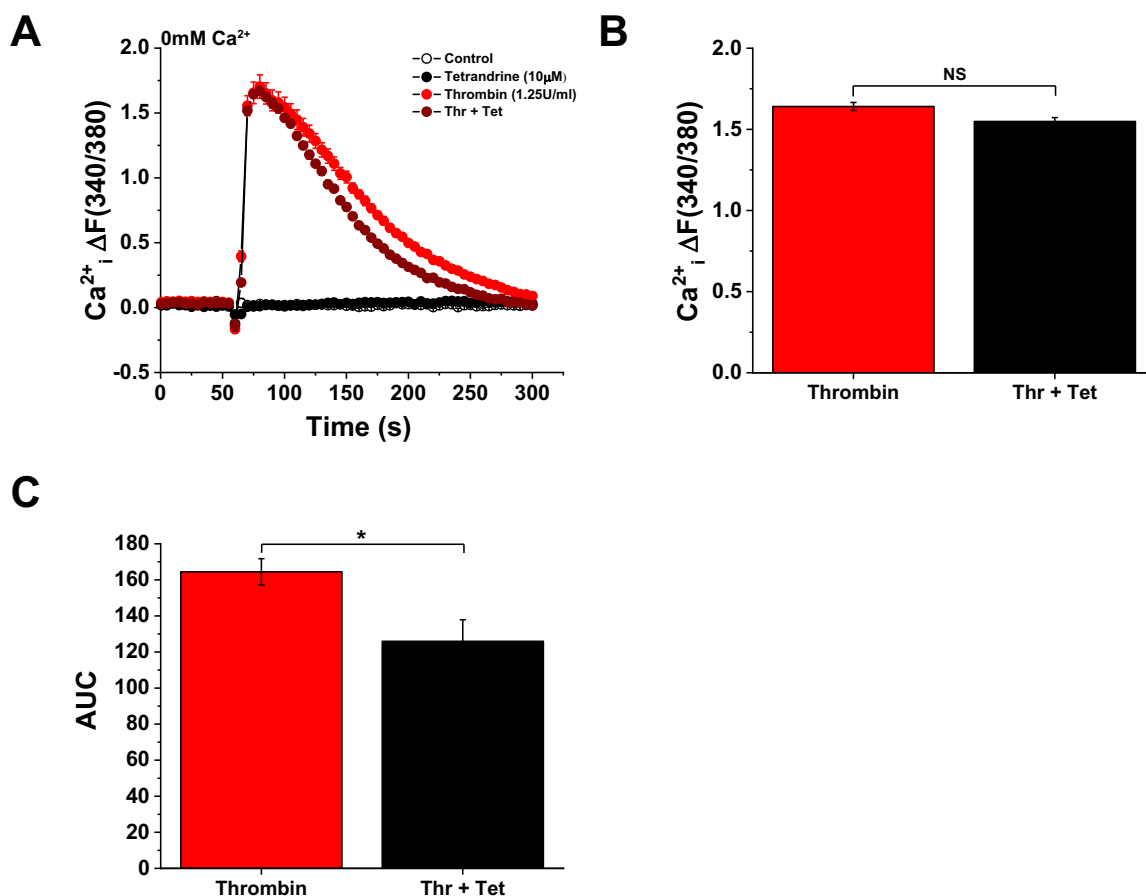


Figure 6.14 Tetrandrine does not inhibit intracellular Ca²⁺ release in response to thrombin.

(A) Representative trace of Ca²⁺ release in HUVECs for 5 minutes evoked by application of 1.25 U/ml thrombin at 60 seconds, cells were pre-treated with 10 μM Tetrandrine (Tet; TPCs inhibitor) for 30 minutes. (B) Peak amplitude mean data of treatments from (A). (C) Mean data of area under the curve (AUC) of treatments from (A). Recordings were obtained in Ca²⁺-free buffer. (n/N=3/15, error bars represent SEM, NS, not significant, * p value < 0.05 by One-way ANOVA).

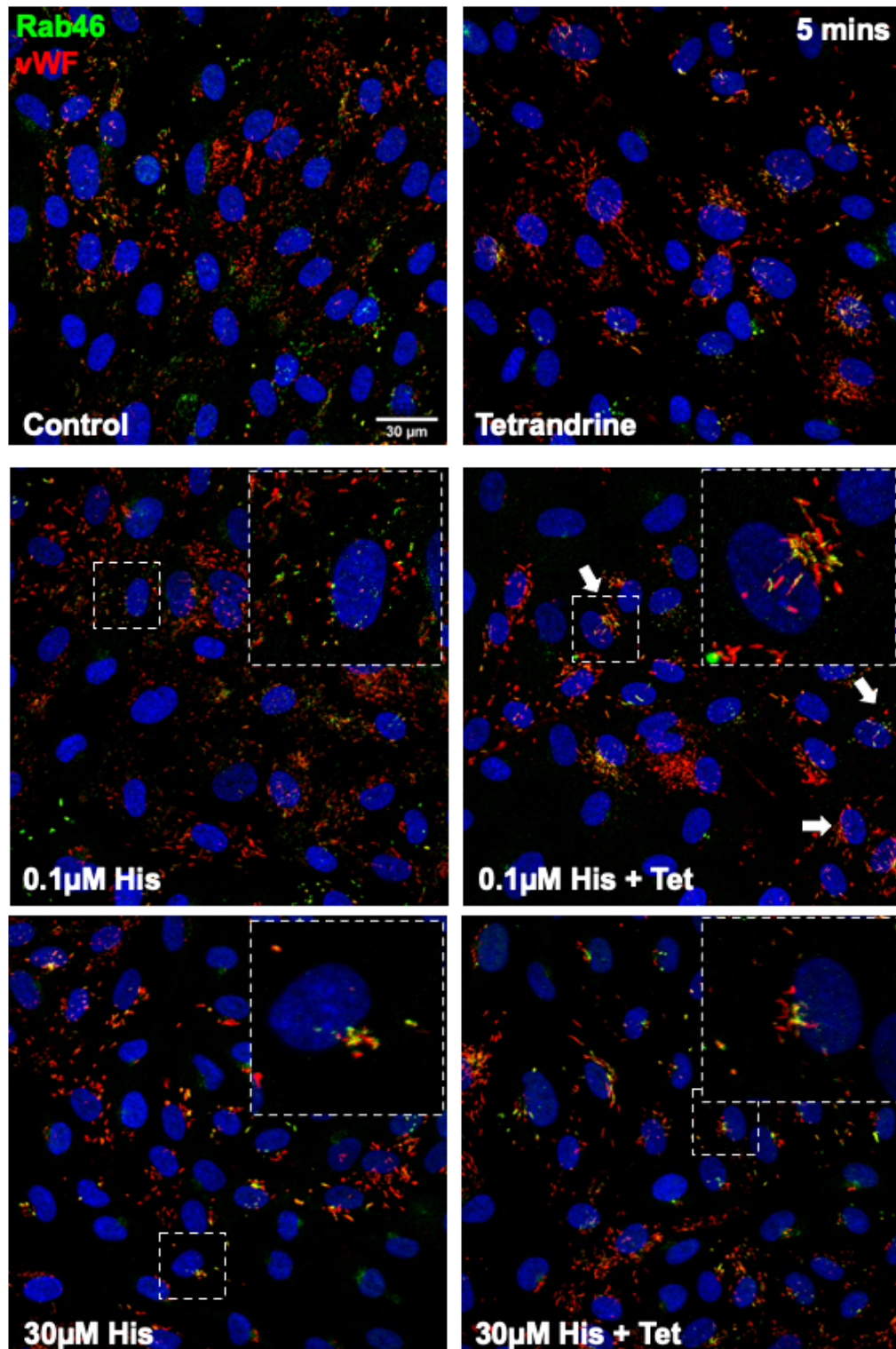


Figure 6.15 Ca^{2+} release from TPCs disperses histamine-induced Rab46 and WPB clusters from the MTOC.

Representative immunofluorescent images of histamine treated HUVECs compared with endothelial cells pre-treated for 30 minutes with $10 \mu\text{M}$ tetrandrine (Tet), stimulated with $0.1 \mu\text{M}$ and $30 \mu\text{M}$ histamine for 5 mins and then fixed and stained for vWF (red) and Rab46 (green). DAPI (blue) shows nuclei. Panels show zoomed-in and cropped cells of interest. Maximum intensity projections from Zeiss LSM 880 z-stack are shown. White arrows indicate perinuclear clusters of vWF and Rab46. Scale bar = $30 \mu\text{m}$.

6.3.3 Localisation of TPCs

Although there have been studies looking at NAADP and TPCs in Ca^{2+} signalling pathways (Esposito et al., 2011; Faviaa et al., 2014c), the endogenous localisation of TPCs in ECs has not been described. In my publication I have previously shown that histamine induces trafficking of both Rab46-positive WPBs towards the MTOC, which can be identified by using pericentrin as a marker. So far this chapter, I have already described compelling findings regarding the role of NAADP-mobilised Ca^{2+} release from TPCs in dispersal of Rab46-positive WPBs clusters from the perinuclear area. In order to further validate the findings described in this chapter so far, it was important to investigate what is the endogenous localisation of TPCs in HUVECs and whether that would be affected by histamine treatment.

To begin with, commercially available anti-TPC1 was purchased. In high-resolution representative images of HUVECs immunostained for TPC1 (green) with previously validated antibody (Hooper et al., 2015) and pericentrin (red), it can be observed that TPC1 is abundantly expressed (Figure 6.16A), consistent with the qPCR data shown above (Figure 6.12). Interestingly, in HUVECs, TPC1 is located at the perinuclear area and co-localises with pericentrin (Figure 6.16B). Furthermore, in HUVECs treated with a high concentration of histamine (30 μM : inducing the characteristic perinuclear clustering of Rab46-positive WPBs) and it can be noted that WPBs not only traffic to the perinuclear area, but are in fact orientated towards TPC1 (Figure 6.17).

Next, although TPC2 mRNA levels in HUVECs were not as high, anti-TPC2 was tested on HUVECs, however, no immunofluorescence signal was detected (data not shown). A commercially available TPC2^{GFP} plasmid was obtained. HUVECs were transfected overnight with the plasmid, and subsequently fixed and additionally immunostained for vWF (red). TPC2^{GFP} was not co-localised with WPBs or replicate aforementioned findings about the endogenous localisation of TPC1. Instead, TPC2^{GFP} vesicles showed rather dispersed localisation throughout the cytoplasm (Figure 6.18). Additionally, in response to histamine treatment, WPBs were clustered and orientated towards the perinuclear area, however, TPC2^{GFP} remained unchanged.

Overall, the data in this section indicate that endogenous TPC1 is localised at the MTOC, which is consistent with our working hypothesis thus far that the Ca^{2+} necessary for the dispersal of WPBs from the perinuclear area is indeed released from TPCs as a highly localised Ca^{2+} release.

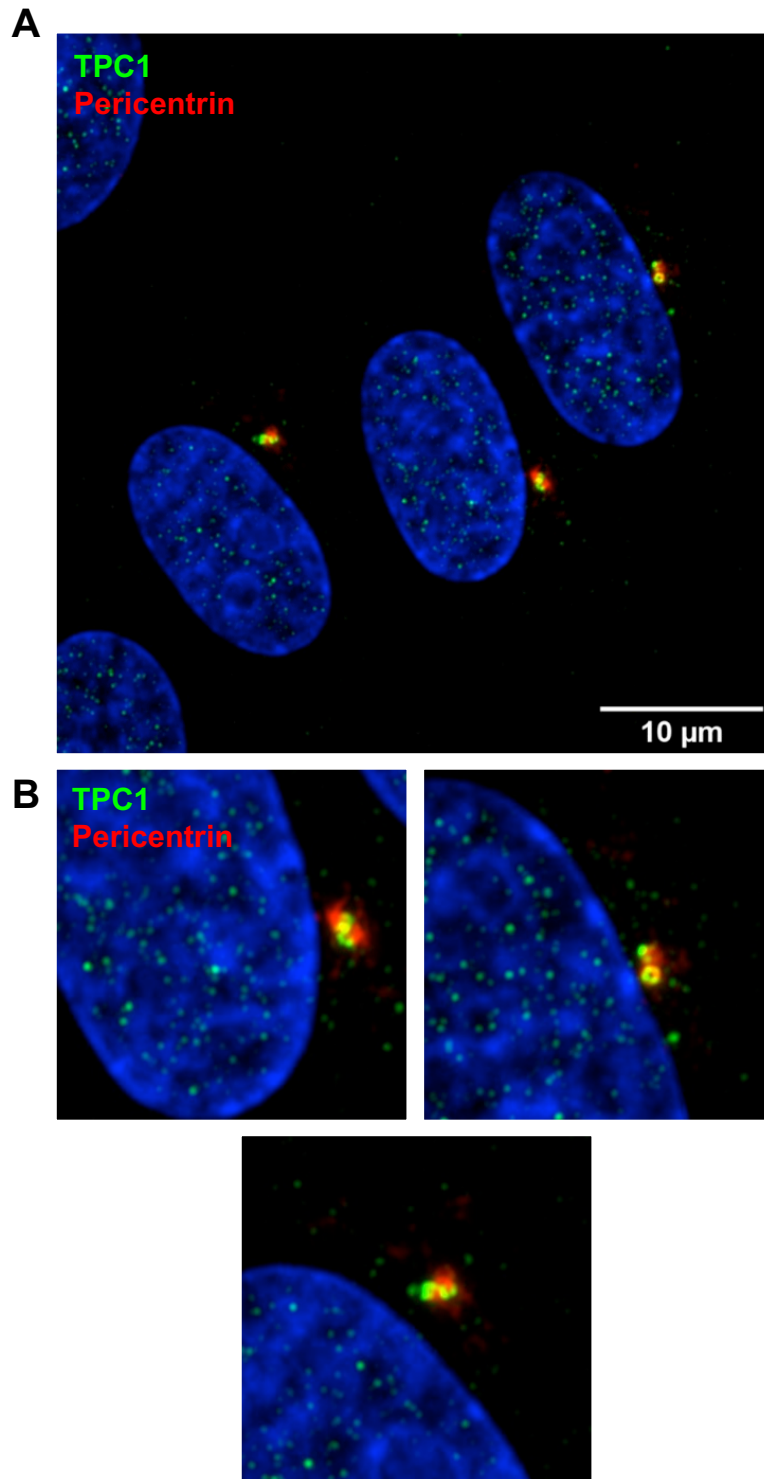


Figure 6.16 Endogenous TPC1 localises to the MTOC in HUVECs.

(A) High-resolution Airy Scan imaging showing detailed localisation of endogenous TPC1 (green) and pericentrin (red; marker of MTOC) in HUVECs. Scale bar = 10 μm . (B) Panels showing zoomed-in and cropped high-resolution images of TPC1 (green) signal co-localised pericentrin (red).

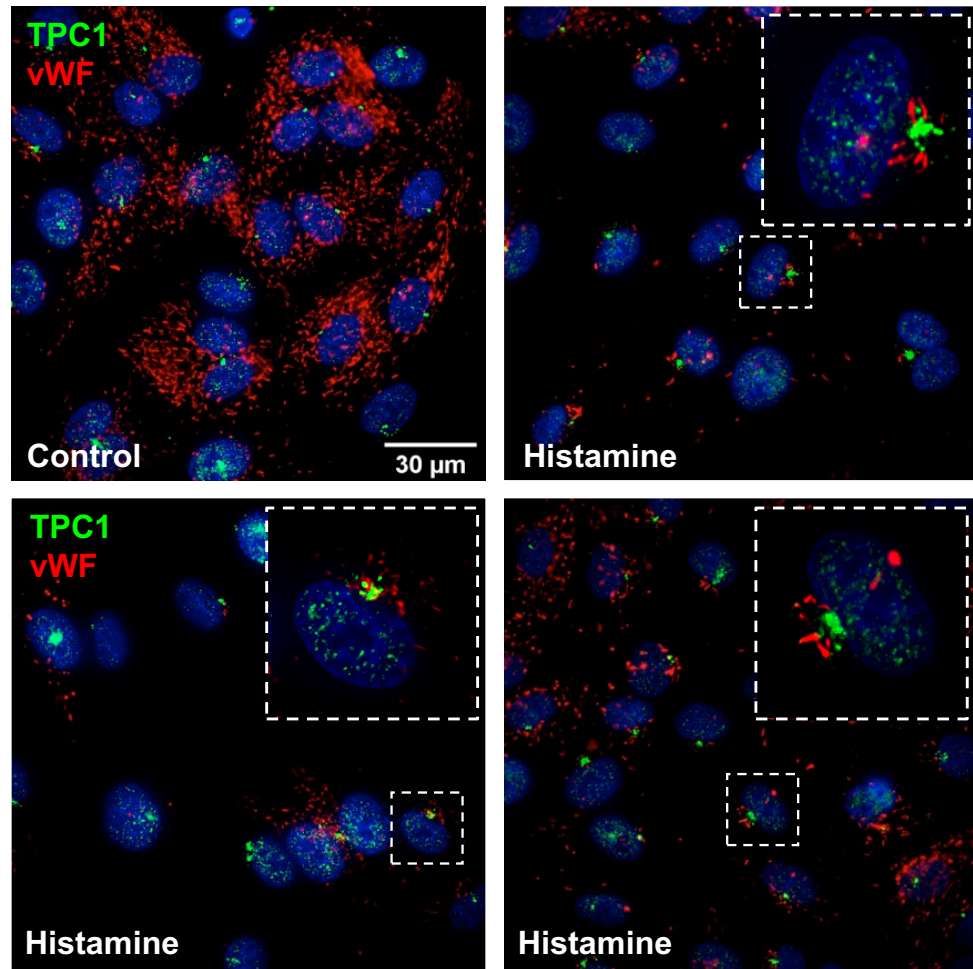


Figure 6.17 WPBs cluster with TPC1 at the MTOC in response to histamine.

Representative immunofluorescent images showing subcellular localisation of endogenous TPC1 (green) and vWF (red; marker of WPBs) in control and 30 μ M histamine treated HUVECs for 5 minutes. DAPI (blue) shows nuclei. Panels show zoomed-in and cropped cells where upon histamine treatment WPBs were orientated towards TPC1. Maximum intensity projections from DeltaVision z-stack are shown. Scale bar = 30 μ m.

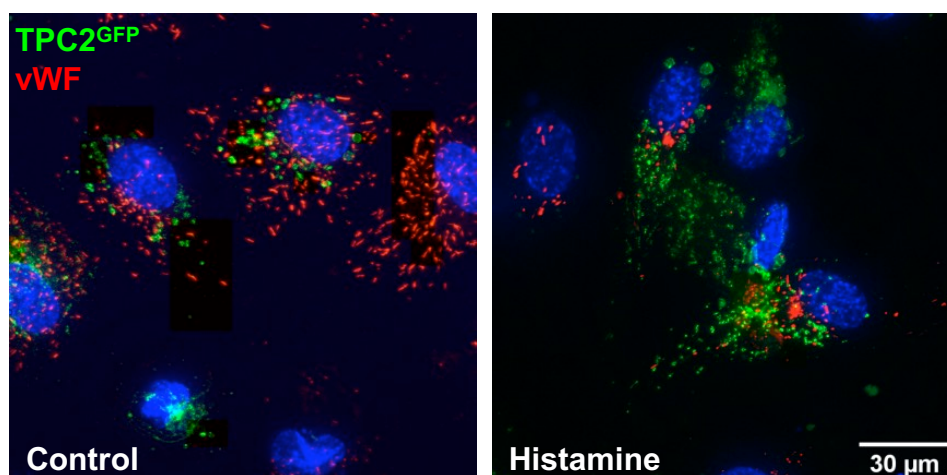


Figure 6.18 TPC2 does not colocalise with WPBs.

Representative immunofluorescent images of HUVECs transfected with TPC2-EGFP (green) for 24 hours and treated with 30 μ M histamine for 5 mins, followed by fixation and staining for vWF (red; marker of WPBs). DAPI (blue) shows nuclei. Maximum intensity projections from DeltaVision z-stack are shown. Scale bar = 30 μ m.

6.3.4 Rab46-positive WPBs interaction with the endo-lysosomes.

In the previous section of this chapter, for the first time, I presented evidence that endogenous TPC1 is localised at the perinuclear area in HUVECs. From literature and Chapter 1 Introduction, it is known that Rab GTPases interact with TPCs and are important for their function (Lin-Moshier et al., 2014). In fact, when mass spec based data from Rab46 (constitutively active mutant) (Pedicini et al., 2021) and TPC1/2 pull downs is compared, the presence of identified common small binding proteins was identified (Figure 6.19A). In addition, due to experimental limitations, it was not possible to immunostain for both TPC1 and Rab46 in order to probe if the two proteins interact in control or histamine stimulated conditions. However, Western blotting analysis of preliminary immunoprecipitation experiments of endogenous Rab46 and TPC1/2 shows that Rab46 interacts with both TPCs in response to histamine (Figure 6.19B).

Taken together the findings in this chapter support that the Ca^{2+} necessary for the dispersal of histamine-induced Rab46-positive WPBs clusters from the MTOC is derived by NAADP-sensitive Ca^{2+} pool. Additionally, I confirmed that in the endothelium the NAADP target Ca^{2+} are TPCs and I presented for the first time data of endogenous localisation of TPC1. Lastly, the novel findings presented herein suggest that WPBs and Rab46 interact with the endo-lysosomes.

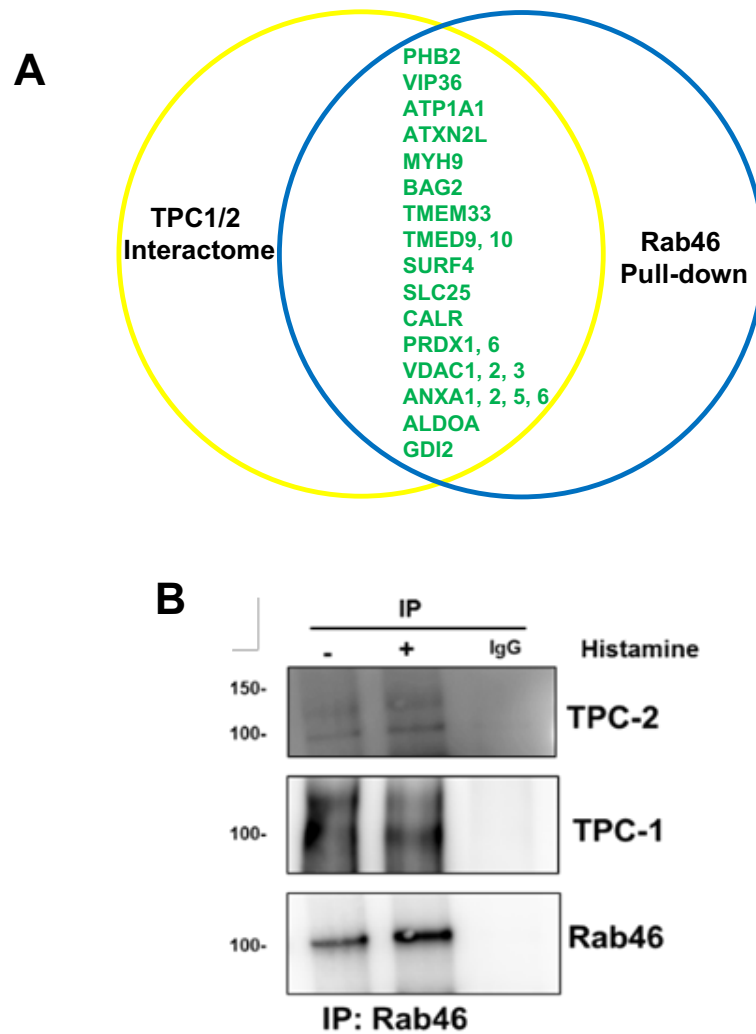


Figure 6.19 Rab46 interacts with TPCs.

(A) Venn diagram depicting the overlap (green) of binding proteins between available TPC1/2 interactome and McKeown's lab Rab46 pulldown data (Pedicini et al., 2021). (B) Western blot of TPC1, TPC2 and Rab46 after immunoprecipitation of endogenous Rab46 from HUVECs treated with 30 μ M histamine or control.

Chapter 7 Discussion

In Miteva *et al.* (2019) it was shown that histamine induces activation of a novel endothelial Rab GTPase, Rab46, and promotes Rab46 interaction with the dynein motor complex promoting trafficking of WPBs towards the MTOC. The data thus far suggests that this interaction selectively triggers trafficking of a subpopulation of WPBs that are devoid of P-selectin but contain other cargo, such as Angiopoietin-2, to the perinuclear area, and the MTOC as I have shown. Concomitantly, histamine rapidly triggers the exocytosis of P-selectin-carrying WPBs at the cell surface of ECs. Notably, such WPBs do not display colocalisation with Rab46 suggesting a potential mechanism whereby Rab46 is specifically recruited to Angiopoietin-2-positive WPBs, or other unexplored WPB subpopulations, not required for the acute immunological response. The data presented in this thesis therefore suggest that Rab46 may fine-tune WPB trafficking in response to distinct agonists, such as histamine, but not thrombin. Over time WPB subpopulations cluster and accumulate at the MTOC, where the EF-hand domain of Rab46 binds to locally released Ca^{2+} , which induces dissociation of Rab46 from the microtubules and disperses clustered WPBs thereafter. Preliminary data from this thesis shows that the Ca^{2+} signal needed for this dispersal is derived from acidic Ca^{2+} stores, such as the endo-lysosomal system, and a potential cross-talk between WPBs and the lysosomes.

7.1 The role of Rab46 in differential trafficking of WPB subpopulations

The orchestration of accurate and agonist-appropriate responses by the vascular endothelium is an elusive, and to some extent, an enigmatic phenomenon. ECs receive signals from multiple agonists, all operating via seemingly converging downstream signalling pathways, cAMP and Ca^{2+} , and yet deliver agonist specific responses. In the previous chapters of this thesis, I have described that ECs pre-package WPBs as an armour of bioactive mediators regulating important vascular functions such as haemostasis, inflammation and angiogenesis. Previous literature provides an initial insight into the complex mechanisms underlying the differential release of cargo from WPBs docked at the cell surface (Zupančič *et al.*, 2002; Royo *et al.*, 2003; Øynebråten *et al.*, 2004; Babich *et al.*, 2008). Some examples include a “lingering kiss” type of exocytosis which occurs during low concentrations of histamine and limits the secretion of WPB cargo >40

kDa. Additionally, agonist-dependent recruitment of an actomyosin ring can control the force necessary for expulsion of vWF without affecting release of other WPB cargo (Babich et al., 2008; Nightingale et al., 2018b). However, to date, there has been no description of physiologically contextual differential WPB release, or the identification of cellular machinery which supports regulation of such release.

Histamine, an amine involved in transient immune and inflammatory responses (Naomasa et al., 1992), and thrombin, a multifunctional serine protease that is involved in the coagulation cascade (Minami et al., 2004), are two potent agonists of WPB exocytosis (Rondaij, Bierings, Kragt, Van Mourik, et al., 2006). Considering the the physiological function of these two agonists (pro-immunogenic vs pro-thrombotic), it is vital that ECs couple distinct stimuli to the selective release of WPB cargo to achieve an appropriate response. This indicates that ECs need to have intracellular machinery to selectively redirect physiologically irrelevant trafficking of cargo and exocytosis. In this thesis I have demonstrated for the first time that thrombin and histamine, elicit differential WPB trafficking in a time-dependent manner; whereby histamine induces perinuclear trafficking of WPBs following 5 to 15 minutes of stimulation, which is not observed when ECs are stimulated with thrombin. In a study by Vinogradova and colleagues, it was reported that thrombin induces perinuclear clustering (Vinogradova et al., 2000). Despite, thrombin causing a typical stress morphological response in the cells I did not observe any perinuclear clustering with thrombin. A possible explanation to this discrepancy is that thrombin response generates cAMP raise in the endothelium (Zhang and Colman, 2007). Another aspect is that in the study by Vinogradova and colleagues the ECs used were from individual donors that suffered from thoracic aorta trauma as opposed, while in this thesis I have used pooled HUVECs from healthy donors. In Miteva *et al.* (2019) it was shown that such histamine-evoked trafficking of WPBs is dependent on Rab46, a novel Rab GTPase in the endothelium (Wilson et al., 2015; Miteva et al., 2019). In addition, in the absence of stimulation a constitutively active mutant of Rab46 mimics histamine stimulation triggering perinuclear clustering of WPBs to the MTOC.

Continuing this work, the findings in this thesis shed more light on an unresolved discrepancy in the literature. Previously, there have been opposing findings regarding mutually exclusive WPB subpopulations containing P-selectin and Angiopoietin-2 (Fiedler et al., 2004b; van Agtmaal et al., 2012). I demonstrated that, not only do WPBs store P-selectin and Angiopoietin-2 in separate subpopulations, but such subpopulations are differentially trafficked in response to acute histamine stimulation. Intriguingly, this is regulated by Rab46 as Rab46

is recruited to Angiotensin-2-positive WPBs and does not display colocalization with P-selectin- positive WPBs in ECs. During transient immune responses chemoattraction and extravasation of leukocytes to the endothelium occurs within minutes (Sun et al., 2012). Consistent with this, the data in this thesis reveals a mechanism whereby upon acute immune responses marked by histamine release in the absence of vascular injury, P-selectin is released at the cell surface, while Rab46 selectively redirects WPBs carrying functionally irrelevant cargo, such as an angiogenic mediator Angiotensin-2 to the MTOC, thereby allowing leukocyte recruitment without inducing cell migration. This proposed mechanism suggests that trafficking of distinct WPB subpopulations is dependent on the physiological context as perinuclear clustering of WPBs at the MTOC is a specific trafficking pattern induced by histamine but not thrombin. The conclusions in this thesis complement previous findings of Fiedler and colleagues who demonstrated that thrombin but not histamine evoked Angiotensin-2 exocytosis from HUVECs, indicating transient anchoring of Angiotensin-2-positive WPBs at the MTOC to prevent release (Fiedler et al., 2004b). Furthermore, Erent and colleagues showed comparative data of WPBs stimulated with either ionomycin, a potent Ca^{2+} ionophore, or histamine, revealing that histamine-stimulated ECs display a significant reserve capacity in the WPB secretory system, which even high concentrations of histamine fail to utilise. The authors proposed that such extra exocytosis capacity may be an important asset during vascular cell injury where very high intracellular Ca^{2+} concentration would signal the need for a rapid and full armour secretion by WPBs (Erent et al., 2007c).

The cellular mechanisms underlying how Rab46 is recruited to WPBs and its effector are currently being investigated by our lab. Understanding the mechanisms of precise Rab46 recruitment together with the signalling pathways that activate Rab46 would shed more light on how histamine can stimulate exocytosis of P-selectin at the plasma membrane to allow for leukocyte adhesion (Rab46 independent), while diverting Angiotensin-2-positive WPB subpopulation to the MTOC (Rab46 dependent). Our lab has also demonstrated that Rab46 depletion increases vWF protein levels suggesting that Rab46 may also play a role in exocytosis (K. T. Miteva et al., 2019). Consistent with the previous observation discussed in this thesis, P-selectin exocytosis remains unaffected by depletion of Rab46. Interestingly, absence of endogenous Rab46 in ECs does not affect mRNA levels of Angiotensin-2, however, protein levels of Angiotensin-2 are reduced and immunofluorescent detection of Angiotensin-2 is reduced in ECs lacking Rab46. This raises the possibility of an additional role of Rab46 recruiting Angiotensin-2 to WPBs. This effect on Angiotensin-2 protein levels requires further exploration. Live imaging studies in ECs would reveal the

dynamics of the relationship between Rab46 and Angiotensin-2 in real-time. In addition, employing *ex vivo* molecular measurements and imaging of ECs isolated from Rab46 null mice could also provide a model with a stable deletion of Rab46.

Overall, the data presented in this thesis suggests that histamine evokes acute perinuclear trafficking and clustering of an Angiotensin-2-positive subpopulation of WPBs at the MTOC as a mechanism to restrict release of Angiotensin-2. However, the possibility of redirection and trafficking of other redundant WPB cargo not needed during an acute inflammatory response cannot be excluded and requires further investigation. Due to time constraints of the project further work on the physiological importance of histamine-specific WPB trafficking was not carried out. Hereinafter, I aim to discuss investigation into the signalling pathways governing histamine evoked trafficking of Rab46-positive WPBs.

7.2 Histamine-induced WPB retrograde trafficking is independent of cAMP and Ca²⁺

WPB regulated exocytosis is primarily split into two groups depending on the second messenger signalling pathways – Ca²⁺ and cAMP (Schillemans et al., 2019c) (although physiologically these may not be mutually exclusive). cAMP-dependent WPB exocytosis is well described in the literature (Rondaij et al., 2004a; Rondaij, Bierings, Kragt, Gijzen, et al., 2006; Van Hooren et al., 2012b; Brandherm et al., 2013). Briefly, cAMP-dependent agonists such as epinephrine or vasopressin cause a slow and gradual WPB release due to the activation and additive effect of two cAMP dependent pathways – the small GTPase RalA and the Epac-Rap1 pathway (Rondaij et al., 2004b; Van Hooren et al., 2012a). Additionally, epinephrine has been found to also trigger perinuclear clustering, also known as retrograde trafficking, of WPBs at the MTOC. PKA-dependent activation of the dynein-dynactin motor complex is responsible for the perinuclear trafficking of WPBs in response to epinephrine (Rondaij, Bierings, Kragt, Gijzen, et al., 2006).

In the previous chapters of this thesis, I have also shown data detailing histamine-evoked perinuclear clustering of a subpopulation of WPBs and a novel endothelial Rab protein, Rab46. Previous studies of histamine-evoked WPB trafficking have not reported the retrograde trafficking we have observed. Possible explanations for this difference in findings could lie in differences in the experimental set up, end point time of measurements and also that histamine-evoked retrograde trafficking is Rab46-dependent, and in Miteva *et al.* (2019) that not all ECs in a

monolayer express Rab46 (K. T. Miteva et al., 2019). It was also shown that the perinuclear area that WPBs cluster at, or more precisely traffic towards, is the MTOC. This histamine-evoked retrograde trafficking towards the MTOC is dependent on the presence of Rab46, the activation of its GTPase domain and interaction with the dynein motor complex (Pedicini et al., 2018).

Interestingly, histamine is an endothelial agonist of WPB exocytosis previously described to trigger intracellular Ca^{2+} pathways. However, histamine is a signalling amine that has a heterogenous family of receptors and it has been shown that G_s -dependent H_2 receptors in fact activate adenylyl cyclase and cAMP signalling pathways downstream (e.g. PKA; Haas and Panula, 2016). Therefore, for this project it was imperative to investigate whether the histamine-evoked perinuclear clustering was also dependent on the cAMP-PKA signalling axis. The widely studied PKA inhibitor, H89, and the cAMP antagonist, Rp-cAMPs, were used. Prior to using these inhibitor, their efficacy was evaluated by measuring phosphorylation of CREB-1, a protein that undergoes PKA-dependent phosphorylation downstream. H89 and Rp-cAMPs had no effect on the histamine-evoked intracellular Ca^{2+} release as expected. H89 and RP-cAMPs at their respective doses did not prevent histamine-induced WPB and Rab46 clustering at the perinuclear area. This data indicates that in ECs, cAMP-PKA signalling is not involved in Rab46-dependent WPB clustering. As such WPB clustering evoked by epinephrine and histamine are likely two separate signalling pathways the endothelium uses for differential trafficking of WPB subpopulations.

It was already established that histamine-induced WPB clustering at the MTOC is Rab46-dependent (Miteva et al., 2019), therefore it was important to determine if Rab46 plays a role in cAMP-dependent perinuclear trafficking. Acute stimulation of ECs with epinephrine and the phosphodiesterase IBMX did not provoke robust WPB clustering, differing to previous studies when cells were treated for longer timepoints. In the absence of endogenous Rab46 (depleted by Rab46 siRNA) it appeared that WPBs still clustered at the perinuclear area, likely due to Rab46-independent trafficking of WPBs and dependent on other trafficking players activated by PKA. The presence of Rab46 on WPBs does not necessarily indicate it plays a role in trafficking or whether Rab46 recognises cAMP-signalling. Further image quantification is needed to solidify the aforementioned findings that Rab46 is indeed not involved in cAMP-dependent trafficking and exocytosis of WPBs. GTPase activity assays would complement and reinforce the data described in this thesis by showing whether the Rab domain of Rab46 is activated in response to cAMP-PKA signalling.

Once confirmed that activation of Rab46 and subsequent Rab46-dependent retrograde trafficking is independent of cAMP-PKA it became clear that a more in

depth investigation into the expression of histamine receptor isoforms in HUVECs was needed. mRNA measurements revealed that primarily H₁R is expressed and from literature it is known that H₁R is a GPCR of G_{q/11} type, previously described to couple to PLC and trigger intracellular Ca²⁺ release from internal Ca²⁺ stores. Out of the other histamine receptor isoforms, only some trace amounts of H₄R were expressed in HUVECs. H₄R expression in HUVECs has not been previously reported and this histamine receptor isoform is primarily detected only in several types of immune cells (Parsons and Ganellin, 2006). Ca²⁺ release in HUVECs was only achieved using only very high concentrations of H₄R specific agonist, suggesting cross reactivity with the H₁R receptor. There were no obvious signs of the agonist triggering retrograde trafficking. However, a better positive control, such as mRNA derived from immune cells, is needed to evaluate the efficacy of set of primers used to determine that our batch of HUVECs express primarily H₁R.

Using a commercially available H₁R selective agonist it was clear that histamine operates via the H₁R to evoke intracellular Ca²⁺ release and trigger retrograde trafficking of Rab46-positive WPBs. Moreover, employing mepyramine, a selective H₁R inverse agonist, abolished any Ca²⁺ release and prevented retrograde trafficking of Rab46 and WPB towards the MTOC evoked by both histamine and the H₁R agonist. This data suggests that in HUVECs histamine binding to the H₁R activates Rab46 and triggers retrograde trafficking of Rab46-positive WPBs along microtubules toward the MTOC. Findings also indicate that Rab46 activation and said retrograde trafficking may be orchestrated by Ca²⁺ signalling pathways. Complementing this, a study by Wang and colleagues proposed that in T cells Rab46 is necessary for dynein motor complex-dependent transport to the MTOC, in which Rab46 and dynein complex interact in a Ca²⁺-dependent manner (Wang et al., 2019).

However, further experiments described in this thesis employing Ca²⁺ chelation and inhibition of Ca²⁺ plasma channels reveal that in the endothelium Rab46 and WPB retrograde trafficking is Ca²⁺ independent. Moreover, when levels of cytoplasmic Ca²⁺ are artificially increased by thapsigargin after histamine stimulation, this reveals dispersing of Rab46-positive WPBs from the MTOC. 30 minutes of thapsigargin has been shown to cause ER stress and Golgi/MTOC fragmentation (Nakagomi et al., 2008). In this thesis experiments utilising thapsigargin were limited to 5 minutes treatments, however in future studies a good control for would be to visualise the Golgi, MTOC and tubulin after 5 minutes treatment to confirm microtubule and centrosome integrity. This observation is further corroborated by the finding that the mutated EF-hand domain of Rab46 that renders Rab46 unable to bind to Ca²⁺ (Rab46^{EFmut}) is also located at the

MTOC in the absence of stimulation by histamine, where it aggregates and becomes anchored. Opposite to endogenous or WT Rab46, Rab46^{EFmut} fails to disperse despite increases in cytoplasmic Ca²⁺ concentration. In addition, our lab has recently published data revealing that despite the lack of Ca²⁺ binding Rab46^{EFmut} is able to bind to and interact with dynein (Pedicini et al., 2021). Together these data show that Ca²⁺ is not necessary for Rab46 activation and dynein-dependent retrograde trafficking to the MTOC, however Rab46-positive WPBs dispersal from the MTOC is driven by binding of Ca²⁺ to the EF-hands of Rab46. The origin of such Ca²⁺ signal is likely to be a highly localised Ca²⁺ microdomain near the perinuclear area. This is not surprising because there are other GTPase proteins that have the ability to use both GTP- and Ca²⁺-binding as two separate signals which act as molecular switches to regulate direction of traffic (retrograde vs anterograde). An example of such is the mitochondrial Rho GTPase, named Miro, which has the ability to switch from dynein-dependent retrograde trafficking to kinesin-dependent anterograde trafficking and vice versa, depending on Ca²⁺ signals binding to the EF-hands of Miro (Tang, 2015). Whether Ca²⁺ binding plays a role in Rab46 trafficking dynamics and potential interaction with the motor protein kinesin remains to be established in future studies following this project.

Nonetheless, the Ca²⁺-independent retrograde trafficking of Rab46-positive WPBs I have described is a crucial difference between other observations in the literature that may reflect differences in the physiology between ECs and T cells. For example, in T cells, upon TCR activation the MTOC traffics to the immunological synapse, and Srikanth and colleagues have shown that Rab46 has an important role in this trafficking that is necessary for downstream activation of the JNK pathway (Srikanth et al., 2016). Additionally, our lab has found that the endothelium expresses only Rab46, the long isoform of the EFCAB4B gene (previously named as cracr2a-a or CRACR2A-L), while T cells also express a short isoform (cracr2a-c: CRACR2A-S) that lacks the Rab domain. Another difference between Rab46 action in T cells and ECs is that in T cells both Rab46 and CRACR2A-S are necessary for regulating store-operated Ca²⁺ entry (SOCE) by means of dispersing Orai1 and Stim1 clusters below the plasma membrane (Srikanth et al., 2010; Srikanth et al., 2016). Previously, our lab has found that endothelial SOCE is unaffected by depletion of Rab46 with CRACR2A specific siRNA (Wilson et al., 2015).

A further key difference between the findings of this thesis and previous reports of Rab46 in T cells is that in T cells Rab46 localisation is notably different. Our lab has proposed that such a discrepancy may be due, at least in part, to the overexpression of Rab46 with a GFP tag (N-termini). Localisation of GFP-tagged

WT Rab46 is similar to Rab46^{EFmut}, particularly following prolonged transfection time points (24 hrs) which indicates that the GFP tag may be impairing binding of Ca²⁺ to the EF-hand domain of Rab46, thereby preventing effective trafficking of WT Rab46. This has proven to be a limiting factor in this project, and in essence excluded the use of this tag for observing Rab46 dynamics using live imaging techniques. A better tagged approach that may be used as a substitute to GFP is the SPOT-Tag stack system. The SPOT-Tag (12 amino acids) is much smaller than GFP and therefore is less likely to disrupt the native function of the Rab46 protein and binding of Ca²⁺ to the EF-hands. This tag system is also validated for super-resolution imaging methods such as dSTORM that may be used to precisely visualise Rab46 mechanisms (Virant et al., 2018).

Finally, it has been discussed thus far that histamine-induced retrograde trafficking of Rab46-positive WPBs towards the MTOC is independent of cAMP-PKA and Ca²⁺, while Ca²⁺ binding to the EF-hand of Rab46 is necessary for the dispersal of Rab46-positive WPBs from the MTOC. However, it is peculiar that despite the fact that H₁R is coupled to intracellular Ca²⁺ release, Ca²⁺ does not seem to be involved in the activation of Rab46 or its interaction with dynein on its way to the MTOC. PKC is a key mediator in the signalling pathway triggered by activation of G_{q/11} GPCRs such as H₁R. Direct activators of PKC such as PMA are potent agonists of WPB exocytosis, however inhibition of both Ca²⁺-dependent and -independent PKC isoforms do not affect histamine-induced WPB exocytosis, suggesting that PKC is not essential for this process (Lorenzi et al., 2008; Xiong et al., 2009). Similarly to PKA inhibition, in order to achieve effective block of PKC very high concentrations of broad spectrum PKC inhibitors are required which raises the risk of numerous off target effects and lack of meaningful results. PKC did not play a role in Rab46-dependent retrograde trafficking of WPBs in response to histamine when using specific PKC activators such as PMA, or with a broad spectrum PKC inhibitor bisindolylmaleimide BIM (data not shown). Rondaij and colleagues have shown that phosphatase inhibition by okadaic acid alone can trigger clustering of WPBs at the perinuclear area (Rondaij, Bierings, Kragt, Gijzen, et al., 2006). It is known that Rab GTPases are widely regulated by phosphorylation (Waschbüsch and Khan, 2020) and likely that there are currently unknown players in the histamine signalling pathway in the endothelium that are regulated by phosphorylation and are independent of PKC. A phosphoproteomic approach may be a suitable option to identify potential phosphorylation pathway clusters involved in the signalling that governs Rab46 activation, its interaction with dynein motor complex and subsequent retrograde trafficking to the MTOC in response to histamine. Additionally, bioinformatics tools that predict phosphorylation sites in a protein's structure could identify

potential phosphorylation sites on Rab46. This would provide more information on how Rab46 is activated and how such activation can be modulated.

The discussed findings reveal more about Rab46 mechanisms; Rab46-positive WPBs retrograde trafficking to the MTOC is independent of both cAMP and Ca^{2+} , however intracellular Ca^{2+} is needed for binding to the Rab46 Ca^{2+} -sensing EF-hand domain to trigger dispersal of WPBs from the MTOC. An important question remains; what are the mechanisms and what is the source of such Ca^{2+} signal?

7.3 Rab46 senses Ca^{2+} release from NAADP-sensitive Ca^{2+} stores

NAADP-induced Ca^{2+} release is a key player in multiple intracellular Ca^{2+} signalling pathways. Despite high research interest in the past two decades, the exact mechanisms of how NAADP evokes Ca^{2+} responses inside cells is yet unknown and is complicated by the fact that NAADP signalling pathways are cell type-specific. Previously, it has been reported that the TPCs are the NAADP receptor and Ca^{2+} release channel since TPC expression is essential for NAADP to trigger Ca^{2+} release from acidic Ca^{2+} stores such as the endo-lysosomes (Calcraft et al., 2009; Ruas et al., 2015). Due to its ubiquitous signalling function, there is still a lot to be uncovered about the exact mechanisms by which NAADP functions. There have been some initial reports of NAADP signalling in the endothelium (Brailoiu et al., 2010a; Esposito et al., 2011; Faviaa et al., 2014c). Esposito and colleagues showed that in the endothelial cell line EA.hy926, histamine operates via the H_1R and the receptor signalling is coupled to NAADP. However, the authors did not observe any NAADP involvement when the cells were treated with thrombin. I successfully confirmed and validated that in the endothelial model system used in this project, HUVECs, that the downstream signalling of the H_1R is indeed coupled to the Ca^{2+} -mobilising messenger, NAADP. Comparing the results with thrombin as a control, it became very clear that there are differences in the Ca^{2+} signatures evoked by different agonists. It also raised the possibility of an intermediate integrator of these signals in ECs, having the ability to recognise and deliver a specialised response when activated by specific stimuli.

The findings that have been presented in this thesis give rise to a hypothesis that Rab46, being an unusually large Rab GTPase that has the ability to sense intracellular Ca^{2+} , is a prime candidate to act as an integrator of NAADP-mobilised Ca^{2+} release in response to histamine. From previous investigation on Rab46 mutants, it is evident that activation of the GTPase domain of Rab46 activity drives the retrograde movement towards the MTOC located in the

perinuclear area, along with its interaction with the dynein motor complex (Miteva et al., 2019). Interestingly, in this thesis I have shown that mutation of the Ca^{2+} -sensing domain of Rab46, the EF-hands, renders Rab46-positive WPBs at the MTOC in the absence of histamine stimulation. This effect is enhanced the longer the EF-hand mutant is overexpressed, suggesting that Rab46 is anchored at the perinuclear area, or it is unable to disperse. Previously, the role of the short version of Rab46 in T cells, CRACR2A-S, is described to be responsible for the dispersal of the Orai1-Stim1 complex in SOCE (Srikanth et al., 2010). Above, I have shown that Ca^{2+} binding of the Rab46 EF-hand is needed in order for Rab46-positive WPBs to disperse from the MTOC. Given that endogenous Rab46 distribution in response to histamine triggers retrograde trafficking and H_1R signalling is coupled to NAADP, it raises the possibility that NAADP-mobilised Ca^{2+} release may be responsible for the dispersal of Rab46 from the MTOC, or lack thereof in high concentrations of histamine. Here, it is important to consider the nature of NAADP signalling in order to understand the proposed hypothesis. NAADP is a Ca^{2+} mobiliser that has a bell-shaped dose response curve and it has the unique properties to self-inhibit the release of Ca^{2+} from acidic Ca^{2+} stores (Berg et al., 2000). Moreover, H_1R agonism rapidly increases NAADP concentration in ECs after 5 minutes (Esposito et al., 2011), a timeframe that coincides with the observation of Rab46 and WPB clusters at the MTOC. Validation of this measurement in HUVECs in collaboration with Professor Antony Galione's lab was planned, but not possible due to time constraints and global circumstances during this project.

Considering all of the experimental findings in this thesis and knowledge from the literature outlined above, it is possible to speculate that the Rab46 and WPB clustering at the MTOC could be in fact due to NAADP self-inhibition. The higher the concentration of H_1R agonist, the higher the intracellular concentration of NAADP would be. Self-inhibition of high levels of NAADP would prevent the localised Ca^{2+} release events from the endo-lysosomal Ca^{2+} stores and Ca^{2+} binding to the EF-hand of Rab46, which in turn would prevent dispersal of the protein. Thus, Rab46-positive WPBs accumulate and remain located at the perinuclear area.

To experimentally challenge this hypothesis, I have used both low and high concentrations of histamine. When cells were treated with low concentrations of histamine accumulation of WPBs and Rab46 was not observed at the MTOC, and it is unclear whether the WPBs undergo active trafficking towards the PM to be released. However, when low concentrations of histamine were applied in conjunction with the NAADP antagonist, Ned19, Rab46-positive WPBs accumulated at the MTOC, indicating the possibility inhibition of Ca^{2+} release by

Ned19 has 'trapped' Rab46-positive WPBs at the MTOC. Therefore, it is plausible to suggest at this low but physiological concentration of histamine, WPBs traffic to the MTOC, where Ca^{2+} released from NAADP-sensitive stores binds to Rab46-positive WPBs disperse. Using higher concentrations of histamine, application of Ned19 didn't have an effect on Rab46 and WPB clustering at the perinuclear area which was reflected in the imaging analysis I used to quantify the distribution of Rab46 at the perinuclear region. More biological repeats and custom, more sensitive image analysis approaches are needed to further validate these preliminary observations. Furthermore, a beneficial complimentary experiment would be to test whether at prolonged histamine treatment the release of WPBs, or certain WPBs subpopulations, would be inhibited by subsequent application of Ned19.

In addition, I have described the first report of endogenous TPC1 localisation in ECs. Interestingly, endothelial TPC1 colocalises at the MTOC and upon stimulation with histamine WPBs accumulate at the MTOC and are orientated towards the channels itself. Preliminary immunoprecipitation, showed that TPC1 and Rab46 co-immunoprecipitate together. It can be speculated that such proximity between the organelles is sufficient for Ca^{2+} release and diffusion from the Ca^{2+} channels located at the lysosomes to reach and bind to Rab46 molecules located on the WPBs. Particularly because the findings in this thesis differ from previous reports of NAADP signalling in the endothelium where researchers described how TPC2 channel is involved in VEGF-mediated neoangiogenesis (Faviaa et al., 2014c) and histamine-induced vWF secretion (Esposito et al., 2011). The expression of both TPC1 and TPC2 in ECs raises the possibility that both channels are present and may have different functions in response to NAADP signalling; TPC2 promoting vWF secretion at the PM while Ca^{2+} from the TPC1 mediating dispersal of Rab46-positive WPBs from the MTOC. This is likely to be governed by their subcellular location, particularly due to the different localisation of TPC1 in ECs compared to other cell types (E. Brailoiu et al., 2009). Nonetheless, these preliminary findings described in this thesis require more experimental repeats and validation before any concrete conclusions are made. The antibody I have used for endogenous TPC1 localisation has to be further validated by TPC1 specific siRNA and antibody controls to control for non-specific binding to tubulin-enriched structures in the cell, for example measure antibody specificity to recombinant TPC1. Additionally, due to species cross-reactivity of the antibodies, colocalisation analysis for TPC1 and Rab46 via high resolution imaging was not established which can be established by either purchasing and validating separate species of antibodies or raising in-house made antibodies in future.

Above, I have proposed a hypothesis suggesting a role of Rab46 as a sensor of NAADP-sensitive Ca^{2+} microdomains. One of the biggest limitations of this project is the lack of live cell imaging data to support this hypothesis. Herein, I have quantified Rab46-positive WPB localisation via unbiased image analysis on Fiji, which analyses a large number of images (and therefore cells) and represents the normalised intensity of Rab46-positive WPBs at the MTOC. However, the analysis does not perform segmentation of clustered WPBs or odd-shaped ECs. More refined image analysis method is needed to account for that complexity. Additionally, super-resolution Ca^{2+} imaging techniques developed by a collaborator, Dr Izzy Jayasinghe, including dSTORM/TIRF, could be utilised to visualise true molecular resolution of highly localised Ca^{2+} release from NAADP-sensitive Ca^{2+} release channels at the perinuclear area needed to disperse Rab46, with the ability to image in different conditions (i.e. NAADP antagonism by Ned19). With a resolving power < 10 nm this technique can be used to quantify the distance between proteins and the likelihood of Ca^{2+} diffusion. Last but not least, this is evidence suggesting a mediator, or multiple mediators, that act as a NAADP binding protein, which in turn binds to TPCs thereby enabling Ca^{2+} release (Calcraft et al., 2009; Lin-Moshier et al., 2014). The existence of such a binding protein is also likely to be cell-type specific considering the range of NAADP functions in different cell types (Galione, 2015a). In preliminary Ca^{2+} measurements of Rab46-depleted HUVECs, I have observed a decrease in histamine-evoked intracellular Ca^{2+} release similar to NAADP inhibition using Ned19, suggesting the possibility of Rab46 as a mediator between NAADP and TPCs. Mapping the TPC interactome revealed that TPCs bind to an unknown Rab GTPase protein in order to release Ca^{2+} (Lin-Moshier et al., 2014), however the exact details of how and why Rab46 would participate in Ca^{2+} release from acidic Ca^{2+} stores, remains unclear and it is beyond the scope of the project (see Future work). It is also important to establish correct controls and reagents for studying lysosomal Ca^{2+} in addition to GPN and nigericin that would enable for further visualisation of the interaction between Rab46 and lysosomal Ca^{2+} . Nonetheless, the findings discussed above present an opportunity for the discovery of new mechanisms and further our understanding of how ECs recognise and fine-tune their secretory signature (inflammation vs thrombosis) while simultaneously receiving a number of Ca^{2+} signals occurring within the cytoplasm.

Chapter 8 Final conclusions and future work

8.1 Summary of key findings

Rab46 (CRACR2A-L) is a novel Rab GTPase in the endothelium that colocalises with WPBs (Wilson et al., 2015; K. T. Miteva et al., 2019). This thesis displays findings revealing the role of Rab46 in differential WPB trafficking in response to acute pro-inflammatory stimulation. I have demonstrated for the first time that Rab46 resides in and labels a P-selectin–negative population of WPBs. Histamine, but not thrombin, activates Rab46 and triggers retrograde trafficking along the microtubules where Rab46 selectively diverts an Angiopoietin-2-2-positive WPB subpopulation, both accumulating at the MTOC. Being an unusually large Rab GTPase, Rab46 also contains an EF-hand that can bind and thus sense Ca^{2+} signals in the cytoplasm (Srikanth et al., 2010; Srikanth et al., 2016). I have shown that such histamine activation of Rab46 is independent of cAMP and Ca^{2+} . Instead, Ca^{2+} binding to the EF-hand of Rab46 is necessary for the dispersal of Rab46-positive WPBs from the MTOC. A key question remains regarding the functional significance of Rab46 and WPB dispersal. One possibility is that this coupling is a means of redirecting WPBs to prevent the secretion of functionally irrelevant cargo, but this will require further investigation.

Both thrombin and histamine trigger intracellular Ca^{2+} signals in ECs. Due to the ubiquitous nature of intracellular Ca^{2+} signalling, specificity of the cellular response to Ca^{2+} signals is achieved by spatio-temporal regulation and amplitude of the Ca^{2+} release, further complicated by the existence of several Ca^{2+} stores within the cell (e.g. ER, endo-lysosomes). The precise cellular localisation of histamine-stimulated Rab46 indicates the involvement of highly localised NAADP-sensitive Ca^{2+} signalling events, most likely released from endo-lysosomal cation channels. Preliminary data in this thesis also show a cross-talk between Rab46 and lysosomes, with Rab46 as a potential candidate for an NAADP binding partner facilitating Ca^{2+} release from NAADP target channels therein. Thus, Rab46 integrates both GTPase transport signals and Ca^{2+} signals to deliver an appropriate cellular response during acute pro-inflammatory stimulation by histamine.

8.2 Conclusion

The innate ability of ECs to be functional ‘multi-taskers’ requires the existence of well-coordinated intracellular response machinery which is able to respond rapidly and simultaneously to multiple physiologically distinct stimuli in the vascular environment. Multiple endothelial agonists signal via converging downstream pathways, however ECs expertly deliver agonist-specific functional

responses. WPBs are the 'vascular first aid kit' which pre-packages and rapidly releases an armour of bioactive cargo following stimulation, in order to fight vascular injury and aid the vasculature to return to homeostasis. The ability to store functionally distinct cargo (i.e haemostatic, inflammatory, angiogenic etc) suggests that WPB exocytosis needs tightly regulated molecular mechanisms to precisely deliver an appropriate functional response. Such mechanisms fundamental to endothelial function are to date not fully understood. Enhancing our understanding of the molecular mechanisms underlying differential release of WPB content upon different agonist stimulation is a key challenge which can have important consequences for clinical interventions. Limiting the risk of thrombosis whilst allowing normal immune responses could open previously unattainable new directions to cardiovascular diseases. All together the data in this thesis describe for the first time a fundamental mechanism that the endothelium is using a novel Rab GTPase, Rab46, to coordinate and couple signals from functionally distinct agonists to precise trafficking, and potentially exocytosis, of WPBs.

Herein, I present Rab46 as a stimulus-coupled regulator of differential WPB trafficking, providing an avenue for discovery of novel precise therapeutics targeting vascular pathophysiology.

8.3 Future work

The new findings in this project open many future avenues for research into the role and signalling pathway of Rab46 in endothelial cells. However, from the discussion of this thesis and clinical findings on CRACR2A, it is evident that Rab46 has the potential to be a crucial player not only in the vasculature, but also in the immune system, and fulfil different, cell-specific roles. Herein, I outline and propose several future work areas that need addressing to enable us to unveil more of Rab46's potential as a future therapeutic target.

8.3.1 Rab46 mechanisms

More work is needed to reveal the exact mechanisms of how Rab46 couples selective stimuli to trafficking of WPBs, and its relationship with NAADP signalling pathways. GTPase proteins are regulated by many effector proteins and Pedicini *et al.* (2021) has published preliminary proteomic results mapping some of the potential effector proteins (e.g. dynein, ATP1 α) of Rab46 (Pedicini *et al.*, 2021). More detailed, future studies will supplement our current knowledge and identify more Rab46 effectors by using other proteomic approaches (i.e. APEX, Mac-tag). Additionally, a method such as XL-MS that has recently been developed for application in native cellular environments may be a suitable option to identify further binding partners of Rab46 (Chan *et al.*, 2018). In order to study protein

interaction partners in live cells to which stimuli have been applied (i.e. histamine vs thrombin), crosslinking reagents could be added to cell cultures and subsequent proteolysis of cell lysates would result in highly complex peptide mixtures, which could be enriched by antibody-based recognition, trypsin digestion, ion-exchange chromatography and LC-MS/MS analysis to identify precise cross-linked partners and positions of cross-linking. However, identification of effectors and mapping the interactome is only the first step. Detailed characterisation has to be performed for each high confidence effector candidate. Previously performed immunoprecipitation assays by Lucia Pedicini to confirm the interaction of ATP1 α with Rab46, for example, however the functional consequence of such interaction remains unclear. Endogenous localisation and effects on WPB trafficking are yet to be confirmed.

In this thesis, I have shown that Rab46-dependent trafficking to the perinuclear area is independent of Ca²⁺, but the dispersal of Rab46-positive WPBs from the MTOC is dependent on Ca²⁺ binding to the EF-hand of Rab46. Moreover, I have shown that Rab46 has the potential to sense NAADP-sensitive Ca²⁺ pool release, likely from TPC1. It has been widely recognised and hypothesised that NAADP mobilises Ca²⁺ from TPCs via an NAADP binding protein, however the molecular identity of this protein to date remains unknown. Preliminary data collected during this project suggests that Rab46 may be interacting directly with TPC1 and this interaction may be responsible for the NAADP proportion of Ca²⁺ released by histamine (Figure 8.1). Proposing Rab46 as an NAADP binding protein involved in Ca²⁺ release from TPCs is an elusive hypothesis. Such interaction of Rab46 with NAADP is likely to be transient and there is a possibility that classical pull down methods are not sensitive enough to detect it. An attainable strategy that may deliver reliable results could be the use of in-gel photoaffinity labelling of NAADP binding and [³²P]-NAADP binding assay, both developed by Professor Antony Galione at the University of Oxford.

An important yet not fully addressed aspect of this project is whether the Rab46-NAADP-TPC axis is involved in differential exocytosis of WPBs. Biochemical assays (i.e. exocytosis measurements via ELISA, Western Blots) in addition to live imaging of WPB cargo (P-sel vs Angiopoietin-2) need to be conducted. There is no doubt that NAADP signalling is a key player in a plethora of physiological events in multiple cell types through NAADP-induced Ca²⁺ release. Therefore, it is likely that there are cell type specific binding partners of NAADP. It is imperative to establish in what other cell types, cellular pathways and target Ca²⁺ channels Rab46 and NAADP are partnering in the regulation of (i.e. immune cells).

Although this is the beginning of defining a novel Rab46 pathway in endothelial cells, future studies employing all the different approaches mentioned above will help to put together more pieces in puzzle of Rab46 mechanisms.

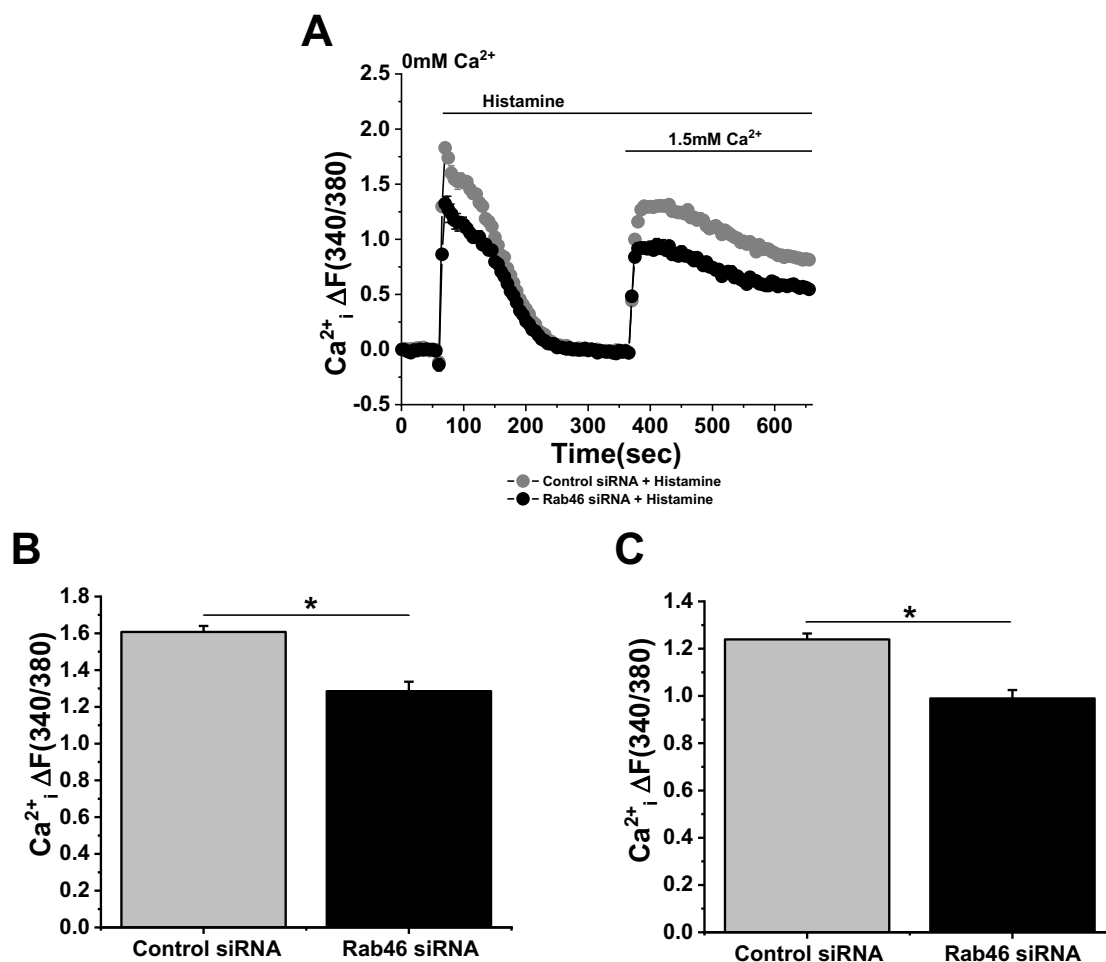


Figure 8.1 Rab46 depletion decreases Ca²⁺ release and entry in response to histamine.

(A) Representative trace of Ca²⁺ release and entry in HUVECs evoked by application of 30 μM histamine at 60 seconds and Ca²⁺ addback (7.5mM Ca²⁺ buffer) at 360 seconds. Rab46 was depleted using CRACR2A specific siRNA for 72 hours prior to Ca²⁺ measurements. Recordings were obtained in Ca²⁺-free buffer. (B), (C) Mean data of peak amplitude (B) Ca²⁺ release and (C) Ca²⁺ entry response (n/N=5/15, error bars represent SEM, *, p value <0.05 by Two-way ANOVA).

8.3.2 Structural studies

To date no structural studies have been performed on Rab46, however, work on the folding and dynamic properties of Rab46 have commenced. Rab GTPase undergo conformational changes during the GTPase cycle, therefore in order to evaluate such changes in Rab46, production of recombinant Rab46 and its domains would provide a useful tool. First of all, structural and conformational changes following GTP and GDP binding could be investigated by using high-resolution Nuclear Magnetic Resonance (NMR) spectroscopy. NMR studies could also be supplemented with IMS/MS and HDX-MS approaches to investigate longer-range conformational rearrangements in response to activating or inhibiting signals (e.g. nucleotide-bound status, Ca^{2+} concentration) and mutations with potential to perturb the function of Rab46. Importantly, the role of Ca^{2+} could be analysed by observing conformational changes induced by Ca^{2+} binding to the EF-hands of Rab46, the presence of a synergistic relationship between activity of the EF-hands and the GTPase domain could be determined. This would be important to establish whether Rab46 has the ability to use binding of those two signals as a switch for bidirectional traffic. Furthermore, a technique called isothermal titration calorimetry (ITC), in which the heat released or absorbed in a chemical reaction following injection of reactants is determined, would permit quantitative studies of ligand binding. This could be used to assess Ca^{2+} binding to Rab46 EF-hands over a range of physiological Ca^{2+} concentrations that occur during intracellular Ca^{2+} release in the cytoplasm. ITC would also decipher the Ca^{2+} binding affinity of Rab46 EF-hands. Homology modelling will be also used to identify residues crucial for the function of Rab46 and give rise to new, more specific experiments such as site-directed mutagenesis. Predicted binding-sites between Rab46 and potential interacting proteins would generate an interactome that could give more clues about different functions Rab46 may play in various systems in the body. Overall, Rab46 atomic structure would allow for identification of specific binding pockets that could serve as targets for small molecules in the search for novel therapies of cardiovascular and immune diseases.

8.3.3 Transgenic mice

The use of transgenic mouse technology is a standard research approach in virtually all fields of biology and provides the ability to not only model many human diseases but to study fundamental mechanisms in an integrated physiological system. There are several hundreds of transgenic lines with expression of foreign genes specifically targeted to desired organelles/cells/tissues that can enable the study of particular pathways. Further, the ability to spatio-temporally control

inactivation or activation of gene expression using the “Cre-lox” technology, or generating a CRISPR mouse model are both powerful approaches to understand fundamental mechanisms. To continue work following this project, endothelial cells, preferably from different vascular beds to account for endothelial heterogeneity and WPB plasticity, need to be isolated from Rab46 null mice to confirm and validate *ex vivo* that the findings described in this thesis occur endogenously, and further detail the functional role of Rab46 in the vasculature. The use of an endothelial-specific Rab46-knockout mouse model would be beneficial to distinguish the specific role of Rab46 in the secretion of WPB subpopulations *in vivo* and determine the effect on animal physiology as a whole. Furthermore, TPCs are the target channels for NAADP signalling and TPC1/TPC2 knockout mouse models can be used to further establish Rab46 as a sensor of NAADP-sensitive Ca^{2+} signalling. Finally, a challenge for this project has been the lack of an anti-Rab46 antibody which is able to sufficiently recognise Rab46 in murine cells or tissues for immunofluorescence assays. However, my supervisor Dr McKeown has initiated an affimer screening project which could be used for future imaging studies using murine *ex vivo* ECs and tissue samples.

List of References

- Aarhus, R., Dickey, D.M., Graeff, R.M., Gee, K.R., Walseth, T.F. and Lee, H.C. 1996. Activation and inactivation of Ca²⁺ release by NAADP⁺. *Journal of Biological Chemistry*. **271**(15), pp.8513–8516.
- Abdullaev, I.F., Bisailon, J.M., Potier, M., Gonzalez, J.C., Motiani, R.K. and Trebak, M. 2008. Stim1 and orai1 mediate crac currents and store-operated calcium entry important for endothelial cell proliferation. *Circulation Research*. **103**(11), pp.1289–1299.
- van Agtmaal, E.L., Bierings, R., Dragt, B.S., Leyen, T.A., Fernandez-Borja, M., Horrevoets, A.J.G. and Voorberg, J. 2012. The shear stress-induced transcription factor klf2 affects dynamics and angiopoietin-2 content of weibel-palade bodies P. H. Reitsma, ed. *PLoS ONE*. **7**(6), p.e38399.
- Aird, W.C. 2007. Phenotypic Heterogeneity of the Endothelium. *Circulation Research*. **100**(2), pp.158–173.
- Aird, W.C. 2005. Spatial and temporal dynamics of the endothelium. *Journal of Thrombosis and Haemostasis*. **3**(7), pp.1392–1406.
- Alevriadou, B.R., Shanmughapriya, S., Patel, A., Stathopoulos, P.B. and Madesh, M. 2017. Mitochondrial Ca²⁺ transport in the endothelium: Regulation by ions, redox signalling and mechanical forces. *Journal of the Royal Society Interface*. **14**(137).
- Altier, C. 2012. GPCR and voltage-gated calcium channels (VGCC) signaling complexes. *Subcellular Biochemistry*. **63**, pp.241–262.
- Ando, J. and Yamamoto, K. 2013. Flow detection and calcium signalling in vascular endothelial cells. *Cardiovascular Research*. **99**(2), pp.260–268.
- András, F. and Merétey, K. 1992. Histamine: an early messenger in inflammatory and immune reactions. *Immunology Today*. **13**(5), pp.154–156.
- Von Andrian, U.H., Chambers, J.D., McEvoy, L.M., Bargatze, R.F., Arfors, K.E. and Butcher, E.C. 1991. Two-step model of leukocyte-endothelial cell interaction in inflammation: Distinct roles for LE CAM-1 and the leukocyte β 2 integrins in vivo. *Proceedings of the National Academy of Sciences of the United States of America*. **88**(17), pp.7538–7542.
- Von Andrian, U.H., Hansell, P., Chambers, J.D., Berger, E.M., Filho, I.T., Butcher, E.C. and Arfors, K.E. 1992. L-selectin function is required for β 2-integrin-mediated neutrophil adhesion at physiological shear rates in vivo. *American Journal of Physiology - Heart and Circulatory Physiology*. **263**(4 32-4).
- Arribas, M. and Cutler, D.F. 2000. Weibel-palade body membrane proteins exhibit differential trafficking after exocytosis in endothelial cells. *Traffic*. **1**(10), pp.783–793.
- Atakpa, P., van Marrewijk, L.M., Apta-Smith, M., Chakraborty, S. and Taylor, C.W. 2019. GPN does not release lysosomal Ca²⁺, but evokes ER Ca²⁺ release by increasing cytosolic pH independent of cathepsin C. *Journal of Cell Science*. **132**(3).
- Atakpa, P., Thillaiappan, N.B., Mataragka, S., Prole, D.L. and Taylor, C.W.

2018. IP3 Receptors Preferentially Associate with ER-Lysosome Contact Sites and Selectively Deliver Ca²⁺ to Lysosomes. *Cell Reports*. **25**(11), pp.3180-3193.e7.
- Babich, V., Meli, A., Knipe, L., Dempster, J.E., Skehel, P., Hannah, M.J. and Carter, T. 2008. Selective release of molecules from Weibel-Palade bodies during a lingering kiss. *Blood*. **111**(11), pp.5282–5290.
- Barozzi, C., Galletti, M., Tomasi, L., De Fanti, S., Palazzini, M., Manes, A., Sazzini, M. and Galiè, N. 2019. A Combined Targeted and Whole Exome Sequencing Approach Identified Novel Candidate Genes Involved in Heritable Pulmonary Arterial Hypertension. *Scientific Reports*. **9**(1).
- Barr, F.A. 2013. Rab GTPases and membrane identity: Causal or inconsequential? *Journal of Cell Biology*. **202**(2), pp.191–199.
- Berg, I., Potter, B.V.L., Mayr, G.W. and Guse, A.H. 2000. Nicotinic acid adenine dinucleotide phosphate (NAADP⁺) is an essential regulator of T-lymphocyte CA²⁺-signaling. *Journal of Cell Biology*. **150**(3), pp.581–588.
- Berridge, M.J. 2002. The endoplasmic reticulum: A multifunctional signaling organelle. *Cell Calcium*. **32**(5–6), pp.235–249.
- Berridge, M.J., Bootman, M.D. and Roderick, H.L. 2003. Calcium signalling: Dynamics, homeostasis and remodelling. *Nature Reviews Molecular Cell Biology*. **4**(7), pp.517–529.
- Berridge, M.J., Lipp, P. and Bootman, M.D. 2000. The versatility and universality of calcium signalling. *Nature Reviews Molecular Cell Biology*. **1**(1), pp.11–21.
- Berriman, J.A., Li, S., Hewlett, L.J., Wasilewski, S., Kiskin, F.N., Carter, T., Hannah, M.J. and Rosenthal, P.B. 2009. *Structural organization of Weibel-Palade bodies revealed by cryo-EM of vitrified endothelial cells* [Online]. [Accessed 24 April 2019]. Available from: www.pnas.org/cgi/content/full/.
- Bers, D.M. and Morotti, S. 2014. Ca²⁺ current facilitation is CaMKII-dependent and has arrhythmogenic consequences. *Frontiers in Pharmacology*. **5**.
- Bevilacqua, L., Navarra, C.O., Pirastu, N., Lenarda, R. Di, Gasparini, P. and Robino, A. 2018. A genome-wide association study identifies an association between variants in EFCAB4B gene and periodontal disease in an Italian isolated population. *Journal of Periodontal Research*. **53**(6), pp.992–998.
- Bevilacqua, M.P., Pober, J.S., Mendrick, D.L., Cotran, R.S. and Gimbrone, M.A. 1987. Identification of an inducible endothelial-leukocyte adhesion molecule. *Proceedings of the National Academy of Sciences of the United States of America*. **84**(24), pp.9238–9242.
- Bhardwaj, R., Hediger, M.A. and Demaurex, N. 2016. Redox modulation of STIM-ORAI signaling. *Cell Calcium*. **60**(2), pp.142–152.
- Bierings, R., Hellen, N., Kiskin, N., Knipe, L., Fonseca, A.V., Patel, B., Meli, A., Rose, M., Hannah, M.J. and Carter, T. 2012. The interplay between the Rab27A effectors Slp4-a and MyRIP controls hormone-evoked Weibel-Palade body exocytosis. *Blood*. **120**(13), pp.2757–2767.
- Biesemann, A., Gorontzi, A., Barr, F. and Gerke, V. 2017. Rab35 protein regulates evoked exocytosis of endothelial Weibel–Palade bodies. *Journal*

of Biological Chemistry. **292**(28), pp.11631–11640.

- Birch, K.A., Poher, J.S., Zavoico, G.B., Means, A.R. and Ewenstein, B.M. 1992. Calcium/calmodulin transduces thrombin-stimulated secretion: Studies in intact and minimally permeabilized human umbilical vein endothelial cells. *Journal of Cell Biology*. **118**(6), pp.1501–1510.
- Bishara, N.B. and Ding, H. 2010. Glucose enhances expression of TRPC1 and calcium entry in endothelial cells. *American Journal of Physiology - Heart and Circulatory Physiology*. **298**(1).
- Bkaily, G., D'Orléans-Juste, P., Naik, R., Pérodin, J., Stankova, J., Abdulnour, E. and Rola-Pleszczynski, M. 1993. PAF activation of a voltage-gated R-type Ca²⁺ channel in human and canine aortic endothelial cells. *British Journal of Pharmacology*. **110**(2), pp.519–520.
- Blatter, L.A., Taha, Z., Mesaros, S., Shacklock, P.S., Wier, W.G. and Malinski, T. 1995. Simultaneous measurements of Ca²⁺ and nitric oxide in bradykinin-stimulated vascular endothelial cells. *Circulation Research*. **76**(5), pp.922–924.
- Bootman, M.D., Fearnley, C., Smyrniak, I., MacDonald, F. and Roderick, H.L. 2009. An update on nuclear calcium signalling. *Journal of Cell Science*. **122**(14), pp.2337–2350.
- Bossu, J.L., Elhamedani, A. and Feltz, A. 1992. Voltage-dependent calcium entry in confluent bovine capillary endothelial cells. *FEBS Letters*. **299**(3), pp.239–242.
- Bossu, J.L., Elhamedani, A., Feltz, A., Tanzi, F., Aunis, D. and Thierse, D. 1992. Voltage-gated Ca entry in isolated bovine capillary endothelial cells: evidence of a new type of BAY K 8644-sensitive channel. *Pflügers Archiv European Journal of Physiology*. **420**(2), pp.200–207.
- Bossu, J.L., Feltz, A., Rodeau, J.L. and Tanzi, F. 1989. Voltage-dependent transient calcium currents in freshly dissociated capillary endothelial cells. *FEBS Letters*. **255**(2), pp.377–380.
- Boulpaep, E., Boron, W., Caplan, M., Cantley, L., Igarashi, P., Aronson, P. and Moczydlowski, E. 2009. Medical Physiology a Cellular and Molecular Approach. *Signal Transduct*. **48**, p.27.
- Brailoiu, E., Churamani, D., Cai, X., Schrlau, M.G., Brailoiu, G.C., Gao, X., Hooper, R., Boulware, M.J., Dun, N.J., Marchant, J.S. and Patel, S. 2009. Essential requirement for two-pore channel 1 in NAADP-mediated calcium signaling. *Journal of Cell Biology*. **186**(2), pp.201–209.
- Brailoiu, G.C. and Brailoiu, E. 2016. Modulation of calcium entry by the endo-lysosomal system. *Advances in Experimental Medicine and Biology*. **898**, pp.423–447.
- Brailoiu, G.C., Brailoiu, E., Parkesh, R., Galione, A., Churchill, G.C., Patel, S. and Dun, N.J. 2009. NAADP-mediated channel 'chatter' in neurons of the rat medulla oblongata. *Biochemical Journal*. **419**(1), pp.91–97.
- Brailoiu, G.C., Gurzu, B., Gao, X., Parkesh, R., Aley, P.K., Trifa, D.I., Galione, A., Dun, N.J., Madesh, M., Patel, S., Churchill, G.C. and Brailoiu, E. 2010a. Acidic NAADP-sensitive calcium stores in the endothelium: Agonist-specific recruitment and role in regulating blood pressure. *Journal of Biological*

Chemistry. **285**(48), pp.37133–37137.

- Brailoiu, G.C., Gurzu, B., Gao, X., Parkesh, R., Aley, P.K., Trifa, D.I., Galione, A., Dun, N.J., Madesh, M., Patel, S., Churchill, G.C. and Brailoiu, E. 2010b. Acidic NAADP-sensitive calcium stores in the endothelium: Agonist-specific recruitment and role in regulating blood pressure. *Journal of Biological Chemistry*. **285**(48), pp.37133–37137.
- Brandherm, I., Disse, J., Zeuschner, D. and Gerke, V. 2013. cAMP-induced secretion of endothelial von Willebrand factor is regulated by a phosphorylation/dephosphorylation switch in annexin A2. *Blood*. **122**(6), pp.1042–1051.
- Braun, A.P. 2014. Some assembly required: SOCE and Orai1 channels couple to NFAT transcriptional activity via calmodulin and calcineurin. *Channels*. **8**(5), pp.383–384.
- Van Breevoort, D., Van Agtmaal, E.L., Dragt, B.S., Gebbinck, J.K., Dienava-Verdoold, I., Kragt, A., Bierings, R., Horrevoets, A.J.G., Valentijn, K.M., Eikenboom, J.C., Fernandez-Borja, M., Meijer, A.B. and Voorberg, J. 2012. Proteomic screen identifies IGFBP7 as a novel component of endothelial cell-specific weibel-palade bodies. *Journal of Proteome Research*. **11**(5), pp.2925–2936.
- Brette, F., Leroy, J., Le Guennec, J.Y. and Sallé, L. 2006. Ca²⁺ currents in cardiac myocytes: Old story, new insights. *Progress in Biophysics and Molecular Biology*. **91**(1–2), pp.1–82.
- Bryantseva, S.A. and Zhapparova, O.N. 2012. Bidirectional transport of organelles: unity and struggle of opposing motors. *Cell Biology International*. **36**(1), pp.1–6.
- Burns, A.R., Bowden, R.A., Abe, Y., Walker, D.C., Simon, S.I., Entman, M.L. and Smith, C.W. 1999. P-selectin mediates neutrophil adhesion to endothelial cell borders. *Journal of Leukocyte Biology*. **65**(3), pp.299–306.
- Cai, X. and Patel, S. 2010. Degeneration of an intracellular ion channel in the primate lineage by relaxation of selective constraints. *Molecular Biology and Evolution*. **27**(10), pp.2352–2359.
- Calcraft, P.J., Ruas, M., Pan, Z., Cheng, X., Arredouani, A., Hao, X., Tang, J., Rietdorf, K., Teboul, L., Chuang, K.T., Lin, P., Xiao, R., Wang, C., Zhu, Y., Lin, Y., Wyatt, C.N., Parrington, J., Ma, J., Evans, A.M., Galione, A. and Zhu, M.X. 2009. NAADP mobilizes calcium from acidic organelles through two-pore channels. *Nature*. **459**(7246), pp.596–600.
- Cancela, J.M., Churchill, G.C. and Galione, A. 1999. Coordination of agonist-induced Ca²⁺-signalling patterns by NAADP in pancreatic acinar cells. *Nature*. **398**(6722), pp.74–76.
- Cang, C., Zhou, Y., Navarro, B., Seo, Y.J., Aranda, K., Shi, L., Battaglia-Hsu, S., Nissim, I., Clapham, D.E. and Ren, D. 2013. MTOR regulates lysosomal ATP-sensitive two-pore Na⁺ channels to adapt to metabolic state. *Cell*. **152**(4), pp.778–790.
- Cao, S., Anishkin, A., Zinkevich, N.S., Nishijima, Y., Korishettar, A., Wang, Z., Fang, J., Wilcox, D.A. and Zhang, D.X. 2018. Transient receptor potential vanilloid 4 (TRPV4) activation by arachidonic acid requires protein kinase A-mediated phosphorylation. *Journal of Biological Chemistry*. **293**(14),

pp.5307–5322.

- Capiod, T. 2011. Cell proliferation, calcium influx and calcium channels. *Biochimie*. **93**(12), pp.2075–2079.
- Carter, T.D. and Ogden, D. 1997. Kinetics of Ca²⁺ release by InsP₃, in pig single aortic endothelial cells: Evidence for an inhibitory role of cytosolic Ca²⁺ in regulating hormonally evoked Ca²⁺ spikes. *Journal of Physiology*. **504**(1), pp.17–33.
- Catterall, W.A. 2011. Voltage-gated calcium channels. *Cold Spring Harbor Perspectives in Biology*. **3**(8), pp.1–23.
- Chan, J.M.S., Monaco, C., Wylezinska-Arridge, M., Tremoleda, J.L., Cole, J.E., Goddard, M., Cheung, M.S.H., Bhakoo, K.K. and Gibbs, R.G.J. 2018. Imaging vulnerable plaques by targeting inflammation in atherosclerosis using fluorescent-labeled dual-ligand microparticles of iron oxide and magnetic resonance imaging. *Journal of Vascular Surgery*. **67**(5), pp.1571-1583.e3.
- Chehab, T., Santos, N.C., Holthenrich, A., Koerdt, S.N., Disse, J., Schubert, C., Nazmi, A.R., Neeft, M., Koch, H., Man, K.N.M., Wojcik, S.M., Martin, T.F.J., Van Der Sluijs, P., Brose, N. and Gerke, V. 2017. A novel Munc13-4/S100A10/annexin A2 complex promotes Weibel-Palade body exocytosis in endothelial cells. *Molecular Biology of the Cell*. **28**(12), pp.1688–1700.
- Chi, J.T., Chang, H.Y., Haraldsen, G., Jahnsen, F.L., Troyanskaya, O.G., Chang, D.S., Wang, Z., Rockson, S.G., Van De Rijn, M., Botstein, D. and Brown, P.O. 2003. Endothelial cell diversity revealed by global expression profiling. *Proceedings of the National Academy of Sciences of the United States of America*. **100**(19), pp.10623–10628.
- Chistiakov, D.A., Orekhov, A.N. and Bobryshev, Y. V. 2017. Effects of shear stress on endothelial cells: go with the flow. *Acta Physiologica*. **219**(2), pp.382–408.
- Chu, Y.X., Fioravante, D., Leitges, M. and Regehr, W.G. 2014. Calcium-Dependent PKC Isoforms Have Specialized Roles in Short-Term Synaptic Plasticity. *Neuron*. **82**(4), pp.859–871.
- Churchill, G.C., Okada, Y., Thomas, J.M., Genazzani, A.A., Patel, S. and Galione, A. 2002. NAADP mobilizes Ca²⁺ from reserve granules, lysosome-related organelles, in sea urchin eggs. *Cell*. **111**(5), pp.703–708.
- Clapham, D.E. 2007. Calcium Signaling. *Cell*. **131**(6), pp.1047–1058.
- Cleator, J.H., Zhu, W.Q., Vaughan, D.E. and Hamm, H.E. 2006. Differential regulation of endothelial exocytosis of P-selectin and von Willebrand factor by protease-activated receptors and cAMP. *Blood*. **107**(7), pp.2736–2744.
- Colicelli, J. 2004. Human RAS superfamily proteins and related GTPases. *Science's STKE : signal transduction knowledge environment*. **2004**(250).
- Conte, I.L., Hellen, N., Bierings, R., Mashanov, G.I., Manneville, J.B., Kiskin, N.I., Hannah, M.J., Molloy, J.E. and Carter, T. 2016. Interaction between MyRIP and the actin cytoskeleton regulates Weibel-Palade body trafficking and exocytosis. *Journal of Cell Science*. **129**(3), pp.592–603.
- Cooke, J.P. 2000. The endothelium: A new target for therapy. *Vascular Medicine*. **5**(1), pp.49–53.

- Cramer, E.M., Meyer, D., Le Menn, R. and Breton-Gorius, J. 1985. Eccentric localization of von Willebrand factor in an internal structure of platelet α -granule resembling that of Weibel-Palade bodies. *Blood*. **66**(3), pp.710–713.
- Cutler, D.F. 2002. Introduction: Lysosome-related organelles. *Seminars in Cell and Developmental Biology*. **13**(4), pp.261–262.
- Dargan, S.L. and Parker, I. 2003. Buffer kinetics shape the spatiotemporal patterns of IP₃-evoked Ca²⁺ signals. *Journal of Physiology*. **553**(3), pp.775–788.
- Davies, S.P., Reddy, H., Caivano, M. and Cohen, P. 2000. Specificity and mechanism of action of some commonly used protein kinase inhibitors. *Biochemical Journal*. **351**(1), pp.95–105.
- Davis, L.C., Morgan, A.J., Chen, J.L., Snead, C.M., Bloor-Young, D., Shenderov, E., Stanton-Humphreys, M.N., Conway, S.J., Churchill, G.C., Parrington, J., Cerundolo, V. and Galione, A. 2012. NAADP Activates two-pore channels on t cell cytolytic granules to stimulate exocytosis and killing. *Current Biology*. **22**(24), pp.2331–2337.
- Davis, L.C., Morgan, A.J. and Galione, A. 2020a. NAADP -regulated two-pore channels drive phagocytosis through endo-lysosomal Ca²⁺ nanodomains, calcineurin and dynamin . *The EMBO Journal*. **39**(14).
- Davis, L.C., Morgan, A.J. and Galione, A. 2020b. NAADP -regulated two-pore channels drive phagocytosis through endo-lysosomal Ca²⁺ nanodomains, calcineurin and dynamin . *The EMBO Journal*. **39**(14).
- Dedkova, E.N. and Blatter, L.A. 2002. Nitric oxide inhibits capcitative Ca²⁺ entry and enhances endoplasmic reticulum Ca²⁺ uptake in bovine vascular endothelial cells. *Journal of Physiology*. **539**(1), pp.77–91.
- Delprato, A., Merithew, E. and Lambright, D.G. 2004. Structure, exchange determinants, and family-wide Rab specificity of the tandem helical bundle and Vps9 domains of Rabex-5. *Cell*. **118**(5), pp.607–617.
- Denis, C., Methia, N., Frenette, P.S., Rayburn, H., Ullman-Culleré, M., Hynes, R.O. and Wagner, D.D. 1998. A mouse model of severe von Willebrand disease: Defects in hemostasis and thrombosis. *Proceedings of the National Academy of Sciences of the United States of America*. **95**(16), pp.9524–9529.
- Denis, C. V., André, P., Saffaripour, S. and Wagner, D.D. 2001. Defect in regulated secretion of P-selectin affects leukocyte recruitment in von Willebrand factor-deficient mice. *Proceedings of the National Academy of Sciences of the United States of America*. **98**(7), pp.4072–4077.
- Detmers, P.A., Lo, S.K., Olsen-Egbert, E., Walz, A., Baggiolini, M. and Cohn, Z.A. 1990. Neutrophil-activating protein 1/interleukin 8 stimulates the binding activity of the leukocyte adhesion receptor CD11B/CD18 on human neutrophils. *Journal of Experimental Medicine*. **171**(4), pp.1155–1162.
- Doyle, E.L., Ridger, V., Ferraro, F., Turmaine, M., Saftig, P. and Cutler, D.F. 2011. CD63 is an essential cofactor to leukocyte recruitment by endothelial P-selectin. *Blood*. **118**(15), pp.4265–4273.
- Dubois, C., Prevarskaya, N. and Vanden Abeele, F. 2016. The calcium-

- signaling toolkit: Updates needed. *Biochimica et Biophysica Acta - Molecular Cell Research*. **1863**(6), pp.1337–1343.
- Duchen, M.R. 2004. Mitochondria in health and disease: Perspectives on a new mitochondrial biology. *Molecular Aspects of Medicine*. **25**(4), pp.365–451.
- Earley, S. and Brayden, J.E. 2015. Transient receptor potential channels in the vasculature. *Physiological Reviews*. **95**(2), pp.645–690.
- Echevarria, W., Leite, M.F., Guerra, M.T., Zipfel, W.R. and Nathanson, M.H. 2003. Regulation of calcium signals in the nucleus by a nucleoplasmic reticulum. *Nature Cell Biology*. **5**(5), pp.440–446.
- Eikenboom, J.C.J., Ploos van Amstel, H.K., Reitsma, P.H. and Briet, E. 1992. Mutations in severe, type III von Willebrand's disease in the Dutch population: Candidate missense and nonsense mutations associated with reduced levels of von Willebrand factor messenger RNA. *Thrombosis and Haemostasis*. **68**(4), pp.448–454.
- Erent, M., Meli, A., Moiso, N., Babich, V., Hannah, M.J., Skehel, P., Knipe, L., Zupančič, G., Ogden, D. and Carter, T. 2007a. Rate, extent and concentration dependence of histamine-evoked Weibel-Palade body exocytosis determined from individual fusion events in human endothelial cells. *Journal of Physiology*. **583**(1), pp.195–212.
- Erent, M., Meli, A., Moiso, N., Babich, V., Hannah, M.J., Skehel, P., Knipe, L., Zupančič, G., Ogden, D. and Carter, T. 2007b. Rate, extent and concentration dependence of histamine-evoked Weibel-Palade body exocytosis determined from individual fusion events in human endothelial cells. *Journal of Physiology*. **583**(1), pp.195–212.
- Erent, M., Meli, A., Moiso, N., Babich, V., Hannah, M.J., Skehel, P., Knipe, L., Zupančič, G., Ogden, D. and Carter, T. 2007c. Rate, extent and concentration dependence of histamine-evoked Weibel-Palade body exocytosis determined from individual fusion events in human endothelial cells. *Journal of Physiology*. **583**(1), pp.195–212.
- Ertel, E.A., Campbell, K.P., Harpold, M.M., Hofmann, F., Mori, Y., Perez-Reyes, E., Schwartz, A., Snutch, T.P., Tanabe, T., Birnbaumer, L., Tsien, R.W. and Catterall, W.A. 2000. Nomenclature of voltage-gated calcium channels. *Neuron*. **25**(3), pp.533–535.
- Escola, J.M., Kleijmeer, M.J., Stoorvogel, W., Griffith, J.M., Yoshie, O. and Geuze, H.J. 1998. Selective enrichment of tetraspan proteins on the internal vesicles of multivesicular endosomes and on exosomes secreted by human B-lymphocytes. *Journal of Biological Chemistry*. **273**(32), pp.20121–20127.
- Esposito, B., Gambarà, G., Lewis, A.M., Palombi, F., D'Alessio, A., Taylor, L.X., Genazzani, A.A., Ziparo, E., Galione, A., Churchill, G.C. and Filippini, A. 2011. NAADP links histamine H1 receptors to secretion of von Willebrand factor in human endothelial cells. *Blood*. **117**(18), pp.4968–4977.
- Fan, M., Wang, X., Peng, X., Feng, S., Zhao, J., Liao, L., Zhang, Y., Hou, Y. and Liu, J. 2020. Prognostic value of plasma von Willebrand factor levels in major adverse cardiovascular events: A systematic review and meta-analysis. *BMC Cardiovascular Disorders*. **20**(1).
- Favaloro, E.J. 2001. Appropriate laboratory assessment as a critical facet in the

- proper diagnosis and classification of von Willebrand disorder. *Best Practice and Research: Clinical Haematology*. **14**(2), pp.299–319.
- Faviaa, A., Desiderib, M., Gambaraa, G., D'Alessioa, A., Ruas, M., Esposito, B., Bufalo, D. Del, Parrington, J., Ziparoa, E., Palombia, F., Galioned, A. and Filippini, A. 2014a. VEGF-induced neoangiogenesis is mediated by NAADP and two-pore channel-2 -dependent ca^{2+} signaling. *Proceedings of the National Academy of Sciences of the United States of America*. **111**(44), pp.4706–4715.
- Faviaa, A., Desiderib, M., Gambaraa, G., D'Alessioa, A., Ruas, M., Esposito, B., Bufalo, D. Del, Parrington, J., Ziparoa, E., Palombia, F., Galioned, A. and Filippini, A. 2014b. VEGF-induced neoangiogenesis is mediated by NAADP and two-pore channel-2 -dependent ca^{2+} signaling. *Proceedings of the National Academy of Sciences of the United States of America*. **111**(44), pp.4706–4715.
- Faviaa, A., Desiderib, M., Gambaraa, G., D'Alessioa, A., Ruas, M., Esposito, B., Bufalo, D. Del, Parrington, J., Ziparoa, E., Palombia, F., Galioned, A. and Filippini, A. 2014c. VEGF-induced neoangiogenesis is mediated by NAADP and two-pore channel-2 -dependent ca^{2+} signaling. *Proceedings of the National Academy of Sciences of the United States of America*. **111**(44), pp.4706–4715.
- Ferraro, F., Kriston-Vizi, J., Metcalf, D.J., Martin-Martin, B., Freeman, J., Burden, J.J., Westmoreland, D., Dyer, C.E., Knight, A.E., Ketteler, R. and Cutler, D.F. 2014. A two-tier golgi-based control of organelle size underpins the functional plasticity of endothelial cells. *Developmental Cell*. **29**(3), pp.292–304.
- Feske, S. 2010. CRAC channelopathies. *Pflugers Archiv European Journal of Physiology*. **460**(2), pp.417–435.
- Feske, S., Gwack, Y., Prakriya, M., Srikanth, S., Puppel, S.H., Tanasa, B., Hogan, P.G., Lewis, R.S., Daly, M. and Rao, A. 2006. A mutation in Orai1 causes immune deficiency by abrogating CRAC channel function. *Nature*. **441**(7090), pp.179–185.
- Fiedler, U., Reiss, Y., Scharpfenecker, M., Grunow, V., Koidl, S., Thurston, G., Gale, N.W., Witzgenrath, M., Rosseau, S., Suttorp, N., Sobke, A., Herrmann, M., Preissner, K.T., Vajkoczy, P. and Augustin, H.G. 2006. Angiopoietin-2 sensitizes endothelial cells to TNF- α and has a crucial role in the induction of inflammation. *Nature Medicine*. **12**(2), pp.235–239.
- Fiedler, U., Scharpfenecker, M., Koidl, S., Hegen, A., Grunow, V., Schmidt, J.M., Kriz, W., Thurston, G. and Augustin, H.G. 2004a. The Tie-2 ligand Angiopoietin-2 is stored in and rapidly released upon stimulation from endothelial cell Weibel-Palade bodies. *Blood*. **103**(11), pp.4150–4156.
- Fiedler, U., Scharpfenecker, M., Koidl, S., Hegen, A., Grunow, V., Schmidt, J.M., Kriz, W., Thurston, G. and Augustin, H.G. 2004b. The Tie-2 ligand Angiopoietin-2 is stored in and rapidly released upon stimulation from endothelial cell Weibel-Palade bodies. *Blood*. **103**(11), pp.4150–4156.
- Finkel, T., Menazza, S., Holmström, K.M., Parks, R.J., Liu, Julia, Sun, J., Liu, Jie, Pan, X. and Murphy, E. 2015. The ins and outs of mitochondrial calcium. *Circulation Research*. **116**(11), pp.1810–1819.

- Fishman, A.P. 1982. Endothelium: a Distributed Organ of Diverse Capabilities. *Annals of the New York Academy of Sciences*. **401**(1), pp.1–8.
- Fitzsimons, C.P., Monczor, F., Fernández, N., Shayo, C. and Davio, C. 2004. Mepyramine, a histamine H1 receptor inverse agonist, binds preferentially to a G protein-coupled form of the receptor and sequesters G protein. *Journal of Biological Chemistry*. **279**(33), pp.34431–34439.
- Franchini, M. and Lippi, G. 2007a. Acquired von Willebrand syndrome: An update. *American Journal of Hematology*. **82**(5), pp.368–375.
- Franchini, M. and Lippi, G. 2007b. The role of von Willebrand factor in hemorrhagic and thrombotic disorders. *Critical Reviews in Clinical Laboratory Sciences*. **44**(2), pp.115–149.
- Fukuda, M. 1991. Lysosomal membrane glycoproteins: Structure, biosynthesis, and intracellular trafficking. *Journal of Biological Chemistry*. **266**(32), pp.21327–21330.
- Furchgott, R.F. and Zawadzki, J. V. 1980. The obligatory role of endothelial cells in the relaxation of arterial smooth muscle by acetylcholine. *Nature*. **288**(5789), pp.373–376.
- Gabe Lee, M.T., Mishra, A. and Lambright, D.G. 2009. Structural mechanisms for regulation of membrane traffic by Rab GTPases. *Traffic*. **10**(10), pp.1377–1389.
- Gale, A.J. 2011. Continuing Education Course #2: Current Understanding of Hemostasis. *Toxicologic Pathology*. **39**(1), pp.273–280.
- Galione, A. 2015a. A primer of NAADP-mediated Ca²⁺ signalling: From sea urchin eggs to mammalian cells. *Cell Calcium*. **58**(1), pp.27–47.
- Galione, A. 2015b. A primer of NAADP-mediated Ca²⁺ signalling: From sea urchin eggs to mammalian cells. *Cell Calcium*. **58**(1), pp.27–47.
- Galione, A. 2011. NAADP Receptors. *Cold Spring Harbor Perspectives in Biology*. **3**(1), pp.1–17.
- Galione, A. and Ruas, M. 2005. NAADP receptors. *Cell Calcium*. **38**(3-4 SPEC. ISS.), pp.273–280.
- Galley, H.F. and Webster, N.R. 2004. Physiology of the endothelium. *British Journal of Anaesthesia*. **93**(1), pp.105–113.
- Gantner, F., Sakai, K., Tusche, M.W., Cruikshank, W.W., Center, D.M. and Bacon, K.B. 2002. Histamine H4 and H2 receptors control histamine-induced interleukin-16 release from human CD8⁺ T cells. *Journal of Pharmacology and Experimental Therapeutics*. **303**(1), pp.300–307.
- Garrity, A.G., Wang, W., Collier, C.M.D., Levey, S.A., Gao, Q. and Xu, H. 2016. The endoplasmic reticulum, not the pH gradient, drives calcium refilling of lysosomes. *eLife*. **5**(MAY2016).
- Genazzani, A.A., Empson, R.M. and Galione, A. 1996. Unique inactivation properties of NAADP-sensitive Ca²⁺ release. *Journal of Biological Chemistry*. **271**(20), pp.11599–11602.
- Giblin, J.P., Hewlett, L.J. and Hannah, M.J. 2008. Basal secretion of von willebrand factor from human endothelial cells. *Blood*. **112**(4), pp.957–964.

- Gilbert, G., Courtois, A., Dubois, M., Cussac, L.A., Ducret, T., Lory, P., Marthan, R., Savineau, J.P. and Quignard, J.F. 2017. T-type voltage gated calcium channels are involved in endothelium-dependent relaxation of mice pulmonary artery. *Biochemical Pharmacology*. **138**, pp.61–72.
- Giorgi, C., Marchi, S. and Pinton, P. 2018. The machineries, regulation and cellular functions of mitochondrial calcium. *Nature Reviews Molecular Cell Biology*. **19**(11), pp.713–730.
- Goligorsky, M.S., Patschan, D. and Kuo, M.C. 2009. Weibel-Palade bodiessentinels of acute stress. *Nature Reviews Nephrology*. **5**(7), pp.423–426.
- Greif, D.M., Sacks, D.B. and Michel, T. 2004. Calmodulin phosphorylation and modulation of endothelial nitric oxide synthase catalysis. *Proceedings of the National Academy of Sciences of the United States of America*. **101**(5), pp.1165–1170.
- Griffiths, G.M. 1996. Secretory lysosomes - A special mechanism of regulated secretion in haemopoietic cells. *Trends in Cell Biology*. **6**(9), pp.329–332.
- Guadagno, N.A. and Progida, C. 2019. Rab GTPases: Switching to Human Diseases. *Cells*. **8**(8), p.909.
- Guibert, C. 2010. Editorial: Plasma membrane Ca²⁺-ATPase equals no NO. *Cardiovascular Research*. **87**(3), pp.401–402.
- Gunaratne, G.S., Yang, Y., Li, F., Walseth, T.F. and Marchant, J.S. 2018. NAADP-dependent Ca²⁺ signaling regulates Middle East respiratory syndrome-coronavirus pseudovirus translocation through the endolysosomal system. *Cell Calcium*. **75**, pp.30–41.
- Guo, J., Zeng, W., Chen, Q., Lee, C., Chen, L., Yang, Y., Cang, C., Ren, D. and Jiang, Y. 2016. Structure of the voltage-gated two-pore channel TPC1 from *Arabidopsis thaliana*. *Nature*. **531**(7593), pp.196–201.
- Guse, A.H. and Diercks, B.P. 2018. Integration of nicotinic acid adenine dinucleotide phosphate (NAADP)-dependent calcium signalling. *Journal of Physiology*. **596**(14), pp.2735–2743.
- Guse, A.H. and Wolf, I.M.A. 2016. Ca²⁺ microdomains, NAADP and type 1 ryanodine receptor in cell activation. *Biochimica et Biophysica Acta - Molecular Cell Research*. **1863**(6), pp.1379–1384.
- Gwack, Y., Feske, S., Srikanth, S., Hogan, P.G. and Rao, A. 2007. Signalling to transcription: Store-operated Ca²⁺ entry and NFAT activation in lymphocytes. *Cell Calcium*. **42**(2), pp.145–156.
- Haak, L.L., Song, L.S., Molinski, T.F., Pessah, I.N., Cheng, H. and Russell, J.T. 2001. Sparks and puffs in oligodendrocyte progenitors: Cross talk between ryanodine receptors and inositol trisphosphate receptors. *Journal of Neuroscience*. **21**(11), pp.3860–3870.
- Haas, A.K., Yoshimura, S.I., Stephens, D.J., Preisinger, C., Fuchs, E. and Barr, F.A. 2007. Analysis of GTPase-activating proteins: Rab1 and Rab43 are key Rabs required to maintain a functional Golgi complex in human cells. *Journal of Cell Science*. **120**(17), pp.2997–3010.
- Haas, H.L. and Panula, P. 2016. Histamine receptors. *Neuropharmacology*. **106**, pp.1–2.

- Haberichter, S.L., Merricks, E.P., Fahs, S.A., Christopherson, P.A., Nichols, T.C. and Montgomery, R.R. 2005. Re-establishment of VWF-dependent Weibel-Palade bodies in VWD endothelial cells. *Blood*. **105**(1), pp.145–152.
- Hallam, T.J., Pearson, J.D. and Needham, L.A. 1988. Thrombin-stimulated elevation of human endothelial-cell cytoplasmic free calcium concentration causes prostacyclin production. *Biochemical Journal*. **251**(1), pp.243–249.
- Halling, D.B., Liebeskind, B.J., Hall, A.W. and Aldrich, R.W. 2016. Conserved properties of individual Ca²⁺-binding sites in calmodulin. *Proceedings of the National Academy of Sciences of the United States of America*. **113**(9), pp.E1216–E1225.
- Hamilton, K.K. and Sims, P.J. 1987. Changes in cytosolic Ca²⁺ associated with von Willebrand factor release in human endothelial cells exposed to histamine. Study of microcarrier cell monolayers using the fluorescent probe indo-1. *Journal of Clinical Investigation*. **79**(2), pp.600–608.
- Hancock, W.O. 2014. Bidirectional cargo transport: Moving beyond tug of war. *Nature Reviews Molecular Cell Biology*. **15**(9), pp.615–628.
- Hannah, M.J., Hume, A.N., Arribas, M., Williams, R., Hewlett, L.J., Seabra, M.C. and Cutler, D.F. 2003. Weibel-Palade bodies recruit Rab27 by a content-driven, maturation-dependent mechanism that is independent of cell type. *Journal of Cell Science*. **116**(19), pp.3939–3948.
- Harrison-Lavoie, K.J., Michaux, G., Hewlett, L., Kaur, J., Hannah, M.J., Lui-Roberts, W.W.Y., Norman, K.E. and Cutler, D.F. 2006. P-selectin and CD63 use different mechanisms for delivery to Weibel-Palade bodies. *Traffic*. **7**(6), pp.647–662.
- Hendrickx, J., Doggen, K., Weinberg, E.O., Van Tongelen, P., Fransen, P. and De Keulenaer, G.W. 2005. Molecular diversity of cardiac endothelial cells in vitro and in vivo. *Physiological Genomics*. **19**, pp.198–206.
- Herrmann, J. and Lerman, A. 2001. The endothelium: Dysfunction and beyond. *Journal of Nuclear Cardiology*. **8**(2), pp.197–206.
- Himmel, H.M., Whorton, A.R. and Strauss, H.C. 1993. Intracellular calcium, currents, and stimulus-response coupling in endothelial cells. *Hypertension*. **21**(1), pp.112–127.
- Van Hinsbergh, V.W.M. 2001. The endothelium: vascular control of haemostasis. *European Journal of Obstetrics and Gynecology and Reproductive Biology*. **95**(2), pp.198–201.
- Hirakawa, S., Hong, Y.K., Harvey, N., Schacht, V., Matsuda, K., Libermann, T. and Detmar, M. 2003. Identification of vascular lineage-specific genes by transcriptional profiling of isolated blood vascular and lymphatic endothelial cells. *American Journal of Pathology*. **162**(2), pp.575–586.
- Hogan, P.G. and Rao, A. 2015. Store-operated calcium entry: Mechanisms and modulation. *Biochemical and Biophysical Research Communications*. **460**(1), pp.40–49.
- Hol, J., K uchler, A.M., Johansen, F.E., Dalhus, B., Haraldsen, G. and  ynebr aten, I. 2009. Molecular requirements for sorting of the chemokine interleukin-8/CXCL8 to endothelial Weibel-Palade bodies. *Journal of*

Biological Chemistry. **284**(35), pp.23532–23539.

- Holthenrich, A., Drexler, H.C.A., Chehab, T., Naß, J. and Gerke, V. 2019. Proximity proteomics of endothelial Weibel-Palade bodies identifies novel regulator of von Willebrand factor secretion. *Blood*. **134**(12), pp.979–982.
- Hon Cheung Lee and Aarhus, R. 1995. A derivative of NADP mobilizes calcium stores insensitive to inositol trisphosphate and cyclic ADP-ribose. *Journal of Biological Chemistry*. **270**(5), pp.2152–2157.
- Hoogduijn, M.J., Smit, N.P., Van Der Laarse, A., Van Nieuwpoort, A.F., Wood, J.M. and Thody, A.J. 2003. Melanin has a role in Ca²⁺ homeostasis in human melanocytes. *Pigment Cell Research*. **16**(2), pp.127–132.
- Hooper, R., Churamani, D., Davidson, S.M., Lin-Moshier, Y., Walseth, T.F., Patel, S. and Marchant, J.S. 2015. TPC1 Knockout Knocks Out TPC1. *Molecular and Cellular Biology*. **35**(10), pp.1882–1883.
- Van Hooren, K.W.E.M., Van Agtmaal, E.L., Fernandez-Borja, M., Van Mourik, J.A., Voorberg, J. and Bierings, R. 2012a. The Epac-Rap1 signaling pathway controls cAMP-mediated exocytosis of Weibel-Palade bodies in endothelial cells. *Journal of Biological Chemistry*. **287**(29), pp.24713–24720.
- Van Hooren, K.W.E.M., Van Agtmaal, E.L., Fernandez-Borja, M., Van Mourik, J.A., Voorberg, J. and Bierings, R. 2012b. The Epac-Rap1 signaling pathway controls cAMP-mediated exocytosis of Weibel-Palade bodies in endothelial cells. *Journal of Biological Chemistry*. **287**(29), pp.24713–24720.
- Hoth, M. and Penner, R. 1992. Depletion of intracellular calcium stores activates a calcium current in mast cells. *Nature*. **355**(6358), pp.353–356.
- Huang, H., Bhat, A., Woodnutt, G. and Lappe, R. 2010. Targeting the ANGPT-TIE2 pathway in malignancy. *Nature Reviews Cancer*. **10**(8), pp.575–585.
- Huang, K.P. 1989. The mechanism of protein kinase C activation. *Trends in Neurosciences*. **12**(11), pp.425–432.
- Hutagalung, A.H. and Novick, P.J. 2011. Role of Rab GTPases in membrane traffic and cell physiology. *Physiological Reviews*. **91**(1), pp.119–149.
- Huynh, W. and Vale, R.D. 2017. Disease-associated mutations in human BICD2 hyperactivate motility of dynein-dynactin. *Journal of Cell Biology*. **216**(10), pp.3051–3060.
- Ishibashi, K., Suzuki, M. and Imai, M. 2000. Molecular cloning of a novel form (two-repeat) protein related to voltage-gated sodium and calcium channels. *Biochemical and Biophysical Research Communications*. **270**(2), pp.370–376.
- James, P.D., Notley, C., Hegadorn, C., Leggo, J., Tuttle, A., Tinlin, S., Brown, C., Andrews, C., Labelle, A., Chirinian, Y., O'Brien, L., Othman, M., Rivard, G., Rapson, D., Hough, C. and Lillicrap, D. 2007. The mutational spectrum of type 1 von Willebrand disease: results from a Canadian cohort study. *Blood*. **109**(1), pp.145–154.
- Jha, A., Brailoiu, E. and Muallem, S. 2014. How does NAADP release lysosomal Ca²⁺? *Channels*. **8**(3), pp.174–175.

- Jilma-Stohlawetz, P., Gorczyca, M.E., Jilma, B., Siller-Matula, J., Gilbert, J.C. and Knöbl, P. 2011. Inhibition of von Willebrand factor by ARC1779 in patients with acute thrombotic thrombocytopenic purpura. *Thrombosis and Haemostasis*. **105**(3), pp.545–552.
- Jones, N., Iljin, K., Dumont, D.J. and Alitalo, K. 2001. Tie receptors: New modulators of angiogenic and lymphangiogenic responses. *Nature Reviews Molecular Cell Biology*. **2**(4), pp.257–267.
- Jung, D.W., Baysal, K. and Brierley, G.P. 1995. The sodium-calcium antiport of heart mitochondria is not electroneutral. *Journal of Biological Chemistry*. **270**(2), pp.672–678.
- Jutel, M., Blaser, K. and Akdis, C.A. 2005. Histamine in allergic inflammation and immune modulation. *International archives of allergy and immunology*. **137**(1), pp.82–92.
- Kadowaki, T., Yamaguchi, Y., Kido, M.A., Abe, T., Ogawa, K., Tokuhisa, M., Gao, W., Okamoto, K., Kiyonari, H. and Tsukuba, T. 2020. The large GTPase Rab44 regulates granule exocytosis in mast cells and IgE-mediated anaphylaxis. *Cellular and Molecular Immunology*. **17**(12), pp.1287–1289.
- Karampini, E., Bierings, R. and Voorberg, J. 2020. Orchestration of Primary Hemostasis by Platelet and Endothelial Lysosome-Related Organelles. *Arteriosclerosis, Thrombosis, and Vascular Biology*. **40**(6), pp.1441–1453.
- Karampini, E., Bürgisser, P.E., Olins, J., Mulder, A.A., Jost, C.R., Geerts, D., Voorberg, J. and Bierings, R. 2021. Sec22b determines Weibel-Palade body length by controlling anterograde endoplasmic reticulum-Golgi transport. *Haematologica*. **106**(4), pp.1138–1147.
- Katsnelson, M.A., Lozada-Soto, K.M., Russo, H.M., Miller, B.A. and Dubyak, G.R. 2016. NLRP3 inflammasome signaling is activated by low-level lysosome disruption but inhibited by extensive lysosome disruption: roles for K⁺ efflux and Ca²⁺ influx. *American Journal of Physiology-Cell Physiology*. **311**(1), pp.C83–C100.
- Khan, I., Sandhu, V., Misquitta, C.M. and Grover, A.K. 2000. SERCA pump isoform expression in endothelium of veins and arteries: Every endothelium is not the same. *Molecular and Cellular Biochemistry*. **203**(1–2), pp.11–15.
- Kilpatrick, B.S., Eden, E.R., Hockey, L.N., Yates, E., Futter, C.E. and Patel, S. 2017. An Endosomal NAADP-Sensitive Two-Pore Ca²⁺ Channel Regulates ER-Endosome Membrane Contact Sites to Control Growth Factor Signaling. *Cell Reports*. **18**(7), pp.1636–1645.
- Kiral, F.R., Kohrs, F.E., Jin, E.J. and Hiesinger, P.R. 2018. Rab GTPases and Membrane Trafficking in Neurodegeneration. *Current Biology*. **28**(8), pp.R471–R486.
- Klöpffer, T.H., Kienle, N., Fasshauer, D. and Munro, S. 2012. Untangling the evolution of Rab G proteins: implications of a comprehensive genomic analysis. *BMC Biology*. **10**.
- Klumperman, J. and Raposo, G. 2014. The complex ultrastructure of the endolysosomal system. *Cold Spring Harbor Perspectives in Biology*. **6**(10).
- Knipe, L., Meli, A., Hewlett, L., Bierings, R., Dempster, J., Skehel, P., Hannah,

- M.J. and Carter, T. 2010. A revised model for the secretion of tPA and cytokines from cultured endothelial cells. *Blood*. **116**(12), pp.2183–2191.
- Knöfler, R., Lange, B.S., Paul, F., Tiebel, O. and Suttrop, M. 2020. Bleeding signs due to acquired von Willebrand syndrome at diagnosis of chronic myeloid leukaemia in children. *British Journal of Haematology*. **188**(5), pp.701–706.
- Knop, M., Aareskjold, E., Bode, G. and Gerke, V. 2004. Rab3D and annexin A2 play a role in regulated of vWF, but not tPA, from endothelial cells. *EMBO Journal*. **23**(15), pp.2982–2992.
- Kobayashi, T., Vischer, U.M., Rosnoblet, C., Lebrand, C., Lindsay, M., Parton, R.G., Kruithof, E.K.O. and Gruenberg, J. 2000. The tetraspanin CD63/lamp3 cycles between endocytic and secretory compartments in human endothelial cells. *Molecular Biology of the Cell*. **11**(5), pp.1829–1843.
- Köhler, R., Brakemeier, S., Kühn, M., Degenhardt, C., Buhr, H., Pries, A. and Hoyer, J. 2001. Expression of ryanodine receptor type 3 and TRP channels in endothelial cells: Comparison of in situ and cultured human endothelial cells. *Cardiovascular Research*. **51**(1), pp.160–168.
- Köhler, R., Degenhardt, C., Kühn, M., Runkel, N., Paul, M. and Hoyer, J. 2000. Expression and function of endothelial Ca²⁺-activated K⁺ channels in human mesenteric artery: A single-cell reverse transcriptase-polymerase chain reaction and electrophysiological study in situ. *Circulation Research*. **87**(6), pp.496–503.
- Kowalczyk, A., Kleniewska, P., Kolodziejczyk, M., Skibska, B. and Goraca, A. 2015. The role of endothelin-1 and endothelin receptor antagonists in inflammatory response and sepsis. *Archivum Immunologiae et Therapiae Experimentalis*. **63**(1), pp.41–52.
- Kumar, P., Kumar, S., Udupa, E.P., Kumar, U., Rao, P. and Honnegowda, T. 2015. Role of angiogenesis and angiogenic factors in acute and chronic wound healing. *Plastic and Aesthetic Research*. **2**(5), p.243.
- Lam, A.K.M. and Galione, A. 2013. The endoplasmic reticulum and junctional membrane communication during calcium signaling. *Biochimica et Biophysica Acta - Molecular Cell Research*. **1833**(11), pp.2542–2559.
- Lanner, J.T., Georgiou, D.K., Joshi, A.D. and Hamilton, S.L. 2010. Ryanodine receptors: structure, expression, molecular details, and function in calcium release. *Cold Spring Harbor perspectives in biology*. **2**(11).
- Laszik, Z., Jansen, P.J., Cummings, R.D., Tedder, T.F., McEver, R.P. and Moore, K.L. 1996. P-selectin glycoprotein ligand-1 is broadly expressed in cells of myeloid, lymphoid, and dendritic lineage and in some nonhematopoietic cells. *Blood*. **88**(8), pp.3010–3021.
- Lenzi, C., Stevens, J., Osborn, D., Hannah, Matthew J., Bierings, R. and Carter, T. 2019. Synaptotagmin 5 regulates Ca²⁺-dependent Weibel–Palade body exocytosis in human endothelial cells. *Journal of Cell Science*. **132**(5).
- Lenzi, C., Stevens, J., Osborn, D., Hannah, Matthew J, Bierings, R. and Carter, T. 2019. Synaptotagmin 5 regulates calcium-dependent Weibel–Palade body exocytosis in human endothelial cells. *Journal of Cell Science*. **132**(5), p.jcs221952.

- Levy, G.G., Nichols, W.C., Lian, E.C., Foroud, T., McClintick, J.N., McGee, B.M., Yang, A.Y., Siemieniak, D.R., Stark, K.R., Gruppo, R., Sarode, R., Shurin, S.B., Chandrasekaran, V., Stabler, S.P., Sabio, H., Bouhassira, E.E., Upshaw, J.D., Ginsburg, D. and Tsai, H.M. 2001. Mutations in a member of the ADAMTS gene family cause thrombotic thrombocytopenic purpura. *Nature*. **413**(6855), pp.488–494.
- Lewis, R.S. 2007. The molecular choreography of a store-operated calcium channel. *Nature*. **446**(7133), pp.284–287.
- Li, H., Burkhardt, C., Heinrich, U.R., Brausch, I., Xia, N. and Förstermann, U. 2003. Histamine upregulates gene expression of endothelial nitric oxide synthase in human vascular endothelial cells. *Circulation*. **107**(18), pp.2348–2354.
- Li, J., Cubbon, R.M., Wilson, L.A., Amer, M.S., McKeown, L., Hou, B., Majeed, Y., Tumova, S., Seymour, V.A.L., Taylor, H., Stacey, M., O'Regan, D., Foster, R., Porter, K.E., Kearney, M.T. and Beech, D.J. 2011. Orai1 and CRAC channel dependence of VEGF-activated Ca²⁺ entry and endothelial tube formation. *Circulation Research*. **108**(10), pp.1190–1198.
- Li, J., Hou, B. and Beech, D.J. 2015. Endothelial Piezo1: Life depends on it. *Channels*. **9**(1), pp.1–2.
- Li, L., Bressler, B., Prameya, R., Dorovini-Zis, K. and Van Breemen, C. 1999. Agonist-stimulated calcium entry in primary cultures of human cerebral microvascular endothelial cells. *Microvascular Research*. **57**(3), pp.211–226.
- Li, P., Wei, G., Cao, Y., Deng, Q., Han, X., Huang, X., Huo, Y., He, Y., Chen, L. and Luo, J. 2018. Myosin IIa is critical for cAMP-mediated endothelial secretion of von Willebrand factor. *Blood*. **131**(6), pp.686–698.
- Li, R.-J., Xu, J., Fu, C., Zhang, J., Zheng, Y.G., Jia, H. and Liu, J.O. 2016. Regulation of mTORC1 by lysosomal calcium and calmodulin. *eLife*. **5**.
- Li, S., Wang, Z., Liao, Y., Zhang, W., Shi, Q., Yan, R., Ruan, C. and Dai, K. 2010. The glycoprotein Iba-von Willebrand factor interaction induces platelet apoptosis. *Journal of Thrombosis and Haemostasis*. **8**(2), pp.341–350.
- Li, Z., Lu, J., Xu, P., Xie, X., Chen, L. and Xu, T. 2007. Mapping the interacting domains of STIM1 and Orai1 in Ca²⁺ release-activated Ca²⁺ channel activation. *Journal of Biological Chemistry*. **282**(40), pp.29448–29456.
- Lillo, M.A., Gaete, P.S., Puebla, M., Ardiles, N.M., Poblete, I., Becerra, A., Simon, F. and Figueroa, X.F. 2018. Critical contribution of Na⁺-Ca²⁺ exchanger to the Ca²⁺-mediated vasodilation activated in endothelial cells of resistance arteries. *FASEB Journal*. **32**(4), pp.2137–2147.
- Lin-Moshier, Y., Keebler, M. V., Hooper, R., Boulware, M.J., Liu, X., Churamani, D., Abood, M.E., Walseth, T.F., Brailoiu, E., Patel, S. and Marchant, J.S. 2014. The Two-pore channel (TPC) interactome unmasks isoform-specific roles for TPCs in endolysosomal morphology and cell pigmentation. *Proceedings of the National Academy of Sciences of the United States of America*. **111**(36), pp.13087–13092.
- Lin-Moshier, Y., Walseth, T.F., Churamani, D., Davidson, S.M., Slama, J.T., Hooper, R., Brailoiu, E., Patel, S. and Marchant, J.S. 2012. Photoaffinity

- labeling of nicotinic acid adenine dinucleotide phosphate (NAADP) targets in mammalian cells. *Journal of Biological Chemistry*. **287**(4), pp.2296–2307.
- Lin, Q., Zhao, L., Jing, R., Trexler, C., Wang, H., Li, Y., Tang, H., Huang, F., Zhang, F., Fang, X., Liu, J., Jia, N., Chen, J. and Ouyang, K. 2019. Inositol 1,4,5-Trisphosphate receptors in endothelial cells play an essential role in vasodilation and blood pressure regulation. *Journal of the American Heart Association*. **8**(4).
- Liou, J., Kim, M.L., Won, D.H., Jones, J.T., Myers, J.W., Ferrell, J.E. and Meyer, T. 2005. STIM is a Ca²⁺ sensor essential for Ca²⁺-store- depletion-triggered Ca²⁺ influx. *Current Biology*. **15**(13), pp.1235–1241.
- Liu, N., Ruan, Y. and Priori, S.G. 2008. Catecholaminergic Polymorphic Ventricular Tachycardia. *Progress in Cardiovascular Diseases*. **51**(1), pp.23–30.
- Livak, K.J. and Schmittgen, T.D. 2001. Analysis of relative gene expression data using real-time quantitative PCR and the 2- $\Delta\Delta$ CT method. *Methods*. **25**(4), pp.402–408.
- Lochner, A. and Moolman, J.A. 2006. The many faces of H89: A review. *Cardiovascular Drug Reviews*. **24**(3–4), pp.261–274.
- López-Sanjurjo, C.I., Tovey, S.C., Prole, D.L. and Taylor, C.W. 2013. Lysosomes shape Ins(1,4,5)P₃-evoked Ca²⁺ signals by selectively sequestering Ca²⁺ released from the endoplasmic reticulum. *Journal of Cell Science*. **126**(1), pp.289–300.
- Lorenzi, O., Frieden, M., Villemin, P., Fournier, M., Foti, M. and Vischer, U.M. 2008. Protein kinase C- δ mediates von Willebrand factor secretion from endothelial cells in response to vascular endothelial growth factor (VEGF) but not histamine. *Journal of Thrombosis and Haemostasis*. **6**(11), pp.1962–1969.
- Lu, X., Kwong, J.Q., Molkentin, J.D. and Bers, D.M. 2016. Individual cardiac mitochondria undergo rare transient permeability transition pore openings. *Circulation Research*. **118**(5), pp.834–841.
- Lückhoff, A. and Busse, R. 1990. Calcium influx into endothelial cells and formation of endothelium-derived relaxing factor is controlled by the membrane potential. *Pflügers Archiv European Journal of Physiology*. **416**(3), pp.305–311.
- Lui-Roberts, W.W.Y., Collinson, L.M., Hewlett, L.J., Michaux, G. and Cutler, D.F. 2005. An AP-1/clathrin coat plays a novel and essential role in forming the Weibel-Palade bodies of endothelial cells. *Journal of Cell Biology*. **170**(4), pp.627–636.
- Lüscher, T.F. and Noll, G. 1995. The pathogenesis of cardiovascular disease: role of the endothelium as a target and mediator. *Atherosclerosis*. **118**(SUPPL.), pp.S81-90.
- Lytton, J., Westlin, M. and Hanley, M.R. 1991. Thapsigargin inhibits the sarcoplasmic or endoplasmic reticulum Ca-ATPase family of calcium pumps. *Journal of Biological Chemistry*. **266**(26), pp.17067–17071.
- Ma, J., Zhang, Z., Yang, L., Kriston-Vizi, J., Cutler, D.F. and Li, W. 2016. BLOC-

- 2 subunit HPS6 deficiency affects the tubulation and secretion of von Willebrand factor from mouse endothelial cells. *Journal of Genetics and Genomics*. **43**(12), pp.686–693.
- MacLennan, D.H., Phillips, M.S. and Zhang, Y. 1996. The Genetic and Physiological Basis of Malignant Hyperthermia *In: Molecular Biology of Membrane Transport Disorders* [Online]. Boston, MA: Springer US, pp.181–200. Available from: http://link.springer.com/10.1007/978-1-4613-1143-0_10.
- Marchant, J.S. and Patel, S. 2015. Two-pore channels at the intersection of endolysosomal membrane traffic. *Biochemical Society Transactions*. **43**, pp.434–441.
- Marchant, J.S. and Taylor, C.W. 1997. Cooperative activation of IP3 receptors by sequential binding of IP3 and Ca²⁺ safeguards against spontaneous activity. *Current Biology*. **7**(7), pp.510–518.
- Markus, H.S., McCollum, C., Imray, C., Goulder, M.A., Gilbert, J. and King, A. 2011. The von willebrand inhibitor ARC1779 reduces cerebral embolization after carotid endarterectomy: A randomized trial. *Stroke*. **42**(8), pp.2149–2153.
- Mayadas, T.N., Johnson, R.C., Rayburn, H., Hynes, R.O. and Wagner, D.D. 1993. Leukocyte rolling and extravasation are severely compromised in P selectin-deficient mice. *Cell*. **74**(3), pp.541–554.
- McEver, R.P., Beckstead, J.H., Moore, K.L., Marshall-Carlson, L. and Bainton, D.F. 1989a. GMP-140, a platelet α -granule membrane protein, is also synthesized by vascular endothelial cells and is localized in Weibel-Palade bodies. *Journal of Clinical Investigation*. **84**(1), pp.92–99.
- McEver, R.P., Beckstead, J.H., Moore, K.L., Marshall-Carlson, L. and Bainton, D.F. 1989b. GMP-140, a platelet α -granule membrane protein, is also synthesized by vascular endothelial cells and is localized in Weibel-Palade bodies. *Journal of Clinical Investigation*. **84**(1), pp.92–99.
- McKenney, R.J., Huynh, W., Tanenbaum, M.E., Bhabha, G. and Vale, R.D. 2014. Activation of cytoplasmic dynein motility by dynactin-cargo adapter complexes. *Science*. **345**(6194), pp.337–341.
- McPhersonx, P.S., Kim, Y.K., Valdivia, H., Knudson, C.M., Takekura, H., Franzini-Armstrong, C., Coronadot, R. and Campbell, K.P. 1991. The brain ryanodine receptor: A caffeine-sensitive calcium release channel. *Neuron*. **7**(1), pp.17–25.
- Ménasché, G., Pastural, E., Feldmann, J., Certain, S., Ersoy, F., Dupuis, S., Wulffraat, N., Bianchi, D., Fischer, A., Le Deist, F. and De Saint Basile, G. 2000. Mutations in RAB27A cause Griscelli syndrome associated with haemophagocytic syndrome. *Nature Genetics*. **25**(2), pp.173–176.
- Mercer, J.C., DeHaven, W.I., Smyth, J.T., Wedel, B., Boyles, R.R., Bird, G.S. and Putney, J.W. 2006. Large store-operated calcium selective currents due to co-expression of Orai1 or Orai2 with the intracellular calcium sensor, Stim1. *Journal of Biological Chemistry*. **281**(34), pp.24979–24990.
- Merten, M. and Thiagarajan, P. 2000. P-selectin expression on platelets determines size and stability of platelet aggregates. *Circulation*. **102**(16), pp.1931–1936.

- Micaroni, M., Perinetti, G., Berrie, C.P. and Mironov, A.A. 2010. The SPCA1 Ca²⁺ Pump and Intracellular Membrane Trafficking. *Traffic*. **11**(10), pp.1315–1333.
- Michalak, M. and Opas, M. 2009. Endoplasmic and sarcoplasmic reticulum in the heart. *Trends in Cell Biology*. **19**(6), pp.253–259.
- Michaux, G. and Cutler, D.F. 2004. How to roll an endothelial cigar: The biogenesis of Weibel-Palade bodies. *Traffic*. **5**(2), pp.69–78.
- Mikoshiba, K. 2007. IP₃ receptor/Ca²⁺ channel: From discovery to new signaling concepts. *Journal of Neurochemistry*. **102**(5), pp.1426–1446.
- Minami, T., Sugiyama, A., Wu, S.Q., Abid, R., Kodama, T. and Aird, W.C. 2004. Thrombin and Phenotypic Modulation of the Endothelium. *Arteriosclerosis, Thrombosis, and Vascular Biology*. **24**(1), pp.41–53.
- Miteva, K.T., Pedicini, L., Wilson, L.A., Jayasinghe, I., Slip, R.G., Marszalek, K., Gaunt, H.J., Bartoli, F., Deivasigamani, S., Sobradillo, D., Beech, D.J. and McKeown, L. 2019. Rab46 integrates Ca²⁺ and histamine signaling to regulate selective cargo release from Weibel-Palade bodies. *Journal of Cell Biology*. **218**(7), pp.2232–2246.
- Mitsunaga, S., Hosomichi, K., Okudaira, Y., Nakaoka, H., Kunii, N., Suzuki, Y., Kuwana, M., Sato, S., Kaneko, Y., Homma, Y., Kashiwase, K., Azuma, F., Kulski, J.K., Inoue, I. and Inoko, H. 2013. Exome sequencing identifies novel rheumatoid arthritis-susceptible variants in the BTNL2. *Journal of Human Genetics*. **58**(4), pp.210–215.
- Miyawaki, A., Llopis, J., Heim, R., Michael McCaffery, J., Adams, J.A., Ikura, M. and Tsien, R.Y. 1997. Fluorescent indicators for Ca²⁺ based on green fluorescent proteins and calmodulin. *Nature*. **388**(6645), pp.882–887.
- Mohri, H., Tanabe, J., Yamazaki, E., Yoshida, M., Harano, H., Matsuzaki, M., Motomura, T.S. and Okubo, T. 1996. Acquired type 2A von Willebrand disease in chronic myelocytic leukemia. *Hematopathology and Molecular Hematology*. **10**(3), pp.123–133.
- Mojiri, A., Alavi, P., Lorenzana Carrillo, M.A., Nakhaei-Nejad, M., Sergi, C.M., Thebaud, B., Aird, W.C. and Jahroudi, N. 2019. Endothelial cells of different organs exhibit heterogeneity in von Willebrand factor expression in response to hypoxia. *Atherosclerosis*. **282**, pp.1–10.
- Morgan, A.J., Davis, L.C. and Galione, A. 2015. Imaging approaches to measuring lysosomal calcium *In: Methods in Cell Biology* [Online]. Elsevier Ltd, pp.159–195. Available from: <http://dx.doi.org/10.1016/bs.mcb.2014.10.031>.
- Morgan, A.J. and Galione, A. 2008. Investigating cADPR and NAADP in intact and broken cell preparations. *Methods*. **46**(3), pp.194–203.
- Morgan, A.J., Platt, F.M., Lloyd-Evans, E. and Galione, A. 2011. Molecular mechanisms of endolysosomal Ca²⁺ signalling in health and disease. *Biochemical Journal*. **439**(3), pp.349–374.
- Morgan, A.J., Yuan, Y., Patel, S. and Galione, A. 2020. Does lysosomal rupture evoke Ca²⁺ release? A question of pores and stores. *Cell calcium*. **86**, p.102139.
- Mountian, I., Manolopoulos, V.G., De Smedt, H., Parys, J.B., Missiaen, L. and

- Wuytack, F. 1999. Expression patterns of sarco/endoplasmic reticulum Ca²⁺-ATPase and inositol 1,4,5 trisphosphate receptor isoforms in vascular endothelial cells. *Cell Calcium*. **25**(5), pp.371–380.
- Van Mourik, J.A., Boertjes, R., Huisveld, I.A., Fijnvandraat, K., Pajkrt, D., Van Genderen, P.J.J. and Fijnheer, R. 1999. von Willebrand factor propeptide in vascular disorders: A tool to distinguish between acute and chronic endothelial cell perturbation. *Blood*. **94**(1), pp.179–185.
- Müller, M.P. and Goody, R.S. 2018. Molecular control of Rab activity by GEFs, GAPs and GDI. *Small GTPases*. **9**(1–2), pp.5–21.
- Murray, A.J. 2008. Pharmacological PKA inhibition: All may not be what it seems. *Science Signaling*. **1**(22), pp.1–7.
- Nakagomi, S., Barsoum, M.J., Bossy-Wetzel, E., Sütterlin, C., Malhotra, V. and Lipton, S.A. 2008. A Golgi fragmentation pathway in neurodegeneration. *Neurobiology of disease*. **29**(2), pp.221–231.
- Nakamura, S., Takemura, T., Tan, L., Nagata, Y., Yokota, D., Hirano, I., Shigeno, K., Shibata, K., Fujie, M., Fujisawa, S. and Ohnishi, K. 2011. Small GTPase RAB45-mediated p38 activation in apoptosis of chronic myeloid leukemia progenitor cells. *Carcinogenesis*. **32**(12), pp.1758–1772.
- Nakayama, S. and Kretsinger, R.H. 1994. Evolution of the EF-hand family of proteins. *Annual Review of Biophysics and Biomolecular Structure*. **23**, pp.473–507.
- Naomasa, N., Norio, N. and Shoso, Y. 1992. The effect of histamine on cultured endothelial cells A study of the mechanism of increased vascular permeability. *European Journal of Pharmacology*. **221**(2–3), pp.325–331.
- Naraghi, M. 1997. T-jump study of calcium binding kinetics of calcium chelators. *Cell Calcium*. **22**(4), pp.255–268.
- Newton-Cheh, C., Johnson, T., Gateva, V., Tobin, M.D., Bochud, M., Coin, L., Najjar, S.S., Zhao, J.H., Heath, S.C., Eyheramendy, S., Papadakis, K., Voight, B.F., Scott, L.J., Zhang, F., Farrall, M., Tanaka, T., Wallace, C., Chambers, J.C., Khaw, K.T., Nilsson, P., Van Der Harst, P., Polidoro, S., Grobbee, D.E., Onland-Moret, N.C., Bots, M.L., Wain, L. V., Elliot, K.S., Teumer, A., Luan, J., Lucas, G., Kuusisto, J., Burton, P.R., Hadley, D., McArdle, W.L., Brown, M., Dominiczak, A., Newhouse, S.J., Samani, N.J., Webster, J., Zeggini, E., Beckmann, J.S., Bergmann, S., Lim, N., Song, K., Vollenweider, P., Waeber, G., Waterworth, D.M., Yuan, X., Groop, L., Orho-Melander, M., Allione, A., Di Gregorio, A., Gurrera, S., Panico, S., Ricceri, F., Romanazzi, V., Sacerdote, C., Vineis, P., Barroso, I., Sandhu, M.S., Luben, R.N., Crawford, G.J., Jousilahti, P., Perola, M., Boehnke, M., Bonnycastle, L.L., Collins, F.S., Jackson, A.U., Mohlke, K.L., Stringham, H.M., Valle, T.T., Willer, C.J., Bergman, R.N., Morken, M.A., Döring, A., Gieger, C., Illig, T., Meitinger, T., Org, E., Pfeufer, A., Wichmann, H.E., Kathiresan, S., Marrugat, J., O'Donnell, C.J., Schwartz, S.M., Siscovick, D.S., Subirana, I., Freimer, N.B., Hartikainen, A.L., McCarthy, M.I., O'Reilly, P.F., Peltonen, L., Pouta, A., De Jong, P.E., Snieder, H., Van Gilst, W.H., Clarke, R., Goel, A., Hamsten, A., Altshuler, D., Jarvelin, M.R., Elliott, P., Lakatta, E.G., Forouhi, N., Wareham, N.J., Loos, R.J.F., Deloukas, P., Lathrop, G.M., Zelenika, D., Strachan, D.P., Soranzo, N., Williams, F.M., Zhai, G., Spector, T.D., Peden, J.F., Watkins, H., Ferrucci, L., Caulfield, M.,

Munroe, P.B., Berglund, G., Melander, O., Matullo, G., Uiterwaal, C.S., van der Schouw, Y.T., Numans, M.E., Ernst, F., Homuth, G., Völker, U., Elosua, R., Laakso, M., Connell, J.M., Mooser, V., Salomaa, V., Tuomilehto, J., Laan, M., Navis, G., Seedorf, U., Syvänen, A.C., Tognoni, G., Sanna, S., Uda, M., Scheet, P., Schlessinger, D., Scuteri, A., Dörr, M., Felix, S.B., Reffelmann, T., Lorbeer, R., Völzke, H., Rettig, R., Galan, P., Hercberg, S., Bingham, S.A., Kooner, J.S., Bandinelli, S., Meneton, P., Abecasis, G., Thompson, J.R., Braga Marcano, C.A., Barke, B., Dobson, R., Gungadoo, J., Lee, K.L., Onipinla, A., Wallace, I., Xue, M., Clayton, D.G., Leung, H.T., Nutland, S., Walker, N.M., Todd, J.A., Stevens, H.E., Dunger, D.B., Widmer, B., Downes, K., Cardon, L.R., Kwiatkowski, D.P., Barrett, J.C., Evans, D., Morris, A.P., Lindgren, C.M., Rayner, N.W., Timpson, N.J., Lyons, E., Vannberg, F., Hill, A.V.S., Teo, Y.Y., Rockett, K.A., Craddock, N., Attwood, A.P., Bryan, C., Bumpstead, S.J., Chaney, A., Ghuri, J., William, R.G., Hunt, S.E., Inouye, M., Keniry, E., King, E., McGinnis, R., Potter, S., Ravindrarajan, R., Whittaker, P., Withers, D., Bentley, D., Groves, C.J., Duncanson, A., Ouwehand, W.H., Boorman, J.P., Cant, B., Jolley, J.D., Knight, A.S., Koch, K., Taylor, N.C., Watkins, N.A., Winzer, T., Braund, P.S., Dixon, R.J., Mangino, M., Stevens, S., Donnely, P., Davidson, D., Marchini, J.L., Spencer, I.C.A., Cardin, N.J., Ferreira, T., Pereira-Gale, J., Hallgrimsdottir, I.B., Howie, B.N., Su, Z., Vukcevic, D., Easton, D., Everson, U., Hussey, J.M., Meech, E., Prowse, C. V., Walters, G.R., Jones, R.W., Ring, S.M., Prembey, M., Breen, G., St. Clair, D., Ceasar, S., Gordon-Smith, K., Fraser, C., Green, E.K., Grozeva, D., Hamshire, M.L., Holmans, P.A., Jones, I.R., Kirov, G., Moskvina, V., Nikolov, I., O'Donovan, M.C., Owen, M.J., Craddock, N., Collier, D.A., Elkin, A., Farmer, A., Williamson, R., McGruffin, P., Young, A.H., Ferrier, I.N., Ball, S.G., Balmforth, A.J., Barrett, J.H., Bishop, D.T., Iles, M.M., Maqbool, A., Yuldasheva, N., Hall, A.S., Bredin, F., Tremelling, M., Parkes, M., Drummond, H., Lees, C.W., Nimmo, E.R., Satsangi, J., Fisher, S.A., Lewis, C.M., Onnie, C.M., Prescott, N.J., Mathew, C.G., Forbes, A., Sanderson, J., Mathew, C., Barbour, J., Mohiuddin, M.K., Todhunter, C.E., Mansfield, J.C., Ahmad, T., Cummings, F.R., Jewell, D.P., Barton, A., Bruce, I.N., Donovan, H., Eyre, S., Gilbert, P.D., Hider, S.L., Hinks, A.M., John, S.L., Potter, C., Silman, A.J., Symmons, D.P.M., Thomson, W., Worthington, J., Frayling, T.M., Freathy, R.M., Lango, H., Perry, J.R.B., Weedon, M.N., Hattersley, A.T., Shields, B.M., Hitman, G.A., Walker, M., Newport, M., Sirugo, G., Conway, D., Jallow, M., Bradbury, L.A., Pointon, J.L., Brown, M.A., Farrar, C., Wordsworth, P., Franklyn, J.A., Heward, J.M., Simmonds, M.J., Cough, S.C.L., Seal, S., Stratton, M.R., Ban, M., Goris, A., Sawcer, S.J. and Compston, A. 2009. Genome-wide association study identifies eight loci associated with blood pressure. *Nature Genetics*. **41**(6), pp.666–676.

Nightingale, T.D., McCormack, J.J., Grimes, W., Robinson, C., Lopes da Silva, M., White, I.J., Vaughan, A., Cramer, L.P. and Cutler, D.F. 2018a. Tuning the endothelial response: differential release of exocytic cargos from Weibel-Palade bodies. *Journal of Thrombosis and Haemostasis*. **16**(9), pp.1873–1886.

Nightingale, T.D., McCormack, J.J., Grimes, W., Robinson, C., Lopes da Silva, M., White, I.J., Vaughan, A., Cramer, L.P. and Cutler, D.F. 2018b. Tuning the endothelial response: differential release of exocytic cargos from

- Weibel-Palade bodies. *Journal of Thrombosis and Haemostasis*. **16**(9), pp.1873–1886.
- Nightingale, T.D., Pattni, K., Hume, A.N., Seabra, M.C. and Cutler, D.F. 2009. Rab27a and MyRIP regulate the amount and multimeric state of VWF released from endothelial cells. *Blood*. **113**(20), pp.5010–5018.
- Nightingale, T.D., White, I.J., Doyle, E.L., Turmaine, M., Harrison-Lavoie, K.J., Webb, K.F., Cramer, L.P. and Cutler, D.F. 2011. Actomyosin II contractility expels von Willebrand factor from Weibel-Palade bodies during exocytosis. *Journal of Cell Biology*. **194**(4), pp.613–629.
- Noy, P.J., Gavin, R.L., Colombo, D., Haining, E.J., Reyat, J.S., Payne, H., Thielmann, I., Lokman, A.B., Neag, G., Yang, J., Lloyd, T., Harrison, N., Heath, V.L., Gardiner, C., Whitworth, K.M., Robinson, J., Koo, C.Z., Maio, A. Di, Harrison, P., Lee, S.P., Michelangeli, F., Kalia, N., Rainger, G.E., Nieswandt, B., Brill, A., Watson, S.P. and Tomlinson, M.G. 2019. Tspan18 is a novel regulator of the Ca²⁺ channel Orai1 and von Willebrand factor release in endothelial cells. *Haematologica*. **104**(9), pp.1892–1905.
- Numata, T., Kiyonaka, S., Kato, K., Takahashi, N. and Mori, Y. 2016. Activation of TRP channels in mammalian systems *In: TRP Channels.*, pp.43–90.
- Ohira, M., Oshitani, N., Hosomi, S., Watanabe, K., Yamagami, H., Tominaga, K., Watanabe, T., Fujiwara, Y., Maeda, K., Hirakawa, K. and Arakawa, T. 2009. Dislocation of Rab13 and vasodilator-stimulated phosphoprotein in inactive colon epithelium in patients with Crohn's disease. *International Journal of Molecular Medicine*. **24**(6), pp.829–835.
- Øynebråten, I., Bakke, O., Brandtzaeg, P., Johansen, F.E. and Haraldsen, G. 2004. Rapid chemokine secretion from endothelial cells originates from 2 distinct compartments. *Blood*. **104**(2), pp.314–320.
- Ozaka, T., Doi, Y., Kayashima, K. and Fujimoto, S. 1997. Weibel-Palade bodies as a storage site of calcitonin gene-related peptide and endothelin-1 in blood vessels of the rat carotid body. *Anatomical Record*. **247**(3), pp.388–394.
- Pang, Z.P. and Südhof, T.C. 2010. Cell biology of Ca²⁺-triggered exocytosis. *Current Opinion in Cell Biology*. **22**(4), pp.496–505.
- Papapetropoulos, A., Fulton, D., Mahboubi, K., Kalb, R.G., O'Connor, D.S., Li, F., Altieri, D.C. and Sessa, W.C. 2000. Angiotensin-1 inhibits endothelial cell apoptosis via the Akt/survivin pathway. *Journal of Biological Chemistry*. **275**(13), pp.9102–9105.
- Park, C.Y., Hoover, P.J., Mullins, F.M., Bachhawat, P., Covington, E.D., Raunser, S., Walz, T., Garcia, K.C., Dolmetsch, R.E. and Lewis, R.S. 2009. STIM1 Clusters and Activates CRAC Channels via Direct Binding of a Cytosolic Domain to Orai1. *Cell*. **136**(5), pp.876–890.
- Paroutis, P., Touret, N. and Grinstein, S. 2004. The pH of the secretory pathway: Measurement, determinants, and regulation. *Physiology*. **19**(4), pp.207–215.
- Parsons, M.E. and Ganellin, C.R. 2006. Histamine and its receptors. *British Journal of Pharmacology*. **147**(SUPPL. 1), pp.S127–S135.
- Patel, J. V., Lim, H.S., Varughese, G.I., Hughes, E.A. and Lip, G.Y.H. 2008.

- Angiotensin-2 levels as a biomarker of cardiovascular risk in patients with hypertension. *Annals of Medicine*. **40**(3), pp.215–222.
- Patel, K.D., Cuvelier, S.L. and Wiehler, S. 2002. Selectins: Critical mediators of leukocyte recruitment. *Seminars in Immunology*. **14**(2), pp.73–81.
- Patel, S. and Docampo, R. 2010. Acidic calcium stores open for business: Expanding the potential for intracellular Ca²⁺ signaling. *Trends in Cell Biology*. **20**(5), pp.277–286.
- Patel, S. and Muallem, S. 2011. Acidic Ca²⁺ stores come to the fore. *Cell Calcium*. **50**(2), pp.109–112.
- Patmore, S., Dhama, S.P.S. and O’Sullivan, J.M. 2020. Von Willebrand factor and cancer; metastasis and coagulopathies. *Journal of Thrombosis and Haemostasis*. **18**(10), pp.2444–2456.
- Pedicini, L., Miteva, K.T., Hawley, V., Gaunt, H.J., Appleby, H.L., Cubbon, R.M., Marszalek, K., Kearney, M.T., Beech, D.J. and McKeown, L. 2018. Homotypic endothelial nanotubes induced by wheat germ agglutinin and thrombin /631/80/86 /631/80/2373 /13/1 /13/89 /13/106 /13/109 /14/63 /38/77 /96/95 /82/51 article. *Scientific Reports*. **8**(1).
- Pedicini, L., Wiktor, S.D., Simmons, K.J., Money, A. and McKeown, L. 2021. Affinity-based proteomics reveals novel binding partners for Rab46 in endothelial cells. *Scientific Reports*. **11**(1), p.4054.
- Peiter, E., Maathuis, F.J.M., Mills, L.N., Knight, H., Pelloux, J., Hetherington, A.M. and Sanders, D. 2005. The vacuolar Ca²⁺-activated channel TPC1 regulates germination and stomatal movement. *Nature*. **434**(7031), pp.404–408.
- Periasamy, M. and Kalyanasundaram, A. 2007. SERCA pump isoforms: Their role in calcium transport and disease. *Muscle and Nerve*. **35**(4), pp.430–442.
- Peyvandi, F., Garagiola, I. and Baronciani, L. 2011. Role of von Willebrand factor in the haemostasis. *Blood Transfusion*. **9**(SUPPL. 2).
- Pisoni, R.L. and Lindley, E.R. 1992. Incorporation of [32P]orthophosphate into long chains of inorganic polyphosphate within lysosomes of human fibroblasts. *Journal of Biological Chemistry*. **267**(6), pp.3626–3631.
- Poeter, M., Brandherm, I., Rossaint, J., Rosso, G., Shahin, V., Skryabin, B. V., Zarbock, A., Gerke, V. and Rescher, U. 2014. Annexin A8 controls leukocyte recruitment to activated endothelial cells via cell surface delivery of CD63. *Nature Communications*. **5**.
- Pozzan, T., Rizzuto, R., Volpe, P. and Meldolesi, J. 1994. Molecular and cellular physiology of intracellular calcium stores. *Physiological Reviews*. **74**(3), pp.595–636.
- Prevarskaya, N., Ouadid-Ahidouch, H., Skryma, R. and Shuba, Y. 2014. Remodelling of Ca²⁺ transport in cancer: How it contributes to cancer hallmarks? *Philosophical Transactions of the Royal Society B: Biological Sciences*. **369**(1638).
- Prole, D.L. and Taylor, C.W. 2019. Structure and function of ip3 receptors. *Cold Spring Harbor Perspectives in Biology*. **11**(4).

- Putney, J.W. 1986. A model for receptor-regulated calcium entry. *Cell Calcium*. **7**(1), pp.1–12.
- Putney, J.W. 2017. Store-operated calcium entry: An historical overview. *Advances in Experimental Medicine and Biology*. **981**, pp.205–214.
- Putney, J.W., Steinckwich-Besançon, N., Numaga-Tomita, T., Davis, F.M., Desai, P.N., D'Agostin, D.M., Wu, S. and Bird, G.S. 2017. The functions of store-operated calcium channels. *Biochimica et Biophysica Acta - Molecular Cell Research*. **1864**(6), pp.900–906.
- Pylypenko, O., Hammich, H., Yu, I.M. and Houdusse, A. 2018. Rab GTPases and their interacting protein partners: Structural insights into Rab functional diversity. *Small GTPases*. **9**(1–2), pp.22–48.
- Rahman, T. and Taylor, C.W. 2009. Dynamic regulation of IP3 receptor clustering and activity by IP3. *Channels*. **3**(4).
- Ralevic, V. 2012. P2X receptors in the cardiovascular system. *Wiley Interdisciplinary Reviews: Membrane Transport and Signaling*. **1**(5), pp.663–674.
- Rastegar-Lari, G., Legendre, P., Ajzenberg, N., Warszawski, J., Meyer, D. and Baruch, D. 2000. Von Willebrand factor binding to heparin in various types of von Willebrand disease. *Hematology Journal*. **1**(3), pp.190–198.
- Reininger, A.J. 2008. Function of von Willebrand factor in haemostasis and thrombosis. *Haemophilia*. **14**(SUPPL. 5), pp.11–26.
- Rinne, A., Banach, K. and Blatter, L.A. 2009. Regulation of nuclear factor of activated T cells (NFAT) in vascular endothelial cells. *Journal of Molecular and Cellular Cardiology*. **47**(3), pp.400–410.
- Rodríguez-Fdez, S. and Bustelo, X.R. 2019. The Vav GEF Family: An Evolutionary and Functional Perspective. *Cells*. **8**(5), p.465.
- Rojo Pulido, I., Nightingale, T.D., Darchen, F., Seabra, M.C., Cutler, D.F. and Gerke, V. 2011. Myosin Va acts in concert with Rab27a and MyRIP to regulate acute von-Willebrand factor release from endothelial cells. *Traffic*. **12**(10), pp.1371–1382.
- Romijn, R.A.P., Bouma, B., Wuyster, W., Gros, P., Kroon, J., Sixma, J.J. and Huizinga, E.G. 2001. Identification of the Collagen-binding Site of the von Willebrand Factor A3-domain. *Journal of Biological Chemistry*. **276**(13), pp.9985–9991.
- Rondaj, M.G., Bierings, R., Kragt, A., Gijzen, K.A., Sellink, E., Van Mourik, J.A., Fernandez-Borja, M. and Voorberg, J. 2006. Dynein-dynactin complex mediates protein kinase A-dependent clustering of Weibel-Palade bodies in endothelial cells. *Arteriosclerosis, Thrombosis, and Vascular Biology*. **26**(1), pp.49–55.
- Rondaj, M.G., Bierings, R., Kragt, A., Van Mourik, J.A. and Voorberg, J. 2006. Dynamics and plasticity of Weibel-Palade bodies in endothelial cells. *Arteriosclerosis, Thrombosis, and Vascular Biology*. **26**(5), pp.1002–1007.
- Rondaj, M.G., Sellink, E., Gijzen, K.A., Ten Klooster, J.P., Hordijk, P.L., Van Mourik, J.A. and Voorberg, J. 2004a. Small GTP-binding protein Ral is involved in cAMP-mediated release of von Willebrand factor from endothelial cells. *Arteriosclerosis, Thrombosis, and Vascular Biology*. **24**(7),

pp.1315–1320.

- Rondaij, M.G., Sellink, E., Gijzen, K.A., Ten Klooster, J.P., Hordijk, P.L., Van Mourik, J.A. and Voorberg, J. 2004b. Small GTP-binding protein Ral is involved in cAMP-mediated release of von Willebrand factor from endothelial cells. *Arteriosclerosis, Thrombosis, and Vascular Biology*. **24**(7), pp.1315–1320.
- Roos, J., DiGregorio, P.J., Yeromin, A. V., Ohlsen, K., Lioudyno, M., Zhang, S., Safrina, O., Kozak, J.A., Wagner, S.L., Cahalan, M.D., Velichelebi, G. and Stauderman, K.A. 2005. STIM1, an essential and conserved component of store-operated Ca²⁺ channel function. *Journal of Cell Biology*. **169**(3), pp.435–445.
- Royo, T., Martínez-González, J., Vilahur, G. and Badimon, L. 2003. Differential intracellular trafficking of von Willebrand factor (vWF) and vWF propeptide in porcine endothelial cells lacking Weibel-Palade bodies and in human endothelial cells. *Atherosclerosis*. **167**(1), pp.55–63.
- Ruas, M., Davis, L.C., Chen, C., Morgan, A.J., Chuang, K., Walseth, T.F., Grimm, C., Garnham, C., Powell, T., Platt, N., Platt, F.M., Biel, M., Wahl-Schott, C., Parrington, J. and Galione, A. 2015. Expression of Ca²⁺ - permeable two-pore channels rescues NAADP signalling in TPC -deficient cells . *The EMBO Journal*. **34**(13), pp.1743–1758.
- Ruggeri, Z.M. 2007. The role of von Willebrand factor in thrombus formation. *Thrombosis Research*. **120**(SUPPL. 1).
- Russell, F.D., Skepper, J.N. and Davenport, A.P. 1998a. Evidence using immunoelectron microscopy for regulated and constitutive pathways in the transport and release of endothelin. *Journal of Cardiovascular Pharmacology*. **31**(3), pp.424–430.
- Russell, F.D., Skepper, J.N. and Davenport, A.P. 1998b. Human endothelial cell storage granules: A novel intracellular site for isoforms of the endothelin-converting enzyme. *Circulation Research*. **83**(3), pp.314–321.
- Sadler, J.E. 1998. Biochemistry and genetics of von Willebrand factor. *Annual Review of Biochemistry*. **67**, pp.395–424.
- Sadler, J.E., Budde, U., Eikenboom, J.C.J., Favaloro, E.J., Hill, F.G.H., Holmberg, L., Ingerslev, J., Lee, C.A., Lillicrap, D., Mannucci, P.M., Mazurier, C., Meyer, D., Nichols, W.L., Nishino, M., Peake, I.R., Rodeghiero, F., Schneppenheim, R., Ruggeri, Z.M., Srivastava, A., Montgomery, R.R. and Federici, A.B. 2006. Update on the pathophysiology and classification of von Willebrand disease: A report of the Subcommittee on von Willebrand factor. *Journal of Thrombosis and Haemostasis*. **4**(10), pp.2103–2114.
- Samanta, A., Hughes, T.E.T. and Moiseenkova-Bell, V.Y. 2018. Transient receptor potential (TRP) channels *In: Subcellular Biochemistry.*, pp.141–165.
- Sanders, Y. V., Eikenboom, J., de Wee, E.M., van der Bom, J.G., Cnossen, M.H., Degenaar-Dujardin, M.E.L., Fijnvandraat, K., Kamphuisen, P.W., Laros-van Gorkom, B.A.P., Meijer, K., Mauser-Bunschoten, E.P., Leebeek, F.W.G., Kors, A., Zweegman, S., Goverde, G.J., Jonkers, M.H., Dors, N., Nijziel, M.R., Meijer, K., Tamminga, R.Y.J., van der Linden, P.W., Ypma,

- P.F., Eikenboom, H.C.J., Smiers, F.J.W., Granzen, B., Hamulyák, K., Brons, P. and de Goede-Bolder, A. 2013. Reduced prevalence of arterial thrombosis in von Willebrand disease. *Journal of Thrombosis and Haemostasis*. **11**(5), pp.845–854.
- Sarma, A. and Yang, W. 2011. Calcium regulation of nucleocytoplasmic transport. *Protein and Cell*. **2**(4), pp.291–302.
- Savage, B., Cattaneo, M. and Ruggeri, Z.M. 2001. Mechanisms of platelet aggregation. *Current Opinion in Hematology*. **8**(5), pp.270–276.
- Schillemans, M., Karampini, E., Van Den Eshof, B.L., Gangaev, A., Hofman, M., Van Breevoort, D., Meems, H., Janssen, H., Mulder, A.A., Jost, C.R., Escher, J.C., Adam, R., Carter, T., Koster, A.J., Van Den Biggelaar, M., Voorberg, J. and Bierings, R. 2018. Weibel-palade body localized syntaxin-3 modulates von willebrand factor secretion from endothelial cells. *Arteriosclerosis, Thrombosis, and Vascular Biology*. **38**(7), pp.1549–1561.
- Schillemans, M., Karampini, E., Kat, M. and Bierings, R. 2019a. Exocytosis of Weibel–Palade bodies: how to unpack a vascular emergency kit. *Journal of Thrombosis and Haemostasis*. **17**(1), pp.6–18.
- Schillemans, M., Karampini, E., Kat, M. and Bierings, R. 2019b. Exocytosis of Weibel–Palade bodies: how to unpack a vascular emergency kit. *Journal of Thrombosis and Haemostasis*. **17**(1), pp.6–18.
- Schillemans, M., Karampini, E., Kat, M. and Bierings, R. 2019c. Exocytosis of Weibel–Palade bodies: how to unpack a vascular emergency kit. *Journal of Thrombosis and Haemostasis*. **17**(1), pp.6–18.
- Schneppenheim, R., Hellermann, N., Brehm, M.A., Klemm, U., Obser, T., Huck, V., Schneider, S.W., Denis, C. V., Tischer, A., Auton, M., März, W., Xu, E.R., Wilmanns, M. and Zotz, R.B. 2019. The von Willebrand factor Tyr2561 allele is a gain-of-function variant and a risk factor for early myocardial infarction. *Blood*. **133**(4), pp.356–365.
- Scholz, A., Plate, K.H. and Reiss, Y. 2015. Angiopoietin-2: A multifaceted cytokine that functions in both angiogenesis and inflammation. *Annals of the New York Academy of Sciences*. **1347**(1), pp.45–51.
- Schröder, J., Lüllmann-Rauch, R., Himmerkus, N., Pleines, I., Nieswandt, B., Orinska, Z., Koch-Nolte, F., Schröder, B., Bleich, M. and Saftig, P. 2009. Deficiency of the Tetraspanin CD63 Associated with Kidney Pathology but Normal Lysosomal Function. *Molecular and Cellular Biology*. **29**(4), pp.1083–1094.
- Schulze, H. and Shivdasani, R.A. 2005. Mechanisms of thrombopoiesis. *Journal of Thrombosis and Haemostasis*. **3**(8), pp.1717–1724.
- Scully, M., Cataland, S.R., Peyvandi, F., Coppo, P., Knöbl, P., Kremer Hovinga, J.A., Metjian, A., de la Rubia, J., Pavenski, K., Callewaert, F., Biswas, D., De Winter, H. and Zeldin, R.K. 2019. Caplacizumab Treatment for Acquired Thrombotic Thrombocytopenic Purpura. *New England Journal of Medicine*. **380**(4), pp.335–346.
- Seabra, M.C., Mules, E.H. and Hume, A.N. 2002. Rab GTPases, intracellular traffic and disease. *Trends in Molecular Medicine*. **8**(1), pp.23–30.
- Seaman, C.D., George, K.M., Ragni, M. and Folsom, A.R. 2016. Association of

- von Willebrand factor deficiency with prevalent cardiovascular disease and asymptomatic carotid atherosclerosis: The Atherosclerosis Risk in Communities Study. *Thrombosis Research*. **144**, pp.236–238.
- Seifert, R., Wenzel-Seifert, K., Burckstummer, T., Pertz, H.H., Schunack, W., Dove, S., Buschauer, A. and Elz, S. 2003. Multiple differences in agonist and antagonist pharmacology between human and guinea pig histamine H1-receptor. *The Journal of pharmacology and experimental therapeutics*. **305**(3), pp.1104–1115.
- Shen, F. and Seabra, M.C. 1996. Mechanism of digeranylgeranylation of rab proteins: Formation of a complex between Monogeranylgeranyl-Rab and Rab escort protein. *Journal of Biological Chemistry*. **271**(7), pp.3692–3698.
- Sherwood, M.W., Prior, I.A., Voronina, S.G., Barrow, S.L., Woodsmith, J.D., Gerasimenko, O. V., Petersen, O.H. and Tepikin, A. V. 2007. Activation of trypsinogen in large endocytic vacuoles of pancreatic acinar cells. *Proceedings of the National Academy of Sciences of the United States of America*. **104**(13), pp.5674–5679.
- Shintani, M., Tada, M., Kobayashi, T., Kajihō, H., Kontani, K. and Katada, T. 2007. Characterization of Rab45/RASEF containing EF-hand domain and a coiled-coil motif as a self-associating GTPase. *Biochemical and Biophysical Research Communications*. **357**(3), pp.661–667.
- Da Silva, M.L. and Cutler, D.F. 2016. Von Willebrand factor multimerization and the polarity of secretory pathways in endothelial cells. *Blood*. **128**(2), pp.277–285.
- Smith, A.C., Won, D.H., Braun, V., Jiang, X., Macrae, C., Casanova, J.E., Scidmore, M.A., Grinstein, S., Meyer, T. and Brumell, J.H. 2007. A network of Rab GTPases controls phagosome maturation and is modulated by *Salmonella enterica* serovar Typhimurium. *Journal of Cell Biology*. **176**(3), pp.263–268.
- Smith, N.L., Felix, J.F., Morrison, A.C., Demissie, S., Glazer, N.L., Loehr, L.R., Cupples, L.A., Dehghan, A., Lumley, T., Rosamond, W.D., Lieb, W., Rivadeneira, F., Bis, J.C., Folsom, A.R., Benjamin, E., Aulchenko, Y.S., Haritunians, T., Couper, D., Murabito, J., Wang, Y.A., Stricker, B.H., Gottdiener, J.S., Chang, P.P., Wang, T.J., Rice, K.M., Hofman, A., Heckbert, S.R., Fox, E.R., O'Donnell, C.J., Uitterlinden, A.G., Rotter, J.I., Willerson, J.T., Levy, D., van Duijn, C.M., Psaty, B.M., Witteman, J.C.M., Boerwinkle, E. and Vasan, R.S. 2010. Association of genome-wide variation with the risk of incident heart failure in adults of European and African ancestry: a prospective meta-analysis from the cohorts for heart and aging research in genomic epidemiology (CHARGE) consortium. *Circulation. Cardiovascular genetics*. **3**(3), pp.256–266.
- Speliotes, E.K., Yerges-Armstrong, L.M., Wu, J., Hernaez, R., Kim, L.J., Palmer, C.D., Gudnason, V., Eiriksdottir, G., Garcia, M.E., Launer, L.J., Nalls, M.A., Clark, J.M., Mitchell, B.D., Shuldiner, A.R., Butler, J.L., Tomas, M., Hoffmann, U., Hwang, S.J., Massaro, J.M., O'Donnell, C.J., Sahani, D. V., Salomaa, V., Schadt, E.E., Schwartz, S.M., Siscovick, D.S., Voight, B.F., Jeffrey Carr, J., Feitosa, M.F., Harris, T.B., Fox, C.S., Smith, A. V., Linda Kao, W.H., Hirschhorn, J.N., Borecki, I.B., McCullough, A., Bringman, D., Dasarathy, S., Edwards, K., Hawkins, C., Liu, Y.C., Rogers, N., Ruth

Sargent, P.A.C., Stager, M., Diehl, A.M., Abdelmalek, M., Gottfried, M.,
 Guy, C., Killenberg, P., Kwan, S., Pan, Y.P., Piercy, D., Smith, M.,
 Chalasani, N., Bhimalli, P., Cummings, O.W., Klipsch, A., Lee, L.,
 Molleston, J., Ragozzino, L., Vuppalachchi, R., Neuschwander-Tetri, B.A.,
 Barlow, S., Derdoy, J., Hoffmann, J., King, D., Siegner, J., Stewart, S.,
 Thompson, J., Brunt, E., Lavine, J.E., Behling, C., Clark, L., Durelle, J.,
 Hassanein, T., Petcharaporn, L., Schwimmer, J.B., Sirlin, C., Stein, T.,
 Bass, N.M., Bambha, K., Ferrell, L.D., Filipowski, D., Merriman, R., Pabst,
 M., Rosenthal, M., Rosenthal, P., Steel, T., Sanyal, A.J., Boyett, S., Bryan,
 D., Contos, M.J., Fuchs, M., Graham, M., Jones, A., Luketic, V.A.C.,
 Sandhu, B., Sargeant, C., Selph, K., White, M., Kowdley, K. V., Gyurkey,
 G., Mooney, J., Nelson, J., Roberts, S., Saunders, C., Stead, A., Wang, C.,
 Yeh, M., Kleiner, D., Doo, E., Everhart, J., Hoofnagle, J.H., Robuck, P.R.,
 Seeff, L., Tonascia, J., Belt, P., Brancati, F., Colvin, R., Donithan, M.,
 Green, M., Isaacson, M., Kim, W., Miriel, L., Sternberg, A., Ünalp, A., Van
 Natta, M., Wilson, L., Yates, K., Willer, C.J., Berndt, S.I., Monda, K.L.,
 Thorleifsson, G., Jackson, A.U., Allen, H.L., Lindgren, C.M., Luan, J., Mägi,
 R., Randall, J., Vedantam, S., Winkler, T.W., Qi, L., Workalemahu, T.,
 Heid, I.M., Steinthorsdottir, V., Stringham, H.M., Weedon, M.N., Wheeler,
 E., Wood, A.R., Ferreira, T., Weyant, R.J., Segrè, A. V., Estrada, K., Liang,
 L., Nemesh, J., Park, J.H., Gustafsson, S., Kilpeläinen, T.O., Yang, J.,
 Bouatia-Naji, N., Esko, T., Kutalik, Z., Mangino, M., Raychaudhuri, S.,
 Scherag, A., Welch, R., Zhao, J.H., Aben, K.K., Absher, D.M., Amin, N.,
 Dixon, A.L., Fisher, E., Glazer, N.L., Goddard, M.E., Heard-Costa, N.L.,
 Hoesel, V., Hottenga, J.J., Johansson, Å., Johnson, T., Ketkar, S., Lamina,
 C., Li, S., Moffatt, M.F., Myers, R.H., Narisu, N., Perry, J.R.B., Peters, M.J.,
 Preuss, M., Ripatti, S., Rivadeneira, F., Sandholt, C., Scott, L.J., Timpson,
 N.J., Tyrer, J.P., van Wingerden, S., Watanabe, R.M., White, C.C.,
 Wiklund, F., Barlassina, C., Chasman, D.I., Cooper, M.N., Jansson, J.O.,
 Lawrence, R.W., Pellikka, N., Prokopenko, I., Shi, J., Thiering, E., Alavere,
 H., Alibrandi, M.T.S., Almgren, P., Arnold, A.M., Aspelund, T., Atwood,
 L.D., Balkau, B., Balmforth, A.J., Bennett, A.J., Ben-Shlomo, Y., Bergman,
 R.N., Bergmann, S., Biebertmann, H., Blakemore, A.I.F., Boes, T.,
 Bonycastle, L.L., Bornstein, S.R., Brown, M.J., Buchanan, T.A., Busonero,
 F., Campbell, H., Cappuccio, F.P., Cavalcanti-Proença, C., Chen, Y.D.I.,
 Chen, C.M., Chines, P.S., Clarke, R., Coin, L., Connell, J., Day, I.N.M., den
 Heijer, M., Duan, J., Ebrahim, S., Elliott, P., Elosua, R., Erdos, M.R.,
 Eriksson, J.G., Facheris, M.F., Felix, S.B., Fischer-Posovszky, P., Folsom,
 A.R., Friedrich, N., Freimer, N.B., Fu, M., Gaget, S., Gejman, P. V., Geus,
 E.J.C., Gieger, C., Gjesing, A.P., Goel, A., Goyette, P., Grallert, H.,
 Gräßler, J., Greenawalt, D.M., Groves, C.J., Guiducci, C., Hartikainen, A.L.,
 Hassanali, N., Hall, A.S., Havulinna, A.S., Hayward, C., Heath, A.C.,
 Hengstenberg, C., Hicks, A.A., Hinney, A., Hofman, A., Homuth, G., Hui, J.,
 Igl, W., Iribarren, C., Isomaa, B., Jacobs, K.B., Jarick, I., Jewell, E., John,
 U., Jørgensen, T., Jousilahti, P., Jula, A., Kaakinen, M., Kajantie, E.,
 Kaplan, L.M., Kathiresan, S., Kettunen, J., Kinnunen, L., Knowles, J.W.,
 Kolcic, I., König, I.R., Koskinen, S., Kovacs, P., Kuusisto, J., Kraft, P.,
 Kvaløy, K., Laitinen, J., Lantieri, O., Lanzani, C., Lecoeur, C., Lehtimäki, T.,
 Lettre, G., Liu, J., Lokki, M.L., Lorentzon, M., Luben, R.N., Ludwig, B.,
 Manunta, P., Marek, D., Marre, M., Martin, N.G., McArdle, W.L., McCarthy,
 A., McKnight, B., Meitinger, T., Melander, O., Meyre, D., Midthjell, K.,
 Montgomery, G.W., Morken, M.A., Morris, A.P., Mulic, R., Ngwa, J.S.,

Nelis, M., Neville, M.J., Nyholt, D.R., O’Rahilly, S., Ong, K.K., Oostra, B., Paré, G., Parker, A.N., Perola, M., Pichler, I., Pietiläinen, K.H., Platou, C.G.P., Polasek, O., Pouta, A., Rafelt, S., Raitakari, O., Rayner, N.W., Ridderstråle, M., Rief, W., Ruukonen, A., Robertson, N.R., Rzehak, P., Sanders, A.R., Sandhu, M.S., Sanna, S., Saramies, J., Savolainen, M.J., Scherag, S., Schipf, S., Schreiber, S., Schunkert, H., Silander, K., Sinisalo, J., Smit, J.H., Soranzo, N., Sovio, U., Stephens, J., Surakka, I., Swift, A., Tammesoo, M.L., Tardif, J.C., Teder-Laving, M., Teslovich, T.M., Thompson, J.R., Thomson, B., Tönjes, A., Tuomi, T., van Meurs, J.B.J., van Ommen, G.J., Vatin, V., Viikari, J., Visvikis-Siest, S., Vitart, V., Vogel, C.I.G., Waite, L.L., Wallaschofski, H., Bragi Walters, G., Widen, E., Wiegand, S., Wild, S.H., Willemsen, G., Witte, D.R., Witteman, J.C., Xu, J., Zhang, Q., Zgaga, L., Ziegler, A., Zitting, P., Beilby, J.P., Farooqi, I.S., Hebebrand, J., Huikuri, H. V., James, A.L., Kähönen, M., Levinson, D.F., Macciardi, F., Nieminen, M.S., Ohlsson, C., Ridker, P.M., Stumvoll, M., Beckmann, J.S., Boeing, H., Boerwinkle, E., Boomsma, D.I., Caulfield, M.J., Chanock, S.J., Adrienne Cupples, L., Smith, G.D., Erdmann, J., Froguel, P., Grönberg, H., Gyllensten, U., Hall, P., Hansen, T., Hattersley, A.T., Hayes, R.B., Heinrich, J., Hu, F.B., Hveem, K., Illig, T., Jarvelin, M.R., Kaprio, J., Karpe, F., Khaw, K.T., Kiemeny, L.A., Krude, H., Laakso, M., Lawlor, D.A., Metspalu, A., Munroe, P.B., Ouwehand, W.H., Pedersen, O., Penninx, B.W., Peters, A., Pramstaller, P.P., Quertermous, T., Reinehr, T., Rissanen, A., Rudan, I., Samani, N.J., Schwarz, P., Spector, T.D., Tuomilehto, J., Uda, M., Uitterlinden, A.G., Valle, T.T., Wabitsch, M., Waeber, G., Wareham, N.J., Watkins, H., Wilson, J.F., Wright, A.F., Carola Zillikens, M., Chatterjee, N., Mc, S.A., Purcell, S., Visscher, P.M., Assimes, T.L., Deloukas, P., Groop, L.C., Haritunians, T., Hunter, D.J., Kaplan, R.C., Mohlke, K.L., O’Connell, J.R., Peltonen, L., Schlessinger, D., Strachan, D.P., van Duijn, Cornelia M., Wichmann, H.E., Frayling, T.M., Thorsteinsdottir, U., Abecasis, G.R., Barroso, I., Boehnke, M., Stefansson, K., North, K.E., McCarthy, M.I., Ingelsson, E., Loos, R.J.F., Dupuis, J., Langenberg, C., Saxena, R., Gloyn, A.L., Rybin, D., Henneman, P., Dehghan, A., Franklin, C.S., Navarro, P., Song, K., Egan, J.M., Lajunen, T., Grarup, N., Sparsø, T., Doney, A., Li, M., Kanoni, S., Shrader, P., Kumari, M., Zabena, C., Rocheleau, G., An, P., Elliott, A., McCarroll, S.A., Payne, F., Roccascaccia, R.M., Pattou, F., Sethupathy, P., Ardlie, K., Ariyurek, Y., Barter, P., Benediktsson, R., Bochud, M., Bonnefond, A., Borch-Johnsen, K., Böttcher, Y., Brunner, E., Bumpstead, S.J., Charpentier, G., Cornelis, M., Crawford, G., Crisponi, L., de Geus, E.J.C., Delplanque, J., Dina, C., Fedson, A.C., Fischer-Rosinsky, A., Forouhi, N.G., Frants, R., Franzosi, M.G., Galan, P., Goodarzi, M.O., Graessler, J., Grundy, S., Gwilliam, R., Hadjadj, S., Hallmans, G., Hammond, N., Han, X., Heath, S.C., Hercberg, S., Herder, C., Hillman, D.R., Hingorani, A.D., Hung, J., Johnson, P.R.V., Antero Kesaniemi, Y., Kivimaki, M., Knight, B., Kyvik, K.O., Lathrop, G.M., Bacquer, O. Le, Li, Y., Lyssenko, V., Mahley, R., Manning, A.K., Martínez-Larrad, M.T., McAteer, J.B., McCulloch, L.J., McPherson, R., Meisinger, C., Melzer, D., Mukherjee, S., Naitza, S., Orrù, M., Pakyz, R., Palmer, C.N.A., Paolisso, G., Pattaro, C., Pearson, D., Peden, J.F., Pedersen, N.L., Pfeiffer, A.F.H., Posthuma, D., Potter, S.C., Province, M.A., Psaty, B.M., Rathmann, W., Rice, K., Roden, M., Rolandsson, O., Sandbaek, A., Sayer, A.A., Scheet, P., Sedorf, U., Sharp, S.J., Shields, B., Sigurðsson, G., Sijbrands, E.J.G., Silveira, A., Simpson, L., Singleton, A., Smith, N.L.,

- Syddall, H., Syvänen, A.C., Tanaka, T., Thorand, B., Tichet, J., van Dijk, K.W., van Hoek, M., Varma, D., Vogelzangs, N., Wagner, P.J., Walley, A., Walters, G.B., Ward, K.L., Wittteman, J.C.M., Yarnell, J.W.G., Zeggini, E., Zelenika, D., Zethelius, B., Zhai, G., Zillikens, M.C., Meneton, P., Magnusson, P.K.E., Nathan, D.M., Williams, G.H., Spranger, J., Cooper, C., Dedoussis, G. V., Lind, L., Morris, A.D., Palmer, L.J., Franks, P.W., Marmot, M., Pankow, J.S., Sampson, M.J., Erich Wichmann, H., Hamsten, A., Altshuler, D., Rotter, J.I., Ferrucci, L., Kong, A., Duijn, Cornelia Mvan, Aulchenko, Y.S., Cao, A., Scuteri, A., Waterworth, D.M., Vollenweider, P., Mooser, V., Sladek, R., Meigs, J.B. and Florez, J.C. 2011. Genome-wide association analysis identifies variants associated with nonalcoholic fatty liver disease that have distinct effects on metabolic traits. *PLoS Genetics*. **7**(3).
- Sporn, L.A., Marder, V.J. and Wagner, D.D. 1986. Inducible secretion of large, biologically potent von Willebrand factor multimers. *Cell*. **46**(2), pp.185–190.
- Springer, T.A. 2014. Von Willebrand factor, Jedi knight of the bloodstream. *Blood*. **124**(9), pp.1412–1425.
- Srikanth, S., Jung, H.J., Kim, K. Do, Souda, P., Whitelegge, J. and Gwack, Y. 2010. A novel EF-hand protein, CRACR2A, is a cytosolic Ca²⁺ sensor that stabilizes CRAC channels in T cells. *Nature Cell Biology*. **12**(5), pp.436–446.
- Srikanth, S., Kim, K. Do, Gao, Y., Woo, J.S., Ghosh, S., Calmettes, G., Paz, A., Abramson, J., Jiang, M. and Gwack, Y. 2016. A large Rab GTPase encoded by CRACR2A is a component of subsynaptic vesicles that transmit T cell activation signals. *Science Signaling*. **9**(420), pp.1–14.
- Srikanth, S., Woo, J.S. and Gwack, Y. 2017. A large Rab GTPase family in a small GTPase world. *Small GTPases*. **8**(1), pp.43–48.
- Starke, R.D., Ferraro, F., Paschalaki, K.E., Dryden, N.H., McKinnon, T.A.J., Sutton, R.E., Payne, E.M., Haskard, D.O., Hughes, A.D., Cutler, D.F., Laffan, M.A. and Randi, A.M. 2011. Endothelial von Willebrand factor regulates angiogenesis. *Blood*. **117**(3), pp.1071–1080.
- Stauffer, B.L., Westby, C.M. and DeSouza, C.A. 2008. Endothelin-1, aging and hypertension. *Current Opinion in Cardiology*. **23**(4), pp.350–355.
- Stenmark, H. 2009. Rab GTPases as coordinators of vesicle traffic. *Nature Reviews Molecular Cell Biology*. **10**(8), pp.513–525.
- Stockschlaeder, M., Schneppenheim, R. and Budde, U. 2014. Update on von Willebrand factor multimers: Focus on high-molecular-weight multimers and their role in hemostasis. *Blood Coagulation and Fibrinolysis*. **25**(3), pp.206–216.
- Stoll, G. and Bendszus, M. 2006. Inflammation and atherosclerosis: Novel insights into plaque formation and destabilization. *Stroke*. **37**(7), pp.1923–1932.
- Straley, K.S. and Green, S.A. 2000. Rapid transport of internalized P-selectin to late endosomes and the TGN: Roles in regulating cell surface expression and recycling to secretory granules. *Journal of Cell Biology*. **151**(1), pp.107–116.

- Streetley, J., Fonseca, A.V., Turner, J., Kiskin, N.I., Knipe, L., Rosenthal, P.B. and Carter, T. 2019. Stimulated release of intraluminal vesicles from Weibel-Palade bodies. *Blood*. **133**(25), pp.2707–2717.
- Sun, W.Y., Abeynaike, L.D., Escarbe, S., Smith, C.D., Pitson, S.M., Hickey, M.J. and Bonder, C.S. 2012. Rapid histamine-induced neutrophil recruitment is sphingosine kinase-1 dependent. *American Journal of Pathology*. **180**(4), pp.1740–1750.
- Swami, A. and Kaur, V. 2017. Von Willebrand Disease: A Concise Review and Update for the Practicing Physician. *Clinical and Applied Thrombosis/Hemostasis*. **23**(8), pp.900–910.
- Tang, B. 2015. MIRO GTPases in Mitochondrial Transport, Homeostasis and Pathology. *Cells*. **5**(1), p.1.
- Taylor, C.W. 1997. Chapter 9 Inositol 1,4,5-trisphosphate receptors. *Principles of Medical Biology*. **8**(C), pp.157–168.
- Taylor, C.W. and Tovey, S.C. 2010. IP(3) receptors: toward understanding their activation. *Cold Spring Harbor perspectives in biology*. **2**(12).
- Tevoufouet, E.E., Nembo, E.N., Dibué-Adjei, M., Hescheler, J., Nguemo, F. and Schneider, T. 2014. Cardiac functions of voltage-gated Ca^{2+} channels: Role of the pharmacoresistant type (E-/R-type) in cardiac modulation and putative implication in sudden unexpected death in epilepsy (SUDEP). *Reviews of Physiology, Biochemistry and Pharmacology*. **167**, pp.115–140.
- Touchot, N., Chardin, P. and Tavitian, A. 1987. Four additional members of the ras gene superfamily isolated by an oligonucleotide strategy: molecular cloning of YPT-related cDNAs from a rat brain library. *Proceedings of the National Academy of Sciences of the United States of America*. **84**(23), pp.8210–8214.
- Tran, Q.K., Ohashi, K. and Watanabe, H. 2000. Calcium signalling in endothelial cells. *Cardiovascular Research*. **48**(1), pp.13–22.
- Tsai, H.-M., Nagel, R.L., Hatcher, V.B., Seaton, A.C. and Sussman, I.I. 1991. The high molecular weight form of endothelial cell von Willebrand factor is released by the regulated pathway. *British Journal of Haematology*. **79**(2), pp.239–245.
- Tscharre, M., Vogel, B., Tentzeris, I., Freynhofer, M.K., Rohla, M., Wojta, J., Weiss, T.W., Ay, C., Huber, K. and Farhan, S. 2019. Prognostic Impact of Soluble P-Selectin on Long-Term Adverse Cardiovascular Outcomes in Patients Undergoing Percutaneous Coronary Intervention. *Thrombosis and Haemostasis*. **119**(2), pp.340–347.
- Ullrich, O., Horiuchi, H., Bucci, C. and Zerial, M. 1994. Membrane association of Rab5 mediated by GDP-dissociation inhibitor and accompanied by GDP/GTP exchange. *Nature*. **368**(6467), pp.157–160.
- Ullrich, O., Stenmark, H., Alexandrov, K., Huber, L.A., Kaibuchi, K., Sasaki, T., Takai, Y. and Zerial, M. 1993. Rab GDP dissociation inhibitor as a general regulator for the membrane association of rab proteins. *Journal of Biological Chemistry*. **268**(24), pp.18143–18150.
- Utgaard, J.O., Jahnsen, F.L., Bakka, A., Brandtzaeg, P. and Haraldsen, G. 1998. Rapid secretion of prestored interleukin 8 from Weibel-Palade bodies

- of microvascular endothelial cells. *Journal of Experimental Medicine*. **188**(9), pp.1751–1756.
- Valentijn, K.M., Van Driel, L.F., Mourik, M.J., Hendriks, G.J., Arends, T.J., Koster, A.J. and Valentijn, J.A. 2010. Multigranular exocytosis of Weibel-Palade bodies in vascular endothelial cells. *Blood*. **116**(10), pp.1807–1816.
- Valentijn, K.M., Sadler, J.E., Valentijn, J.A., Voorberg, J. and Eikenboom, J. 2011. Functional architecture of Weibel-Palade bodies. *Blood*. **117**(19), pp.5033–5043.
- Venturi, E., Pitt, S., Galfré, E. and Sitsapesan, R. 2012. From Eggs to Hearts: What Is the Link between Cyclic ADP-Ribose and Ryanodine Receptors? *Cardiovascular Therapeutics*. **30**(2), pp.109–116.
- Vinogradova, T.M., Roudnik, V.E., Bystrevskaya, V.B. and Smirnov, V.N. 2000. Centrosome-directed translocation of Weibel-Palade bodies is rapidly induced by thrombin, calyculin A, or cytochalasin B in human aortic endothelial cells. *Cell motility and the cytoskeleton*. **47**(2), pp.141–153.
- Virant, D., Traenkle, B., Maier, J., Kaiser, P.D., Bodenhöfer, M., Schmees, C., Vojnovic, I., Pisak-Lukáts, B., Endesfelder, U. and Rothbauer, U. 2018. A peptide tag-specific nanobody enables high-quality labeling for dSTORM imaging. *Nature Communications*. **9**(1), p.930.
- Vischer, U. and Wagner, D. 1994. von Willebrand factor proteolytic processing and multimerization precede the formation of Weibel-Palade bodies. *Blood*. **83**(12), pp.3536–3544.
- Vischer, U.M. and Wagner, D.D. 1993. CD63 is a component of Weibel-Palade bodies of human endothelial cells. *Blood*. **82**(4), pp.1184–1191.
- Vischer, U.M. and Wollheim, C.B. 1997. Epinephrine induces von Willebrand factor release from cultured endothelial cells: Involvement of cyclic AMP-dependent signalling in exocytosis. *Thrombosis and Haemostasis*. **77**(6), pp.1182–1188.
- Voorberg, J., Fontijn, R., Calafat, J., Janssen, H., Van Mourik, J.A. and Pannekoek, H. 1993. Biogenesis of von Willebrand factor-containing organelles in heterologous transfected CV-1 cells. *EMBO Journal*. **12**(2), pp.749–758.
- Wagner, D.D. 1990. Cell Biology of von Willebrand Factor. *Annual Review of Cell Biology*. **6**(1), pp.217–242.
- Wagner, D.D., Mayadas, T. and Marder, V.J. 1986. Initial glycosylation and acidic pH in the Golgi apparatus are required for multimerization of von Willebrand factor. *Journal of Cell Biology*. **102**(4), pp.1320–1324.
- Wagner, D.D., Saffaripour, S., Bonfanti, R., Sadler, J.E., Cramer, E.M., Chapman, B. and Mayadas, T.N. 1991. Induction of specific storage organelles by von Willebrand factor propeptide. *Cell*. **64**(2), pp.403–413.
- Walsh, D.A., Perkins, J.P. and Krebs, E.G. 1968. An adenosine 3',5'-monophosphate-dependant protein kinase from rabbit skeletal muscle. *Journal of Biological Chemistry*. **243**(13), pp.3763–3765.
- Wang, P., Chintagari, N.R., Gou, D., Su, L. and Liu, L. 2007. Physical and functional interactions of SNAP-23 with annexin A2. *American journal of*

respiratory cell and molecular biology. **37**(4), pp.467–476.

- Wang, X., Zhang, X., Dong, X.P., Samie, M., Li, X., Cheng, X., Goschka, A., Shen, D., Zhou, Y., Harlow, J., Zhu, M.X., Clapham, D.E., Ren, D. and Xu, H. 2012. TPC proteins are phosphoinositide- Activated sodium-selective ion channels in endosomes and lysosomes. *Cell*. **151**(2), pp.372–383.
- Wang, Y., Huynh, W., Skokan, T.D., Lu, W., Weiss, A. and Vale, R.D. 2019. CRACR2a is a calcium-activated dynein adaptor protein that regulates endocytic traffic. *Journal of Cell Biology*. **218**(5), pp.1619–1633.
- Waschbüsch, D. and Khan, A.R. 2020. Phosphorylation of Rab GTPases in the regulation of membrane trafficking. *Traffic*. **21**(11), pp.712–719.
- Wei, A.-H. and Li, W. 2013. Hermansky-Pudlak syndrome: pigmentary and non-pigmentary defects and their pathogenesis. *Pigment cell & melanoma research*. **26**(2), pp.176–192.
- Weibel, E.R. 2012. Fifty years of Weibel-Palade bodies: The discovery and early history of an enigmatic organelle of endothelial cells. *Journal of Thrombosis and Haemostasis*. **10**(6), pp.979–984.
- WEIBEL, E.R. and PALADE, G.E. 1964. New Cytoplasmic Components in Arterial Endothelia. *The Journal of cell biology*. **23**(1), pp.101–112.
- Westra, J., de Groot, L., Plaxton, S.L., Brouwer, E., Posthumus, M.D., Kallenberg, C.G.M. and Bijl, M. 2011. Angiopoietin-2 is highly correlated with inflammation and disease activity in recent-onset rheumatoid arthritis and could be predictive for cardiovascular disease. *Rheumatology*. **50**(4), pp.665–673.
- Willebrand, E.A. Von 1999. Hereditary pseudohaemophilia. *Haemophilia*. **5**(3), pp.223–231.
- Wilson, L.A., McKeown, L., Tumova, S., Li, J. and Beech, D.J. 2015. Expression of a long variant of CRACR2A that belongs to the Rab GTPase protein family in endothelial cells. *Biochemical and Biophysical Research Communications*. **456**(1), pp.398–402.
- Wolff, B., Burns, A.R., Middleton, J. and Rot, A. 1998. Endothelial cell ‘memory’ of inflammatory stimulation: Human venular endothelial cells store interleukin 8 in Weibel-Palade bodies. *Journal of Experimental Medicine*. **188**(9), pp.1757–1762.
- Wong, C.O. and Yao, X. 2011. TRP channels in vascular endothelial cells. *Advances in Experimental Medicine and Biology*. **704**, pp.759–780.
- Woo, J.S., Srikanth, S., Kim, K.-D., Elsaesser, H., Lu, J., Pellegrini, M., Brooks, D.G., Sun, Z. and Gwack, Y. 2018. CRACR2A-Mediated TCR Signaling Promotes Local Effector Th1 and Th17 Responses. *The Journal of Immunology*. **201**(4), pp.1174–1185.
- Wu, K.K., Frasier-Scott, K. and Hatzakis, H. 1988. Endothelial cell function in hemostasis and thrombosis. In: S. Chien, ed. *Advances in experimental medicine and biology* [Online]. Boston, MA: Springer US, pp.127–133. Available from: https://doi.org/10.1007/978-1-4684-8935-4_15.
- Wu, M.M., Covington, E.D. and Lewis, R.S. 2014. Single-molecule analysis of diffusion and trapping of STIM1 and Orai1 at endoplasmic reticulum-plasma membrane junctions. *Molecular Biology of the Cell*. **25**(22),

pp.3672–3685.

- Xiong, Y., Huo, Y., Chen, C., Zeng, H., Lu, X., Wei, C., Ruan, C., Zhang, X., Hu, Z., Shibuya, M. and Luo, J. 2009. Vascular endothelial growth factor (VEGF) receptor-2 tyrosine 1175 signaling controls VEGF-induced von Willebrand factor release from endothelial cells via phospholipase C- γ 1- and protein kinase A-dependent pathways. *Journal of Biological Chemistry*. **284**(35), pp.23217–23224.
- Yamaguchi, Y., Sakai, E., Okamoto, K., Kajiya, H., Okabe, K., Naito, M., Kadowaki, T. and Tsukuba, T. 2018. Rab44, a novel large Rab GTPase, negatively regulates osteoclast differentiation by modulating intracellular calcium levels followed by NFATc1 activation. *Cellular and Molecular Life Sciences*. **75**(1), pp.33–48.
- Yamamoto, K., Sokabe, T., Matsumoto, T., Yoshimura, K., Shibata, M., Ohura, N., Fukuda, T., Sato, T., Sekine, K., Kato, S., Isshiki, M., Fujita, T., Kobayashi, M., Kawamura, K., Masuda, H., Kamiya, A. and Ando, J. 2006. Impaired flow-dependent control of vascular tone and remodeling in P2X4-deficient mice. *Nature Medicine*. **12**(1), pp.133–137.
- Yamamoto, N., Watanabe, H., Kakizawa, H., Hirano, M., Kobayashi, A. and Ohno, R. 1995. A study on thapsigargin-induced calcium ion and cation influx pathways in vascular endothelial cells. *Biochimica et Biophysica Acta - Molecular Cell Research*. **1266**(2), pp.157–162.
- Yancopoulos, G.D., Davis, S., Gale, N.W., Rudge, J.S., Wiegand, S.J. and Holash, J. 2000. Vascular-specific growth factors and blood vessel formation. *Nature*. **407**(6801), pp.242–248.
- Yáñez, M., Gil-Longo, J. and Campos-Toimil, M. 2012. Calcium binding proteins. *Advances in Experimental Medicine and Biology*. **740**, pp.461–482.
- Yang, Z., Kirton, H.M., MacDougall, D.A., Boyle, J.P., Deuchars, J., Frater, B., Ponnambalam, S., Hardy, M.E., White, E., Calaghan, S.C., Peers, C. and Steele, D.S. 2015. The Golgi apparatus is a functionally distinct Ca²⁺ store regulated by the PKA and Epac branches of the β 1-adrenergic signaling pathway. *Science Signaling*. **8**(398), pp.1–12.
- Yau, J.W., Teoh, H. and Verma, S. 2015. Endothelial cell control of thrombosis. *BMC Cardiovascular Disorders*. **15**(1), p.130.
- Zahradník, I., Györke, S. and Zahradníková, A. 2005. Calcium activation of ryanodine receptor channels - Reconciling RyR gating models with tetrameric channel structure. *Journal of General Physiology*. **126**(5), pp.515–527.
- Zenner, H.L., Collinson, L.M., Michaux, G. and Cutler, D.F. 2007. High-pressure freezing provides insights into Weibel-Palade body biogenesis. *Journal of Cell Science*. **120**(12), pp.2117–2125.
- Zerial, M. and McBride, H. 2001. Rab proteins as membrane organizers. *Nature Reviews Molecular Cell Biology*. **2**(2), pp.107–117.
- Zhang, D. and Aravind, L. 2010. Identification of novel families and classification of the C2 domain superfamily elucidate the origin and evolution of membrane targeting activities in eukaryotes. *Gene*. **469**(1–2), pp.18–30.

- Zhang, F. and Li, P.L. 2007. Reconstitution and characterization of a Nicotinic Acid Adenine Dinucleotide Phosphate (NAADP)-sensitive Ca²⁺ release channel from liver lysosomes of rats. *Journal of Biological Chemistry*. **282**(35), pp.25259–25269.
- Zhang, F., Xu, M., Han, W.Q. and Li, P.L. 2011. Reconstitution of lysosomal NAADP-TRP-ML1 signaling pathway and its function in TRP-ML1 ^{-/-} cells. *American Journal of Physiology - Cell Physiology*. **301**(2).
- Zhang, L., Yang, N., Park, J.W., Katsaros, D., Fracchioli, S., Cao, G., O'Brien-Jenkins, A., Randall, T.C., Rubin, S.C. and Coukos, G. 2003. Tumor-derived vascular endothelial growth factor up-regulates angiopoietin-2 in host endothelium and destabilizes host vasculature, supporting angiogenesis in ovarian cancer. *Cancer Research*. **63**(12), pp.3403–3412.
- Zhang, M., Abrams, C., Wang, L., Gizzi, A., He, L., Lin, R., Chen, Y., Loll, P.J., Pascal, J.M. and Zhang, J.F. 2012. Structural basis for calmodulin as a dynamic calcium sensor. *Structure*. **20**(5), pp.911–923.
- Zhang, S.L., Yu, Y., Roos, J., Kozak, J.A., Deerinck, T.J., Ellisman, M.H., Stauderman, K.A. and Cahalan, M.D. 2005. STIM1 is a Ca²⁺ sensor that activates CRAC channels and migrates from the Ca²⁺ store to the plasma membrane. *Nature*. **437**(7060), pp.902–905.
- Zhang, W. and Colman, R.W. 2007. Thrombin regulates intracellular cyclic AMP concentration in human platelets through phosphorylation/activation of phosphodiesterase 3A. *Blood*. **110**(5), pp.1475–1482.
- Zhang, Z.H., Lu, Y.Y. and Yue, J. 2013. Two Pore Channel 2 Differentially Modulates Neural Differentiation of Mouse Embryonic Stem Cells. *PLoS ONE*. **8**(6).
- Zhu, M.X., Ma, J., Parrington, J., Galione, A. and Mark Evans, A. 2010. TPCs: Endolysosomal channels for Ca²⁺ mobilization from acidic organelles triggered by NAADP. *FEBS Letters*. **584**(10), pp.1966–1974.
- Zografou, S., Basagiannis, D., Papafotika, A., Shirakawa, R., Horiuchi, H., Auerbach, D., Fukuda, M. and Christoforidis, S. 2012. A complete rab screening reveals novel insights in Weibel-Palade body exocytosis. *Journal of Cell Science*. **125**(20), pp.4780–4790.
- Zografu 2012. Accepted manuscript. . (August).
- Zupančič, G., Ogden, D., Magnus, C.J., Wheeler-Jones, C. and Carter, T.D. 2002. Differential exocytosis from human endothelial cells evoked by high intracellular Ca²⁺ concentration. *Journal of Physiology*. **544**(3), pp.741–755.